University of Zurich[UZH]

Department of Geography

Analysis of decadal glacier changes on active volcanoes in Latin America

GEO 511 Master's Thesis

Author
Johannes Reinthaler
15-727-720

Supervised by
PD Dr. Christian Huggel, UZH
Dr. Frank Paul, UZH
Dr. Hugo Delgado, UNAM, hugo@geofisica.unam.mx

Faculty representative
Prof. Dr. Andreas Vieli

29.09.2017
Department of Geography, University of Zurich

Analysis of decadal glacier changes on active volcanoes in Latin America

Cover picture: view on Pico de Orizaba (Mexico) and Glaciar Jamapa

By Johannes Reinthaler

Abstract

Glaciers on active volcanoes are subject to changes related to both, climate fluctuation and volcanic activity. This thesis analyses glacier area change of active Latin American volcanoes during the last three decades using multispectral satellite images in combination with a database reporting volcanic eruptions. A main focus was on the influence of volcanic activity on glacier area and the change of volcanic activity over time by combining glacier area changes with volcano and eruption data.

Glacier outlines were obtained for three time steps: around 1985, 2000 and 2015 using a semi-automated band ratio method with satellite images form Landsat 4/5, 7, 8 and Sentinel-2. Volcanic activity was analysed using a modified version of the Smithsonian volcano database that contains volcano and eruption data of all Holocene volcanoes of Latin America (except countries without glacier-covered volcanoes). Finally, volcanoes with a hazard potential were identified and ideas for further research suggested.

In total, glacier outline of 59 volcanoes across Latin America could be derived. Results show, that on average, glaciers on active volcanoes lost around 50% of their size in the last 30 years with an average change rate of -1.8%/y. Small glaciers, especially in tropical regions lost more area than large or extratropical glaciers. Glaciers in Mexico had the highest change rate during the study period (-2.3%/y), followed by Chile and Argentina between 35° S and 38° S (-2.14%/y), Peru/Bolivia (-1.53%/y) and Colombia/Ecuador (-1.38%/y). In southern South America (south of 41° S), the glacier change rate was much lower (-0.60%/y). Two volcanoes lost their entire glacier area within the time period, being Popocatepetl in Mexico and Tungurahua in Ecuador. Both volcanoes experienced extensive eruptions that contributed to the area loss.

Surprisingly, overall glacier retreat slowed down since 2000 (-0.66%/y) comparison with the period 1985-2000 (-1.14%/y). Also, glaciers on volcanoes that experienced eruptions during the study period show a higher area loss (on average -2.05%/y) than glaciers on volcanoes without eruptions (on average -1.56%/y).

Because volcanic activity increased during the last deglaciation (likely due to the unloading of ice), a similar response to climate change but on a much smaller scale could be expected following the recent glacier retreat. Investigations of volcano data have shown, that volcanic activity on glacier-covered volcanoes experienced variations during the Holocene, partly following climate and glacier fluctuations. Period with increased volcanic activity were found between 7100 BP and 6700 BP, 2300 BP and 1500 BP, and after 1820AD. All of which correlate with warming or warm periods.

How much the glacier retreat since the LIA influenced and will affect the volcanic activity still remains an open discussion with further research needed.

Zusammenfassung

Gletscher gelten als wichtige Klimaindikatoren und werden oft als natürliche Thermometer des Erdklimas betrachtet (Vaughan et al., 2013). Sie verändern ihre Größe infolge von äußeren Bedingungen wie Temperatur, Niederschlag und Erdwärme. Gerade der Einfluss der Erdwärme ist für die Gletscher, die auf Vulkanen vorkommen, von besonderer Wichtigkeit.

Diese Arbeit befasst sich mit den Veränderungen der Gletscherflächen in den letzten drei Jahrzehnten auf aktiven Vulkanen in Lateinamerika. Untersucht wird der Einfluss von Vulkanausbrüchen während der Untersuchungsperiode und deren Auswirkung auf die Gletscherfläche. Neben den Gletscherveränderungen wird auch die Entwicklung der vulkanischen Aktivität während des Holozäns untersucht, und diese mit den Veränderungen der Gletscherflächen und des Klimas verglichen. Studien haben bestätigt, dass es eine Verbindung zwischen Gletscherauflast und vulkanischer Aktivität gibt. Nach der letzten Eiszeit, als global großen Mengen an Eis abschmolzen, wurde eine zwei- bis sechsmal höhere Vulkanaktivität festgestellt (Huybers & Langmuir, 2009; Maclennan et al., 2002; Jull & Mckenzie, 1996). Jedoch ist es bis zu diesem Zeitpunkt noch unklar, wie sich der gegenwärtige Klimawandel auf die vulkanische Aktivität auswirkt.

Außerdem werden in dieser Arbeit gletscherbedeckte Vulkane mit einem hohen Gefahrenrisiko identifiziert, die entweder einen Mangel an Überwachung aufweisen oder eine besondere Gefahr für die Bevölkerung darstellen könnten.

Für die Berechnung der Gletscherflächen wurden folgende drei Zeitpunkte gewählt: die Jahre 1985, 2000 und 2015. Zur Berechnung dieser wurden verschiedene multi-spektrale Satelliten benutzt: Landsat 4-5 (für 1985 und 2000), Landsat 7 (für 2000), Landsat 8 (für 2015) und Sentinel 2A (für 2015). Alle Bilder sind frei über die Homepage des U.S. Geological Survey (USGS) verfügbar und können direkt heruntergeladen werden. Um die Gletscherflächen zu berechnen wurden sie in das Programm ArcGIS importiert. Da die ausgewählten Satelliten alle auch über einen Kanal im kurzwelligen infraroten Bereich verfügen, konnte die Gletscherkartierung anhand der spektralen Eigenschaften von Eis durchgeführt werden. Im Vergleich zu Fels oder zur Vegetation absorbiert Eis den Großteil des kurzwelligen infraroten Lichtes und kann somit klar unterschieden werden. Diese Kategorisierung anhand der spektralen Eigenschaften funktioniert halb automatisch und kann auf allen Gletschern angewandt werden. Schwierigkeiten ergeben sich sobald der Gletscher mit Schutt oder Asche bedeckt ist oder im Schatten liegt. Außerdem können optische Sensoren, wie sie in den Landsat und Sentinel-2 Satelliten eingebaut sind nicht durch dicke Wolken penetrieren.

Um die vulkanische Aktivität zu untersuchen wurde eine Vulkandatenbank, ähnlich der „Smithsonian“ Vulkandatenbank benutzt. In ihr sind alle Vulkaneigenschaften und Vulkanausbrüche der im Holozäns aktiven Vulkane von Lateinamerika gespeichert. Daraus konnte die Entwicklung der

Ausbruchshäufigkeit ermittelt werden um diese mit der Entwicklung des Klimas zu vergleichen. Die Datenbank wurde in zwei Gruppen unterteilt: Vulkane mit Gletscherbedeckung und Vulkane ohne Gletscher. Anhand dieser Unterteilung lässt sich der Unterschied der Eruptionsraten aufgrund von Gletscherveränderungen herauslesen.

Die wichtigsten Ergebnisse kurz aufgelistet:

- Es wurden Gletscherflächen für 59 Vulkane berechnet.
- Alle Gletscher verloren zwischen 1985 und 2015 an Fläche (durchschnittlich 50%).
- Größte Flächenverluste in Mexico (-2.3%/y), in Peru und Bolivien (-1.53%/y) und zwischen 35°S-38° S (-2.14%/y).
- Geringe Flächenverluste zwischen 33° S-35° S (-0.76%/y) und südlich von 41°S (-0.60%/y).
- Allgemein geringerer Flächenverlust zwischen 2000 und 2015 (-0.66%/y) im Vergleich zu 1985 bis 2000 (-1.14%/y).
- Gletscher auf Vulkanen welche eine oder mehrere Vulkanausbrüche während der Untersuchungsperiode erlebt haben, zeigen größere Flächenverluste auf (Durchschnittlich -1.41%/y im Vergleich zu -0.85%/y für Gletscher ohne Vulkanausbrüche).
- Die vulkanische Aktivität während des Holozäns unterlag einigen Schwankungen. Perioden mit hohen Ausbruchsraten auf Vulkanen mit Gletscherbedeckung waren zwischen 7100 BP und 6700 BP, 2300 BP und 1500 BP und nach 1820 AD. Diese Perioden korrelieren größtenteils, wenn auch mit einer Verzögerung mit Erwärmungs- oder Warmperioden wo mit einer geringen Gletscherbedeckung zu rechnen ist.
- Die meisten (64%) der Ausbrüche (seit 1500 AD) der Vulkane mit Gletscherbedeckung südlich von 24° S starteten zwischen November und April und 50% zwischen November und Februar. Dies könnte am Einfluss von der saisonalen Schneebedeckung liegen, da keine Trends für tropische Vulkane festgestellt werden konnte.
- 29 der 74 gletscherbedeckten aktiven Vulkane in Lateinamerika werden derzeit nicht überwacht. Einige von diesen befinden sich in unmittelbarer Umgebung von Großstädten (z.B. Iztaccíhuatl in Mexico oder Illiniza in Ecuador). Für acht der untersuchten Vulkane konnten keine Gefahrenkarten gefunden werden.

Table of Content

Table of Figures

Tables

1 Introduction and Motivation

Glaciers are widely considered as a good climate indicators and often referred to as a "natural thermometer" for the Earth`s climate (Vaughan et al., 2013). They adjust to changes of the climatic forcing by changing their size. The sources of these changes can be temperature variations but also changes in precipitation, radiation or geothermal heat. The latter is particularly important for glaciers that are located on active volcanoes, as volcanic eruptions and the related heat release can enhance glacier melt.

Apart from being a climate indicator, glaciers are also an important hydrological reservoir on a regional scale and will be more important in the future for the water management in dry regions and increasing population. Furthermore, especially for glaciers on active volcanoes, sudden melting of ice or lake outbursts can cause hazards like lahars and GLOFs (Glacier lake outburst floods) and can expose the local population at risk (Lescinsky & Fink, 2000). Many volcanoes lie in proximity to highly populated regions that could be affected by these hazards. Lahars have caused many fatalities in the past, most recently at Pinatubo (1991) and Nevado del Ruiz (1985).

Volcanic eruptions on glacier-covered volcanoes and the related heat release can greatly influence the glacier mass balance of the glacier by strongly enhancing basal melt, ultimately leading to massive glacier shrinkage (e.g. eruption of Mount Hudson 1991). On the other hand, the presence of an ash cover might insulate the underlying ice and prevent surface melting. Thus, glacier changes need to be monitored regularly to understand the impact of the volcanic activity and climate change, and safe the population from volcanic hazards.

Additionally, studies have shown, that glacier changes on active volcanoes and the associated load variation can have an influence on volcanic activity and eruption rates. After the last deglaciation (12000BP-7000BP), eruption rates were globally two to six times higher than background levels and about 30 times larger in Iceland (Huybers & Langmuir, 2009; Maclennan et al., 2002; Jull & Mckenzie, 1996). However, it is not quite understood how today's much smaller climate variations along with the recent massive glacier shrinkage will influence the volcanic activity, eruptive cycle, explosivity and what the response time of volcanoes will be. This is mostly due to the lack of data about how glacier change affects the volcanic activity and eruption style (Tuffen, 2010). In Latin America, some studies of glacier-covered volcanoes have been made (Rivera & Bown, 2013; Huggel et al., 2007b) but no research on a continental scale that includes all glacier-covered volcanoes has been performed. By using a continental scale, the data pool is much larger and statistical analyses of glacier changes and volcanic activity over time get more significance.

By using satellite remote sensing, it is now possible to quantify glacier changes over a 30-year time period (1985-2015). With multispectral satellite images (Landsat 4/5, 7, 8 and Sentinel-2), glaciers can be mapped with the band ratio method which is based on the different spectral properties of snow and ice. Challenges and limitation of glacier mapping from space such as volcanic ash, cloud cover, shadows and seasonal snow need to be quantified and kept to a minimum. Comparing glacier area data with a volcanological database and knowledge about the climate and glacier history during the Holocene will lead the path to identify the connection between climate change, glacier variation, and volcanic activity.

1.1 Scientific questions

The main goal of this thesis is the analysis of multi-decadal glacier changes (1985-2015) on active volcanoes in Latin America and identification of possible links between their activity and observed glacier change. The following research questions will align with the main goal of the thesis:

1) How have glaciers on Latin American volcanoes changed over the past three decades?

2) Can the changes be derived robustly given the problems with seasonal snow in previous studies?

3) Is it possible to provide evidence of a possible difference between glacier changes on volcanoes that have experienced eruptions and volcanoes that have been quiet during the study period?

4) Is there any evidence of the level or changes in volcanic activity related to glacier change?

5) Can we identify ice-capped volcanoes with substantial hazard potential for downstream communities?

1.2 Approach and work flow

In order to solve the research questions and reach the main goal of this thesis, the work flow presented in Figure 1 is followed. The first step is to define the study region, and to determine, which comprises the glacier-covered volcanoes of Latin America are. To identify these volcanoes, online research about them as well as expert knowledge are used. With high resolution satellite images, as available in Google Earth, a pre-selection has been performed. Later, when analysing satellite images from Landsat and others, the selection is being finalised. In total, 74 volcanoes that have or until recently had some glacier cover could be found. For 59 of them, the glacier area is being calculated. Glacier areas are generated for three time steps (around 1985, 2000 and 2015). After the identification and calculation of all glacier-covered volcanoes, the work flow separates into two parts: the glacier part and the volcano part.

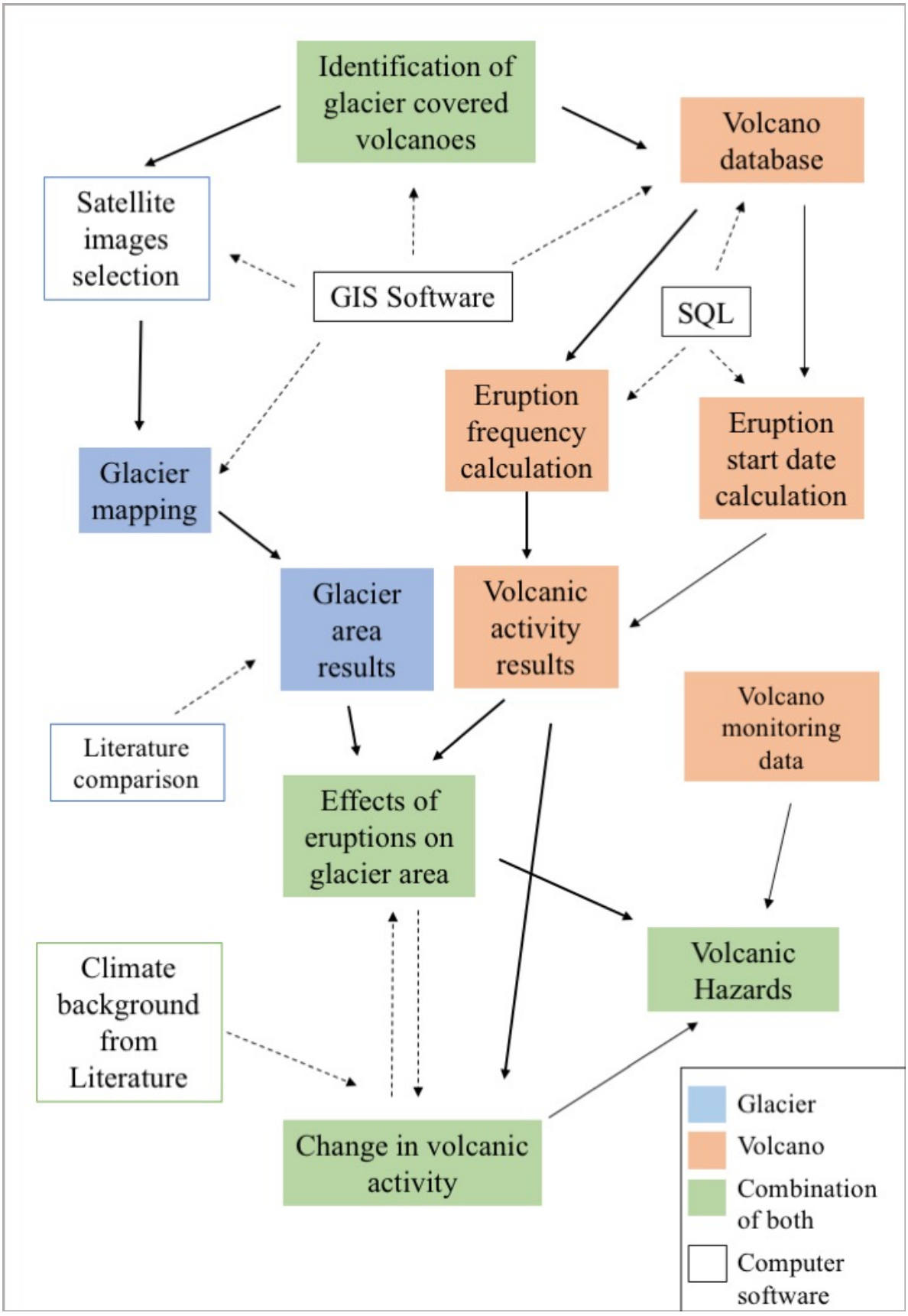

Figure 1: Schematic overview of the general work flow and steps to combine glacier data with volcano data. Colours according to the field of study. Solid lines mark the main workflow, dashed lines computer programs used and secondary work.

In order to calculate glacier outlines from space first, satellite images must be found and processed to map them and perform area calculations. The selection is done considering cloud cover and minimal seasonal snow. By using GIS software (ArcGis) the band ratio method is applied to create glacier outlines and calculate glacier areas. The results are being compared with each other and to data found in the literature.

For the volcanology part, a research study in Mexico was performed to work in cooperation with the UNAM (Universidad Nacional Autónoma de México), providing access to volcano data for all active volcanoes of Latin America. Using this data, the eruptive history can be analysed for both glacier-covered and non glacier-covered volcanoes. Database access is managed by using SQL queries within the pgAdmin 3 program. Eruptions frequencies over time for different magnitudes can be calculated as well as the geographic influence on the eruption start date. Additionally, the volcano monitoring database Glovoremid is used to get an up-to-date state of all monitoring installations for the valid volcanoes.

When combining glacier area results and volcanic activity data, the effects of volcanic eruptions on glacier area can be analysed. Further, the change of volcanic activity over time can be determined by comparing glacier change results and literature knowledge about the climate history with volcanic activity results.

The synthesis of all analysed datasets helps to identify glacier-covered volcanoes, which could be subject of volcanic hazards for the surrounding population.

1.3 Structure of the thesis

The above workflow is presented in the following sections: (1) Introduction, (2) Scientific background and Study area, (3) Data and methods, (4) Results, (5) Discussion, and (6) Conclusion.

In Chapter one, an introduction and motivation to the topic are given. Furthermore, the main objectives and research questions are listed. Finally, an overview of the approach and work flow is shown.

In chapter two, the scientific background about volcano-ice interactions, the effects of ash on glaciers and glacier-volcanic hazards are described. Additionally, the connection between glacier unloading due to climate change and the response of volcanic activity are being discussed. Also, the study area is being described in terms of its glaciological, climatological and geological context.

In Chapter four, first, the results of the glacier area calculations are listed and illustrated. Secondly, volcanic eruption time series on different time scales as well as results of the eruption start date are

being displayed. Finally, after combining glacier results and volcano data, the influence of volcanic eruptions on glacier area is shown.

In Chapter five, results are being discussed. Starting with the results of the glacier area calculations, challenges and uncertainties, also sources of errors are presented. Additionally, a comparison between elaborated results and literature data is made. Secondly, the influence of eruptions on glacier area is being discussed for a selection of volcanoes. Thirdly, the discussion continues with putting the glacier fluctuation in a broader context by explaining the connection between climate and volcanic activity during the Holocene and giving an outlook on possible future changes. In addition, some volcanoes with a high hazard potential or the lack of adequate monitoring are described. Finally, suggestions for improvements for future research are given.

In Chapter six a conclusion is made to wrap up the main results and to give an outlook for the future. The thesis ends with literature references as well as maps of selected glaciers and tables of the used satellite images can be found in the appendix.

2 Scientific background and study area

2.1 Volcano-ice interaction and the global climate

The interaction between glaciers and volcanoes is based on a two-way coupling of processes. (A) An increase in the volcanic activity and geothermal heat flux lead to a decrease of the glacier area and volume. Following the (B) pressure reduction due to the unloading of ice, volcanoes show an increase in eruption likelihood (Albino et al., 2010). This feedback cycle was very distinct during the last major deglaciation were according to Maclennan et al. (2002), the volcanic activity in Iceland increased by a factor of 30-50. For Iceland, models indicate, that the recent glacier retreat of Vatnajökull has an effect on the mantle melting rate by increasing it to about $0.014 km^3/y$ which is about 10% (Pagli & Sigmundsson, 2008). Because for Latin America, volcanological conditions are different since mantle melting is not very common and glaciers do not form large ice shields except in Patagonia, but rather form small ice caps, the Icelandic model cannot be assigned to the Latin American stratovolcanoes. For them, changes in crustal stress due to ice unloading that affect the pressure inside the magma chamber are more important than mantle melting (Jellinek et al., 2004).

Concerning the effects of climate fluctuation on volcanic eruptions, the connection is widely recognized (Capra, 2006; Maclennan et al., 2002; Huybers & Langmuir, 2009). Unloading of a large amount of ice reduces the magmatic pressure inside the magma chamber. As magma chambers are usually located close to the surface, they are sensitive to load changes from above. The pressure change also effects the lava composition. Pinel & Jaupart (2005) suggest, that in case of ice unloading either new magma can flow into the magma chamber from deeper sources or the magma gets denser and therefore regresses to a more primitive stage. Further, it is also possible that dykes will shut off due to the reduction of pressure. Depending on the size and depth of the magma chamber the eruption likelihood may increase or not. Albino et al. (2010) mentioned that shallow, spherical magma chambers filled with compressible magma show the biggest triggering effect.

Although the influence of load variation on magma chambers is well understood, some questions remain such as what the effects on the volcanic activity will be, what the response time of the volcano will be and how the increase in volcanic activity scales to the amount of load variation (Tuffen, 2010).

On a longer timescale, volcanism and climate variations show interactions and feedback effects. Volcanic eruptions influence the global CO_2 cycle in two ways. More volcanic CO_2 in the atmosphere can contribute to global warming. The ejected aerosols of an eruption on the other hand, show a cooling effect like after the Pinatubo eruption in 1991. Huybers & Langmuir (2009) suggest that tropical eruptions initially show more of a cooling effect because the aerosols block the sun. While high latitude volcanoes – which are important for deglaciation processes as they contain more ice volume – seem to

have a warming effect. In addition, glacial variability may pace the timing of low-frequency eruptions so as to coincide with deglaciations. They further say that anomalies in volcanic activity cause an imbalanced carbon budget. With two to six times larger volcanic emission rate during the last deglaciation, the CO_2 concentration was raised by 20-80ppm. Thus, the rise in CO_2 can be understood as feedback induced by the deglaciation itself through the volcanic activity.

The main question that remains is, whether tectonic changes initiated the increase of volcanic activity which then started a positive feedback or if the rate of volcanism is led by the climate (Tuffen & Betts, 2010). This question can be seen as a "chicken and egg" question and is at this point difficult to answer. Many other factors influence the feedback processes and the global climate (e.g. sea level changes or reactions of the biosphere).

2.2 Effects of ash layers on the glacier mass balance

Volcano-ice interaction can be seen on a global scale with the feedback effects and CO_2 cycle, but also on a local scale. Volcanic activity can greatly influence the extent and shape of the local glacier. One volcanic process that influences the glacier extent is the presence of an ash layer on top of the ice. It could originate from an eruption of the same volcano or a nearby active volcano. Similarly, bigger volcanic edifices can be found closer to the volcanic crater and finer material further away.

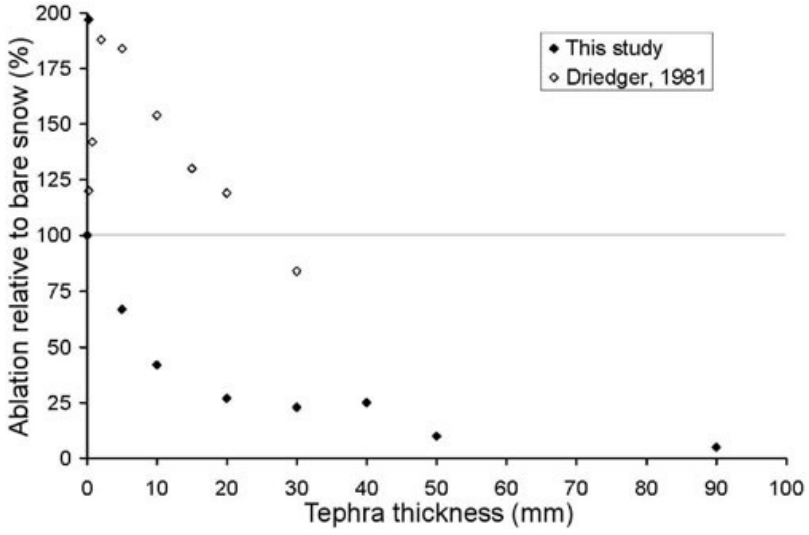

Figure 2: Relation between tephra thickness and ablation relative to a tephra-free surface. Data from two different studies are being compared (Brock et al., 2007).

The presence of an ash or tephra layer has an insulation effect if the layer is thick enough. The critical thickness was given as around 5 mm for ash tephra (Brock et al., 2007). Lapilli, because of its porosity and therefore a large volume of air has a higher insulating effect than ash and therefore, has an even more positive impact on the mass balance. In Figure 2, the relation between the tephra thickness and the ablation compared with bare snow can be seen. A thin layer on the other hand, especially fine particles coming for example from fumarolic activity, darkens the snow and therefore amplifies the snowmelt by reducing the surface albedo (Brock et al., 2007). Figure 3 shows the dark coloured ice of Cayambe glacier.

Figure 3: Satellite image of Cayambe glacier. Note the ash covered dark ice (source: Google maps).

2.3 Glacier-volcanic hazards

The volcano ice-interaction can cause serious hazards effecting the surrounding population. For instance, the eruption and the following lahar of Nevado del Ruiz in Colombia caused more than 25.000 deaths in 1985. The source of the hazard can be of eruptive or non-eruptive origin. During an eruption, melting of ice can be caused by: (1) a pyroclastic flow, (2) a lava flow, (3) basal melting due to a sub glacier eruption, (4) the ejection of water from the crater lake or (5) by tephra deposition (Delgado Granados et al., 2015a). The consequence of these melting processes are often lahars like the one cited above. Lahars are volcanic debris flows, consisted of melt water and volcanic deposits such as ash and

other tephra deposits. They can also occur without an eruption as ice-rock and debris avalanches, which may include tephra deposits. Also, exterior factors like heavy rain events may trigger a lahar (Huggel et al., 2007b). A scheme of the possibilities of the lahar generation can be seen in Figure 4.

Moreover, glacier volcanic hazards can also be caused by an increase of geothermal heat flow. A lateral sill intrusion will lead to a continuous melting of the surrounding ice while a dyke intrusion will originate a rapid melting around the surface area. Both can form a sub-glacial lake which could eventually break out (Delgado Granados et al., 2015a). Grímsvötn in Iceland is a good example of were the lake bursts out once the threshold level is reached. In Iceland, these types of outburst floods are also known as Jökulhlaups. On steep stratovolcanoes, jökulhlaups can transform into lahars if they come in contact with tephra and debris.

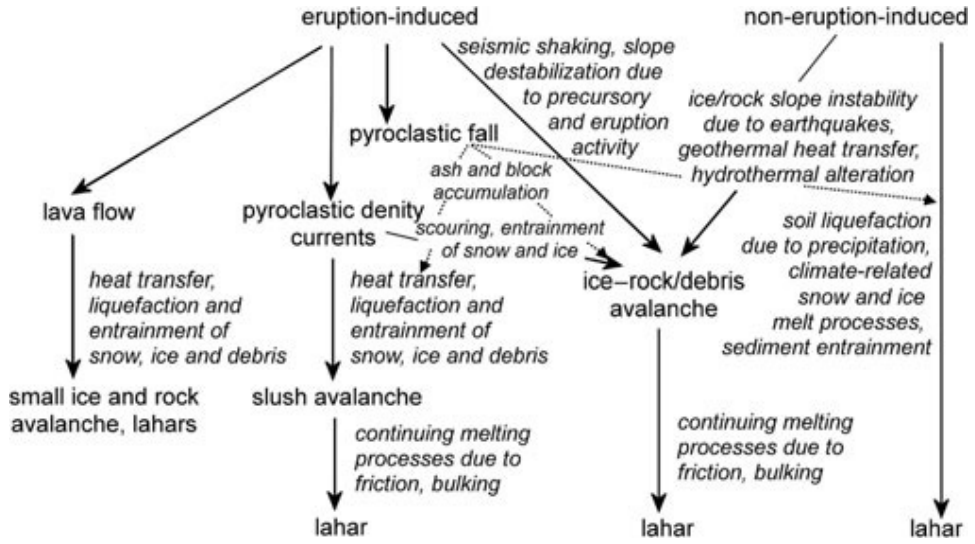

Figure 4: Scheme of possibilities to generate lahars. Dotted lines do not indicate triggering, but facilitation of mass movements (Huggel et al., 2007b).

A further hazard that can be found on glacier-covered volcanoes is the possibility of volcanic collapses. Capra (2006) mentioned that during the late Pleistocene and Holocene, several volcanic collapses occurred, triggered by climate change and glacier retreat. The most recent volcanic collapse occurred on Mount Saint Helens in 1980. Several factors contribute to the instability of a volcano: It is possible that prior to a collapse, the volcano was already unstable, which got enhanced by magmatic intrusions into the volcanic edifice, the accumulation of pyroclastic deposits, a sub-volcanic spreading and a weakening due to hydrothermal alteration. These factors can contribute to the instability but mostly do not act as triggers. An earthquake or a heavy rain storm can further weaken the volcanic structure and

trigger a collapse (McGuire et al., 1996). During deglaciation, unloading of ice and melt water circulation may further have caused rock weakening and loss of cohesion (Capra, 2006).

Even though the current glacier retreat and pressure change is generally small, McGuire (2013) claims that it may be sufficient to trigger a geospheric response. Such events can represent a big hazard to the surrounding population and need to be carefully monitored. Rising temperature can not only decrease the glacier extent, but also weaken the ice masses itself. Geothermal heat and the presence of fumaroles may further contribute to the ice instability. According to Huggel (2009), this can lead to large ice avalanches and potential lateral collapses. To prevent it, long term monitoring, as well as early warning and event reconstruction are essential (Huggel et al., 2007a).

2.4 Study area - Geographical and geological overview

The study area is defined as the glacier-covered active volcanoes in Latin America. This includes volcanoes in Mexico, Colombia, Ecuador, Peru, Bolivia, Argentina, and Chile. All volcanoes are located along the Latin American part of the Cordillera, more specific the South American Andes and the trans Mexican volcanic belt (MVB).

The Andes are the longest transcontinental mountain range in the world, stretching from the Scotia sea to the Caribbean Sea (Diaz & Graham, 1996; Bradley et al., 2009; Seidel & Free, 2003). The length of the mountain range is about 10000km and the width varies from 200 to 700km. Many mountains exceed the altitude of 6000m, making it the world highest mountain range outside Asia. Also, the world's highest active volcano (Ojos del Salado) lies within the Andes. The MVB is part of the North American Cordillera. North America's highest volcano, Pico de Orizaba, is located on the southern end of the Mexican volcanic chain (Gaffen et al., 2000; Diaz & Graham, 1996).

2.4.1 Plate tectonics and Volcanism

The American Cordillera stretch along the Pacific Ring of Fire, a volcanic belt that runs along the borders of the Pacific Ocean. The eastern side of the ring of fire is characterized by the subduction of oceanic crust underneath the continental crust of the Americas. The American Cordillera were formed due to the collision and subduction of former Farallon plate and the North and South American plate. Now the relicts of the Farallon plate, the Juan de Fuca, Rivera, Cocos and Nazca plates still push towards the continent. Additionally, the Antarctic plate gets subducted underneath the South American plate at the southern end of South America (see Figure 5).

South American plate tectonics and volcanism

In South America, the subduction of the Nazca and Antarctic plate is responsible for the volcanism. The convergence rate of the Nazca and the South American plate is about 7-9 cm/y, whereas the convergence rate with the Antarctic plate is only about 2 cm/y (Seidel & Free, 2003).

Within the Andes there are also two subplates that are part of the mountain formation process: The North Andean plate in the north and the Altiplano plate in the centre (see Figure 5). Both plates show different movements or have different genesis compared to the South American plate and can, therefore, be considered as independent subplates (Freymueller et al., 1993; Allmendinger et al., 1997). The subducted slab shows different inclinations along the subduction zone, ranging from shallow dipping (<10°) to more steep zones (≈30°) (details in following paragraphs) (Sold et al., 2016).

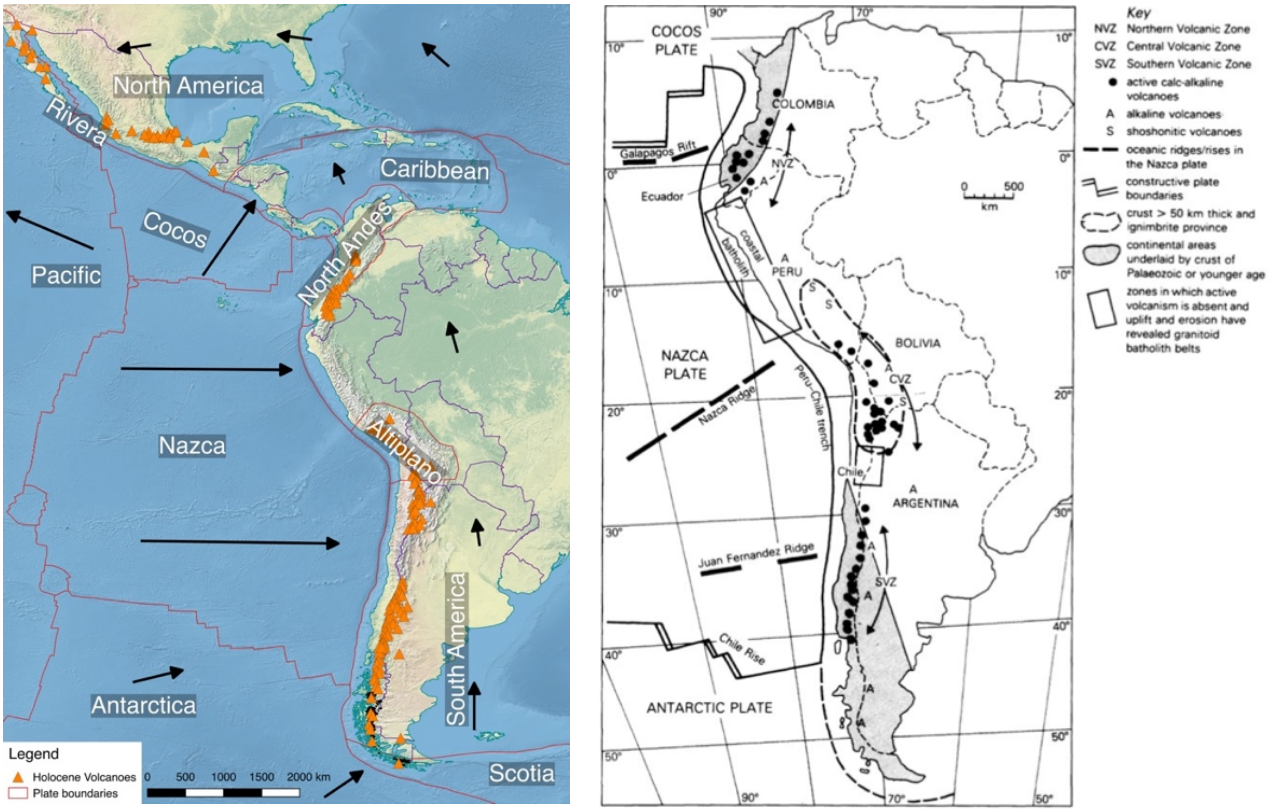

Figure 5: Tectonic setting and volcano distribution of South and Central America (left, own image, right after Wilson 1989).

The volcanoes of South America are located along the Andean Volcanic Belt. In total, there are 60 historically active volcanoes and another 118 with Holocene activity. In total, this gives 178 active volcanoes of the 1511 volcanoes worldwide (Simkin and Siebert, 1994). The Andean volcanic belt can

be subdivided into four main volcanic zones: The Northern Volcanic zone (NVZ), the Central Volcanic Zone (CVZ), the Southern Volcanic Zone (SVZ) and the Austral Volcanic Zone (AVZ). Each of them can be further subdivided into segments according to their petrologic, geologic and tectonic characteristics (Seidel & Free 2003). Tectonic and volcanic characteristic of the volcanic zones of the Andes can be seen in Table 1.

The **NVZ** (12°N-5° S) includes volcanoes of Colombia and Ecuador (see Figure 6). There are 36 volcanoes with Holocene activity. They are located in the Cordillera Real (Ecuador) or Central (Colombia) as well as the Cordillera Occidental and the intermountain valley that lies between the two mountain chains (Gaffen et al., 2000). Lavas of the NVZ are mostly basaltic/andesitic and andesitic which show similarities in the mineralogy and major element characteristics of island arch volcanism (Gaffen et al., 2000). The crust shows mafic oceanic characteristics and pervasive strike-slip deformation. The age of the crust is younger than in the central and southern Andeans, having its origin in the Late Cretaceous and Cenozoic Era. The thickness of the crust ranges from 40 to 60 km (Govett, 2017). Below the NVZ the subducted slab shows an angle of about 25-30° and a convergence rate of 7 cm/y (Gutscher et al. 1999).

Between the NVZ and the CVZ, there is a volcanic gap, called the Peruvian gap (5°-14°S). This is because of shallow dipping of the slab due to the presence of the buoyant aseismic Nazca ridge. The northern end of the flat segment corresponds to the boundary between the Northern Central Andes and the Northern Andes. Indices of the boundary are the Dolores-Guayaqil megashear in Ecuador and the Huancabamba deflection in Peru. The southern end of the flat segment is characterized by an abrupt bend in the Nazca plate at the northern end of the Peruvian Altiplano (Gutscher et al. 1999).

The **CVZ** (14°-27° S) holds 69 volcanoes and stretches from Peru over Bolivia to the northern part of Chile and Argentina (15-33°S) (see Figure 6). Volcanoes are restricted to the western Cordillera Occidental, about 240-300km from the trench and do not appear in the Cordillera Oriental (Stern, 2004). The lava is intermediate to acidic in their composition (andesite, dacite, rhyolite ignimbrite). This petrologic composition might be explained by the presence of a Precambrian basement, underneath the CVZ whereas the crust of the other zones, especially in the NVZ is much younger (Mesozoic Cenozoic) (Wilson 1989; Stern 2004). The presence of the Precambrian basement as well as crustal shortening and magmatic underplating also explains the very large thickness (>70km) of the crust (Stern, 2004). The convergence rate is about 7-9 cm/y and the dip of the sub ducted slab is around 25°. The slab reaches a total depth of more than 400 km, where is breaks off (Dorbath et al. 1996).

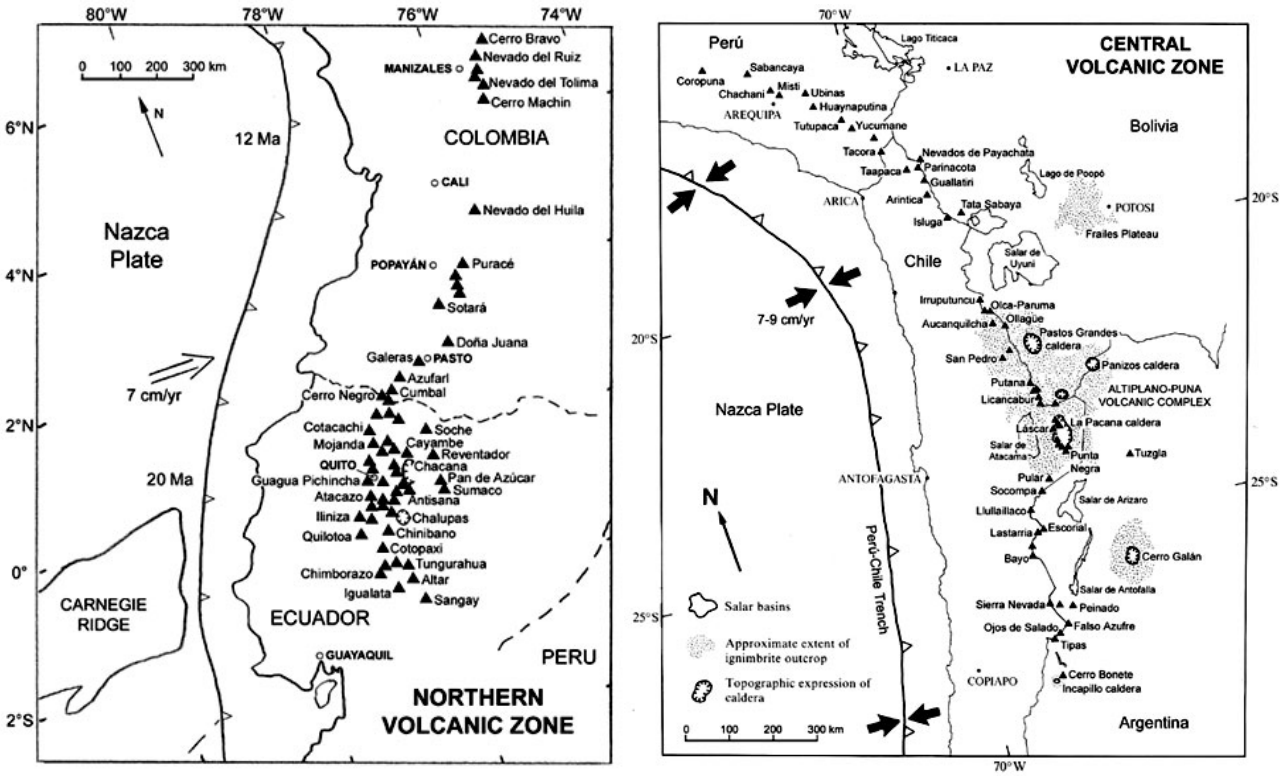

Figure 6: Overview and volcano distribution of the NVZ (left) and CVZ (right) (Stern 2004).

South of the CVZ there is a second volcanic gap called the Pampean flat slab segment (27°-33°S). It is driven by the subduction of the Juan Fernandez Ridge at a shallow angle underneath the South American plate (Wilson, 1989). The northern end of the volcanic gap is a seismic discontinuity at about 27°S following a gradual decrease of the subduction angle to the south (González-Ferrán et al. 1985; Cahill and Isack 1992). In the south, the boundary of the flat slab segment is a sharp bend at the locus of the Juan Fernandez ridge (Cahill and Isack 1992).

The **SVZ** (33°-46° S) includes 69 volcanoes with Holocene activity stretching from the Juan Fernandez Ridge in the north until the Chile Rise in the south (see Figure 7). The major rock types are high alumina basalt and basaltic andesite. The convergence rate is about 7-9 cm/y and the subduction angle of the slab varies from 20° in the north to >25° further south. The crustal thickness decreases from >50 km at the northern end to 30-35 km in the south. The basement of the crust shows Paleozoic and early Mesozoic ages (Stern, 2004). An important tectonic feature of the SVZ is the Liquiñe-Ofqui fault zone which controls the location of the large stratovolcanoes (Cembrano et al. 1996).

In the northern segment, many volcanoes are located on the continental divide forming a narrow chain of volcanoes approximately 290 km east of the trench. Further south the so-called transitional SVZ is characterized by a >200 km wide volcanic belt approximately 270-280 km east of the trench. The central segment is a broad arc (120 km width) of volcanoes with an intra-arc basin (Stern, 2004). South of the

Valdivia Fracture Zone (39°S) the arc is only 80km wide and the intra-arc basin disappears. This is due to the younger oceanic lithosphere that is being subducted (Herron 1981). The southern segment of the SVZ consists of 13 volcanic centers, all located in Chile, west of the continental divide about 270 km east of the trench.

The Patagonian volcanic gap (46°-49°S) is located at the Chile Rise/Trench triple junction and is caused by the subduction of the Chile Rise underneath the South American plate during the last 8 million years. Due to the subduction of the ridge, no Beinoff zone of seismicity occurs below the gap. The subduction of the Chile Rise also resulted in the formation of basaltic back arc volcanism as part of the Patagonian plateau (Stern, 2004).

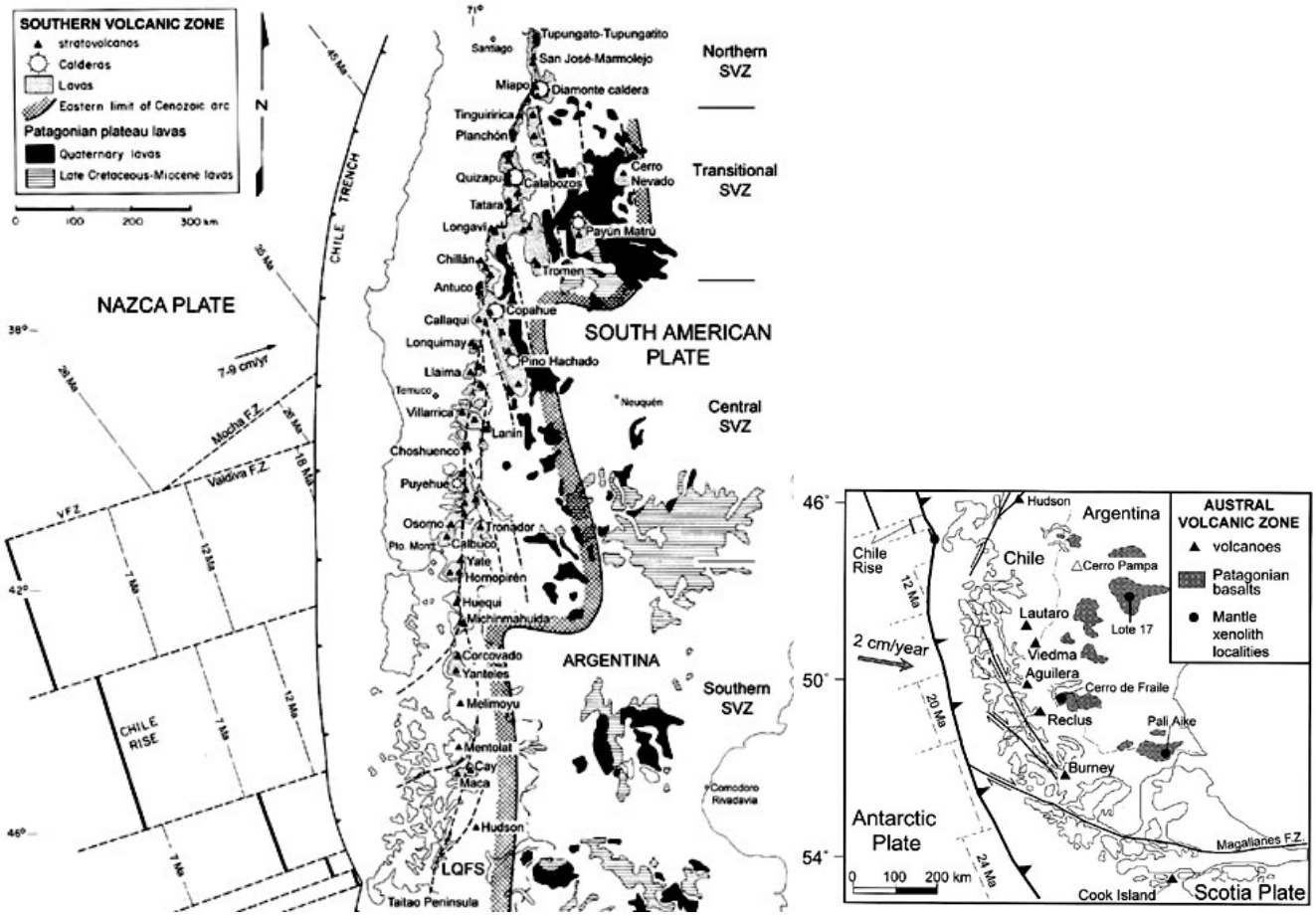

Figure 7: Overview and volcano distribution of the SVZ (left) and AVZ (right) (Stern, 2004).

The **AVZ** (49°-55°S) is the southernmost volcanic zone of the Andes (see Figure 7). Sometimes it is considered as one with the SVZ (Wilson, 1989) but there is a key difference, the Antarctic plate gets subducted underneath the South American plate and not the Nazca plate with a speed of only about

2 cm/y (Stern, 2004). The crust below the AVZ has a thickness of less than 35 km. Most volcanoes are located underneath the Northern and Southern Patagonian ice shield and until this moment, no pre Holocene eruption is known (Stern, 2004). This may also be related to the remoteness of the area and the glacier cover. The major rock types are adakitic hornblende, andesite and dacite (Stern and Killian 1996). A specialty of this zone is, that neither basalt nor basaltic andesite nor rhyolite are present.

Table 1: Tectonic and volcanic characteristic of the volcanic zones of the Andes (Wilson, 1989).

	SVZ (45–33°S)	CVZ (26–18°S)	NVZ (2°S–5°N)
dip of seismic zone	<25°	*c.* 25–30°	*c.* 20–30°
depth to seismic zone	*c.* 90 km	*c.* 140 km	*c.* 140 km
maximum crustal elevation	2000–4000 m	5000–7000 m	4000–6000 m
crustal thickness	30–35 km	50–70 km	40 km
crustal age	Mesozoic–Cenozoic	Precambrian–Palaeozoic	Cretaceous–Cenozoic
composition of volcanics	basalt with minor andesite and dacite	andesite–dacite with dacite–rhyolite ignimbrites	basaltic andesite to andesite
SiO_2 (wt.%)	50–69	56–66	53–63
K_2O (wt.%)	0.4–2.8	1.4–5.4	1.4–2.2
	medium-K series	high-K series	medium-K series
$\delta^{18}O$	5.2–6.8	6.8–14.0	6.3–7.7
$^{87}Sr/^{86}Sr$	0.7037–0.7044	0.7054–0.7149	0.7036–0.7046
$^{206}Pb/^{204}Pb$	18.48–18.59	17.38–19.01	18.72–18.99
$^{207}Pb/^{204}Pb$	15.58–15.62	15.53–15.68	15.59–15.68
$^{208}Pb/^{204}Pb$	38.32–38.51	38.47–39.14	38.46–38.91

Mexican plate tectonics and volcanism

The trans Mexican volcanic belt (**MVB**) in Mexico is a 1000 km long Neogene continental arch with an east west direction along the margin of the North American plate (Ferrari et al., 2012). The origin of the volcanism is the subduction of the Cocos and Rivera plate underneath the North American plate along the Meso-American trench. There are also other interpretations of the MVB, like the involvement of rift processes (Márquez et al. 1999) or the presence of a hot spot (Verma 2002). The fact that the MVB does not have a constant distance to the Mesoamerican trench and only the western part the volcanic arc is parallel to the trench indicates, that other processes rather than only the subduction might be evolved in the volcanism. The MVB can be divided into three sectors: The western-, central-, and eastern sector (Ferrari, 2000). Convergence rates vary from 2 cm/y on the northern end and gradually increases to around 6 cm/y on the southern end of the MVB (Pardo & Sufirez, 1995).

The glacier-covered volcanoes of Mexico all lay in the eastern (oriental) sector. It is characterized by large stratovolcanoes, calderas and andesitic and rhyolite dome complexes (Ferrari, 2000). Major rock types of the glacier-covered volcanoes are andesite and basaltic andesite as well as dacite (Global Volcanism Program 2013c). Underneath the volcanoes, old Precambrian to Paleozoic crust with a thickness of 50-55 km can be found (Ferrari et al., 2012). The subducted slab of the eastern sector as

part of the Cocos Plate shows a 15° dip in the first 80 km from the coast, followed by a flat segment until about 200 km inland (Kim et al., 2010). Beneath the volcanic front, the inclination of the slab increases greatly to about 75° until it breaks off in a depth of 500 km at a distance of 400 km from the trench (Husker & Davis, 2009). This flat slab segment might explain the non-parallel chain of volcanoes towards the trench. Figure 8 shows the location of the Mexican volcanoes along with the depth of the underlying slab (isolines).

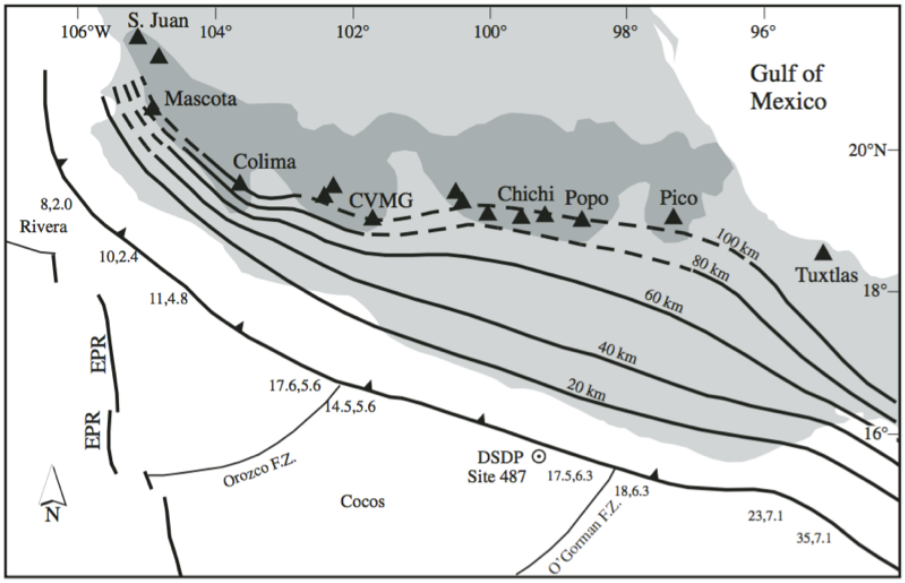

Figure 8: Generalized tectonic map of the Mexican subduction system and the Trans-Mexican Volcanic Belt (dark grey field). Isolines show the depth of the subducted slab. The first number along the plate boundary indicates the age of the oceanic slab, thesecond number shows the convergence rate (from Gómez-Tuena et al., (2007)).

2.5 Climatological background and glacier distribution

The climate of the Andes and Mexico varies largely due to its long north-south extension. The key requirements for the presence of glaciers are a temperature below 0°C and sufficient solid precipitation. Due to the high temperatures in the tropic, glaciers can only be found on the highest peaks. In the southern Andes, the climate favors the formation of large glaciers and ice fields. The intersection of the ELA (equilibrium line altitude) often also called snow line (lower limit of permanent snowcover) with the terrain determines the altitude at which glacier accumulation and ablation are equal (Benn & Evens, 2010; ALPECOLe, 2011) In the tropics, glacier can only be found at an altitude over 4700m altitude (Cáceres, 2010). Towards the south and north, the snow line first increases in Bolivia and Mexico due to the dry conditions, then gradually decreases to just 1000m in in Patagonia (Benn & Evens, 2010;

Aniya et al., 1996). The next section will firstly describe the glacier distribution and climatic context of the tropics and subtropics, and secondly the dry and wet Andes will be looked at in more detail.

2.5.1 Tropical and subtropical glaciers

In **Mexico**, glaciers can only be found on the three highest peaks, the dormant volcanoes of Pico de Orizaba (5610m) and Iztaccíhuatl (5239m) and the recently very active Popocatepetl (5426m). The largest glacier is situated on Pico de Orizaba. There, snowfall can occur throughout the year although winters are generally dry. Snow that falls on the south and southeastern side always melts rapidly due to the intense solar radiation and glaciers occur mostly on the northern side (White, 2002). The second largest ice mass can be found on Iztaccíhuatl near Mexico City. Here, most of the solid precipitation occurs in the dry period between March and May (Delgado Granados et al., 2015b). Due to the often cloudy days during summer and the presence of fresh snow, melting is generally low during this season (White, 2002). Currently there are two major glacier systems left on Iztaccíhuatl: El Pecho (the chest) and la Pancha (the belly) (Schneider et al., 2008). Glaciers on the nearby Popocatepetl volcano (5426m) suffered continuous thinning and recede since the beginning of the last eruptive period in 1994 (Andrés et al., 2007). Because of ongoing volcanic activity and climate change, the glacier on Popocatepetl became extinct in late 2000 (Delgado Granados et al., 2007).

In **Colombia**, glaciers are located on the highest peaks of the Cordillera Central and Cordillera Oriental above an altitude of 4700m. The temperature does not vary significantly throughout the year with the mean monthly temperature not varying more than ±2 °C. The 0° isotherm is at about 4800m which roughly also corresponds to the ELA (Hoyos-Patiño, 1998). Differences in the snow line are caused by variation in moisture and precipitation. Short term variations of the snow line are caused by changes in precipitation while long term changes are driven by temperature changes (Hoyos-Patiño, 1998).

In **Ecuador**, the glaciers are located very close to the equator and are therefore a good example for tropical glacier cover. Glaciers occur on the highest peaks, mostly as ice caps at the summit of volcanoes. The monthly mean temperature does not vary significantly throughout the year. Two different sources of moisture can be found in Ecuador. While in the Western Cordillera, the precipitation comes from the Pacific Ocean, the wettest months are March and April, the Eastern Cordillera gets its precipitation from the Amazon basin, and is evenly distributed throughout the year. The average snow line is about 4800-4900m, but it can vary, depending on precipitation characteristics and slope orientation. Snow can fall throughout the year but the months of December-February and July to September generally show maximum glacier exposure and minimal snow cover (Jordan & Hastenrath, 1998).

Peru currently holds the world's largest area of ice in the tropics. The ELA in Peru is at an altitude of around 5900m (value corresponds for Ampato volcanic complex) (Alcalá et al., 2010). Precipitation generally comes from the Amazon and Paraná basin. Therefore, a precipitation gradient from east to west can be found. Precipitation amounts on the mountains vary between 1200-2500mm/y, which results in a snow accumulation of 2 to 3 m at an altitude of 4800-5100 m (Morales-Arnao, 1998).

Generally speaking, tropical Andean glaciers have some unique characteristics. The primary controller of the radiation budget is the albedo as the sun intensity is constant throughout the year. Through the albedo, the ablation is also linked with the accumulation. The occurrence of solid precipitation controls changes in the energy fluxes through the change of albedo. On an inter annual and decadal time scale, the sea surface temperature is the main controller of the mass balance (Rabatel et al., 2013). Furthermore, global climate change affects glacier mass balance on a decadal scale. In the Andean region, the SST is influenced by the El Niño Southern Oscillation phenomena (ENSO). Generally, La Niña events are characterized by low temperatures and high amounts of snowfall. These have a positive impact on the mass balance. On the other hand, cloud cover is generally reduced during El Niño events which impact the incoming short wave radiation. Therefore, the annual mass balance is more likely to be negative during El Niño years and positive during la Niña years (Francou et al., 2004).

2.5.2 Glaciers in the dry Andes

Due to climatic differences, the Southern Andes are divided into two parts: The dry and wet Andes. An overview of the glacier distribution of the dry and wet Andes can be seen in Figure 9. The dry Andes are located between 17.5°S and 35°S and are partly in Bolivia, Chile and Argentina. In the very dry northern part (until 28°S), glaciers occur as small ice patches on the highest peaks, of which some are higher than 6000 m. As fresh snow gets often blown away, glaciers may only be found on the leeward side of a mountain (Lliboutry, 1998). The snowline altitude in this region is amongst the highest in the world due to the lack of precipitation. A constant high-pressure system prevents any moist air from coming into the continent. Nevertheless, snowfall occurs through local convection systems and occasional moist inflow from the Amazon basin.

Generally, north of 25°S, September is the month with the least amount of snow cover. Because of the high variability in precipitation, the snow line is not always clearly visible. In dry years, only a few snow patches may remain on a glacier after the melt season and in wet years, the whole glacier may be covered with snow (Lliboutry, 1998). Also, common for the dry Andes is the formation of penitentes, irregular blades of ice resulting from different evaporation-sublimation rates. For the formation of penitentes, low relative humidity, high short wave radiation and a high solar angle are required (Benn & Evens, 2010).

Further south (31°-35°S) the precipitation is higher and real glaciers can be found. Because the moisture comes from the Pacific Ocean, an increase of the ELA towards the east of about 1500m can be found (Lliboutry, 1998). Glaciers are comparably large, considering the moderate latitude and glacier tongues are often debris covered. This makes is difficult, to create glacier outlines using satellite images, as the ice is often hidden underneath a layer of debris. Further, surging glaciers have been identified in this region. An example is Glaciar del Nevado which advanced 2 km from 16.02. to 26.08.1984.

Figure 9: Chile and Argentina showing the occurrence of glaciers in the Dry Andes (Desert Andes and Central Andes) and in the Wet Andes (Lakes Region and Patagonian Andes) (Lliboutry, 1998).

2.5.3 Glaciers in the wet Andes

The wet Andes, south of 35°S receive in comparison to the dry Andes more precipitation. Between 35°S and 45°S, 37 volcanoes are covered with a total of 300 km^2 of ice. Further south, in the Patagonian Andes, glaciers are larger and two major ice fields can be found. The Southern Patagonian ice field being the largest with around 13.200 km^2 (Davies & Glasser, 2012).

From the northern high-pressure system, a steep north-south atmospheric pressure gradient can be found. South of 45° constant westerly winds bring moist air from the ocean and result in heavy precipitation and snowfall over the southern part of the Andes. From October to April the high pressure system can fluctuate to higher latitudes and bring cloudless weather to the Patagonian region (Lliboutry, 1998). Additionally, a constant temperature gradient from north to south is present. While the average annual temperature at sea level at 37° S is 13.7 °C it drops to 6.5 °C at 53° S. Precipitation rates are increasing southwards. At 35° S, the precipitation rate is in the Andes about 1500mm/yr water

equivalent; at 39° S, it increases to almost 5000 mm/yr. The northern and southern Patagonian Ice Field receive about 6000-7500 mm. In the Patagonian region, precipitation decreases sharply from west to east. Most of the precipitation falls on the west side of the Patagonian ice field and only 200-300 mm reaches the Patagonian pampa to the east (Lliboutry, 1998). Figure 10 shows the southern Andes as a cross section from 30°S to 48°S. Note the gradual decrease of the snow line towards the south.

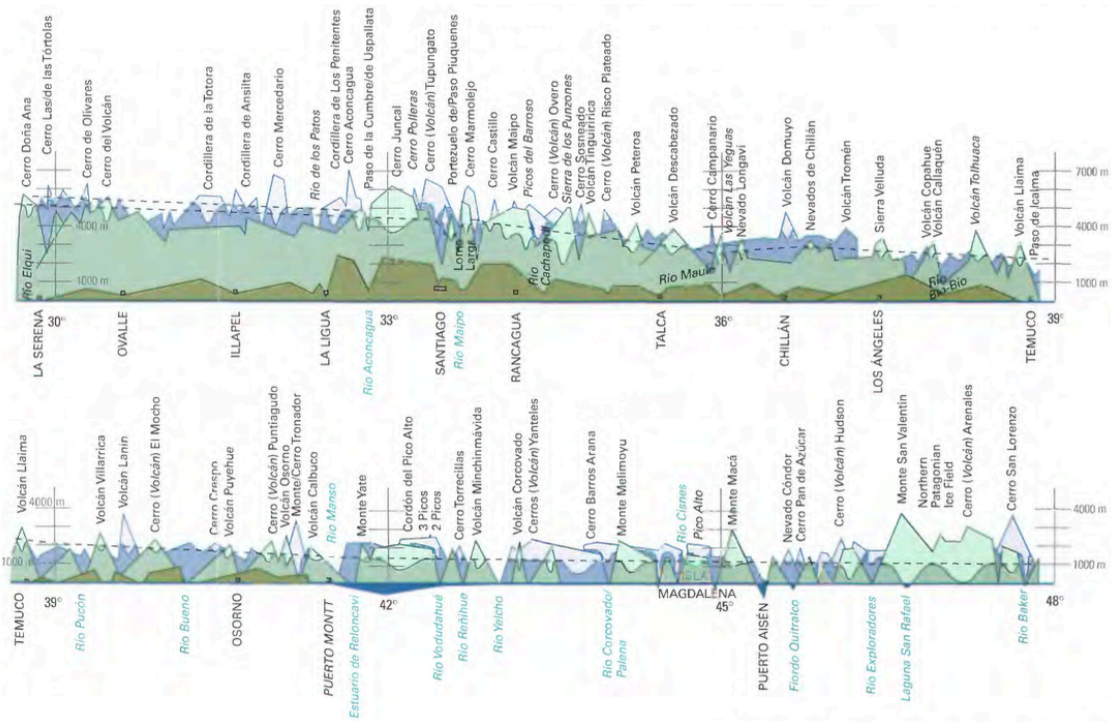

Figure 10: Southern Andes seen from the west. The green-tinted low area is the Coast. The dashed line represents the snow line. Mountain summits above the snow line are shown in a lighter tint (modified from Lliboutry, 1956).

2.6 Glacier retreat and climatic trends

Glacier changes can be seen as a natural thermometer as they adjust their extent according to climate changes (Vaughan et al., 2013). Glaciers in the tropical Andes reached their maximum LIA extent in the late 17th and early 18th century and are retreating since then at an increased rate since the 1970s (Rabatel et al., 2013). In the southern Andes, glaciers reached their LIA maximum in the late 17th and early 19th century and are retreating since then with some minor advances in the 1980s but an increased retreat rate in recent times (Masiokas et al., 2009). Figure 11 shows a selection of glaciers on active volcanoes with their relative change in glacier area since the LIA. The data comes from several literature sources.

Glacier area values from the LIA could only be found for a few volcanoes. Since 1850 until the early 2000s, the selected glaciers (listed in Figure 11) lost between 11% and 90% of their area. Southern glaciers like the Patagonian ice fields and Mount Hudson lost the least amount of area but large amounts of mass, whereas tropical glaciers show a much higher area loss rate without contributing noticeably to sea level rise (Rignot et al., 2003).

The problem is, that area data for LIA extents are rare and mostly front variations of glacier tongues are reported. LIA glacier advances and front variation changes have been recorded for many glaciers. The period of the maximum LIA extent varies from region to region depending on the local climate and ENSO impact. In Ecuador, the maximum LIA extent was dated to around 1730, in Peru 1630, in Bolivia the second half of the 17th century, in Chile, data varies suggesting a maximum extent between 1550 in dry Andes until the mid 1800s in the southern Andes (Vuille et al., 2008; Masiokas et al., 2009; Garibotti & Villalba, 2009; Winchester & Harrison, 1996). In Mexico, the LIA advance phase ended in the mid 19th century (Cortés Ramos & Delgado Granados, 2012). Since their maximum extent, glaciers have been retreating continuously in all regions with some minor advances in between. An overview about the dates of the LIA maximum and temperature as well as precipitations trends are listed in Table 2.

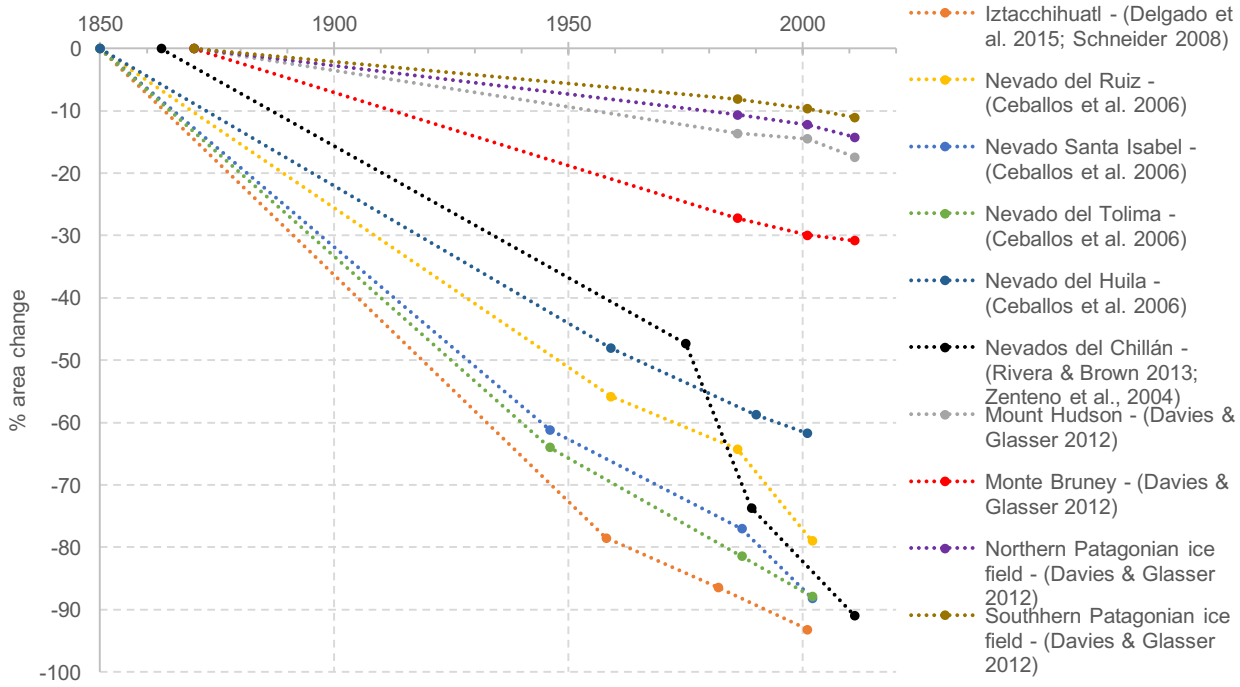

Figure 11: Area loss of selected glaciers on active volcanoes since the LIA. Dashed lines mark tropical glaciers, solid lines mark extratropical glaciers.

Considering only glacier changes during the last decades, more literature data is available. According to the literature, most glaciers show an area loss rate of around 1%/y. Thereby, tropical glaciers generally experience a larger area decrease than extra tropical glaciers. As an exception, Nevados de Chillàn, an active volcano in Southern Chile has lost 83% of its size between 1975 and 2011 (-2.3%/y) (Rivera & Bown, 2013). A comparison between literature data and the results are made in the discussion part.

2.6.1 Climate change in the Southern Andes

Climate data has shown that high altitude stations in the Andes experienced a warming trend in the last decades. Low elevation stations along the coast of Chile show in contrast to higher elevations a slight cooling trend in the last decades. The atmosphere sounding data of Puerto Montt, for example shows a cooling trend of -0.1 °C/decade from the surface to an altitude of 10 km (Falvey & Garreaud, 2009). In central (Quintero) and northern Chile (Antofagasta), this cooling trend can only be seen near the surface and changes to a warming trend at an altitude of 500 m and 1000 m respectively (see Figure 12). In southernmost South America, no cooling trend but a slight warming trend is being observed, even at low elevation stations (Rosenblüth et al., 1997).

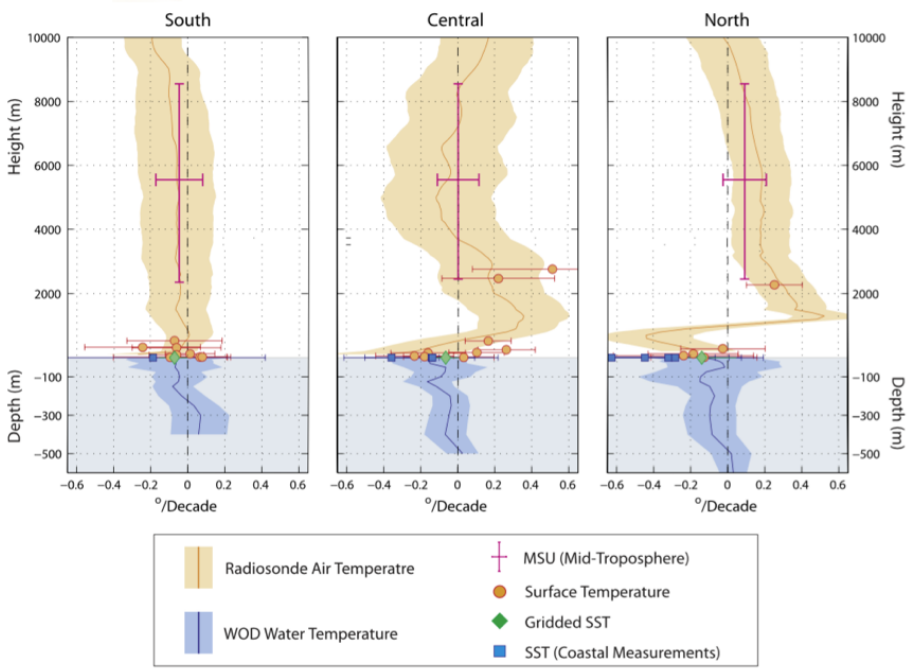

Figure 12: Vertical profile and Temperature trend in (a) southern, (b) central and (c) northern Chile (Falvey & Garreaud 2009).

Furthermore, precipitation decreased in southern Chile in the last decades. The precipitation reduction is highest at 39° S with a decrease of 450 mm in the last 70 years (Bown & Rivera, 2007). According to Giese et al. (2002), this precipitation reduction is related to more frequent negative ENSO events since 1976. The decrease of precipitation in combination with the high sensitivity of glaciers in maritime climates and a warming in higher elevation might explain the ongoing fast glacier shrinkage in the Southern Andes in the last decades to some extent (Paul & Mölg, 2014). Rivera et al. (2006) suggested that the ELA has been raised by 100 m between 1976 and 2004/2005 in southern Chile. Looking at the future climate evolution, Rivera et al. (2017) project a temperature increase until 2100 in comparison to the period 1986-2005 of 1.2 °C - 5.3 °C for northern Chile and 0.8 °C - 3.4 °C for central Chile. Precipitation will decrease between 30° S and 43° S by 5-10%.

2.6.2 Climate change in the tropical Andes and Mexico

In the tropical Andes, temperatures have been rising by 0.1 °C/decade in the last 70 years. The observed reduction in glacier area is thus considered to be directly connected to air temperature rise, SST and the ENSO (Rabatel et al., 2013). If this trend continues, many glaciers in the tropical Andes will disappear in the future. In Peru, temperatures were increasing by 0.35-0.39 °C/decade between 1951 and 1999 with an increased warming trend since the mid 1970s (Vuille et al., 2008). Changes in precipitation quantities are less significant than changes in temperature. Vuille et al. (2008) further said, that regions north of 11° S (Ecuador and northern Peru) experienced a slight precipitation increase in the last decades. Southern Peru and Bolivia on the other hand, is moving towards dryer conditions. Furthermore, changes are an increase in relative humidity, especially in northern Ecuador and southern Colombia. Additionally, studies of cloud cover variations from outgoing long wave radiation have shown that the inner tropics experienced an increase in convective activity and high clouds. In the outer tropics, a reduction of cloud cover could be observed (Vuille et al., 2008).

In Mexico, the climate tends to change towards slightly warmer and dryer conditions. According to Delgado Granados et al. (2015) most of the glacier retreat is related to a decrease in precipitation and only a small part of it results from the increase of temperature.

Table 2: Overview over the temperature and precipitation trends of the different regions.

Region	Mexico	Tropics	Dry Andes	Wet Andes
LIA maximum	mid 19th century	mid 17th - 18th century	16th-17th century	18th and 19th century
Temperature trend	slight increase	increase	increase	slight increase
Precipitation trend	decrease	slight increase	slight decrease	decrease

3 Data and Method

3.1 Glacier mapping

As glaciers are key indicators of climate change (Vaughan et al., 2013), their regular area monitoring is essential to investigate climatic impacts. Also, for other products like volume change and runoff, the outlines of a glacier are required. Glacier area can be mapped with satellite images using a semiautomatic band ratio method introduced by Paul (2002). It is based on glacier classification using the spectral reflectance properties of snow and ice. Snow and ice absorb most of the short-wave infrared (SWIR) compared to the visible or near infrared (VNIR) (Paul et al., 2016). By using multispectral Earth Observing satellites that feature a SWIR band, this method can be applied for a rapid and precise glacier outline generation, at least for clean ice. To clearly distinguish glacier area from non-glacier are, the raw digital numbers (DNs) of a VNIR band need to be divided by the SWIR band. This results in glaciers visually standing out bright against a dark surrounding. To clearly distinguish between glacier and non-glacier area, a threshold value is applied. The resulting binary glacier map can then be transformed into glacier outlines in vector format (Paul et al., 2016).

3.1.1 Data used for glacier mapping

For the calculation of the present and past glacier outlines, data from multi-temporal Landsat 4 or 5 Thematic mapper (TM), Landsat 7 Enhanced Thematic Mapper Plus (ETM+), Landsat 8 Operational Land Imager (OLI), and Sentinel-2A MultiSpectral Instrument (MSI) sensors were used. The respective bands for Landsat are 3/5 or 4/5 (for TM and ETM+), 4/6 or 8/6 for OLI and bands 4/11 for MSI. Initially, ASTER images were also considered as a possible source but due to the sufficient availability of Landsat and Sentinel-2 images, these were preferred. The large advantage of the selected satellites is, that the images are easily and freely accessible and cover the whole time period.

Since Landsat TM scenes are available since 1985, the study period was divided into three time steps: 1985, 2000 and 2015. In case, no useful images could be found in the specific year, also the surrounding years were considered. Because of the data availability starting in 1985, only few images could be found for the first year. It was the initial goal to select images as early as possible but due to extensive could cover, seasonal snow and a limited number of scenes, the first useful scene was chosen. The majority of images for the first time-step are coming from 1986 and only few could be found from 1985. In the results and discussion part 1985 always refers to the first time step, even though not all scenes were taken from that year. The same applies for time steps 2000 and 2015.

The following satellite images were (see Table A 1 in Appendix): In total, 72 different scenes were selected to map glacier outlines, of which 38 are Landsat TM scenes (24 for time step 1985 and 14 for 2000), 11 Landsat ETM+, 20 Landsat OLI, and 3 Sentinel-2. In the case of partial could cover, additional images from different dates were taken into account to create an outline without gaps. Below, details and technical properties about the satellites for each time step are listed. In Tables 3-6, spectral bands of all sensors are shown and bands that have been used for glacier mapping are highlighted in yellow.

Data used for time step one (around 1985):

For this time step, the images from the Landsat 4 and 5 TM (Thematic Mapper) satellite were used. Landsat 4 and 5 were launched by NASA in 1982 and 1984 and orbit the Earth in a 16-day repeat cycle. They were discontinued in 2001 (Landsat 4) and 2013 (Landsat 5).

Each scenes of both satellites consist of seven spectral bands with a resolution of 30 m (band 6 has a resolution of 120 m). The scene size is approximately 170 km north-south and 183k m east-west. As a shortwave-infrared band is also included, the data can be used for glacier mapping using the band ratio method. The file size for all seven bands is around 350 MB uncompressed. Details about the Landsat 4/5 bands, their wavelength and resolution are listed in Table 3.

Table 3: Landsat 4-5 TM bands and their wavelength and resolution. Band 6 was acquired at 120m but resampled to 30m. Bands in yellow were used for glacier mapping (U.S. Geological Survey, 2016b) *Accessed 27.02.2017.*

Landsat 4-5 - Thematic Mapper (TM)	Wavelength (µm)	Resolution (m)
Band 1 - Blue	0.45-0.52	30
Band 2 - Green	0.52-0.60	30
Band 3 - Red	0.63-0.69	30
Band 4 - Near Infrared (NIR)	0.76-0.90	30
Band 5 - Shortwave Infrared (SWIR) 1	1.55-1.75	30
Band 6 - Thermal	10.40-12.50	120 (30)
Band 7 - Shortwave Infrared (SWIR) 2	2.08-2.35	30

Data used for time step two (around 2000):

For this time step, additionally to the still available Landsat 4-5 TM scenes, the newer Landsat 7 ETM+ scenes were also considered. If available, Landsat 7 were preferred over Landsat 4-5 TM scenes due to their better image quality.

Landsat 7 was launched in 1999 and performed well until May 2003, when a hardware component failed (the so-called scan-line-corrector) leaving wedge-shaped spaces of missing data on each scene (NASA, 2017). However, the central part of the scenes could still be used in the case the target is located there. In terms of the functionality, Landsat 7 is very similar to Landsat 4-5 but also features a panchromatic channel with a resolution of 15 m. Also, the resolution of the thermal band was upgraded from 120 m to 60 m. The file size for all eight bands is around 500 MB uncompressed. Details about the Landsat 7 bands, their wavelength and resolution are shown in Table 4.

Table 4: Landsat 7 ETM+ bands and their wavelength and resolution. Band 6 was acquired at 60m but resampled to 30m. Bands in yellow were used for glacier mapping Source (U.S. Geological Survey, 2016b) *Accessed 27.02.2017.*

Landsat 7 - Enhanced Thematic Mapper Plus (ETM+)	**Wavelength (µm)**	**Resolution (m)**
Band 1 - Blue	0.45-0.52	30
Band 2 - Green	0.52-0.60	30
Band 3 - Red	0.63-0.69	30
Band 4 - Near Infrared (NIR)	0.77-0.90	30
Band 5 - Shortwave Infrared (SWIR) 1	1.55-1.75	30
Band 6 - Thermal	10.40-12.50	60 (30)
Band 7 - Shortwave Infrared (SWIR) 2	2.09-2.35	30
Band 8 - Panchromatic	0.52-0.90	15

Data used for time step three (around 2015):

For this time step, satellite scenes from newer satellites featuring better image quality and higher spacial resolution have been used. Landsat 8 Operational Land Imager (OLI) satellite was launched in 2013 and orbits around the Earth since then with a return period of 16 days and an 8-day offset from Landsat 7. Landsat 8 has 11 bands, 8 multispectral bands (1-7,9) one panchromatic band (8) and two thermal bands (10-11). Products are delivered with a radiometric resolution of 16 bits and have a file size of about 2 GB uncompressed (U.S. Geological Survey, 2016a). For glacier mapping, a ratio with bands 4 and 6 (red/SWIR) or 8 and 6 (pan/SWIR) are used (Paul et al., 2016). The advantage of band 8 is its higher 15m resolution. Details about the Landsat 8 bands, their wavelength and resolution are listed in Table 5.

Table 5: Landsat 8 OLI bands and their wavelength and resolution. Band 10 and 11 were acquired at 100m but resampled to 30 m. Bands in yellow were used for glacier mapping Source: U.S. Geological Survey, 2016b, *accessed 27.02.2017.*

Landsat 8 - Operational Land Imager (OLI) and Thermal Infrared Sensor (TIRS)	Wavelength (µm)	Resolution (m)
Band 2 - Blue	0.45 - 0.51	30
Band 3 - Green	0.53 - 0.59	30
Band 4 - Red	0.64 - 0.67	30
Band 5 - Near Infrared (NIR)	0.85 - 0.88	30
Band 6 - Shortwave Infrared (SWIR) 1	1.57 - 1.65	30
Band 7 - Shortwave Infrared (SWIR) 2	2.11 - 2.29	30
Band 8 - Panchromatic	0.50 - 0.68	15
Band 10 - Thermal Infrared (TIRS) 1	10.60 - 11.19	100 (30)
Band 11 - Thermal Infrared (TIRS) 2	11.50 - 12.51	100 (30)

As an additional data source, images from the new Sentinel-2 satellite were also taken into account. The European twin satellites Sentinel 2A and B surround the Earth in the same orbit but with a phase of 180°. This leads to a high revisit frequency of 5 days at the equator. Sentinel-2A was launched by ESA in June 2015 and has 13 spectral bands, four at a resolution of 10m, six at 20 m and three at 60m. The field of view is about 290 km for each scene (ESA, 2017). The file size of a Sentinel-2 image tile is about 600 MB covering 100x100 km. Because Sentinel-2B was launched only in March 2017, only data from Sentinel-2A is used for this study. This led to a smaller amount of data being already available and therefore images were only considered additionally to Landsat 8 images. Details about the Sentinel-2 bands, their wavelength and resolution is listed in Table 6.

Table 6: Sentinel-2 bands and their wavelength and resolution.

Sentinel-2	Wavelength (µm)	Resolution (m)
Band 2 – Blue	0.46-0.52	10
Band 3 – Green	0.54-0.58	10
Band 4 – Red	0.65-0.68	10
Band 8 – NIR	0.78-0.90	10
Band 11 – SWIR	1.57-1.66	20
Band 12 – SWIR	2.10-2.28	20

3.1.2 Scene selection

In order to get the best possible results, the right images need to be selected. Generally, the images with the least amount of snow are preferred as they only display the glacier ice without any seasonal snow. The date on which there is the minimal snow cover varies by the region and can be different each year. As there are no seasons in the tropics, most of the year could feature the date of minimal snow cover. An additional limitation in tropical areas is the frequent presence of a cloud cover. Most scenes from the tropical region were taken in the months of December and January with additional ones from November and February. During these months, the snow cover and cloud cover seemed to be at a minimum. In Mexico, even though it is in the northern hemisphere where usually the date of minimal snow cover can be found at the end of the summer, images were chosen from February to March. This corresponds to the end of the dry season as in May the wet season starts and more snow lies on the mountains.

For Chile and Argentina, the date of minimal snow cover is again in line with the end of the summer. Most images were taken from February-April, generally before the first large snow fall of the year. As this date can vary from year to year, the date of minimal snow cover also varies. For some glaciers, no images without snow and clouds could be found. In such cases, scenes from different dates were combined so that all of the glacier perimeter is covered.

Satellite images from Landsat as well as Sentinel-2 can directly be displayed and downloaded free of charge from the homepages of the USGS using their Glovis image browser (http://glovis.usgs.gov) and the Sentinel Science hub. These web-based applications offer numerous filters for selection, among others can be filtered and searched according to their location (Path/Row) or their acquisition date. All scenes are available as orthorectified images in Geotiff format. To reduce the amount of disk space needed for image storage, full resolution preview images can be downloaded in jpg format. These preview images are false color composites (TM equivalent bands 543 as RGB) and are pratical for an initial evaluation of glacier area and comparison to other images with potentially a smaller amount of seasonal snow. The file size is with about 10 MB much smaller than the full L1T products. Once suitable images are found, they can be downloaded and imported into GIS software. For this study, the program ArcGis was used under the license of the University of Zurich. The usage of other GIS software would also be possible but ArcGIS was chosen due to the larger experience with this software.

3.1.3 Generation of glacier outlines and area calculation

Once images are loaded into ArcGIS, it is important that they have the correct projection. As default, they are geo-referenced to the rectangular coordinate system UTM with the WGS1984 datum.

Depending on the location, the UTM zone varies. Combining images from more than one zone results in area changes as the UTM projection is not conservative for area. Therefore, for each UTM zone a new ArcGIS project was created.

After the images have the right projection, the band ratio calculation can be performed. Additional to the SWIR band, the red or the near infrared band can be used. Using the near infrared band instead of the red band results in a reduced sensitivity to atmospheric scattering and might thus miss glaciers in shadows. The red band, on the other hand performs better in shadow and does not misclassify vegetation in shadow as glaciers (Paul et al., 2013c). For Landsat 4/5 and 7 images, the NIR band was chosen over the red band due to an assuming better performance. When dealing with Landsat 8 images, band 8 (panchromatic) was preferred over the NIR or red band due to its higher resolution.

In order to calculate the band ratio, both images need to have the same resolution. When working with Landsat 8, the panchromatic band has a resolution of 15m and therefore the SWIR band has been resampled from 30 m to 15 m prior to any calculations. Table 7 shows an overview of all satellites used and their respective bands, resolutions, and threshold values.

Table 7: Overview of used satellites for the specific time period with their bands, resolution and threshold values.

Satellite	Time period	Bands used	Resolution	Threshold value
Landsat 4/5 TM	1985-2013	4/5	30m	1.6-2.0
Landsat 7 ETM+	1999-2003	4/5	30m	1.6-2.0
Landsat 8 OLI	2013-	4/6 or 8/6	30m or 15m	1.3-1.4
Sentinel-2	2015-	4/11	10m	≈ 1.4

When performing the band-ratio calculation, the pixel values need to be transformed from integer to float to have decimals for precisely setting the threshold value later. This can be done using the raster calculator as follows: *result = band4/float(band5);*

Applying a threshold value converts the ratio image into a binary image (two unique values). The command when using the raster calculator reads as follows: *result = ratio_image>threshold_value 1,0;* which means that all pixels which have a value greater than the selected threshold values are set to one, all others to zero. Next, all zero values need to be transformed into no data values. The command reads as follows: *result = setnull(ratio_image== 0, 1);* this step removes the polygons surrounding ice free areas.

If there are many small units within or near the glacier outline or single pixels that are isolated from the main glacier area, a median (or majority) filter can be applied. This reduces the total number of polygons and fills small gaps. It calculates the median value of the neighbouring cells (3x3 kernel) and corrects the glacier outline accordingly. The median filter helps to eliminate small snow patches and fills gaps resulting from rocks on the glacier (Raup et al., 2007).

The big advantages of using a median filter are the reduction of errors and the uniform correction of the glacier outlines for all glaciers. Because the median filter works the same for all glaciers, subjective interpretation can be minimized and therefore the data output is more uniform and reproducible.

Finally, the resulting area can be converted from raster into vector data by using the functions *raster to polygon;* The resulting polygons are being merged into one polygon per volcano as the volcano is seen as a whole. Accordingly, it is not required to calculate drainage divides.

3.1.4 Challenges and limitations

With a resolution of 30 m (TM), the accuracy of the observable glacier changes is limited. In general, it can be said, that the accuracy of the mapping needs to be larger than the glacier changes to get reasonable results. Furthermore, with a 30 m resolution, ice patches smaller than 0.01 km^2 cannot be properly recognized (Paul et al., 2016). It is thus recommended to use the highest possible resolution to get the best results, especially in regions dominated by small ice masses.

Because the band ratio method is based on the different spectral properties of ice and snow compared to bare soil or vegetation, it only performs well, when ice or snow is exposed at the surface. A debris-covered glacier, as the name says, is covered by a layer of debris and with no or only small patches of ice which are visible from above. The missing classification of debris-covered glaciers is one of the major weaknesses of the band ratio method and all other methods when mapping glaciers. Hence, manual editing has to be applied when debris-covered glacier parts need to be included. Paul et al., (2013b) suggest using high resolution images like available in Google Earth ™ to visually interpret the debris covered part, even if the images were not taken on the same date.

Apart from debris cover, glaciers on active volcanoes may also have a temporary ash layer on top of the ice following an eruption. If the ash layer is relatively thin the thermal band of the Landsat satellites can be useful to determine the glacier outline. As the resolution is 120 m for Landsat 4/5, 100 m for Landsat 8 and 60 m for Landsat 7, it is not as good as the other bands, it should only be used as an additional indicator and not for primary mapping.

Another limitation of the band ratio method is the, sometimes poor performance in cast shadow. Due to the low reflectance of both channels (NIR and SWIR), ice bodies in regions with shadows have also low values when calculating the ratio (Paul, 2002). By using a lower threshold value, ice in cast shadow can be mapped as well but performance might be degraded in other areas. In such a case, a compromise of several tested threshold values needs to be found to get the best performance over the entire glacier area. Another option is to use a different threshold value only for the shadow area and combine it with the result of the shadow free area afterwards. In any case, manual correction might be required for parts in cast shadows (Paul et al., 2016).

The great advantage of well-established semi-automated method over manual glacier digitizing is that the outlines are reproducible and not generalized. Additionally, it is much less time consuming if the method is applied for a large number of glaciers (Paul et al., 2013a).

3.2 Volcano data

By analyzing volcano data, it was possible to read out trends and changes in the volcanic activity of glacier and non glacier-covered volcanoes during the Holocene. To do so, a modified version of the Smithsonian volcano database was used. It uses the same catalog and data as the Smithsonian database but with the possibility to access all data via a locally stored database. This makes it easier to filter out valid data and combine tables with each other. The database was named “South American and Mexican Volcano database”. The major difference of this database to the Smithsonian database is, that it does only include volcanoes from South America and Mexico and does not include all other volcanoes like the volcanoes of Central America as there are currently no glaciers present.

Even though many eruptions from the past have not been reported and are unknown until this day, changes in eruption frequency can be identified and compared with results of glacier and climatological studies. With increasing age the completeness of the database decreases, but because it does so for all volcanoes, the data can still be used to describe eventual changes of the activity of glacier-covered volcanoes in comparison to non glacier-covered once. Statistical tests were applied to verify the significance of the differences. The investigation of volcano data focuses on changes in eruption frequency meaning the total number of eruptions over time but also on large magnitude eruption frequency. The frequency was studied on different time scales, according to the data density over time. First, the whole Holocene was analyzed, then the last 4000 years and further eruptions since 1500, 1850 and 1980. The latter was combined with the elaborated glacier area results. Furthermore, analyzation of the eruption start month and the potential connection with the presence of seasonal snow was made. Finally, information about the number of people living close to the volcano was used to determine

volcanoes with possible hazard potential. Below, the most important features of the database are being explained in more detail.

3.2.1 South American and Mexican Volcano database.

The database is based on the PostgresSQL database management system. The data was initially imported from the server of the UNAM in collaboration with the local staff. It is divided into tables, one for each volcano property. Each property will be explained in more detail in the coming sections. To access data from the database, SQL queries are used. This makes it possible to access many records and combine tables with a single query. To display and access the date, the program PgAdmin3 was used. It is an open source software that allows the administration and development of Postgres SQL databases. With its user-friendly interface, it provides a visual help and makes it possible to easily access, edit, write and export data. Further, it is secure and allows backups.

The time period covered in the data base is the Pleistocene and Holocene epochs. All the volcanoes that likely have been active since then, appear in the database. The boundary between Pleistocene and Holocene was set to 10.000BP as it was defined at the 1969 International Union for Quaternary Research (INQUA) Congress (Siebert et al., 2010).

The database contains 400 volcanoes and 237 of them have shown Holocene activity and are therefore relevant for this study. An active volcano is according to the definition a volcano that has had an eruption or has shown other evidence of activity within the Holocene (Siebert et al., 2010). As in this study only active volcanoes are considered, Pleistocene volcanoes are not relevant. Anyhow, the data of the Pleistocene volcanoes are also stored in the database and can be accessed if necessary. The country with the most glacier-covered volcanoes is Chile with 51 volcanoes, 13 of which are on the border to either Argentina or Bolivia. It was the initial goal to calculate glacier areas for all 74 glaciers covered volcanoes. Because the glaciers of Northern Chile/Argentina and Bolivia are mostly very small ($<0.5km^2$) they were excluded from the study. With a 30m resolution image it was not possible to clearly identify ice versus snow and therefore no precise results could be made. Further, the volcanic caldera of Atuel was also excluded because of its large size (25km diameter) and no clear borders. Many small separate glaciers lie within the caldera but not a continuous ice mass. Additionally, no new glacier outlines were made for the Patagonian ice fields due to their big size and the amount of already existing data. In total, it was possible to finalize results for 59 glaciers covered volcanoes. The number of volcanoes for each country is listed in Table 8.

Table 8: Number of analysed volcanoes per country.

Country	Number	Country	Number
Argentina (entirely within)	3	Chile - Argentina	6
Chile (entirely within)	33	Ecuador	7
Chile - Bolivia	1	Mexico	3
Colombia	4	Peru	2
Total	59		

Eruption reporting

Of the 237 Holocene active volcanoes, 1374 eruptions are currently known. 1208 of them are confirmed, the rest is either unconfirmed (153) or discredited (13). The database was updated to the date of August 2017. The frequency of observed eruptions over time shows a clear trend, only 290 eruptions are older than 2000 years. The frequency of volcanic eruptions during the Holocene can be seen in Figure 13. In recent years, the dating techniques and stratigraphic studies have been improved and we can expect to update the database in the future and to extend the eruptive history of the volcanoes. After the arrival of the Spanish and other colonialists in Latin America, the number of reported eruptions increased largely. Almost 70% of the known eruptions are dated after 1500, almost 50% after 1850 and about 11% after 1985. This relation clearly shows how much the reporting of volcanic eruption impacts the number of known eruptions.

Since the increase of the world population and the construction of monitoring stations, the number of known eruptions further increased. As mentioned by Siebert et al. (2010) the number of reported eruptions during the last centuries always increased after a big eruption, since the general interest was larger and therefore led to global attention and media coverage. A decline in the global eruption reporting number can be seen during the world wars and the great depression as the people were occupied and therefore did not report as many eruptions. As larger eruptions leave more traces behind, it makes it easier to date older large magnitude eruptions. 56 of the 117 Holocene eruptions (48%) with a VEI of 4 or larger are older than 2000 years.

Concerning glacier-covered volcanoes, a total number of 763 eruptions have occurred in the Holocene. Of which only 141 (18%) are older than 2000 years. Of the 763 eruptions, around 70% occurred after 1500, almost 50% after 1850 and around 11% after 1980. Large magnitude eruptions are more spread out in time and the lack of known eruptions in the past is not as big as for small eruptions. In the database, there are 62 known eruptions on glacier-covered volcanoes with a VEI of 4 or more. Of these, around 50% are older than 2000 years.

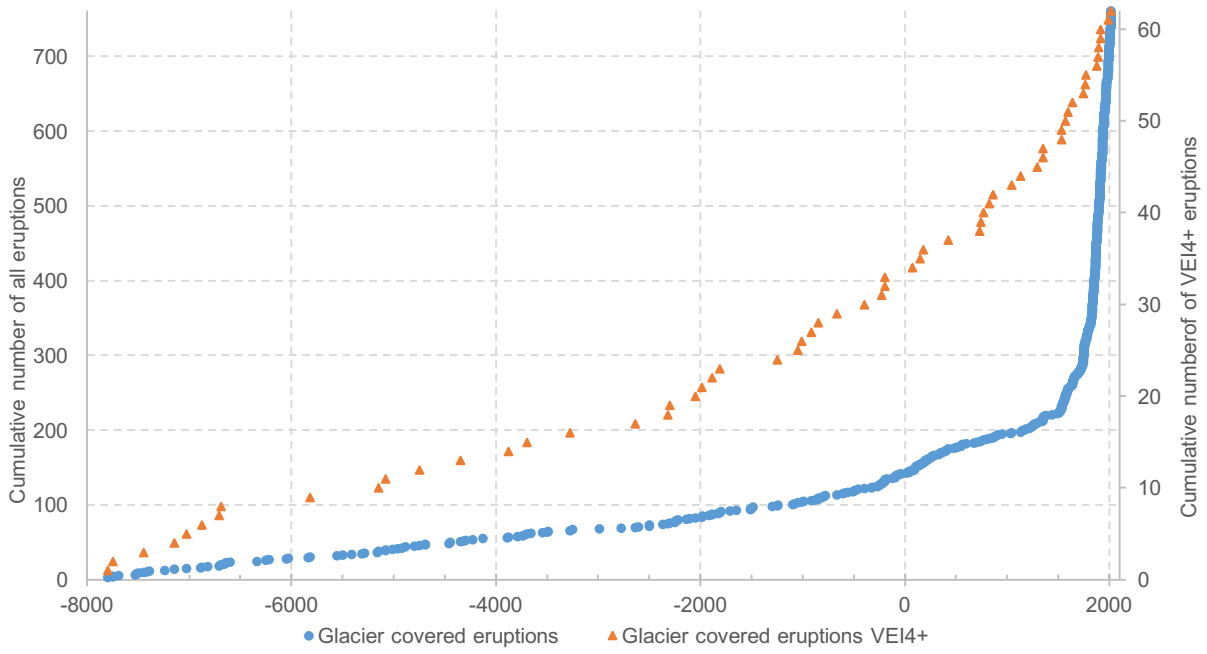

Figure 13: Cumulative Holocene eruptions on glacier-covered volcanoes in Mexico and South America. Secondary axis shows the cumulative number of VEI4+ eruptions.

Volcano data

The database is filled with various information about the history and the state of the volcano and its properties. Below, the main volcano characteristics and database properties are being listed.

Volcano Identification

First, each volcano has a name and an identification number (id). The latter is the same as used in the Smithsonian database (six-digit number). As for each volcano, also each eruption has its own id number (five-digit number). This makes a connection between a volcano and an eruption in the database possible. The volcano number is unique and can be linked to several eruptions. As some volcanoes are known under more than just name, also the synonyms are stored in the database to prevent confusion.

Localization

The volcanoes are categorized in regions, sub-regions and political units (countries). The region is a wider form of localizing a volcano on a global scale. In this case, there are only two regions: “Mexico

& Central America" and "South America". Each region is divided into sub-regions, for example, volcanoes from Chile can be in the sub-region "Northern Chile, Bolivia and Argentina", "Central Chile and Argentina" and "Southern Chile and Argentina". Along with the names for the regions and sub-regions also an id code for each of them is stored in the database.

For a more precise localization also the longitude and latitude values are saved. Using these coordinates, the volcanoes can easily be visualized in GIS software like QGis or ArcGis. Finally, the altitude is listed in meters above sea level.

Population

To identify hazards related to volcanic eruptions, it is essential to know, how many people live around a volcano. In the database, there is the number of people stored, that live within a specific distance from the volcano. The four distance groups are: within 5km, 10km, 30km, and 100km.

Further volcanic information

A further characteristic of the volcano is the volcano type, which is the main morphological characteristic (e.g. Stratovolcano, Caldera or Shield volcano). A subgroup of the types are the volcano features (e.g. Dome, Vent, Cone or Geyser). Each volcano can have more than one type and contain several features.

To summarize the lithospheric character of the volcano, the rock type is stored in the database. In the original Smithsonian database, the major rock type as well as minor rock types are listed. In this version only the major rock types, are present, but it can consist of a combination of more than one rock type (e.g. Andesite/Basaltic Andesite). Figure 14 shows an overview of the main volcanic rock types in an alkali-silica diagram.

A more general description of the geological setting gives the section tectonic setting. It describes what type of plate movement is connected with the volcano (e.g. compressional continental).

Finally, an estimation of the volume of the volcano is given for some volcanoes. This is an indication of the size and the eruption history. The larger the volume the greater also the eruptions or the eruption frequency and magnitude must have been.

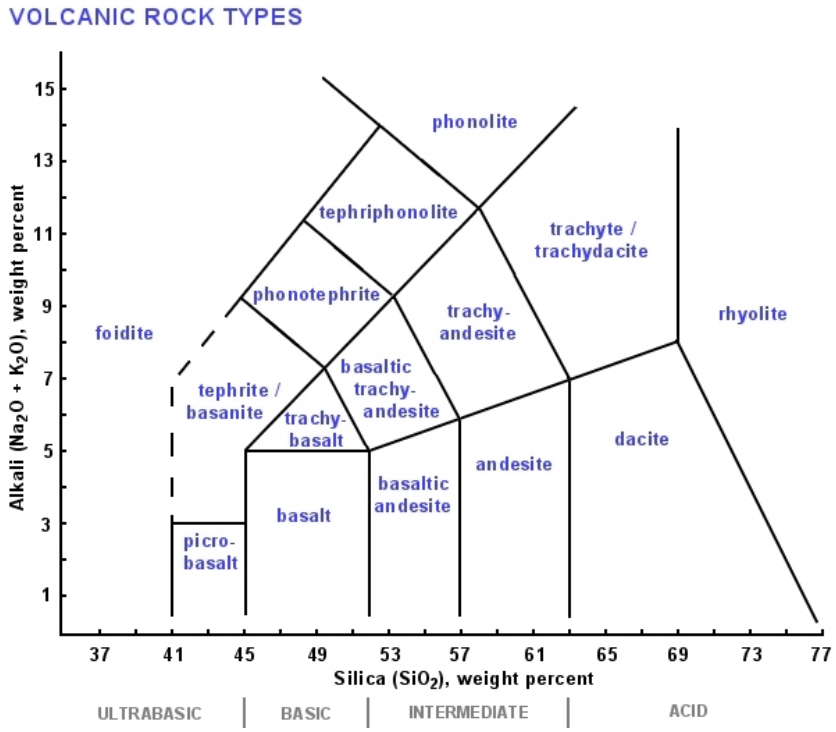

Figure 14: Volcanic rock types in an alcali-silica diagram (http://geology.about.com/od/more_igrocks/ss/igneous-rock-classification-diagrams.htm#step3).

Eruption data

The second big field next to the volcano data is the eruption data. An eruption is defined according to Siebert et al., (2010) as an event that involves explosive ejection of fragmented material or the effusion of molten lava, or both.

As volcanic eruptions can vary greatly in terms of the duration, the knowledge of their start and stop dates are important. As we go back in time the exact dates have often not been reported or only the year is roughly known, without knowing the month or day. The start date is for the observer easier to tell than the stop date, as a typical eruption ends with a gradual decrease of activity, so the exact time when the eruption stops is hard to tell. Knowing the start and stop date, the duration of the eruption can be calculated.

Additionally, to the dates, also the uncertainties of the dates are shown in the database. The uncertainties can be expressed using a specific amount of days or months or the start and stop date can have a "greater than" or "smaller than" sign to indicate that the eruption occurred after or before the listed date. Also, ongoing eruptions are shown in the database, indicated with a "greater than" sign.

Eruption characteristics

The location on the volcano, on which the eruption occurred is described as the "eruption vent description". For example, an eruption could take place in the central vent or could be a flank eruption. An important characterization is also the subglacial eruption which is one feature of the vent description. An eruption can have a single or multiple vent description entries, but out of the database, it is not clear if they occurred at the same time or at different dates as the eruption only has one start and stop date.

A more detailed eruption description is listed under the field "event type". Here, many characteristics of an eruption are described like the type of tephra (e.g. ash, pumice or bombs), seismic activity, hazard events (e.g. lahar, pyroclastic flow or tsunami), consequences to the population (fatalities and property damage), observations (e.g. loud noise, lightning or volcanic smoke) or pre-eruptive indicia's (e.g. thermal anomaly and inflation). In total 47 different "event types" are stored in the database.

Volcanic explosivity index (VEI)

To describe the magnitude of an eruption the volcanic explosivity index (VEI) is used. As there is no instrumental determined magnitude scale like for example for earthquakes the VEI was introduced to describe the magnitude of an eruption. It is a logarithmic scale ranging from 0 to 8. The VEI combines multiple aspects of an eruption like the volume of explosive material, the eruptive cloud height and other descriptive terms (Siebert et al., 2010). A table with the different VEIs and the corresponding features and eruption examples can be seen in Table 9.

Table 9: Volcanic Explosivity Index (VEI) criteria, description and example (Siebert et al., 2010).

VEI	**0**	**1**	**2**	**3**	**4**	**5**	**6**	**7**	**8**
General Description	Non-explosive	Small	Moderate	Moderate-large	Large	Very large	—>	—>	—>
Qualitative description	Gentle	Effusive	Explosive	——>	Cataclysmic /paroxysmal	—>	—>	—>	—>
Max erupted volume of tephra (m^3)	10^4	10^6	10^7	10^8	10^9	10^{10}	10^{11}	10^{12}	$>10^{12}$
Eruption cloud column height (km)	<0.1	0.1-1	1-5	3-15	10-25	>25			
Eruption Type	Hawaiian	Hawaiian/ Strombolian	Strombolian/ Vulcanian	Vulcanian /Plinian	Vulcanian/ Plinian	Plinian/ Ultra Plinian	Plinian/ Ultra Plinian	Ultra Plinian	Ultra Plinian
Volcano example	Masaya (1570)	Poás (1991)	Ruapehu (1971)	Nevado del Riuz (1985)	Pelée (1902)	St. Helens (1980)	Kraka-tau (1883)	Tambo-ra (1815)	Yellows tone (Pleisto-cene)

Eruptive Volume

The volume of ejected material is known for some of the historical eruptions. To get an estimation of the volume, field work is required and therefore not all eruptions yet have volume data. Also, it is important to know that the eruption volume data is only an estimation and large uncertainties can occur. In the database, the eruption volume is separated into the total volume, tephra volume and lava volume. Additionally, the references of the volume estimations are listed.

3.2.2 Glovoremid (Global Volcano Research and Monitoring Institutions Database)

Glovoremid is a database focusing on the monitoring of volcanoes and is linking monitoring with research institutions. It supports the communication between scientists and technician and will help to reduce the risk of volcanic hazards. The database was developed in 2013 by adopting the VOMODA database for a worldwide usage (Ortiz-Guerrero et al., 2015).

The Glovoremid database was developed to work hand in hand with the already existing database of the Smithsonian Institute and the LaMEVE database for large magnitude eruptions. The same identification numbers for the volcanoes were used and therefore it can also be integrated into the database used in this master thesis. Glovoremid is hosted at the Instituto de Geofisica (UNAM) and can be accessed online in English and Spanish by users globally (Ortiz-Guerrero et al., 2015).

Monitoring in Latin America

Of the 314 Holocene volcanoes in total Latin America, 202 do not have any monitoring installation at the moment. Mexico and Chile have the largest number of unmonitored volcanoes (32 and 50, respectively). In comparison to the total number of volcanoes, 64% of Chilean and 82% of the Mexican volcanoes are currently not monitored. Three countries, Argentina, Bolivia, and Honduras do not have any on-site monitoring station but as some volcanoes lie on the border they might be monitored from the neighboring country (Ortiz-Guerrero et al., 2015).

Considering glacier-covered volcanoes, 29 of the 74 Holocene active volcanoes do currently not have any monitor installation. Some of them have seen historical eruptions like Viedma (1988), Cerro Arenales (1979), Tromen (1822) or Llullaillaco (1877). The non-monitored volcanoes are located under the Patagonian ice field or far away from major cities. Therefore, the monitoring priority was shifted towards volcanoes that pose a higher risk to the population. Nevertheless, 45 of the 74 glacier-covered volcanoes are currently under monitoring. Most of them (31) are located in Chile. This makes Chile the

country with the most monitored volcanoes, 31 out of 51 are under observation. In Colombia, all 4 glacier-covered volcanoes possess monitoring installation.

The general monitoring focuses on volcanoes that have shown activity in the recent history. Many Holocene volcanoes that are still considered as active but without historical eruptions are not monitored. However, 30 unmonitored volcanoes have had eruptions since the 16th century.

As a quantification of the hazard potential due to the number of people within 100km the population exposure indices (scale from 1-7) are used (Ortiz-Guerrero et al., 2015). Currently, monitoring focuses on three major aspects: seismology, deformation and gas monitoring. The amount of monitoring effort is categorized in 5 monitoring levels. Level 0 means not monitored, Level 1 corresponds to only seismology, Level 2 seismology and deformation and Level 3 seismology, deformation and gas monitoring. Level 4 and 5 just have more instruments installed (Ortiz-Guerrero et al., 2015).

4 Results

4.1 Inventory of glaciers on volcanoes in Latin America

Glacier area changes of the ice masses on active volcanoes of Latin America could be determined using the band-ratio method explained in the previous chapter. In total, glacier area data of 59 volcanoes were derived. For the other 15 remaining volcanoes that possibly have or had glaciers, the method using satellite images was not sufficient to perform good results. This is because the ice masses are either too small to be detected by a 30m resolution image of older images or too big in which case with only a few available images it was difficult to get a sufficient outcome. This applies for volcanoes is northern Chile and Argentina, where glaciers appear more like multiyear firn patches. Data for the Patagonian ice fields were taken from the literature as a lot of studies have already been made.

Of the glacier on the 59 volcanoes, a frequency analysis performed. The related histogram of glacier area at the different time points is shown ins Figure 15. The distribution is very wide, reaching from glaciers as small as 0.1 km^2 (which is the smallest possible size at which a reasonable result can be calculated all the way) to large glaciers with more than 200 km^2. In 1985, no glacier was in the class of 0.5 or below, whereas in 2015 around 13% of the glaciers are smaller than 0.5 km^2. Note that in 2015 there were two glaciers less than in 1985 and 2000 as they melted away after 2000.

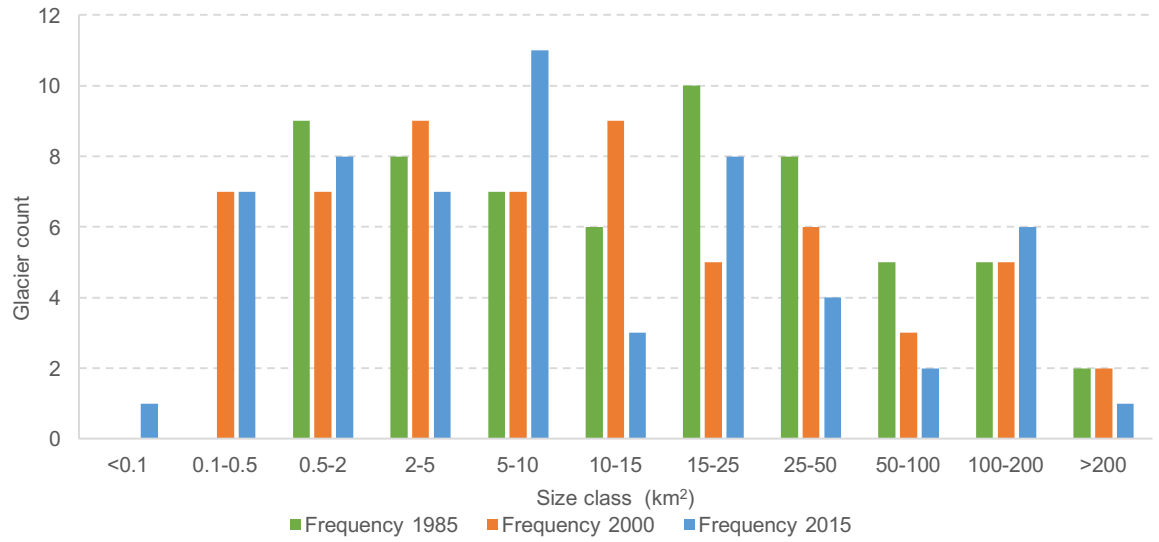

Figure 15: Number of glaciers per size class for 1985, 2000 and 2015.

Furthermore, the total glacier area per size class was calculated. Results are shown in Figure 16. The largest amount of glacier area is made up of glaciers between 100 km^2 and 200 km^2. For 2015, more that 50% of the total area was found within this size class. For 1985 and 2000 it was 34% and 38% respectively. Small glaciers, even though there are many of them, only make up a fraction of the total glacier area. Glaciers smaller than 50 km^2 (76% of glacier for 1985, 80% for 2000 and 83% for 2015 are within the size class) only contribute about 25% to the total glacier area (24.5% for 1985, 24% for 2000 and 27% for 2015).

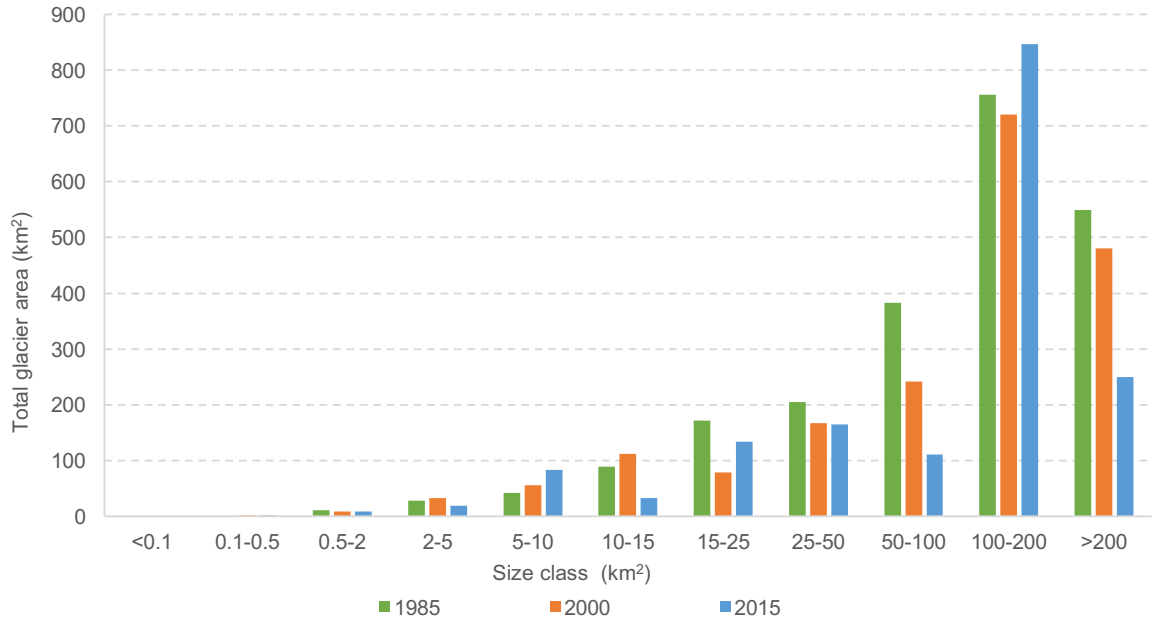

Figure 16: Glacier area covered in each size class for 1985, 2000 and 2015.

4.2 Glacier change

All glaciers on observed volcanoes lost area between 1985 and 2015. Therefore, all values indicating a glacier change relate to area loss. Only a few glaciers have shown an advance during the time frame, but this will be explained further below. Figure 17 shows the histogram of relative area change values.

The histogram shows that the change results are not normally distributed and a large spread of the results is present. The average change off all glaciers is -49.8% between 1985 and 2015. Looking at the change rate per year, the average is -1.83%/y for the whole time period.

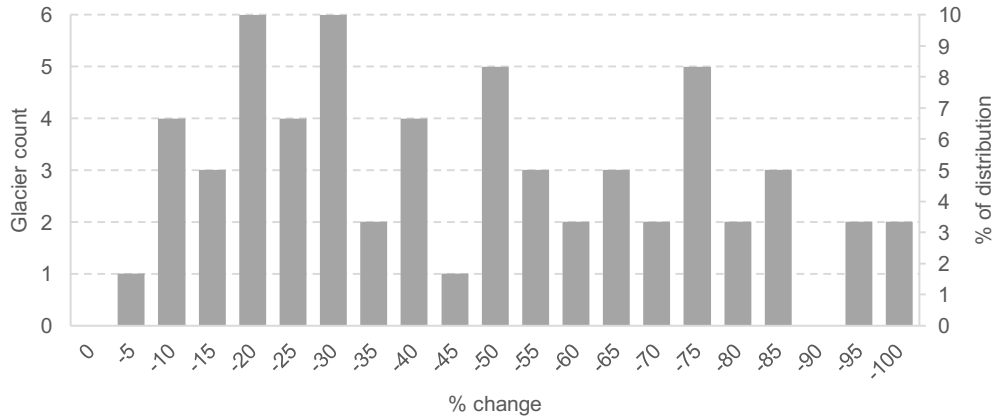

Figure 17: Frequency and distribution of percentage glacier change.

In Figure 18 the glacier change rate is plotted against the glacier area of around 1985. It is clearly visible that the area change rate increases towards small glaciers. The curve resembles a "hockey stick" illustrating exponential increase in relative area change with decreasing glacier area. Large glaciers might have a larger absolute change, but the relative change is much smaller than for small glaciers. There is also a large spread in the change rates of glaciers smaller than about 20 km^2, likely reflecting their different climatic setting, response time and possible volcanic impacts.

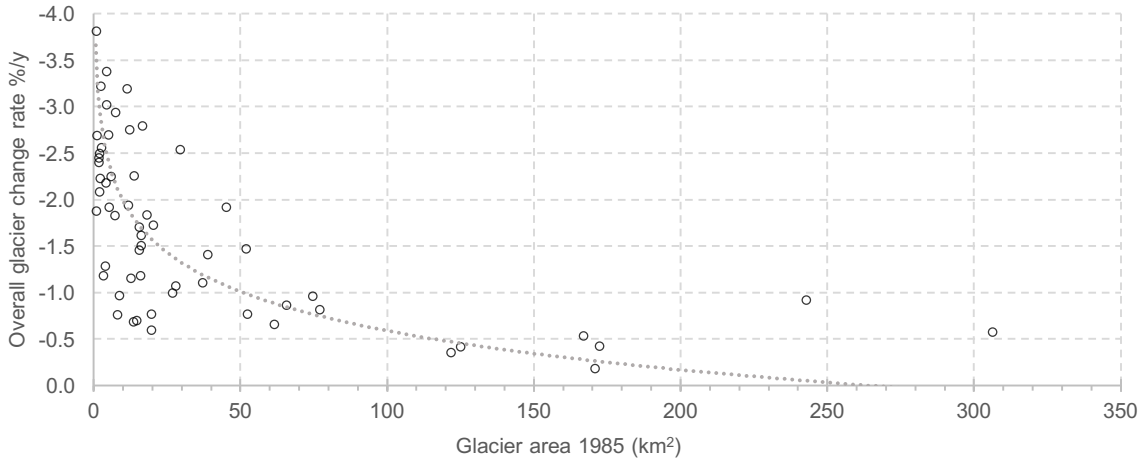

Figure 18: Glacier change rate (1985-2015) in compare with the glacier size of around 1985.

Glaciers with no change or an increase in area could not be observed. Two volcanoes lost their entire glacier cover, these are Popocatepetl in Mexico and Tungurahua in Ecuador. Looking at the glacier change rate values, most glaciers had an overall change rate between -0.25%/y and -3.25%/y. Generally,

the change rate was higher between 1985 and 2000 in compare to after 2000. Figure 19 shows the histogram of glacier change rate values. Between 1985 and 2000, 13 glaciers had a change rate of more than -4.0%/y. After 2000, no glacier had a change rate that high.

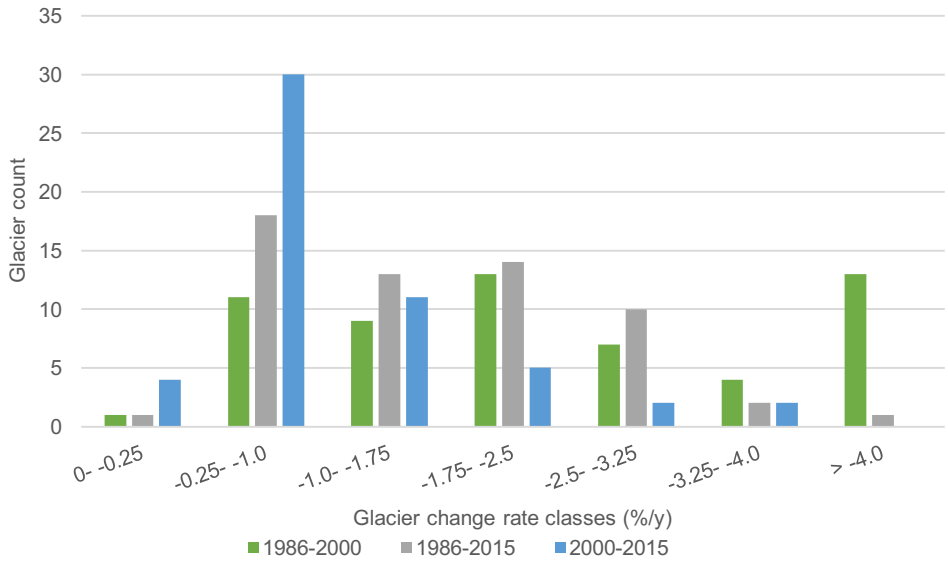

Figure 19: Frequency of glacier change rates. Comparing the change rates of the whole study period versus the first and second half.

4.3 Glacier change according to region

Due to the large geographical distances of the volcanoes and the resulting variability in climate conditions, also the glacier change rates are not the same for all regions. An overview of the location of the analysed glaciers and the corresponding region is shown in Figure 20.

Change rates in % per year can be seen in Figure 21 for the time periods of 1985-2000 in comparison to 2000-2015. It is striking, that all regions show a lower retreat rate in recent years relative to 1985-2000. Before 2000 the shrinkage rate for all regions was -1.14%/y whereas after 2000 decreased to -0.66%/y. The biggest changes were found in subtropical Mexico. There, the glacier change during the whole study period was -2.30%/y whereas for the glaciers of Colombia and Ecuador the change rate was “only” -1.38%/y. Glaciers in Peru/Bolivia changed by -1.53%/y while along the Chilean-Argentinean border, between 33° S and 45°S the change rate was -0.85%/y with a local maximum between 35 and 38° S (-2.14%/y). South of 45° S, the rate decreased to -0.59%/y, which is the lowest of all regions.

Figure 20: Overview of the location of the 59 analysed glacier-covered volcanoes within their corresponding region and sub-region.

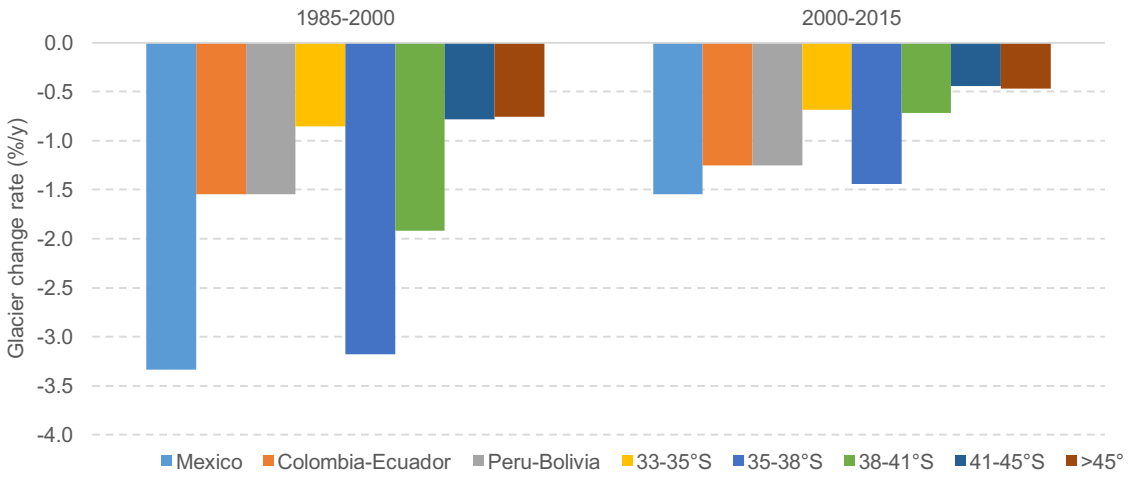

Figure 21: Glacier change rate for each region. Comparing change rates of 1985-2000 to 2000-2015. Averages were calculated using the absolute area values. Hence big glaciers have more impact on the outcome.

4.3.1 Glacier change Mexico

In present day Mexico, there are only two glacier-covered volcanoes remaining. Glacier area change of all studied volcanoes over time can be seen in Figure 23. At the time at which the satellite image of Popocatepetl for 2000 was taken, almost 50% of the glacier area in comparison to 1987 was still left. As no glacier area was detected in 2015, the exact date of the extinction could not be determined. Delgado Granados et al., (2007) mentioned, that the glacier on Popocatepetl became extinct in late 2000. The other two volcanoes, Iztaccíhuatl and Pico de Orizaba remained quiet during the study period, nevertheless its glaciers underwent large relative area loss with -57.6% and -66.1% respectively. The largest still remaining ice mass can be found on Pico de Orizaba with an area of 0.63 km^2 as of February 2017 down from 1.85 km^2 in 1986. A map showing the glacier outlines of Pico de Orizaba can be seen in Figure 22. In all of Mexico, there remain 0.90 km^2 of glacier ice, down from 3.12 km^2 in 1986. In Tables 10, all glacier results of Mexico are listed.

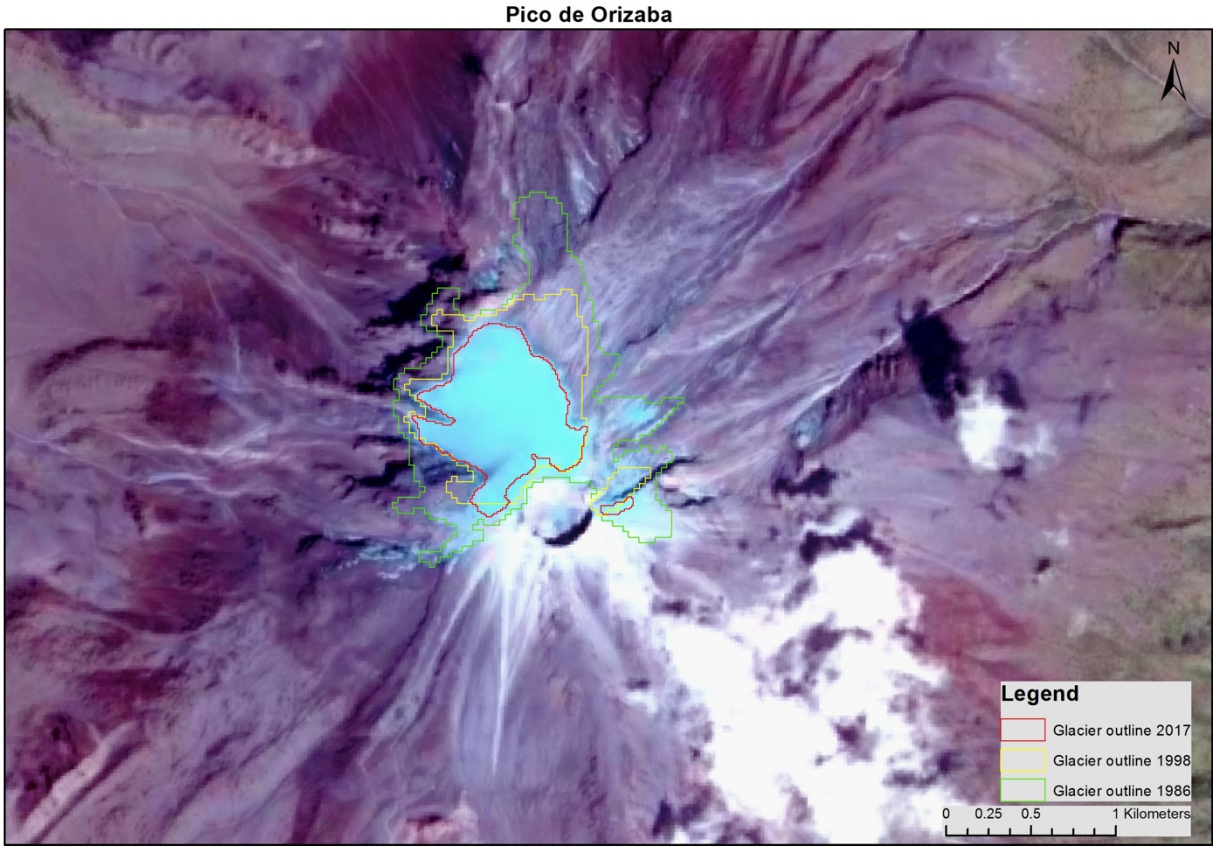

Figure 22: Glacier outlines of Pico de Orizaba from 1986 (green), 1998 (yellow) and 2017 (red).

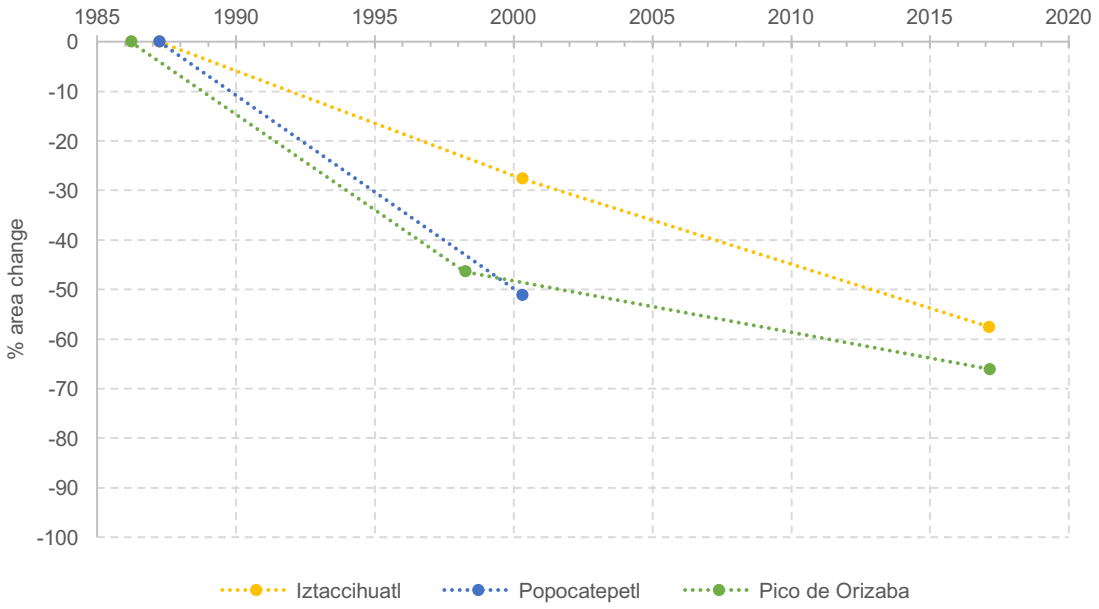

Figure 23: Glacier area change of Mexico.

Table 10: Glacier area calculation results of Mexico.

Volcano name	Eruptions	Area 1985 km² (date)	Area 2000 km² (date)	Area 2015 km² (date)	Area change total (%)	%/y 1986-2000	%/y 2000-2015	%/y total
Iztaccihuatl (5230m)		0.64 (1987)	0.46 (2000)	0.27 (2017)	-57.6	-2.06	-1.74	-1.88
Popocatepetl (5436m)	1994, 1996, 2004, 2005	0.63 (1987)	0.31 (2000)		-100.0	-3.81		-3.81
Pico de Orizaba (5636m)		1.85 (1986)	0.99 (1998)	0.63 (2017)	-66.1	-3.76	-1.02	-2.08
Total	4	3.12	1.76	0.90	-71.2	-3.33	-1.54	-2.30

4.3.2 Glacier change in Colombia and Ecuador

In Colombia and Ecuador some of the most active glacier-covered volcanoes of Latin America can be found. The peaks reach high altitudes and can, therefore, sustain a permanent ice cover even in a tropical climate. The area change within the study period varies greatly between the different volcanoes (see Figure 24). The general retreat rate of the tropical glaciers in Colombia and Ecuador is -1.38%/y between 1986 and 2015. The relative area loss of the whole area is -40.1%. All results are listed in Table 11. The volcano of Tungurahua showed the strongest shrinkage with -11.93%/y (or -85.7%) from 1991 to 1998. In 1998, only 0.10 km^2 of the initial 0.70 km^2 remained and after the eruption of 1999, the glacier disappeared completely. Other glaciers like Cayambe, Cotopaxi and Antisana showed a much smaller glacier area decrease with -0.60%/y, -0.66%/y and -0.71%/y (or -17.5%, -20.8%, -22.9%) respectively. Even though Cotopaxi had an eruption in 2015 (VEI 2) it seemed like it did not have an immediate impact on the overall glacier area. The ice-free area around the crated has widened starting from 2002 due to fumarolic activity (Delgado Granados et al., 2015a). After the 2015 eruption, parts of the glacier are covered with a layer of ash. This might have reduced the ablation rates if the ash layer is thicker than about 10 mm.

Another glacier that lost large amount of its area is Nevado Santa Isabel. It is with 4944 m the lowest glacier-covered volcano in Colombia and the whole tropical region. In 1987, its peaks were still covered by a continuous ice cap (7.14 km^2) which broke apart in the following years with only 0.91km^2 remaining in 2016. This results in an area loss of -7.2% or -2.93%/y. Huggel et al. (2007) mentioned that since the LIA until 2002 the glacier has lost almost 90% of its area with an increased retreat rate in recent years. This would mean that since the LIA the Santa Isabel glacier lost 97% of its area. A map showing the glacier outlines since 1987 of Santa Isabel are can be seen in Figure 25.

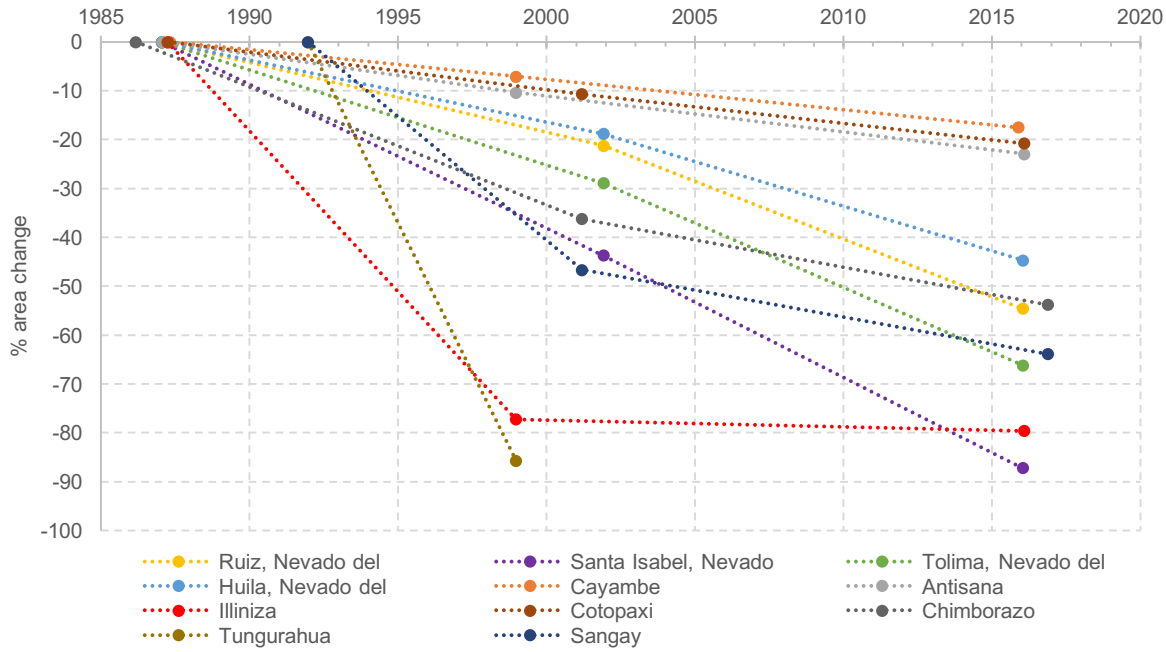

Figure 24: Glacier area change of Colombia and Ecuador.

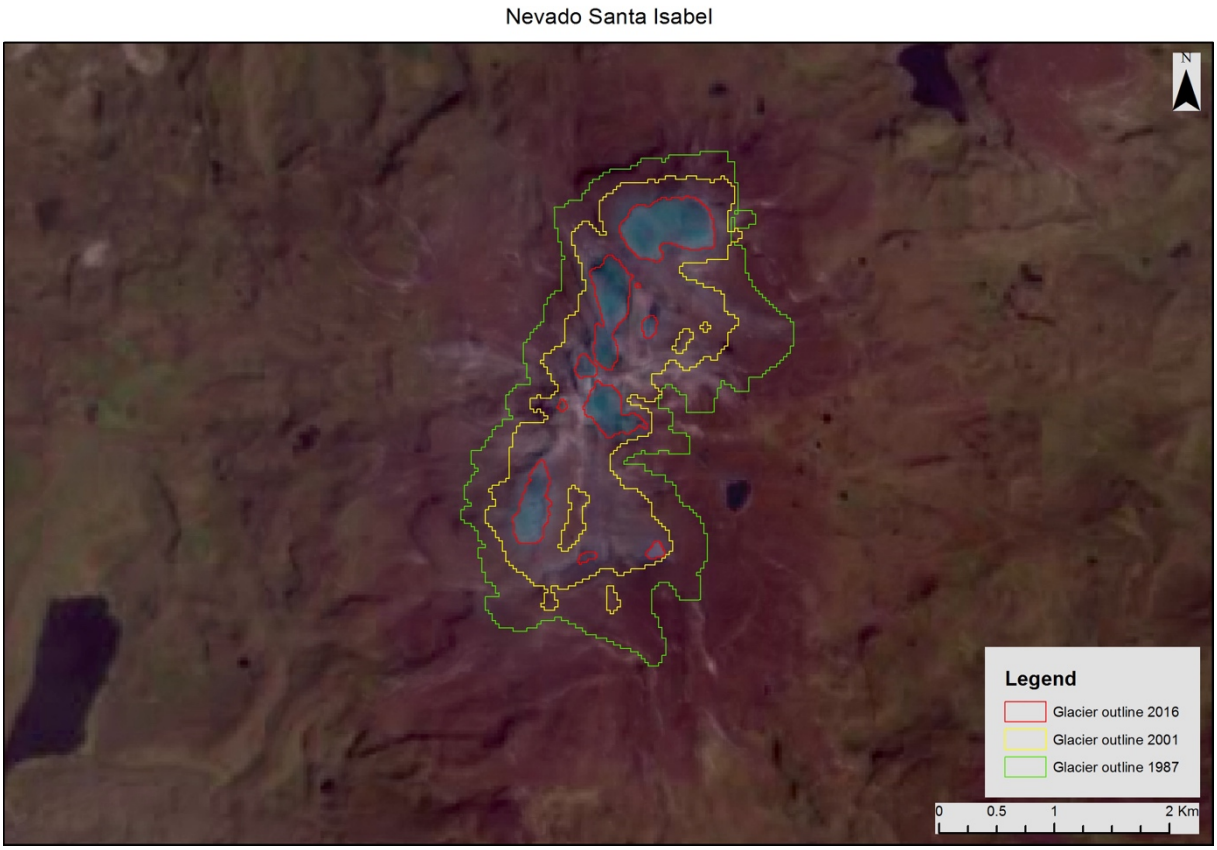

Figure 25: Glacier outlines of Nevado Santa Isabel from 1987 (green), 2001 (yellow) and 2016 (red).

Nevado del Ruiz, the most active ice capped volcano of Colombia lost 54.5% of its area from 1987 to 2016 at a retreat rate of -1.83%/y. Apart from several volcanic eruptions and the connected ash layers on the ice, fumarolic activity affected the glacier area especially around the crater rim (Huggel et al., 2007b).

In terms of the change in the shrinkage rate, some glaciers show an increase and others a decrease of change rate. All Colombian glaciers have a higher retreat rate in recent years in comparison to the 80s and 90s. In Ecuador, all glaciers except Cayambe have a lower retreat rate in recent years compared to before 2000. Cáceres et al. (2008) explained that Antisana had positive bass balance and a front advance in the years 1999 and 2000. The advance is probably related with the La Niña years at the same time (Francou et al., 2004).

The exact reason for the differences between the Colombian and Ecuadorian glaciers is unclear and difficult to answer with the data available. This would require more detailed studies on the glaciers including meteorological measurements.

Table 11: Glacier area calculation results of Colombia and Ecuador.

Volcano name	Eruptions	Area 1985 km^2 (date)	Area 2000 km^2 (date)	Area 2015 km^2 (date)	Area change total (%)	%/y 1986-2000	%/y 2000-2015	%/y total
Ruiz, Nevado del (5321m)	1985, 1994,2012, 2014, 2015	17.87 (1987)	14.08 (2001)	8.13 (2016)	-54.5	-1.39	-2.30	-1.83
Santa Isabel, Nevado (4944m)		7.14 (1987)	4.02 (2001)	0.91 (2016)	-87.2	-2.87	-3.01	-2.93
Tolima, Nevado del (5200m)		1.95 (1987)	1.39 (2001)	0.66 (2016)	-66.1	-1.89	-2.58	-2.23
Huila, Nevado del (5365m)	2007, 2008, 2008	16.04 (1987)	13.02 (2001)	8.87 (2016)	-44.7	-1.23	-1.79	-1.50
Cayambe (5790m)		19.42 (1987)	18.05 (1998)	16.02 (2015)	-17.5	-0.59	-0.60	-0.60
Antisana (5753m)		19.51 (1987)	17.48 (1998)	15.04 (2016)	-22.9	-0.85	-0.71	-0.77
Illiniza (5248m)		0.99 (1987)	0.23 (1998)	0.20 (2016)	-79.6	-6.42	-0.13	-2.69
Cotopaxi (5911m)	2015	14.42 (1987)	12.88 (2001)	11.42 (2016)	-20.8	-0.75	-0.66	-0.70
Chimborazo (6310m)		15.42 (1986)	9.83 (2001)	7.13 (2016)	-53.8	-2.35	-1.09	-1.71
Tungurahua (5023m)	1993, 1999, 2010, 2010, 2015	0.70 (1991)	0.10 (1998)		-100.0	-11.93		-11.93
Sangay (5286m)	1934-2016<	1.73 (1991)	0.92 (2001)	0.62 (2016)	-63.8	-4.93	-1.07	-2.50
Total	15	115.20	92.0	69.01	-40.1%	-1.54	-1.25	-1.38

4.3.3 Glacier change in Peru and Bolivia/Chile

After the initial search of ice-capped volcanoes in the CVZ, 13 volcanoes were found that could have a permanent ice cap. As the border region of Bolivia and northern Chile/Argentina is one of the driest places on Earth, glacier presence is only determined by the availability of solid precipitation as temperatures are generally very low in high altitudes. The absence of precipitation leads to one of the highest ELA in the world, currently at more than 5000-6000m. Even though the highest mountain peaks are over 6000 m, glaciers could not be found on many volcanoes. What could be found are snow patches that are most probably multiyear, as they appeared in several satellite images of different years. Because theses snow patches could not be undoubtedly being classified as glaciers with an image resolution of 30m, these volcanoes were excluded. Moreover, such small potential ice masses are most likely not having a big impact on the volcanic behavior and are therefore not relevant for the study. The excluded volcanoes are (from north to south): Pular, Llullaillaco, Sierra Nevada, Cerro el Condor, Nevado de Incahuasi, Ojos del Salado, Tipas, and Copiapo. To investigate potential glacier changes on these volcanoes, local observation as well as satellite images and aerial photos with better resolution than available from Landsat is required. They have thus to be investigated in a future study.

The four remaining active volcanoes in the CVZ that still contain a large ice cover are Coropuna, Sabancaya, Parinacota, and Guallatiri. Their glacier area change is shown in Figure 26. During the study period, they lost on average 59% of their area, in total 45.3% of the glacierized area disappeared. Sabancaya and Gaullatiri lost the most with a change rate of -2.54%/y and -2.69%/y. Nevado Coropuna was the least affected by the change, only loosing -0.86%/y or 26.5% of its area.

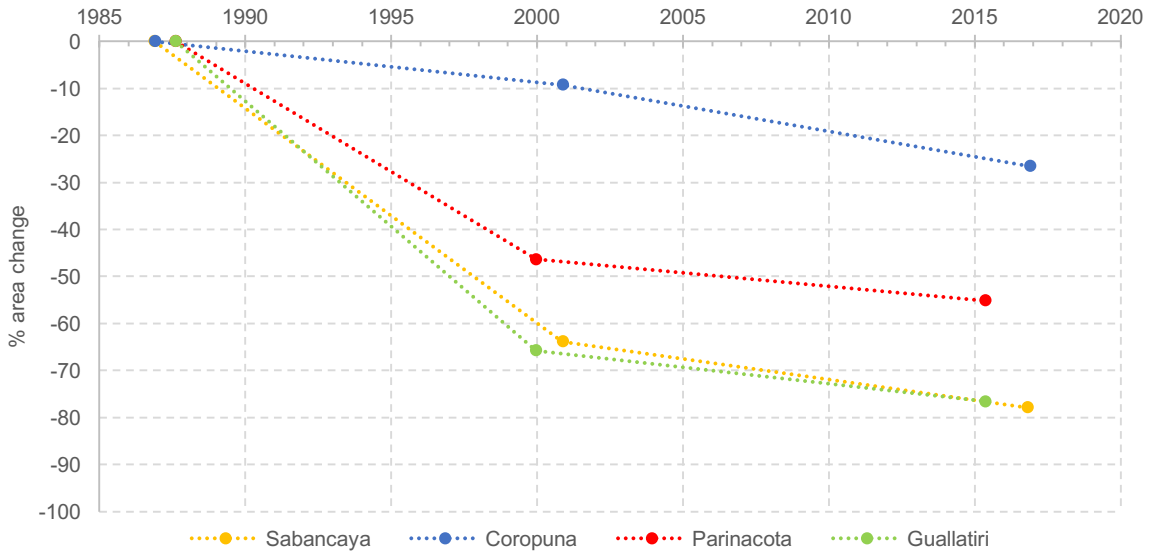

Figure 26: Glacier area change of Peru and Bolivia/Chile.

Interesting is the observation, that all volcanoes except Coropuna had a faster change rate before 2000 and a slower one in the second period. Sabancaya glacier had a continuous ice cap in 1986 that broke apart into many pieces in the following years. This led to a fast shrinkage of the glacier in a short period of time. Even though the distance between Sabancaya and Coropuna is not large, the glaciers showed very different behaviour. The glaciers of Coropuna still form a large ice cap around the summit that is affected by climate forcing. Sabancaya on the other hand with its relatively flat sections covered by glaciers, reached a threshold where the climate could not support a permanent snow cover any more and the glacier broke into many pieces. A similar process occurred on Nevado Santa Isabel in Colombia. Furthermore, Sabancaya is one of the most active volcanoes in the region with a total of nine eruptions since 1986. A map showing the glacier outlines since 1986 of Sabancaya are can be seen in Figure 27.

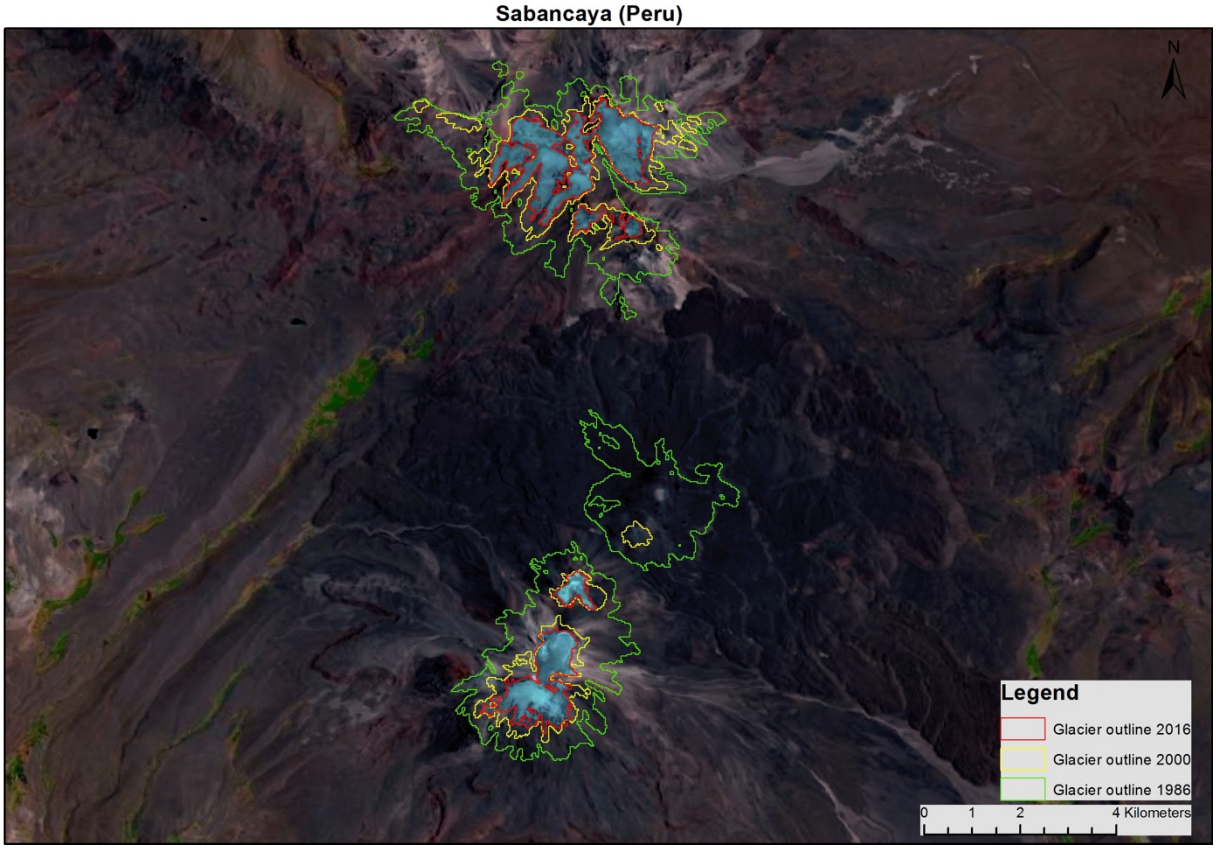

Figure 27: Glacier outlines of Sabancaya from 1986 (green), 2000 (yellow) and 2016 (red).

Currently, all four volcanoes contain an ice area of 61.02 km^2 down from 111.50 km^2 in 1986. Coropuna is by far holding the largest portion of the ice with still 48.15 km^2. All results from this sub-region are listed in Table 12.

Table 12: Glacier area calculation results of Peru and Bolivia/Chile.

Volcano name	Eruptions	Area 1985 km^2 (date)	Area 2000 km^2 (date)	Area 2015 km^2 (date)	Area change total (%)	%/y change 1986-2000	%/y change 2000-2015	%/y change total
Coropuna (6377m)		65.55 (1986)	59.46 (2000)	48.15 (2016)	-26.5	-0.65	-1.05	-0.86
Sabancaya (5967m)	1986, 1987, 1988, 1990, 2000, 2003, 2014, 2015, 2016<	29.36 (1986)	10.61 (2000)	6.49 (2016)	-77.9	-4.46	-0.86	-2.54
Parinacota (6336m)		11.69 (1987)	6.27 (1999)	5.24 (2015)	-55.2	-3.66	-0.56	-1.94
Guallatiri (6071m)	2015	4.90 (1987)	1.68 (1999)	1.15 (2015)	-76.6	-5.20	-0.68	-2.69
Total	10	111.50	78.02	61.02	-45.3	-2.23	-0.95	-1.53

4.3.4 Glacier change in Chile and Argentina

The region of Chile and Argentina contains most of the glacier-covered active volcanoes of which 41 were studied in this thesis. Because of the large number of volcanoes, a sub classification was done to better display the results. This division was done according to their geographical distribution and the volcanological context. The groups are 33-35°S, 35-38°S, 38-41°S, 41-45°S in the SVZ and more than 45°S in the AVZ. Because the volcanoes along the Chilean-Argentinean border lie along a line in north south direction, they can be grouped according to their latitude.

Glacier change between 33-35° S

Between 33° and 35° much larger glaciers can be found than further north as we enter the wet Andes. Large debris covered glacier tongues flow in the valleys of the volcanoes Tupungatito, San Jose and Palomo. The debris-covered tongues were manually mapped as it was not possible to apply the band ratio method on heavily debris-covered parts. Only the thermal band was used as a help to identify the debris cover. Other than that, high resolution satellite images and aerial photos like in Google Earth were used to better understand the extent of the debris cover. Furthermore, the RGI glacier inventory was taken into account to localize the debris covered parts. However, it can only be used as a guide, because outlines refer to the year 2000 and are generalized to some degree.

For Tupungatito and San Jose, the image of 2001 contains some snow and can therefore need to be interpreted with caution. As no better satellite image could be found, the calculated values are listed in the results Table 13. Nevertheless, the comparison from 1986 and 2015 is still valuable. Tupungatito and San Jose lost during the 29 year study period the least amount of area with a change rate of only -0.18%/y (or -5.3%) and -0.42%/y (or -12.5%). These are some of the lowest values found in all of Latin America, and much lower than the surrounding ice caps. An explanation could be the present debris

cover that has an insulating effect on the glacier. For a better understanding of the debris cover of these glaciers, higher resolution images or on-site measurements are required, as an area calculation does not give any clues about thickness change. With almost no front variation change, the thickness change is more important to understand the impact of climate change and volcanic activity on the glacier.

The further south located Calabozos volcano, on the other hand, lost most of its area (-96.2%) during the study period. This leads to a change rate of -3.22%/y which is one of the highest of all observed glaciers. A map showing the glacier outlines since 1986 of Calabozos are can be seen in Figure 28.

The glaciers on Descabezado Grande and Cerro Azul lost much of its area between 1986 and 1999 and then remained almost constant. The calculated area gain should not be seen as a glacier advance as it is very small and within the uncertainty of 0.1 km^2. Most likely some snow was mapped as well because, considering the small area, a 15 m resolution image of 2015 could detect more small snow patches than the 30 m image from 1999. Only looking at the summit crater glacier of Descabezado Grande, it seems like there were no large changes or a small increase in area between 1999 and 2015.

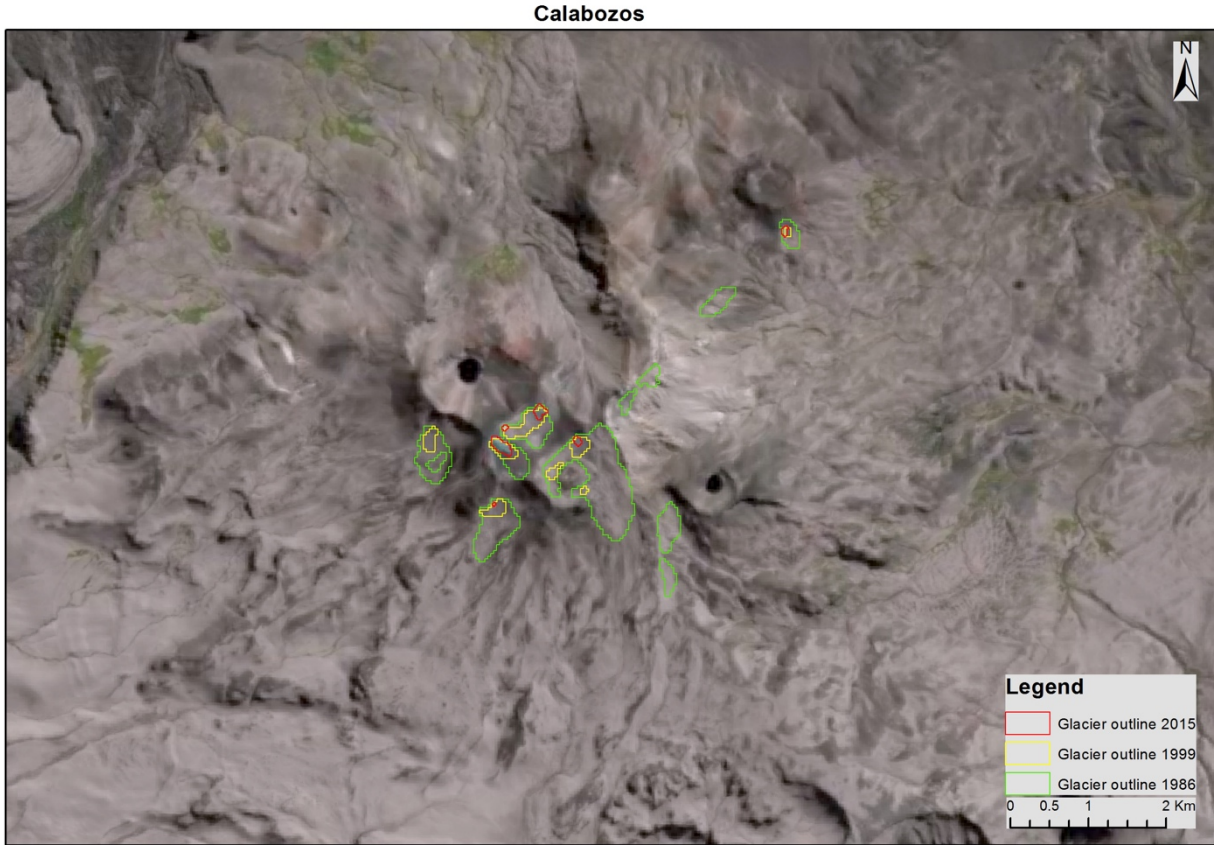

Figure 28: Glacier outlines of Calabozos from 1986 (green), 2000 (yellow) and 2015 (red).

Generally, the change rates vary greatly even though the glaciers are located close to each other. With a difference of 90.9% between the area change of Tupungatito and Calabozos, the spread within the same sub-region is higher than for any other sub-region. Moreover, the change rates shifted after the year 2000 from -2.78%/y before to -0.67%/y after. All results from this sub-region can be seen in Figure 29 and Table 13.

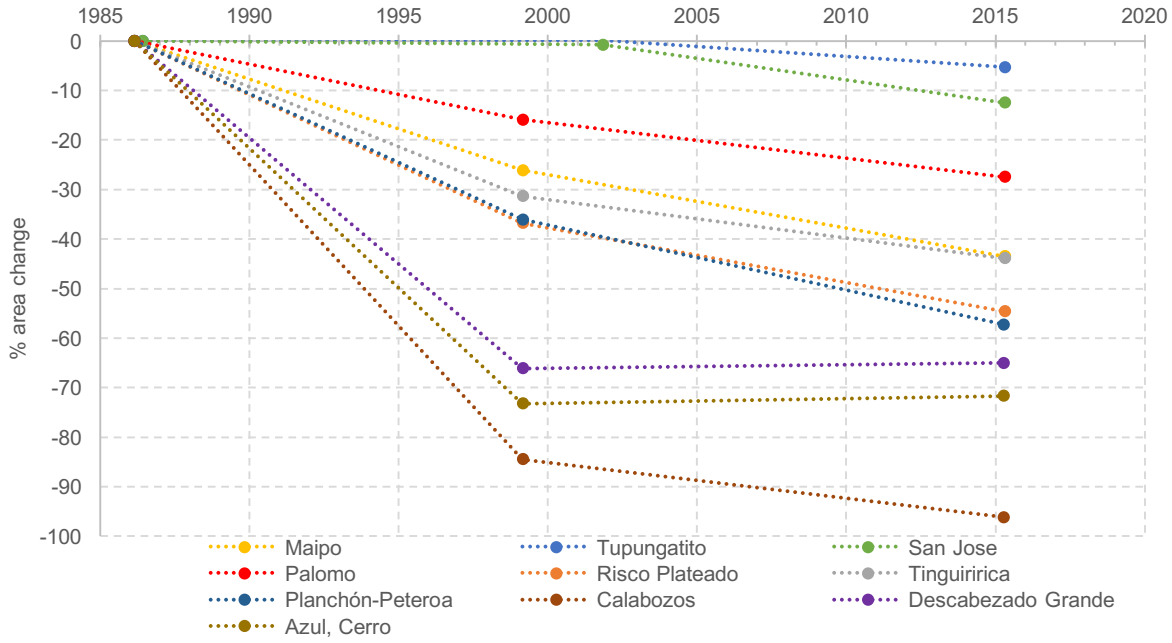

Figure 29: Glacier area change of Chile/Argentina between 33° S and 35° S.

Table 13: Glacier area calculation results of Chile and Argentina between 33° S and 35° S.

Volcano name	Eruptions	Area 1985 km² (date)	Area 2000 km² (date)	Area 2015 km² (date)	Area change total (%)	%/y change 1986-2000	%/y change 2000-2015	%/y change total
Tupungatito (5660m)	1986, 1987	170.77 (1986)	171.12 (2001)	161.67 (2015)	-5.3	0.01	-0.40	-0.18
San Jose (6070m)		172.22 (1986)	170.85 (2001)	150.77 (2015)	-12.5	-0.05	-0.84	-0.42
Maipo (5323m)		15.33 (1986)	11.32 (1999)	8.66 (2015)	-43.5	-1.96	-1.05	-1.45
Palomo (4860m)		242.63 (1986)	204.09 (1999)	175.93 (2015)	-27.5	-1.19	-0.70	-0.92
Risco Plateado (4999m)		6.98 (1986)	4.42 (1999)	3.17 (2015)	-54.6	-2.76	-1.08	-1.83
Tinguiririca (4280m)	1994	51.79 (1986)	35.55 (1999)	29.06 (2015)	-47.1	-2.65	-0.71	-1.58
Planchón-Peteroa (3977m)	1991, 1998, 2010, 2011	44.90 (1986)	28.72 (1999)	19.20 (2015)	-57.2	-2.70	-1.28	-1.92

Calabozos (3508m)		2.15 (1986)	0.33 (1999)	0.08 (2015)	-96.2	-6.34	-0.71	-3.22
Descabezado Grande (3953m)		4.06 (1986)	1.38 (1999)	1.42 (2015)	-65.0	-4.96	0.07	-2.18
Azul, Cerro (3788m)		1.54 (1986)	0.41 (1999)	0.44 (2015)	-71.7	-5.49	0.10	-2.40
Total	7	712.38	628.19	550.40	-22.7	-0.85	-0.68	-0.76

Glacier change between 35-38° S

Between 35° and 38°S, the glaciers on active volcanoes are smaller than further north. This is due to the lower altitude of the peaks. Glacier area changes for all volcanoes of this sub-region can be seen in Figure 31. Domuyo with 4709 m, is the highest in the sub-region. The lowest volcano that still holds a permanent ice cover is Tolguaca with 2806m. The twin volcanoes of Antuco and Sierra Velluda have both been studied even though Sierra Velluda did not show any Holocene activity. By comparing the two glaciers it is possible to see eventual influences of the volcanoes as Antuco is still an active volcano but did not have any eruptions in the study period. The results of Sierra Velluda were excluded from the general analysis (average etc.) and just used for the comparison with Antuco volcano.

The two mountains show different area change rates even though they next to each other. Antuco is losing on average 1.92%/y (or -53.1%) and Sierra Velluda 1.13%/y (or -31.4%). Especially between 1989 and 2000, Antuco had with -2.77%/y a much higher change rate than Sierra Velluda (-1.13%/y). One needs to keep in mind that the glacier of Sierra Velluda is much larger and therefore also has a longer response time to the climate impact. How much of the change is due to the volcanic activity remains unclear, no eruptions have been reported on Antuco but fumarolic activity remains present. A map of the glacier outlines of Antuco and Sierra Velluda can be seen in Figure 30.

In total (excluding Sierra Velluda) 42.79 km^2 of ice, down from 110.05 km^2 in 1985 could be found on the nine volcanoes. This leads to an overall change rate of -2.14%/y (or -61.8%). The same shift of the change as in the previous sub-region could be observed with a higher change rate (-3.18%/y) before 2000 and a lower one (-1.44%/y) in the more recent period. One exception is the volcano Copahue, that had with -2.00%/y a large change rate between 1989 and 1999 but lost much of its area after 1999 with an even higher change rate of -3.88%/y. Copahue is a very active volcano with seven eruptions after 1992, the most recent one being in 2014 and 2015. Of the 8.99km^2 in 1999, only 1.30km^2 remained in 2016. Another very active volcano of this sub-region is Nevados de Chillan. The glacier on it had a change rate of -5.37%/y before 2000 and -0.93%/y after 2000. The volcano experience eruptions in 2003 and 2016 and an uncertain eruption in 2009. Furthermore, it also had a very active phase between 1973 and 1986, which also affected the glacier extent. How this eruption affected the glacier can be seen in Figure 11. Glacier change results for all volcanoes of this sub-region are listed in Table 14.

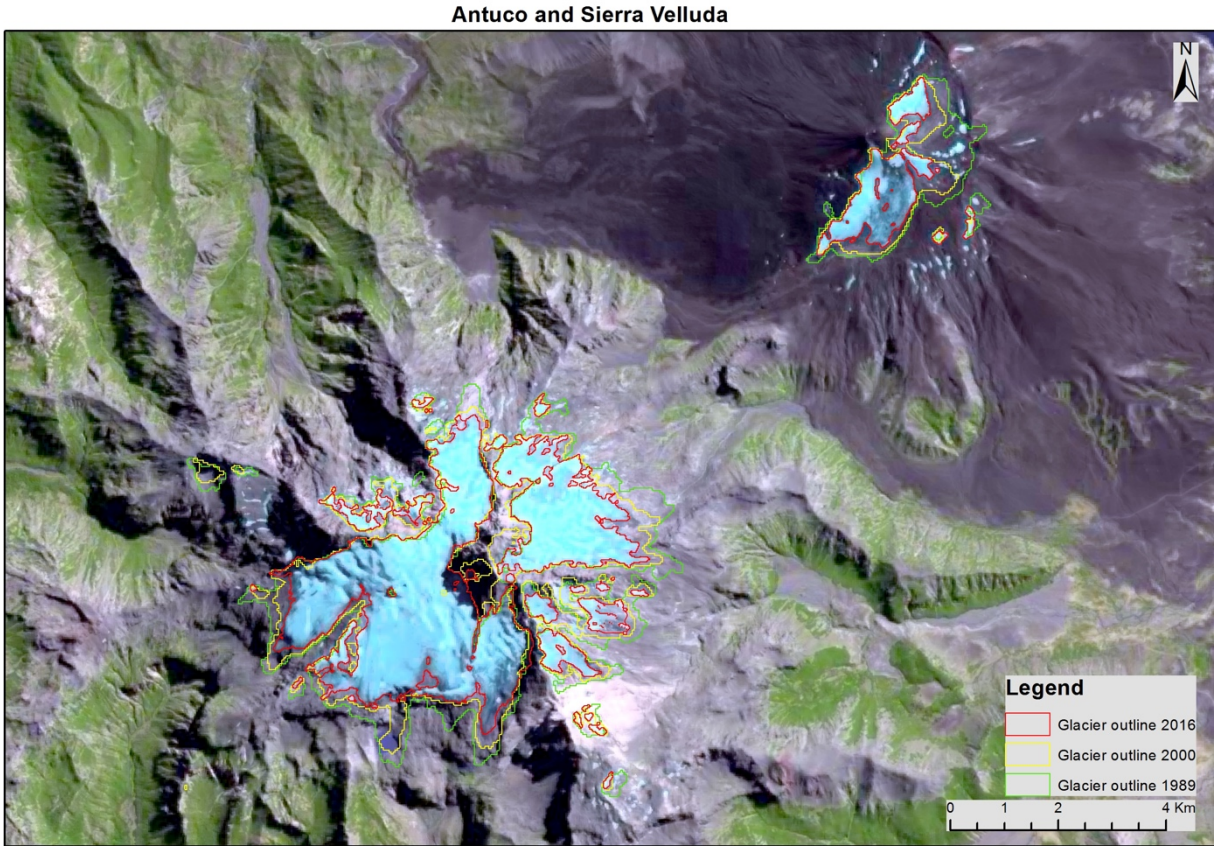

Figure 30: Glacier outlines of Antuco (right) and Sierra Velluda (left) from 1986 (green), 2000 (yellow) and 2015 (red).

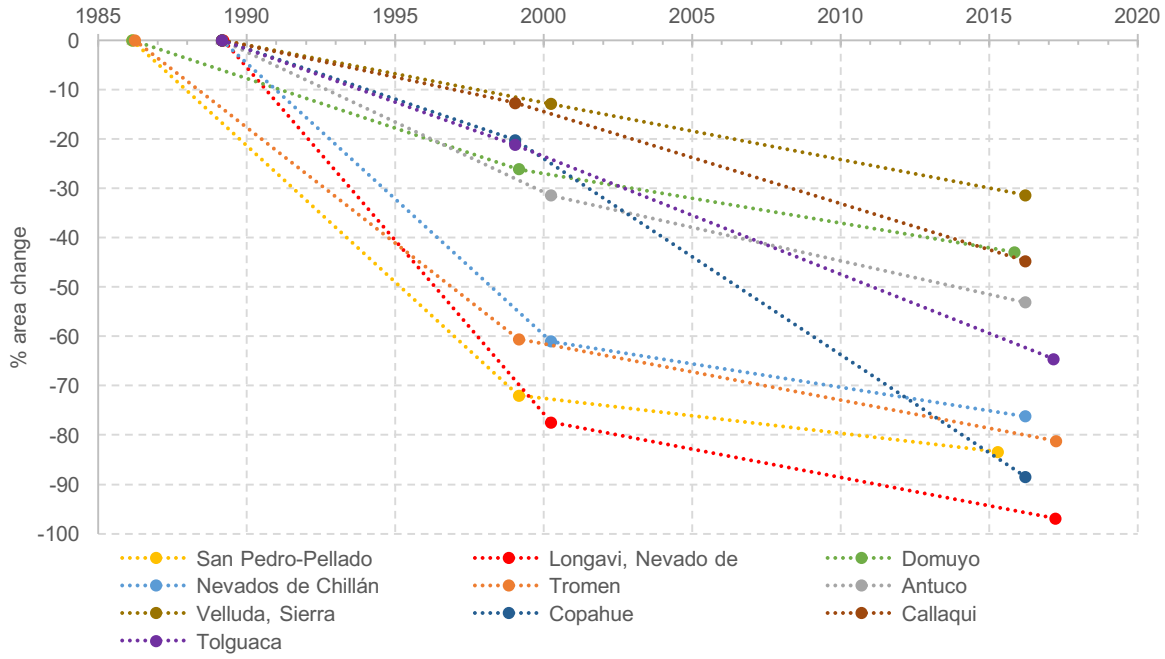

Figure 31: Glacier area change of Chile/Argentina between 35° S and 38° S.

Table 14: Glacier area calculation results of Chile and Argentina between 35° S and 38° S.

Volcano name	Eruptions	Area 1985 km² (date)	Area 2000 km² (date)	Area 2015 km² (date)	Area change total (%)	%/y change 1986-2000	%/y change 2000-2015	%/y change total
San Pedro-Pellado (3621m)		16.46 (1986)	4.61 (1999)	2.73 (2015)	-83.4	-5.40	-0.69	-2.79
Longavi, Nevado de (3242m)		4.23 (1989)	0.95 (2000)	0.13 (2017)	-96.9	-6.85	-1.12	-3.38
Domuyo (4709m)		38.64 (1986)	28.56 (1999)	22.05 (2015)	-42.9	-1.96	-0.98	-1.41
Nevados de Chillán (3212m)	2003, 2009, 2016>	12.14 (1989)	4.73 (2000)	2.89 (2016)	-76.2	-5.37	-0.93	-2.75
Tromen (3978m)		2.44 (1986)	0.96 (1999)	0.46 (2017)	-81.2	-4.57	-1.11	-2.56
Antuco (2979m)		5.07 (1989)	3.47 (2000)	2.38 (2016)	-53.1	-2.77	-1.32	-1.92
Velluda, Sierra (3585m)	*Not active*	*25.95 (1989)*	*22.61 (2000)*	*17.82 (2016)*	*-31.4*	*-1.13*	*-1.13*	*-1.13*
Copahue (2953m)	1992, 1994, 1995, 2000, 2012, 2014, 2015	11.27 (1989)	8.99 (1999)	1.30 (2016)	-88.5	-2.00	-3.88	-3.19
Callaqui (3164m)	2009, 2012	16.03 (1989)	14.00 (1999)	8.86 (2016)	-44.8	-1.26	-1.82	-1.61
Tolguaca (2806m)		5.66 (1989)	4.46 (1999)	2.01 (2017)	-64.6	-2.09	-2.34	-2.25
Total	12	111.94	70.73	42.79	-61.8	-3.18	-1.44	-2.14

Glacier change between 38-41° S

The sub-region between 38° S and 41° S contains with Llaima and Villarica some of the most active ice-capped volcanoes in entire Latin America. Large parts of the Villarica glacier are covered by a thick layer of ash that works as an insulating layer for the ice. As the band ratio method is not applicable for thick debris or ash covers, the ash covered parts of Villarica and the nearby Lanin were manually mapped. Furthermore, already existing studies (Rivera et al., 2008) were taken into account to define the glacier outlines. Even though Villarica underwent 15 eruptions during the study period, the glacier change rate is with -0.77%/y smaller than for many other glaciers. As mentioned before, this is likely due to the insulating effect of an ash or debris cover.

In general, every glacier of these sub-regions except Puyehue Cordón Caulle had a higher change rate before 2000 than recently (see Figure 33). Overall, the change rate of this sub-regions was -1.91%/y before 2000 and -0.72%/y after 2000 (or a loss of 24.5% and 12.5%). Puyehue Cordón Caulle was only holding a glacier inside the crater and some small patches of snow outside the crater rim. By 1999 the glacier in the crater lost some of its area but still covered most of the crater base and its sides. In 2011, the volcano saw a VEI 5 eruption that affected the glacier extent greatly. In 2015 ice could only be found

on the inner north slope of the crater and the glacier on the crater base disappeared completely (See Figure 32).

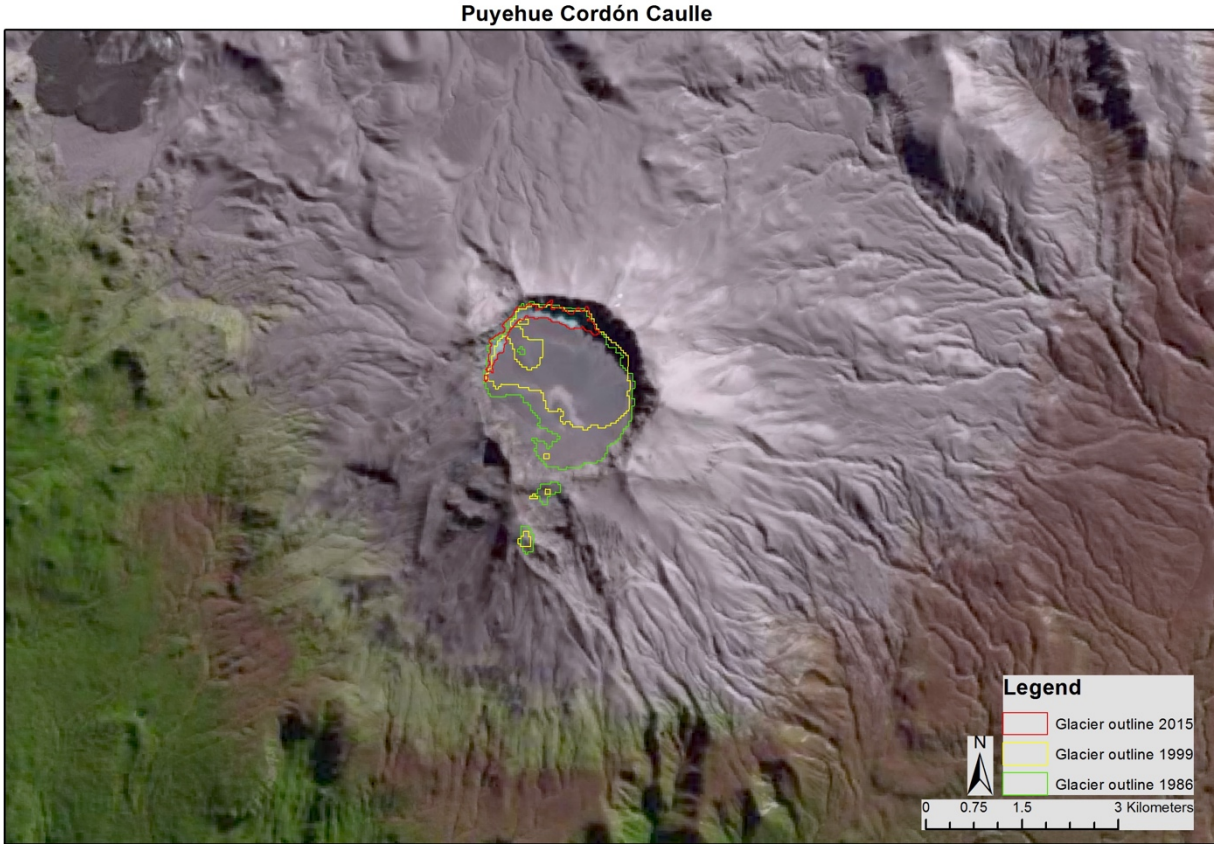

Figure 32: Glacier outlines of Puyehue Cordón Caulle from 1986 (green), 1999 (yellow) and 2015 (red).

Lonquimay, which erupted in 1988, lost most of its area after the eruption from 1.59 km^2 in 1986 to just 0.37 km^2 in 1999. All glaciers on the flanks of the volcano disappeared, only the crater glacier remained as the eruption took place on the NE flank of the volcano. Between 1999 and 2015 the glacier did not change dramatically, the glacier in the crater shrank slightly but a small glacier on the south side recovered where there already was a glacier in 1986. Area change results for all glaciers are listed in Figure 33 and Table 15.

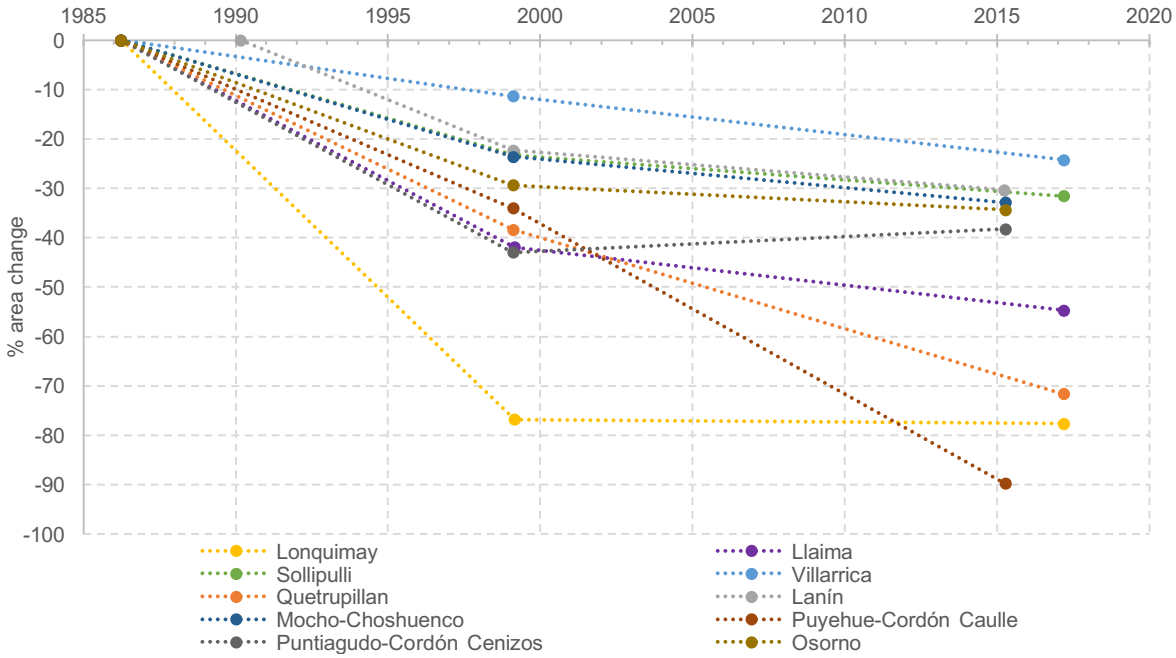

Figure 33: Glacier area change of Chile/Argentina between 38° S and 41° S.

Table 15: Glacier area calculation results of Chile and Argentina between 38° S and 41° S.

Volcano name	Eruptions	Area 1985 km² (date)	Area 2000 km² (date)	Area 2015 km² (date)	Area change total (%)	%/y change 1986-2000	%/y change 2000-2015	%/y change total
Lonquimay (2832m)	1988	1.59 (1986)	0.37 (1999)	0.36 (2017)	-77.7	-5.80	-0.05	-2.45
Llaima (3125m)	1990, 1992, 1994, 1995, 1997, 1998, 1998, 2002, 2003, 2007, 2008	20.02 (1986)	11.62 (1999)	9.06 (2017)	-54.7	-3.17	-0.69	-1.73
Sollipulli (2282m)		26.77 (1986)	20.54 (1999)	18.31 (2017)	-31.6	-1.76	-0.45	-1.00
Villarrica (2847m)	1991, 1992, 1994, 1995, 1996, 1996, 1998, 2003, 2004, 2008, 2009, 2009, 2012, 2013, 2014	52.18 (1986)	46.25 (1999)	39.51 (2017)	-24.3	-0.86	-0.70	-0.77
Quetrupillan (2360m)		13.68 (1986)	8.43 (1999)	3.88 (2017)	-71.6	-2.91	-1.79	-2.26
Lanín (3776m)		15.80 (1990)	12.27 (1999)	11.01 (2015)	-30.3	-2.43	-0.48	-1.18
Mocho-Choshuenco (2422m)		37.02 (1986)	28.29 (1999)	24.86 (2015)	-32.9	-1.79	-0.56	-1.10
Puyehue-Cordón Caulle (2236m)	1990, 2011	4.10 (1986)	2.71 (1999)	0.42 (2015)	-89.8	-2.58	-3.37	-3.02
Puntiagudo - Cordón Cenizos (2493m)		3.71 (1986)	2.12 (1999)	2.29 (2015)	-38.3	-3.26	0.29	-1.29
Osorno (2659m)		12.46 (1986)	8.80 (1999)	8.18 (2015)	-34.4	-2.22	-0.30	-1.15
Total	29	187.35	141.39	117.89	-37.1	-1.91	-0.72	-1.22

Glacier change between 41-45° S

The glaciers on active volcanoes between 41° and 45° S show a very similar behavior (see Figure 35). Their average change rate of the volcanoes is -0.77%/y smaller than further north in Chile. Also, the spread of the results is considerably smaller, the standard deviation being is only 0.27.

There have been no eruptions been taking place within the study period, the eruption of Calbuco in 2015 took place after the area for 2015 was calculated. Nevertheless, the volcanic activity might have had an impact on the glacier change as Calbuco showed the largest area loss of all the volcanoes in this subgroup. An increase of geothermal heat flux is common prior to an eruption and could, therefore, influence the melt rate. However, how much this influence could have been remains unclear, as no detailed investigations are available.

The three biggest glaciers in this sub-region, Tronador, Michinmahuida and Melimoyu showed the smallest change rate with -0.42%/y, -0.53%/y and -0.36%/y (or -12.4%, -15.9%, -11.0%) respectively. These three volcanoes also hold the largest glacier area for this sub-region. A few kilometers west of Michinmahuida the glacier free Volcan Chaitén is located. It erupted in 2008 and covered the nearby glacier with a 10-20 cm thick layer of ash deposits (Alfano et al., 2011). This had an insulating effect, and glacier Amarillo on Michinmahuida experienced two advances in 2007 and 2009 (Rivera et al., 2012). However, as the advance already started before the eruption, a direct connection is unlikely. Rivera et al. (2009) proposed that the advances could be connected to an increase in volcanic activity of Michinmahuida and Chaitén. This leads to more geothermal heat and more basal meltwater resulting in a sudden glacier advance. Between 2007 and 2009, the glacier Amarillo advanced about 234 m (Rivera et al., 2012). A map of Volcán Chaitén and the glacier outlines of Michinmahuida can be seen in Figure 34.

In total 512.19km^2 of glacier area remained in 2015 down from 625.24 km^2 in 1985. This results in an overall area loss of 18.1% which is half the amount of the glacier loss in tropical regions and more than three times less than between 35°- 38° S. All glacier change results for this sub-region are listed in Table 16.

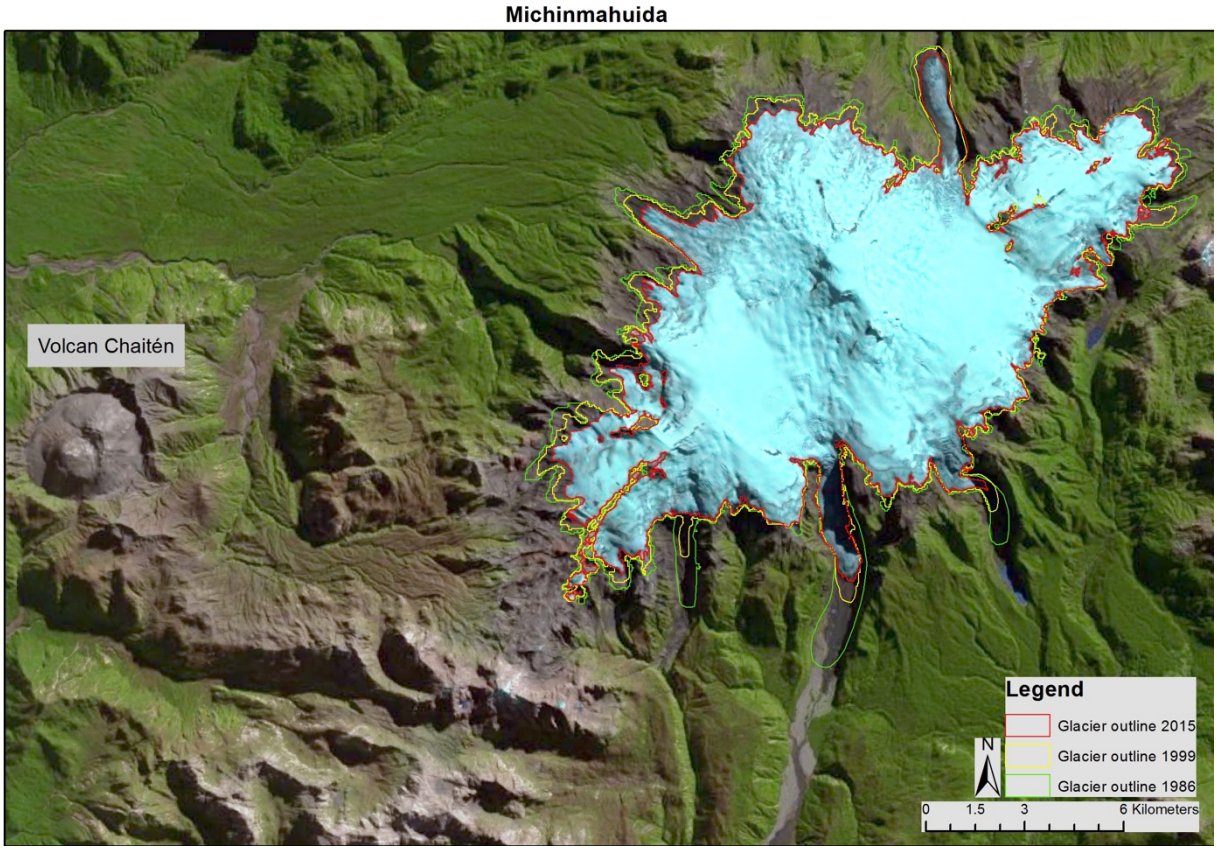

Figure 34: Glacier outlines of Michinmahuida from 1986 (green), 1999 (yellow) and 2015 (red).

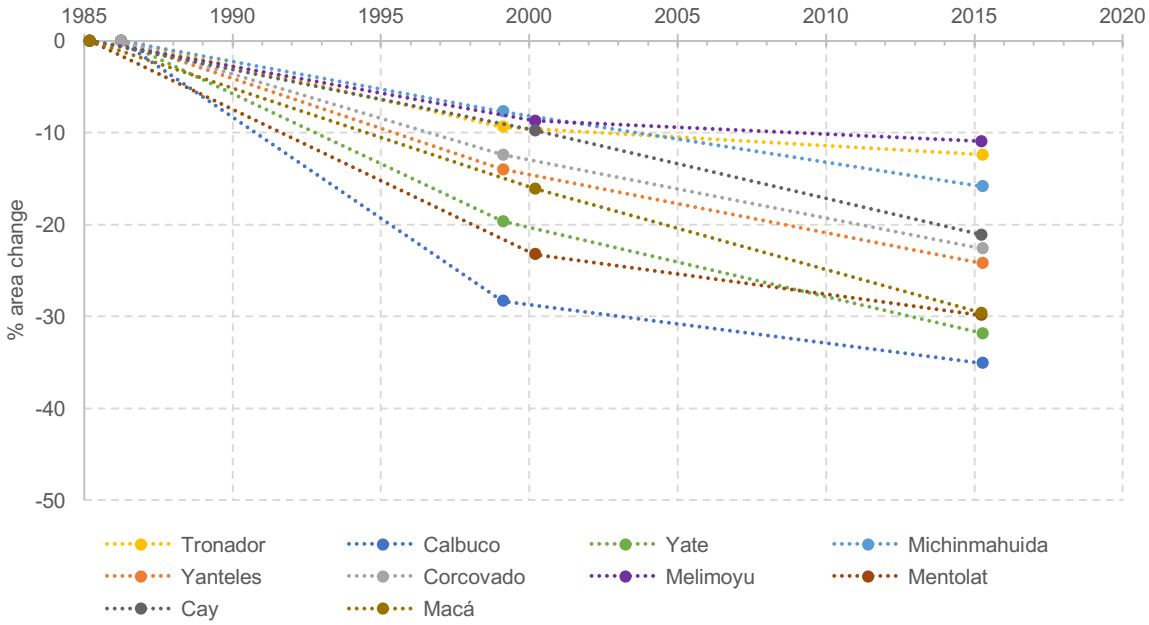

Figure 35: Glacier area change of Chile/Argentina between 41° S and 45° S.

Table 16: Glacier area calculation results of Chile and Argentina between 41° S and 45° S.

Volcano name	Eruptions	Area 1985 km^2 (date)	Area 2000 km^2 (date)	Area 2015 km^2 (date)	Area change total (%)	%/y change 1986-2000	%/y change 2000-2015	%/y change total
Tronador (3491m)		124.79 (1986)	113.09 (1999)	109.28 (2015)	-12.4	-0.71	-0.18	-0.42
Calbuco (1974m)	2015	3.06 (1986)	2.19 (1999)	1.98 (2015)	-35.1	-2.15	-0.41	-1.18
Yate (2187m)		27.80 (1986)	22.34 (1999)	18.95 (2015)	-31.8	-1.49	-0.74	-1.07
Michinmahuida (2452m)		166.76 (1986)	153.93 (1999)	140.31 (2015)	-15.9	-0.58	-0.49	-0.53
Yanteles (2049m)		76.86 (1986)	66.08 (1999)	58.26 (2015)	-24.2	-1.06	-0.61	-0.81
Corcovado (1826m)		8.01 (1986)	7.02 (1999)	6.20 (2015)	-22.6	-0.94	-0.62	-0.76
Melimoyu (2400m)		121.56 (1985)	110.95 (2000)	108.25 (2015)	-11.0	-0.57	-0.14	-0.36
Mentolat (1660m)		8.65 (1985)	6.64 (2000)	6.07 (2015)	-29.9	-1.51	-0.43	-0.97
Cay (2090m)		13.32 (1985)	12.01 (2000)	10.50 (2015)	-21.1	-0.64	-0.74	-0.69
Macá (2960m)		74.43 (1985)	62.46 (2000)	52.39 (2015)	-29.6	-1.05	-0.88	-0.96
Total	1	625.24	556.71	512.19	-18.1	-0.78	-0.44	-0.60

Glacier change south of 45° S

South of 45° S, the volcanism is part of the AVZ. Active volcanoes with glacier coverage are Mount Hudson and Monte Bruney apart from Cerro Arenale, Lautaro, Viedma, Aguilera and Reclus, which are located underneath the Northern and Southern Patagonian ice fields. Glacier area changes for the studied volcanoes can be seen in Figure 37.

In 1991, Mont Hudson experienced one of the biggest eruptions seen in recent decades (VEI 5). It had a large influence on the glacier as according to Rivera & Bown (2013) 20 km^2 got destroyed in the caldera due to the eruption of 1991, but it was able to recover some of its loss. Mount Hudson experienced another minor eruption in 2011, which covered large parts of the caldera with a thick ash layer. Due to the ash layer, the band ratio method was not working as it cannot detect ice underneath a thick ash cover. Therefore, the ice extent inside of the caldera was manually mapped and estimated which may result in additional uncertainties. Nevertheless, as this was done for all time points the data are still comparable. Glacier Huemules, which is the main glacier tongue and outflow of the caldera is also largely debris covered and retreated about 3.8 km between 1985 and 2015. A map of the glacier outlines of Mount Hudson can be seen in Figure 36.

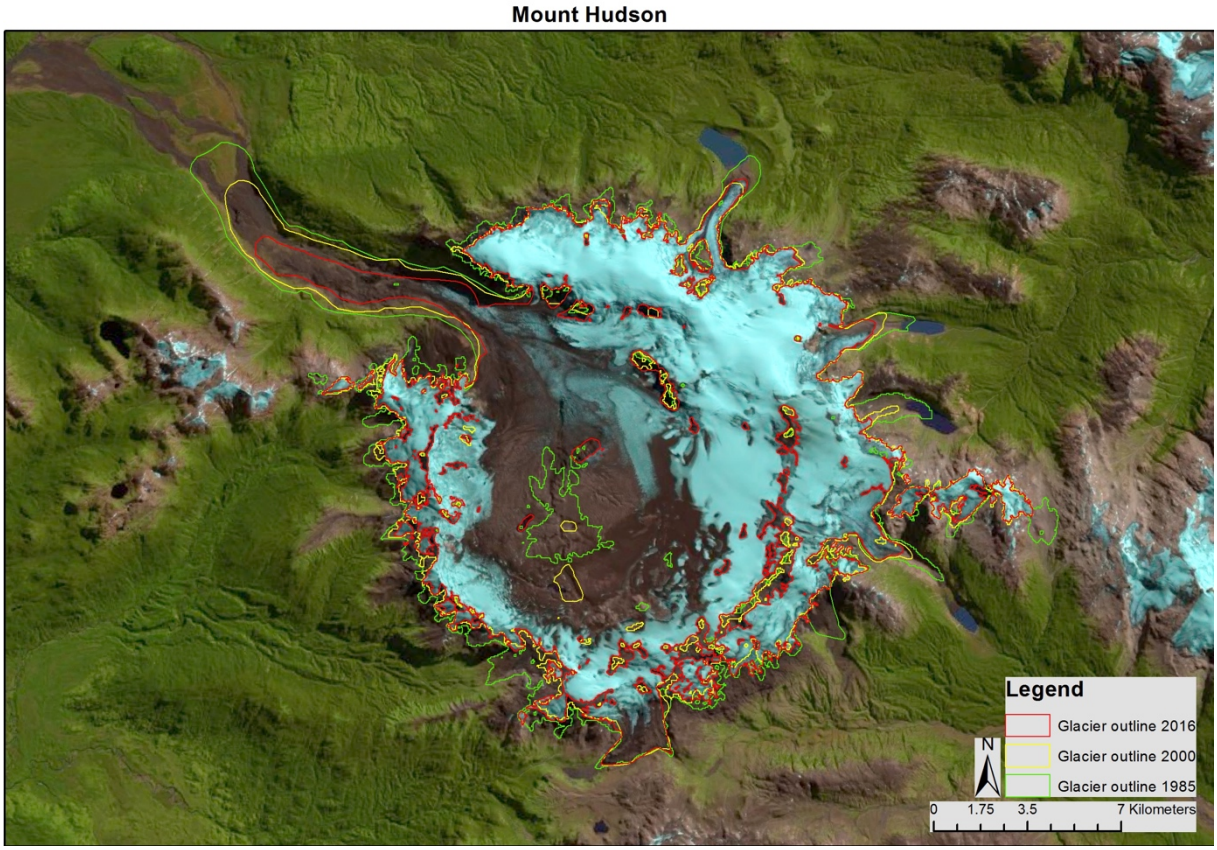

Figure 36: Glacier outlines of Mount Hudson from 1985 (green), 2000 (yellow) and 2016 (red).

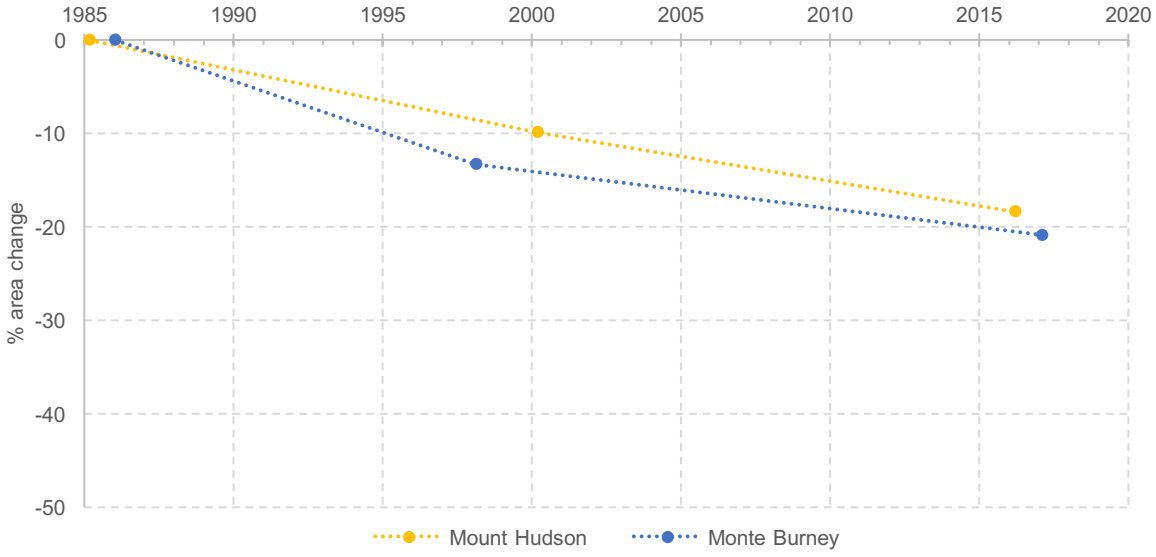

Figure 37: Glacier area change of Chile south of 45° S.

Both glaciers, on Mount Hudson and Monte Bruney had a larger change rate before 2000 with -0.64%/y and -1.07%/y (or -9.9% and -13.3%) and a smaller one after 2000 with -0.52%/y and -0.39%/y (or -8.5% and -7.6%), or respectively. This result matches with the general trend of less glacier retreat after the year 2000 as observed in all of Latin America.

In total, 298.53 km^2 of ice remain on the two mountains, down from 367.64 km^2. This results in an area loss of 18.8%, which is almost the same as between 41° and 45°S (-18.1%). All glacier change results for this sub-region are listed in Table 17.

Table 17: Glacier area calculation results of Chile south of 45° S.

Volcano name	Eruptions	Area 1985 km^2 (date)	Area 2000 km^2 (date)	Area 2015 km^2 (date)	Area change total (%)	%/y change 1986-2015	%/y change 2000-2015	%/y change total
Mount Hudson (1905m)	1991, 2011	306.18 (1985)	275.92 (2000)	249.90 (2016)	-18.4	-0.64	-0.52	-0.58
Monte Burney (1758m)		49.00 (1986)	44.40 (1998)	42.03 (2017)	-20.9	-1.07	-0.39	-0.66
Total	2	367.64	329.21	298.53	-18.8	-0.75	-0.47	-0.59

4.3.5 Further glacier change analysis

Glacier area changes can be compared with various other factors to better understand their reasons. In this section, the focus lies on geographical differences between the regions.

When comparing the change rate with the latitude of the volcanoes, some interesting trends can be seen. Figure 38 shows the annual change rate versus latitude and initial glacier area, coded by circles of the respective size. In low latitudes (20° N-20° S), change rates of the glaciers average to -2.51%/y between 1985 and 2015. The change rate of Tungurahua glacier is not shown in Figure 38 as it is with -11.93%/y much higher than for the other glaciers. South of 33° S, the change rates are generally lower with an average of -1.53%/y. An exception is the latitude zone between 35°-38° S where change rates are higher than further north and south. South of 39° S, change rates generally decrease with an average of -1.04%/y. The Puyehue-Cordón Caulle being the only exception with a change rate of -3.02%/y.

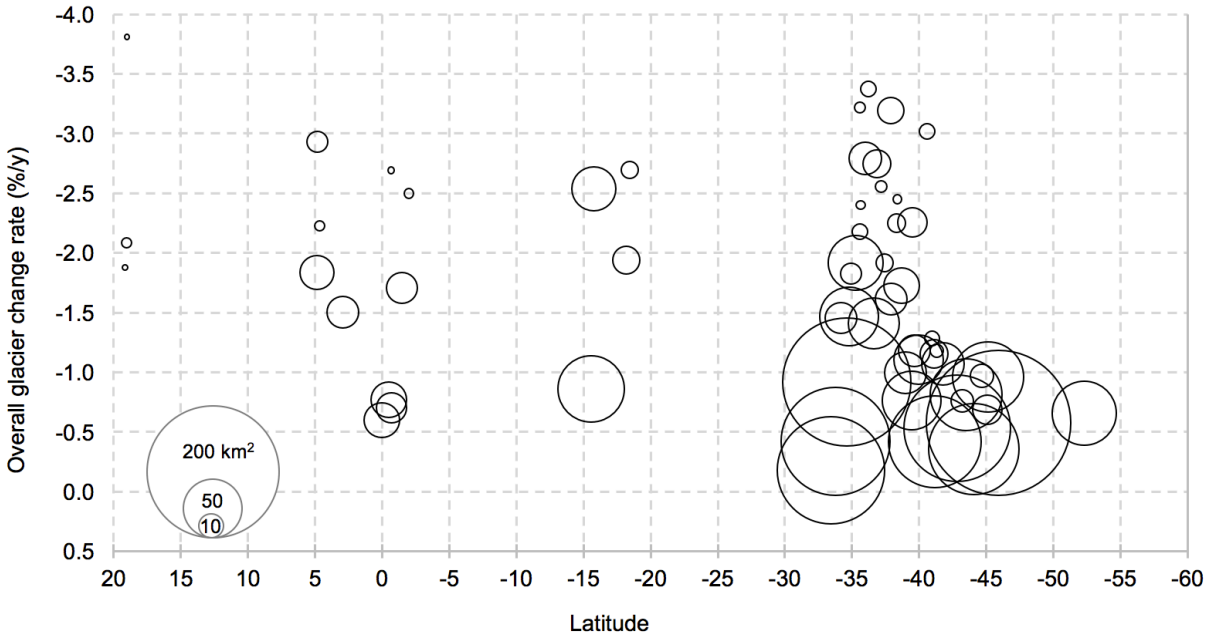

Figure 38: Glacier change rates (1985-2015) in comparison to the respective latitude. Circle size indicates the initial glacier area. Tungurahua in is not visible due to its high change rate of -11.93%/y.

4.4 Presentation of volcano and eruption data

4.4.1 History of volcanic eruptions

To compare the eruption evolution of the volcanoes of Latin America, the database was divided into two groups, one group with volcanoes that have or had a glacier coverage and volcanoes without any glacier. As it remains unclear for all volcanoes if they might have had a glacier in the past, the state in 1985 was chosen. All volcanoes that had some ice in 1985 fall into the group of glacier-covered volcanoes. During the Little Ice Age, some other volcanoes might have had a glacier as well and lost it during the last century. Which volcanoes that might be, is difficult to say during the lack of related studies.

In total, 74 volcanoes had some ice in 1985 and 163 volcanoes did not have any ice. The comparison of the two volcano groups was done on different time scales to better understand trends and changes in the volcanic activity. In Figure 39 the cumulative number of eruptions of both, glacier-covered and glacier free volcanoes in the Holocene as well as the number of eruptions per 500 year intervals are shown. In total 761 eruptions have been recorded on the 74 glacier-covered volcanoes. This means that on average, there have been about 10 eruptions per volcano. On the other hand, 611 eruptions took place on the 163 non glacier-covered volcanoes (≈4 eruptions per volcano). Even though the number of volcanoes is more than the twice the number for glacier free volcanoes, fewer eruptions took place. This means that

glacier-covered volcanoes are generally more active with more eruptions than non glacier-covered volcanoes. In the early Holocene, until -7000BC more eruptions are known from non glacier-covered volcanos. This is due to the fact that more of these volcanoes exist and that generally only big eruptions are known from that time. Between 5160BC and 4690BC there seemed to be a period with a larger number of eruptions on glacier-covered volcanoes with eruptions of volcanoes that have recently been quiet like Santa Isabel, Corcovado or Nevado de Longavi. This period falls into the time of the Holocene climate optimum which took place in South America from 5500 – 4000BC and after a possible glacier advance during the 8.2 kiloyear event (7500 C^{14} BP), a period of globally cold temperatures (Kim et al., 2002; Vázquez-selem & Heine, 2004).

Figure 39: Evolution of Holocene eruptions on currently glacier-covered volcanoes versus non glacier-covered volcanoes. The y-axis has on a logarithmic scale to simplify the visualisation. a) Cumulative number of eruptions (dots) and number of eruptions per 500 years (lines). Arrows indicate periods with high eruption rates on glacier-covered volcanoes. b) eruptions per 500 years per volcano.

Investigating the eruption evolution at different time scale, Figure 40 shows the number of eruptions per century in the last 4000 years. On average, 2.6 (2.3) eruptions per century took place from 2000 to 500 BC on glacier-free (covered) volcanoes. Between 330 BC and 500 AD, a shift in the eruption frequency occurred. On glacier-covered volcanoes the average increased about six eruptions per century, whereas on glacier free volcanoes the average remained the same. Focusing on at large magnitude eruption (VEI 3 and higher), the same trend could be observed. Whereas the eruption rate of glacier free volcanoes did not change significantly, the eruption rate of glacier-covered volcanoes changed from 1.4 eruptions per century (average between 2000 BC to 1500 AD) to 2.8 eruptions per century between 200 BC until 400 AD.

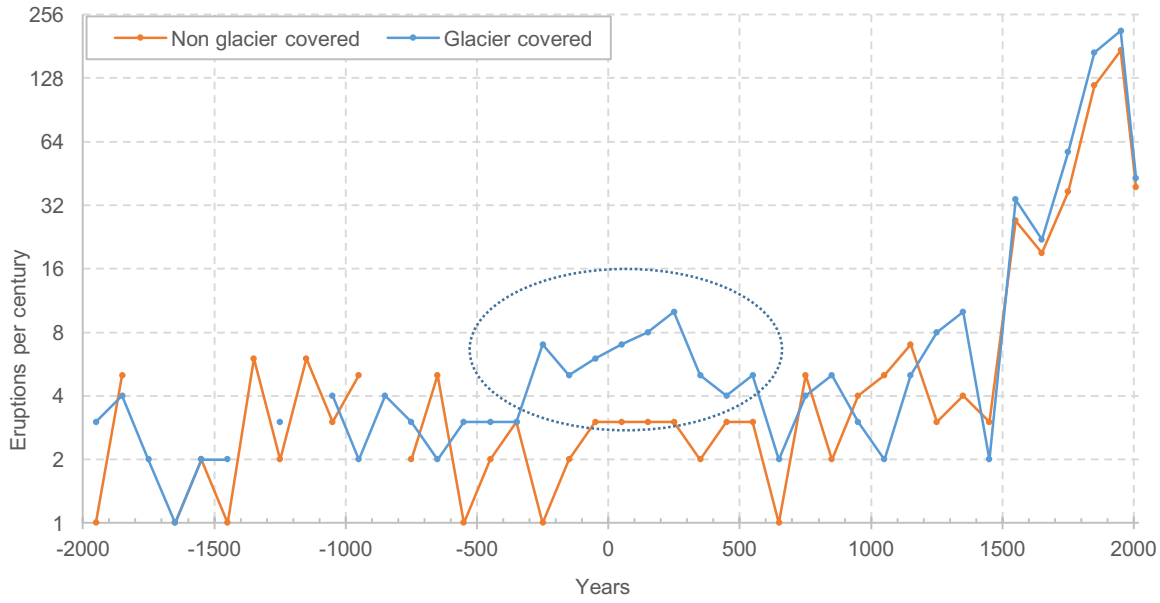

Figure 40: Volcanic evolution of the last 4000 years of both glacier-covered and glacier-free volcanoes. Data are shown as eruptions per century. The y-axis has a logarithmic scale to simplify the visualisation. The last dots represent eruptions after the year 2000.

For the eruption evolution after 1500 the following statements can be made. With the arrival of the Europeans in South America the knowledge and documentation of occurring eruptions increased largely. With more people living in the areas near the volcanoes also the number of known eruption increased. In Figure 41 the number of eruptions per decade is shown since 1500 is shown. Between 1500 and 1730, the average eruption rate for glacier-covered volcanoes was 2.75 eruptions per decade. For glacier free covered volcanoes, the eruption frequency was 2.1 per decade for the same time period. Two peaks in volcanic eruption frequency on glacier-covered volcanoes occurred afterwards. The first being between 1740-1760 and the second after 1820. Especially between 1820 and 1950, the number of

eruptions on glacier-covered volcanoes was much larger than on non glacier-covered volcanoes despite that there are much more active non glacier-covered volcanoes. Between 1820 and 1950 on average 22 eruptions occurred per decade on glacier-covered volcanoes in comparison with just 13.5 on non glacier-covered once. If we compare the eruption frequency between 1500-1730 is compared to 1820-1950, the rate of glacier-covered volcanoes increased eightfold while on glacier free volcanoes only six-fold. This increase in eruption frequency correlates with the end of the LIA which had its maximum between 1550 and mid 1850 depending on the region. In Ecuador the maximum LIA extent was in 1730, in Peru 1630, in Bolivia the second half of the 17th century, in the central Andes in the 16th century, in the southern Andes in the mid 19th century (Vuille et al., 2008; Garibotti & Villalba, 2009; Winchester & Harrison, 1996; Masiokas et al., 2009).

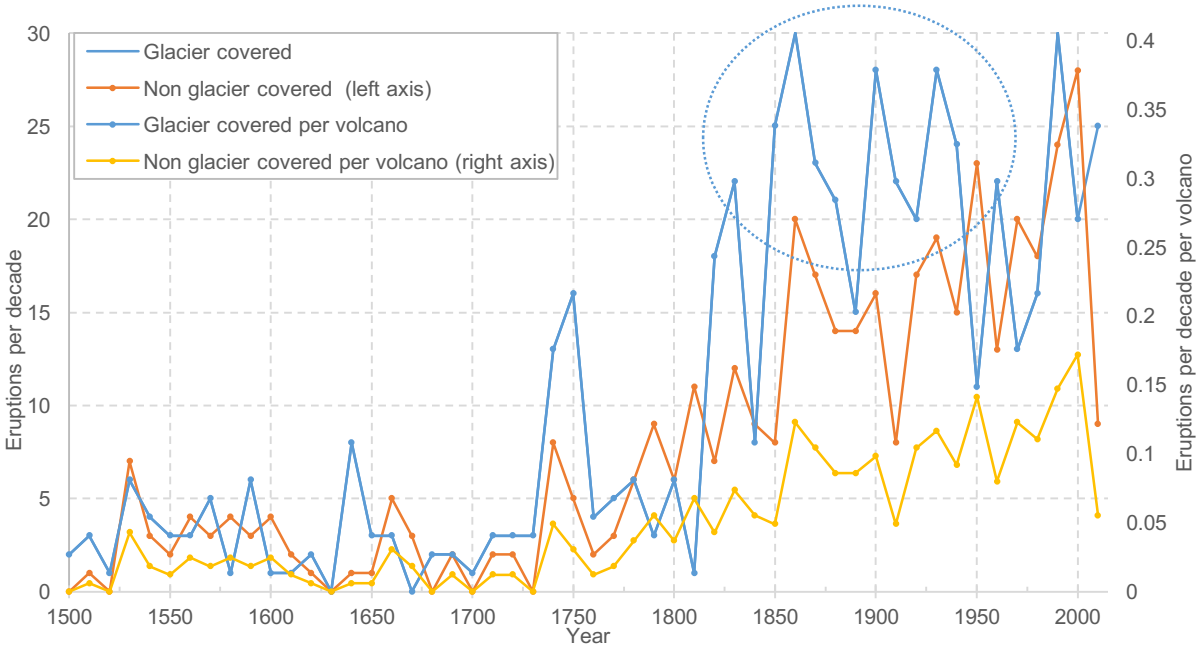

Figure 41: Volcanic evolution since 1500 of both glacier-covered and glacier free volcanoes. Data are shown in eruptions per decade (left axis) and eruptions per decade per volcano (right axis). The blue line can be read from both axes. The last dots stand for eruptions after the year 2010.

The eruption frequency since 1850 shows no significant trend in the number of eruptions on glacier-covered volcanoes. On average 11 eruptions occurred every 5 years or 2.2 eruptions per year. For eruptions on glacier-free volcanoes, a slight increase in the eruption frequency can be seen even though it is not a significant.

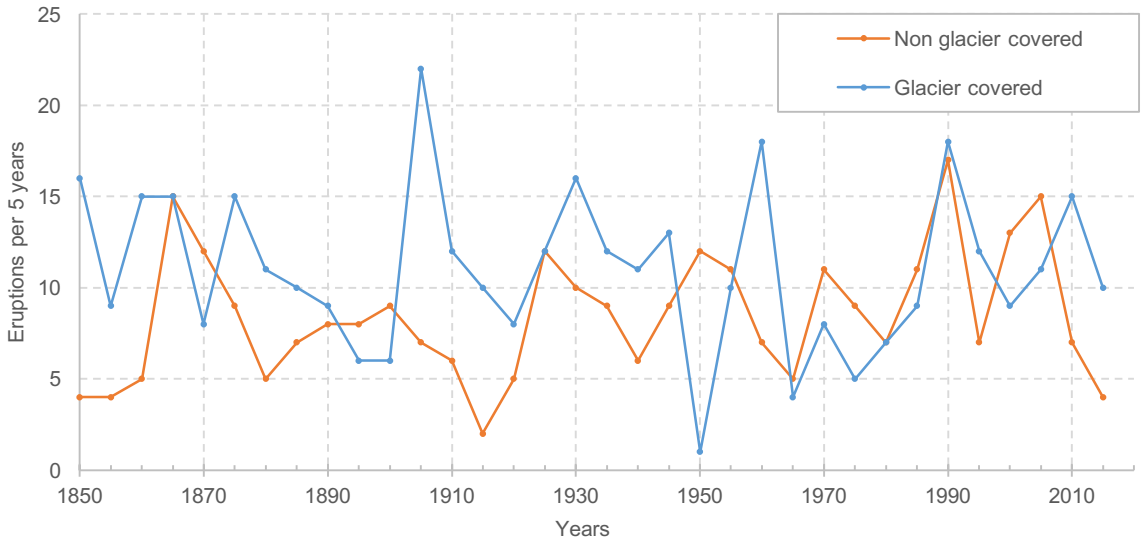

Figure 42: Volcanic evolution since 1850 of both glacier-covered and non glacier-covered volcanoes. Data is shown in eruptions per five years. The last dot stands for eruptions after the year 2015.

Finally, the history of eruption frequency since 1980 can be seen in Figure 43. This time frame also represents the study period of the glacier area calculations. On glacier free volcanoes, two eruptions occurred on average per year with no increase noteworthy increase during the time period. On the other hand, on glacier-covered volcanoes the average eruption frequency lies at 2.4 eruptions per year, with a slight increase in recent years, more exactly since 2008 (average of 3.4 between 2008 and 2016).

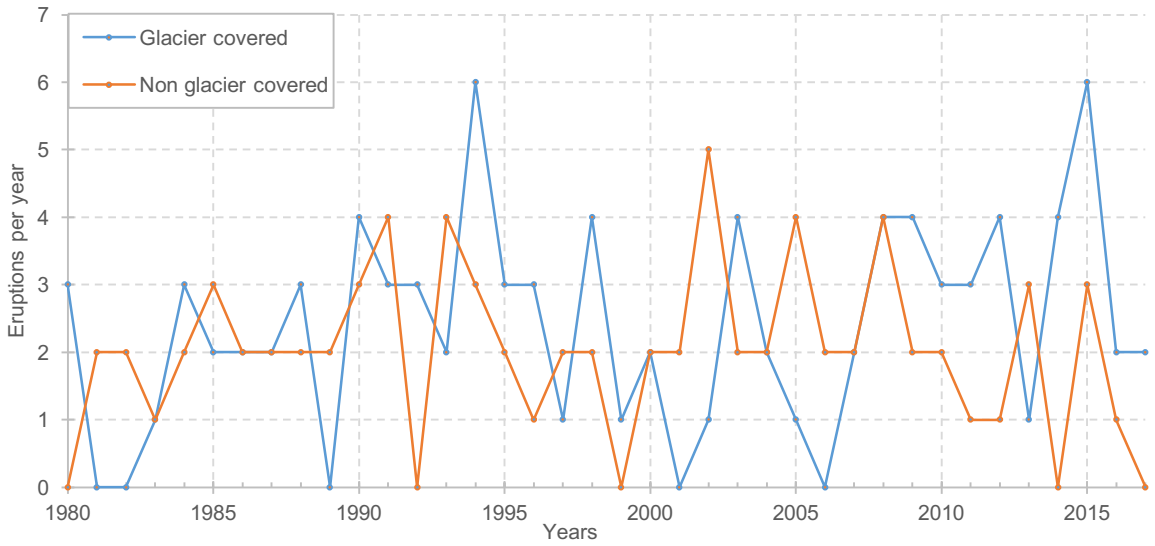

Figure 43: Volcanic evolution since 1980 of both glacier-covered and non glacier-covered volcanoes. Data is shown in eruptions per year.

By showing different time scales, trends can be seen, that would not be visible at another scale. By looking at the eruption frequency since 1500 an increase of eruptions on glacier-covered in compared to glacier free volcanoes can be found between 1820 and 1950. Figure 42 depicting the eruption frequency since 1850 shows the opposite trend with an increasing number of eruptions on glacier free volcanoes. When trying to find such variations, it is important to consider the time frame and time scale to not overlook or falsely interpret possible trends.

4.4.2 Eruption start date

Not only the glacier extent can have an influence on the eruption likelihood, also the seasonal snow cover can have an impact. Albino et al. (2010) mentioned that the eruption likelihood of Katla volcano in Iceland is largest when the snow cover is smallest. The last nine major eruptions of Katla all started during the summer under such conditions.

As the eruption database also contains the start date for the most recent eruptions, the likelihood of the eruption per month can be calculated. As there are no seasons and also no seasonal snow cover for tropical volcanoes, their eruption start dates are compared with the extra-tropical glacier-covered volcanoes to see if there is a significant difference. Figure 44 shows the percentage of the eruption start data for each month for extra-tropical versus tropical volcanoes. The boundary between tropics and extra tropics was chosen to be 24° S. In total, for 353 tropical and subtropical eruptions the start month is known, for extra-tropical eruptions, the number is 232.

To simplify the calculation the year was cut in half to analyse how many eruptions occurred during the summer/winter half and how much during the winter half. For the extratropical eruptions (only glacier-covered volcanoes), 63.8% started between November and April when the snow cover is generally lowest. The other 36.2% started between May and October. For the tropical volcanoes, it was almost 50-50. 53.3% started during the summer half and 46.7% during the winter months. After performing a statistical t-test, the difference seems to be significant (p two tail=0.01).

The difference between the frequency of summer and winter eruption start is with 27.6% not as striking as for Katla volcano in Iceland where all major eruptions started during the summer period, but still, shows a significant difference in comparison to low latitude eruptions. The variation between the months of tropical and subtropical eruptions starting months is very low and can only be a random error (that could be even more reduced with increasing sample size). Most months have a similar amount of eruptions starting, ranging from 7.3-9.9%/month. Only the month of September showed a lower eruption likelihood with only 5.6%. An interesting fact is, that for extratropical eruptions on glacier-covered

volcanoes, almost 50% started in the four months of November to February and the other 50% in the eight months of March to October.

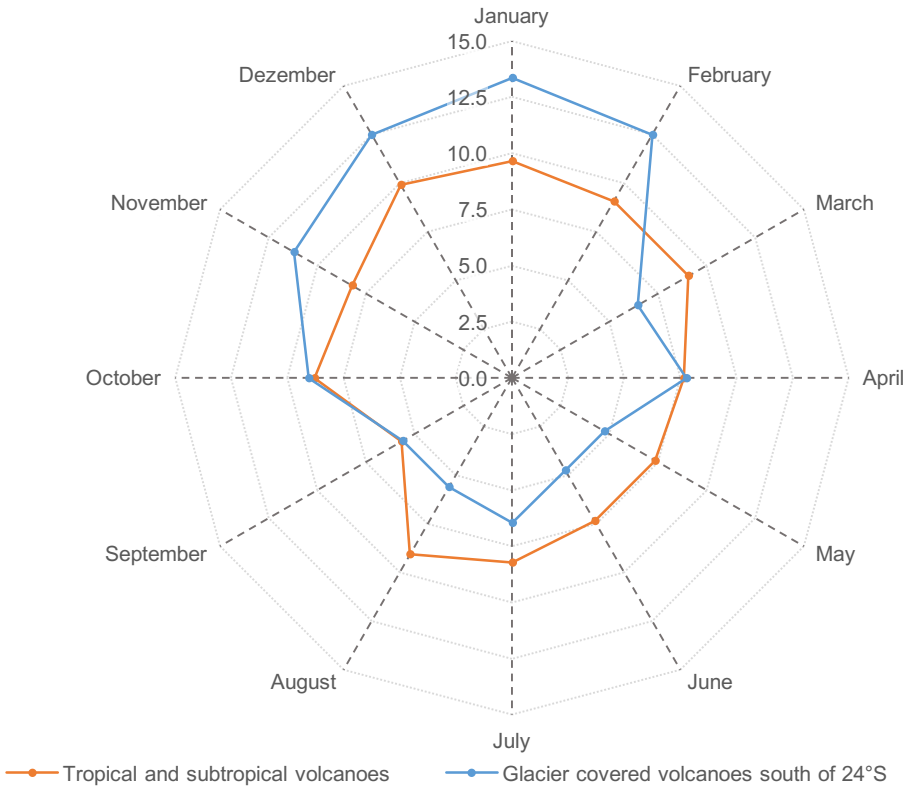

Figure 44: Eruption start date (month) of all volcanoes in the tropics and subtropics versus glacier-covered volcanoes in the extra-tropics (south of 24° S) since the year 1500. Data are shown in percentage of all eruptions for each month.

4.5 Combination of glacier results and volcano data.

Combing glacier change data with volcanic eruption data, possible differences between glaciers on volcanoes that experienced eruptions versus glaciers on volcanoes that did not show any sight of activity can be seen. Keep in mind that all the volcanoes listed in the graphs below are considered active, therefore fumaroles, geysers, and other volcanic features could be present even though no eruption occurred. The glacier change data was split into two groups: the first group consists of all glaciers of volcanoes that experienced an eruption within the study period. The second group consists of glaciers on volcanoes that did not erupt but are still considered as active. By comparing these, the effect of a volcanic eruption on the glacier can be seen. In total 19 volcanoes erupted during the study period, some just once, others multiple times. In Figure 45 the glacier change of the volcanoes with versus without

eruption can be seen. The error bars indicate the standard deviation of both the glacier change and the investigation date. Change rate numbers are listed in Table 18.

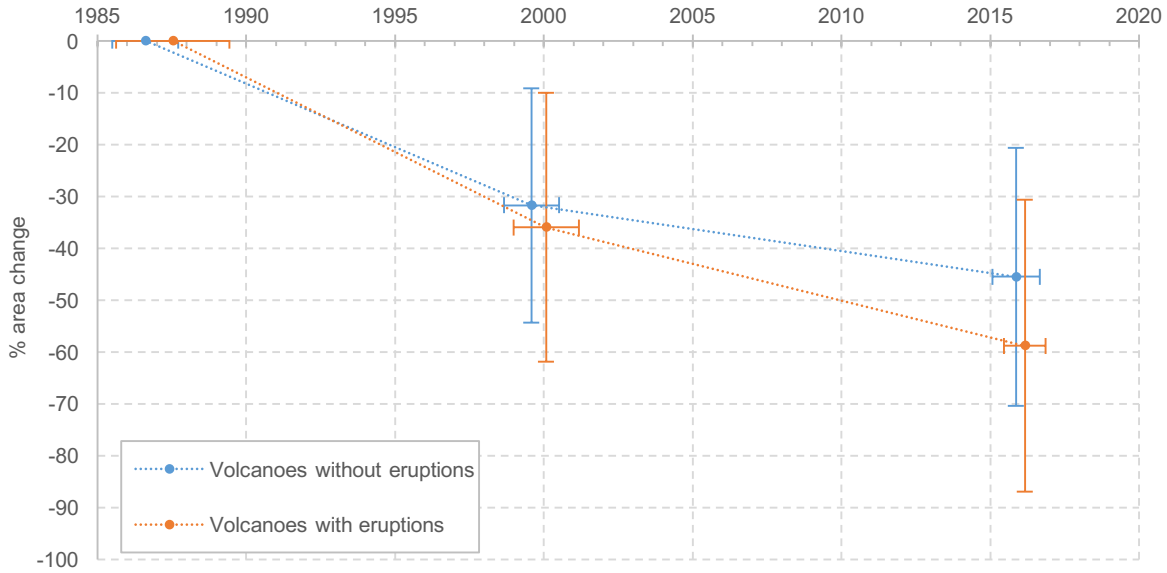

Figure 45: Average glacier area change of volcanoes that experienced an eruption since 1985 versus volcanoes without any eruption.

Table 18: Average glacier change rate of volcanoes with eruptions versus without eruptions.

Glacier change rate	1985-2000 (%/y)	2000-2015 (%/y)	1985-2015 (%/y)
Volcanoes with eruptions	-2.87	-1.42	-2.05
Volcanoes without eruptions	-2.45	-0.85	-1.56

After performing a statistical t-test to examine if there is a significant difference between the glacier change between glacier on volcanoes with eruptions versus without eruptions, the result was, that the difference is not significant for the 95% confidence interval but significant for the 90% interval (p-value = 0.054). Even though the result is not significant, there is clearly a difference between the two groups. As there are only 19 volcanoes which had an eruption, the data pool is too limited. With a larger dataset, the change will be clearer and the significance level would rise.

Next, the influence of the volcanic activity on glacier change is analyzed. To quantify volcanic activity, the number of eruptions and their magnitude are important. To do so, a weighted volcanic activity index was invented to combine both factors. The activity index is the sum of eruption number within the study period plus one point for each VEI step. For example, the volcano Guallatiri had one eruption with the VEI of one. This results in an activity index of one. Popocatepetl had four eruptions, three with a VEI 2

and one with VEI 3, therefore the activity index is 9 (2+2+2+3). Most active volcanoes were Llaima (19), Villarrica (16), Sabancaya (14), Copahue (13) and Tungurahua (13).

Figure 46 shows the glacier change rate along with the respective activity index. All glacier which were not directly affected by an eruption were grouped as one point (black point in the graph). The result is, that there is a slight increase in the glacier change rate with increasing volcanic activity, but the correlation is very small. Volcanoes like Villarica and Llaima had relatively small change rates even though the volcanic activity was very high. This is due to the fact that multiple eruptions have covered the ice with a thick layer of ash and therefore prevented it from melting. Tungurahua and Popocatepetl on the other hand lost its entire glacier because of multiple eruptions and no time for the glacier to recover.

Another reason why the correlation is so small is given by the many other factors playing a role in glacier change rates, like climate change impacts or glacier size. Nevertheless, the volcanic activity can have sometimes a large effect on glacier area.

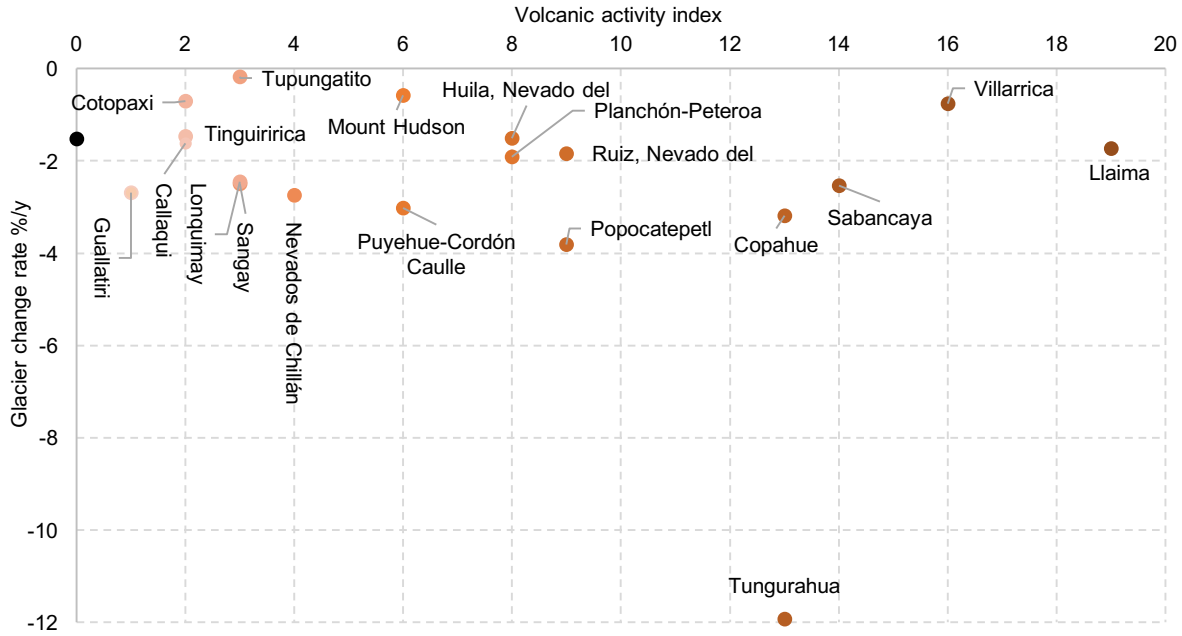

Figure 46: Glacier change rate of volcanoes with eruptions and their respective activity index. The average change rate of volcanoes without eruptions is indicated by the black dot.

5 Discussion

5.1 Glacier mapping

Deriving glacier outlines using satellite images and the semi-automated band ratio method has been proven to be a useful and reliable tool. The main advantages are its fast performance and reproducibility of results. When applying the method to all glaciers data are comparable with only little subjective interpretation (e.g. for the threshold). Nevertheless, some limitations remain: Paul et al., (2013c) mention that debris cover is still one of the biggest limitations of automated glacier outline generation as these regions are not included by any of the so far developed methods. As for debris, also volcanic ash worsens the performance greatly and manual editing is needed. If the debris cover is very thin, the thermal band (with lower resolution) might be used to identify underlying ice (Raup et al., 2007).

Another limitation mentioned by Paul et al., (2013c) was poor performance in cast shadows. As active volcanoes mostly have a constant slope gradient and only few steep rock faces, shadows were not a big problem in this study. For less active and more eroded volcanoes, shadows were still a problem, but with the right selection of the threshold value when calculating the glacier outline, errors could be kept to a minimum.

Initially one of the concerns was if the 30 m resolution of the Landsat TM images was good enough to perform well. Paul et al., (2003) compared the outcomes of different image resolutions with the result that 30 m images on average produce a 2-5% smaller glacier area than when manually editing using high resolution images (in that case Ikonos). Differences for debris free areas tend to be larger for small glaciers and smaller for large glaciers. Comparing image resolution from Landsat TM (30 m) to Landsat OLI (15 m) and Sentinel-2 (10 m) results seem be similar in accuracy (Paul et al., 2016). Higher resolution images perform better if the glacier size is very small (<0.1 km^2) but also have a more time demanding workflow. When manually editing debris covered parts, higher resolution images come in handy to clearly define the glacier outline. When using 30 m images it is sometimes almost impossible to clearly see the glacier terminus under a debris cover. In that case, high-resolution images from other sources like Google maps should be considered. When analyzing images from the 1980s, it gets more difficult to obtain high-resolution images. Maps from other publications or aerial photos are useful to map debris-covered parts. When availably, also the GLIMS and RGI glacier inventories can be used to verify the edits.

One of the major limitations of optical sensors is the presence of clouds. This is because passive sensors like used in the Landsat satellites cannot penetrate thick layers of clouds. If only a thin layer of cirrus clouds is present, images can still be used as the light can still penetrate through these clouds (i.e. they are optically thin). Among the most important steps to get precise and robust results is the availability

of cloud-free images with no seasonal snow. As glacier-covered volcanoes, especially in tropical regions reach very high altitudes, they attract thick clouds over their summits. This is because passive sensors like used in the Landsat satellites cannot penetrate thick layers of clouds. If only a thin layer of cirrus clouds is present, images can still be used as the light can break through these clouds (i.e. they are optically thin). Especially in Ecuador, cloud cover was the biggest issue for finding useful images. With its tropical climate and the large amount of convection, volcano peaks are often cloud covered. Rarely, an image could be found where all volcano peaks within one image were free of clouds. Furthermore, for some volcanoes, no image for the specific time frame could be found where all glaciers were free of clouds. Therefore, a combination of more than one image was used and resulting glacier outlines were merged together. Volcanoes affected by this are Cayambe, Antisana, Illiniza, Cotopaxi, Chimborazo as well as Sangay. The latter showed the most cloud cover with only few images showing the glacier as a whole.

The second big challenge while searching for satellite images was the presence of seasonal snow. In the case of Ecuador, if a useful cloud free image was found it was not certain that it also represents the minimal snow cover. Therefore, the selection of useful images got even smaller. In order to minimize the errors evolving from mapping seasonal snow, the right images need to be selected. Previous studies like Liu et al. (2013); Peduzzi et al. (2010) and Pfeffer et al. (2014) have had difficulties with seasonal snow whilst glacier mapping. Especially the Randolph glacier inventory (RGI) still has many poorly elaborated glacier outlines in South America due to the presence of seasonal snow that have been mapped as glacier. Visual and manual correction is needed to update the glacier inventory which is time consuming and still in the process (Pfeffer et al., 2014). More satellites that overfly the region more frequently would be a solution or a method that can break through clouds and work by night like radar technology.

For extra-tropical areas, especially for the time steps of 2000 and 2015 the available data was sufficient to find useful images without or only little seasonal snow and no cloud cover. But for 1985 only Landsat 4/5 images were available, so fewer useful images could be found. Consequently, the following years were also considered until a good image could be found. Hence, in such cases the study period got shortened, but without compromising data quality.

5.2 Literature comparison

To verify the glacier area data and glacier change results, a comparison with existing glacier change studies from the literature is necessary. In total, glacier data from the literature for 28 of the 59 volcanoes could be found. To provide a realistic comparison, data from the same time period were selected. As this is not always possible, especially as only few studies have been published after 2015, the next best

dataset was chosen. On average, data from the literature were taken from around 1982 and 2007. Because it was not evitable, some results from the 1950s and 1960s were considered as well to at least be able to calculate a change rate. Because the area selection in the literature is not always the same as in this study (e.g. sometimes only a part of the volcanic glacier is considered) changes in absolute have not been determined. Nevertheless, change rates per year could still be compared.

In Figure 47, glacier change rates of each volcano are compared against the selected literature data. In general, the coefficient of determination (R^2) is 0.78 or 78%. Overall, change rates taken from the literature seem to be lower than the results from this study. The average change rate of the 28 volcanoes with literature values show a change rate of -1.36%/y in comparison to -1.38%/y in this study. The mean values are in very good agreement, but do not show clearly the differences between the datasets. For 11 for the 28 volcanoes, glacier area change rates were larger in the literature, for the other 17 volcanoes they were smaller. Looking at the trend line in Figure 47 it seems that glaciers with small change rates were underestimated in the literature whereas glaciers with high change rates have been overestimated. Also, the occurrence of volcanic eruptions make a comparison more difficult as the study periods are not exactly the same and volcanic eruptions could be included in one but not in the other period.

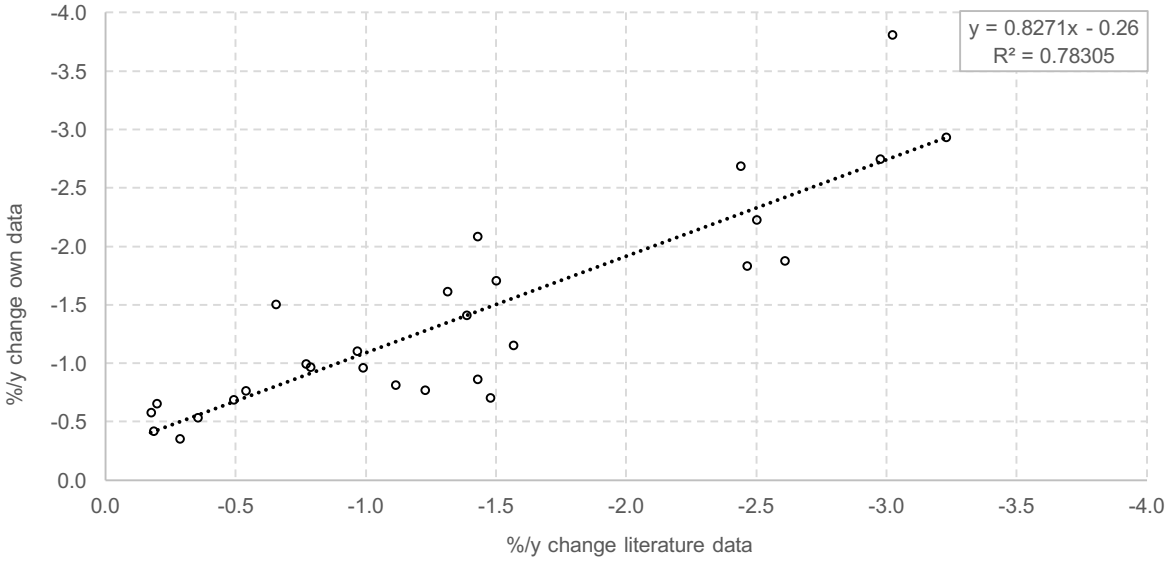

Figure 47: Comparison between glacier change results of this thesis (1985-2015) against data from different literature sources (average of 1982-2007).

5.3 Influence of eruptions on glacier change

The results have shown that glaciers on volcanoes that experienced eruptions melt faster than volcanoes without recorded eruptions. This increase in melt rates likely comes from the heat release during a volcanic eruption. Where and how much the contact with the ice is made, depends on the eruption style. Geothermal fields, hot springs or fumaroles can contribute to the melt rate on an active volcano via basal melting even though no eruption occurs. A sudden increase in geothermal activity may indicate an upcoming eruption also increases the melt rate. During an eruption, contact between ice and volcanic edifices can occur underneath the ice during a sub-glacial eruption or by tephra fall from the top. The latter can originate from the same volcano as the glacier is situated or a nearby one. Hot volcanic edifices might initially accelerate the melt rate by releasing heat and lowering the albedo but form an insulation after reaching a critical thickness (about 10 mm, depending on the grain size). Additional to tephra fall, pyroclastic flows and lava domes can contribute to glacier melt. Sub-glacial eruptions can either be a sill or dyke intrusion, a dome generation or lava flow. All of which can form a sub-glacial lake that might end up in an outburst flood.

To answer which of these factors contributed most to the overall difference between glacier change rates on volcanoes with eruptions and without is hard to determine. To do so, every eruption needs to be analyzed carefully to understand the processes which occurred. Further, not all glaciers on volcanoes with eruption had a noticeable increase in glacier melt rate. Some examples are the volcanoes Cotopaxi, Villarica, Tupungatito and Mount Hudson which all had a glacier change rate of less than -0.8%/y. For Cotopaxt in Ecuador, only one eruption occurred during the study period starting on the 14.08.2015 and ending on the 24.01.2016 just a few days before the satellite image for the glacier mapping was chosen (02.02.2016). On that image, large parts of the ice were still covered with ash and tephra. Troncoso et al. (2017) says that the ash layer was very thin (under 2 mm) which would initially lead to an increase of the melt rate. For Villarica volcano in Chile, large parts of the glacier are covered by a thick layer of tephra. This prevents the ice from melting even though 15 eruptions occurred since 1991 which makes Villarica one of the most active of all volcanoes of South America. Nevertheless, the glacier change rate is in comparison to glaciers on its surrounding volcanoes relatively small (-0.77%/y).

Tupungatito has one of the largest ice masses in central Chile. As of 2016, the glacier of Tupungatito and the nearby Pleistocene Tupungato volcano covers an area of 162 km^2, down from 171 km^2 in 1986. During the study period, two eruptions occur, a very small VEI1 eruption in 1986 and a VEI2 eruption in 1987. The latter triggered a mud-flow, which killed 49 people in the region. The eruption was limited to the crater area and only parts of the ice were covered with an ash layer (Global Volcanism Program 1987). Because of the size of the ice mass, this small volcanic eruption was probably not big enough to significantly change the glacier balance.

Mount Hudson, a large stratovolcano north of the Patagonian ice fields, has experienced two eruptions within the study period. A VEI5 eruption in 1991 which was the second largest eruption globally of the 20th century and a small VEI1 eruption in 2011. Rivera & Bown (2013) suggests that 20 km^2 of ice was destroyed within the caldera during the 1991 eruption which partly recovered afterwards. For other glaciers, the volcanic activity contributed much more towards glacier melt. Examples for this are Tungurahua (Ecuador) and Popocatepetl (Mexico), which lost their entire glacier cover within the study period but also Copahue, Sabancaya and Puyhue-Cordón Caulle which lost most of their area.

5.4 Influence of climate change on volcanic eruptions

Many studies have shown that an increase in volcanic activity has been observed following major deglaciation events (Huybers & Langmuir, 2009; Maclennan et al., 2002; Jull & Mckenzie, 1996; McGuire, 2015). According to Huybers & Langmuir (2009) the increase of volcanic activity during the last deglaciation between 18-7 ka was statistically highly significant ($p>0.1$). As this study only analysed eruption frequencies, it remains unclear if glacier retreat only affects the eruption frequency or also the eruption magnitude (Tuffen, 2010). Figure 48 shows the temperature evolution of the Holocene in southern South America. Red rectangles indicate the periods with increased volcanic activity of glacier-covered volcanoes. Periods of increased activity occur during periods with an increasing temperature and glacier retreats. Interestingly, no increased volcanic activity could be found directly after the 8200 BP temperature low. Studies of sea surface evolution showed, that there was a rapid warming between 8000-7500 BP in the Southeast Pacific and that weak ENSO variability/intensity led to a very warm SST between 7500 and 5000 BP off the coast of mid latitude South America (Kim et al., 2002). This would have led to massive glacier retreat, shortly followed by an increase of volcanic between around 7100 BP and 6700 BP. If there was volcanic response after the 8200 BP event, it was not immediate but had a lag time of around 1000 years.

Furthermore, glacier advances have been observed in the Southern Andes between 2700-2000 BP (Glasser et al., 2004). Having its peak at around 2300-2500 BP, the initiation of the retreat is directly followed by an increase of volcanic activity between (2300-1500 BP). This implies that there was almost no lag time of smaller glacier changes and volcanic activity on ice-caped volcanoes with mostly shallow magma chambers (like in Latin America) would react fast to unloading processes. Interestingly, not all periods of glacier retreat showed also a signal in the volcanic activity. Apart from the 8.2 ka BP event, there were also glacier advances between 5400-4800 BP (Kilian & Lamy, 2012; Glasser et al., 2004). No immediate increase in volcanic activity could be found but a period of higher activity between 4400-3800 BP.

As we have seen, the lag times can vary significantly. For the last deglaciation, the lag time of the volcanic activity holds large uncertainties. Jellinek et al. (2004) proposed, that the lag time of the volcanic activity following a deglaciation is 3200 ± 4200 y and 11200 y ± 2300 y for silicic and basaltic volcanism respectively. The lag time and scale of volcanic changes following smaller glacier changes like the current glacier retreat also still holds large uncertainties.

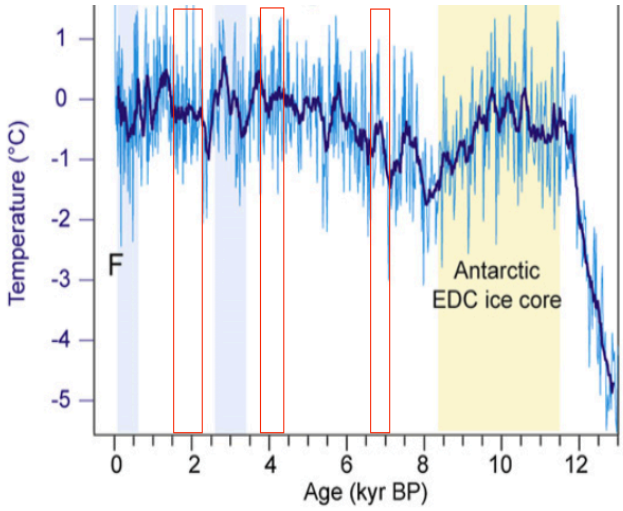

Figure 48: Temperature variation in Southern South America during the Holocene. Red rectangles indicate period with increased volcanic activity. (Modified after Kilian & Lamy 2012)

5.5 Change in volcanic activity in the last decades (centuries) and possible future change

Glaciers in Latin America reached their maximum LIA extent between 1550 and the early 19th century depending on the region. Volcanic activity increased significantly after 1820 from 2.75 eruptions per decade between 1500 and 1740 to 21 eruptions per decade from 1820 until today. In part, this increase can be explained by the raising awareness of people towards eruptions and the general increase in reported eruptions (also for non glacier-covered eruptions). Nevertheless, the increase of eruptions on glacier-covered volcanoes is larger than on ice free volcanoes. If this difference is related to glacier retreat, then the lag time was very small, only a few decades to a century.

Since glaciers continue to retreat after the LIA, it remains unclear how much the future melting influences the volcanic activity and the possibility of volcano related hazards. In Iceland, unloading of ice leads to an increase in mantle melting and magma production. Stratovolcanoes, like most volcanoes in Latin America, are more affected by crustal stress changes that lead to pressure changes in the magma chamber (Pagli & Sigmundsson, 2008). Ice unloading also effects the eruptions style, leading to more explosive eruptions under a thinning ice cover. If thinning continues, more volcanoes might shift from intrusive eruption towards explosive eruptions (Tuffen, 2010).

Apart from the unloading effects, many other feedback processes come into play, that influences glaciers and climate. The glacier breakup can be accelerated by Jökulhlaups and debris flows triggered by eruptions, or rock-ice avalanches triggered by seismic activity. Furthermore, due to the lack of mechanical support after the unloading of ice, hazards can stretch from rock avalanches to volcanic collapses (McGuire, 2015).

With ongoing climate change, some glaciers will disappear completely like we have already seen on Popocatepetl and Tungurahua. Hazards from lahars might be reduced due to the limited availability of water and ice even though new crater lakes might form. Also, eruption styles are likely to be less explosive if no ice or water is present with less phreatomagmatic activity (Tuffen, 2010).

5.6 Eruption starting date

According to Albino et al. (2010), eruptions also follow a seasonal pattern, depending on the snow cover. For Katla volcano in Iceland, all nine eruptions since 1580 started in Summer (between May and November). Also for the extratropical volcanoes in Latin America, 64% of the known eruptions since 1500 started during the summer (between November and April). Tropical and subtropical volcanoes have a similar eruption frequency all around the year without a seasonal pattern. How much the snow cover influences the eruption start is not clear, as the period of snow cover can vary for each volcano, especially as the study region spans over many different climatic zones. Further investigations would be needed for each volcano with the knowledge about the present snow cover to verify these results. Nevertheless, it is interesting to see that also small load changes like the seasonal snow cover might have an influence on triggering volcanic eruptions. If this is the case, then also the current glacier retreat and the resulting weight unloading should have an influence on the volcanic activity.

5.7 Volcanoes with large hazard potential

In many scientific papers (e.g. McGuire 2013; Tuffen 2010; Gilbert et al. 1996) the Chilean volcano Solipulli was mentioned as a possible future hazard regarding load variation changes and increased volcanic activity. Sollipulli is a 4 km wide glacier filled caldera, lying between the active Llaima and Villarrica volcanoes. Recent eruptions always took place at the rim of the caldera. The last known eruption took place in 1240, the last big eruption (VEI5) occurred 2900 years ago. Once the ice load (currently around 6 km^3) gets reduced, eruptions at the caldera center could occur again, leading to potential devastating hazards (Gilbert et al., 1996). Even though there are no big cities in close proximity, around 500.000 people live within a distance of 100 km.

Of all the volcanoes that could lead to hazards for the surrounding population most are under constant monitoring. Information about monitoring installations can be accessed on the Glovoremid database. Further, many volcanoes with a large hazard potential already have hazard maps for a better preparation in case of an eruption. However, some volcanoes such as Iztaccihuatl in Mexico are not monitored. This volcano is located within the proximity of the megacity Mexico City were 27 million people live within

a distance of 100 km and 210.000 within 15 km. The latter could therefore be affected by lahars originating the volcano. Even though the volcano has been quiet during the Holocene, fumaroles could be observed underneath the glacier. An eruption is currently unlikely, but indirect hazards like the formation of a glacier lake or a slope destabilization by glacier retreat and permafrost thawing are possible (Schneider et al., 2008).

Of the non-monitored glacier-covered volcanoes (currently 29), most did not show any activity in recent time (see Table 19). For some, evidence of Holocene activity is uncertain. Nevertheless, some volcanoes experienced eruptions in recent history like Monte Bruney and Yanteles. The latter might have experienced a small eruption in 1835 but this could not be verified (Global Volcanism Program 2013b). Little is known about Yanteles, partly also because it is located in a poorly populated area. However, if signs of activity can be found, the volcano should be monitored to provide early warning in case of an upcoming eruption. All volcanoes that are entirely within the Argentinian territory are currently not being monitored. Risco Plateado and Domuyo are still considered as active volcanoes as they showed activity during the Holocene. The latter holds with 22 km^2 a significant glacier area and big lahars could follow an eruption. In case signs of activity are present, the volcanoes should be monitored and hazard maps should be elaborated.

Table 19: List of analysed volcanoes without permanent monitoring installation.

Name (Country)	Glacier area 2015 (km^2)	Hazard map Y/N	Last eruption	Population 30km	Population 100km
Iztaccihuatl (Mexico)	0.27	Y	Holocene	1.036.172	27.276.280
Illiniza (Ecuador)	0.2	N	Holocene	158.371	3.941.221
Palomo (Chile)	175.93	Y	Holocene?	4.732	965.894
Risco Plateado (Argentina)	3.17	N	Holocene?	522	190.076
Calabozos (Chile)	0.08	N	Holocene	1.023	305.637
San Pedro-Pellado (Chile)	2.73	Y	Holocene	4.155	500.494
Longavi, Nevado de (Chile)	0.13	Y	4890BC	3.901	753.797
Domuyo (Argentina)	22.05	N	Holocene?	1.425	30.006
Tolguaca (Chile)	2.01	Y	4000BC	13.873	567.185
Tronador (Chile-Argentina)	109.28	N	Holocene?	1.293	380.976
Yate (Chile)	18.95	Y	1090	6.135	315.418
Yanteles (Chile)	58.26	N	4920BC maybe 1835	1.348	44.899
Cay (Chile)	10.50	N	Holocene?	104	74.787
Monte Burney (Chile)	48.63	N	1910	0	3.309

5.8 Suggestions for improvements and further research

Combining recent glacier data with volcano data to detect possible connections between glacier change and volcanic activity is a relatively new field of study and has never been applied on a continental scale before. Most existing studies (Albino et al., 2010; Pinel & Jaupart, 2005; Capra, 2006) that analyze the link between glacier unloading and volcanic activity focuses on changes following the last deglaciation on single volcanoes or regions. These studies use mass changes of glacier ice to calculate the effect of the underlying magma chamber. Models have been developed to simplify the effects of unloading on the volcano (Jull & Mckenzie, 1996; Sigmundsson et al., 2010).

To identify a change in volcanism due to glacier change, 30 years as a study period is a comparably short time frame because the lag time of volcanoes might be very long. Initially, an extension of the glacier change calculation to the LIA extent was considered. Because data and literature availability for LIA glacier extends are very rare, only a 30-year period was chosen. However, this time period allowed application of the band ratio method for generating time-series of glacier outlines for active volcanoes in Latin America. The question remains, if an extension to the LIA period would improve the robustness of the conclusions in or if it would still be an insufficient time span.

A further possible improvement to determine the link between glacier changes and volcanism would be the analysis of glacier mass changes instead of area changes. Even though area analysis gives a good approximation about the amount of ice on a volcano, mass changes are essential to calculate the effects of unloading processes. As it was not feasible to calculate mass changes for all glacier-covered volcanoes due to missing ice thickness data, it can be recommended to follow this approach in future studies. With modern technologies and increasingly available DEMs, it is possible to calculate decadal mass changes from space. Currently, only few glaciers have long enough time series of mass balance measurements and especially for remote glacier-covered volcanoes, only few data are available.

To better understand the relationship between glacier change and volcanic activity, climatologic influences on the glaciers should be removed to only see the influence of the volcano. This requires accurate climatologic data from each volcano. Another approach would be to look at the evolution of the 0° isotherm (FLH) over time. Some studies have already shown the connection between FLH and glacier change, especially in tropical regions as its altitude determines whether there is a possibility for solid precipitation (Schauwecker et al., 2017; Bradley et al., 2009). Atmospheric sounding data for many stations all over the world are available for more than 50 years and would be a good tool to combine with the here presented glacier change data.

Another approach would be to compare glacier change on active volcanoes with non-volcanic glaciers in the same region. As climate change impacts should be similar for both types, it can be ruled out as a governing force to maybe reveal the influence of the volcanic activity on the glacier. However, also in

this continental-scale study, a main limitation to perform valid statistical analysis is the small data pool with only 59 volcanoes. The first step to improve this would be to include the missing volcanoes from Latin America to increase the amount of data and better read out trends. Further, a worldwide approach of all glacier-covered volcanoes would allow increasing the data pool to its maximum. Future projects are required to advance this field of study.

6 Conclusions

The main goal of this thesis was, to analyse glacier change on active volcanoes in Latin America and combine the results with volcano data to see the effect of volcano eruptions on glaciers and how the volcanic activity has changed in the past. Eruptions on glacier-clad volcanoes can first greatly influence the mass balance of the glacier and secondly can cause hazards for the surrounding population. Because the volcanic activity significantly increased during the last deglaciation, a similar response, but on a smaller scale, can be expected following the recent glacier retreat, in particular for volcanoes where large amounts of ice have been removed. By analysing volcano data of the whole Holocene, trends and changes in the volcanic activity have been identified. Volcanic eruption frequencies of glacier-covered volcanoes revealed that volcanic activity follows a climatic fluctuation, influenced by the Earth's climate and glacier load. Additionally, eruptions seem to be more likely to start when the mountain is not covered with large amounts of snow.

Multispectral satellite images from Landsat 4/5, 7, 8 and Sentinel-2 were used to generate glacier outlines with the well-established band ratio method. Limitations of this method emerged due to the image selection process, as optical image data especially suffer from cloud cover in tropical regions and ash layers from volcanic eruptions. For several glaciers debris-covered tongues had to be digitized manually, reducing the accuracy of the glacier mapping.

On average, glaciers on active volcanoes lost around 50% of their size in the last 30 years with an average change rate of -1.8%/y. Glaciers in Mexico had the highest change rate during the study period (-2.3%/y), followed by Chile and Argentina between 35° S and 38° S (-2.14%/y), Peru/Bolivia (-1.53%/y) and Colombia/Ecuador (-1.38%/y). In southern South America (south of 41° S), the glacier change rate was much lower (-0.60%/y).

When comparing glaciers on volcanoes that experienced and eruption with dormant volcanoes, differences in the change rate were observed. On average, glaciers on volcanoes with eruptions (without eruption) had a change rate of -2.05%/y (-1.56%/y) between 1985 and 2015. Tow volcanoes (Popocatepetl and Tungurahua) lost their entire glacier cover during the study period, influenced by extensive volcanism.

This thesis has analysed volcano-ice interactions related to the coupling of the Earth system and its complex interactions between volcanic activity and climate fluctuations. Moreover, glacier-covered volcanoes expose the downstream population at high risk, requiring their frequent monitoring and improved understanding of potential relations between glacier retreat and volcanic activity. This thesis presented a first analysis of the available databases for Latin America, and results indicated that further research is needed to investigate how the current glacier shrinkage affects the volcanic activity and if

we can expect an increase in volcanic eruptions or eruption magnitude in the future. This would require detailed studies of glacier mass change over the past decades to century on all glacier-covered volcanoes and a comparison to an extended database of volcanic eruptions (e.g. considering also volcanoes in North America).

Acknowledgement

It is time to thank all the people that made this work possible. Without their help, it would not be possible to study and conclude this Master studies.

First, I would like to thank Christian Huggel and Frank Paul from the University of Zurich for their supervision and support during the thesis. They have been a great help and always had time for my questions. Even though their time was limited I never felt left alone and I could always count on their support.

Secondly, I want to give special thanks to Hugo Delgado from Mexico (UNAM) that made it possible that I could go to work at the UNAM for more than two months. I felt very welcome there and had to opportunity to learn many new things that contributed to my thesis. Concerning the work at the UNAM I also want to thank Natalie Ortiz for all her help on the handling of the volcano database and the company outside of the university.

In combination to the research stay in Mexico I also want to thank the SEP (Swiss snow, ice and permafrost society), which supported me financially and made my stay in in Mexico possible.

Further, I want to thank my flatmates, Dilara Perver, Bianca Sola Claudio and Francesco Wennubst and all my friends for their support and motivation during the writing period. Nice, that I can always count on you.

Finally, I want give the biggest thank to my parents and family. From childhood on, they always supported me and made it possible that I could go to university.

Literature

Albino, F., Pinel, V. & Sigmundsson, F. (2010). Influence of surface load variations on eruption likelihood: application to two Icelandic subglacial volcanoes, Grímsvötn and Katla. *Geophysical Journal International*. 181. p.pp. 1510–1524.

Alcalá, J., Palacios, D. & Zamorano, J.J. (2010). Glacial recession in the Tropical Andes from the Little Ice Age : the case of Ampato Volcanic Complex (Southern Peru). *6th Alexander von Humboldt International Conference*.

Alfano, F., Bonadonna, C., Watt, S.F.L., Pyle, D.M. & Connor, L.J. (2011). Tephra stratigraphy and eruptive volume of the May, 2008, Chaitén eruption, Chile. *Bull Volcanol*. 73. p.pp. 613–630.

Allmendinger, R.W., Jordan, T.E., Kay, S.M. & Isacks, B.L. (1997). The evolution of the Altiplano-Puna plateau of teh Central Andes. *Annu. Rev. Earth Planet*. 25. p.pp. 139–174.

ALPECOLe (2011). *snow line*. [Online]. 2011. Available from: http://www.geo.uzh.ch/microsite/alpecole/static/course/glossary-term-snow_pl_line.htm. [Accessed: 25 September 2017].

Andrés, N., Zamorano, J., SanJosé, J., Atkinson, A. & Palacios, D. (2007). Glacier retreat during the recent eruptive period of Popocatépetl volcano, Mexico. *Annals of Glaciology*. 45. p.pp. 73–82.

Aniya, M., Sato, H., Naruse, R., Skarca, P. & Casassa, G. (1996). The Use of Satellite and Airborne Imagery to Inventory Outlet Glaciers of the Southern Patagonia Icefield, South America. *Photogrammetric Engineering and Remote Sensing*. 62 (December). p.pp. 1361–1369.

Benn, D.I. & Evens, D.J.A. (2010). *Glaciers & Glaciation*. 2nd editio. London: Hodder education.

Bown, F. & Rivera, A. (2007). Climate changes and recent glacier behaviour in the Chilean Lake District. *Global and Planetary Change*. 59. p.pp. 79–86.

Bradley, R.S., Keimig, F.T., Diaz, H.F. & Hardy, D.R. (2009). Recent changes in freezing level heights in the Tropics with implications for the deglacierization of high mountain regions. *Geophysical Research Letters*. 36. p.pp. 1–4.

Brock, B., Rivera, A., Casassa, G., Bown, F. & Acuña, C. (2007). The surface energy balance of an active ice-covered volcano: Villarica Volcano, Southern Chile. *Annals of Glaciology*. 45. p.pp. 104–114.

Cáceres, B. (2010). *Actualización del inventario de tres casquetes glaciares del Ecuador*.

Cáceres, B., Maisincho, L., Manciati, C., Loyo, C., Cuenca, E., Villacís, M., Freire, D., Francou, B., Cadier, E. & Guamanzara, C. (2008). *Glaciare del Ecuado: Antisanay Carihuayrazo*.

Capra, L. (2006). Abrupt climatic changes as triggering mechanisms of massive volcanic collapses. *Journal of Volcanology and Geothermal Research*. 155. p.pp. 329–333.

Cortés Ramos, J. & Delgado Granados, H. (2012). The recent retreat of Mexican glaciers on Citlaltépetl Volcano detected using ASTER data. *The Cryosphere Discussion*. 6. p.pp. 3149–3176.

Davies, B.J. & Glasser, N.F. (2012). Accelerating shrinkage of Patagonian glaciers from the Little Ice Age (AD 1870) to 2011. *Journal of Glaciology*. 58 (212). p.pp. 1063–1084.

Delgado Granados, H., Julio, P., Huggel, C., Ortega, S. & Alatorre, M.A. (2007). Chronicle of a death

foretold: Extinction of the small-size tropical glaciers of Popocatépetl volcano (Mexico). *Global and Planetary Change*. 56. p.pp. 13–22.

Delgado Granados, H., Julio Miranda, P., Carrasco Núñez, G., Pulgarín Alzate, B., Mothes, P., Moreno Roa, H., Cáceres Correa, B.E. & Cortés Ramos, J. (2015a). Hazards at Ice-Clad Volcanoes: Phenomena , Processes , and Examples From Mexico, Colombia, Ecuador and Chile. In: W. Haeberli & C. Whiteman (eds.). *Snow and ice-related hazards, risks, and disasters*. pp. 607–646.

Delgado Granados, H., Vázquez Selem, L., Cortés Ramos, J., Julio Miranda, P., Ontiveros González, G. & Soto Molina, V.H. (2015b). *Reporte Mexicano de Cambio Climático - La Criósfera en México*. Ciudad de Mexico.

Diaz, H.F. & Graham, N.E. (1996). Recent changes in tropical freezing heights and the role of sea surface temperature. *Nature*. 383. p.pp. 152–155.

ESA (2017). *Sentinel-2*. [Online]. 2017. Available from: https://sentinel.esa.int/web/sentinel/missions/sentinel-2. [Accessed: 15 March 2017].

Falvey, M. & Garreaud, R.D. (2009). Regional cooling in a warming world: Recent temperature trends in the southeast Pacific and along the west coast of subtropical South America (1979 – 2006). *Journal of Geophysical Research*. 114. p.pp. 1–16.

Ferrari, L. (2000). Avances en el conocimiento de la Faja Volcánica Transmexicana durante la última década. *Boletin de la Sociedad Geologica Mexicana*. 53. p.pp. 84–92.

Ferrari, L., Orozco-esquivel, T., Manea, V. & Manea, M. (2012). Tectonophysics The dynamic history of the Trans-Mexican Volcanic Belt and the Mexico subduction zone North America Pacific Plate. *Tectonophysics*. [Online]. 522–523. p.pp. 122–149. Available from: http://dx.doi.org/10.1016/j.tecto.2011.09.018.

Francou, B., Vuille, M., Favier, V. & Ca, B. (2004). New evidence for an ENSO impact on low-latitude glaciers: Antizana 15, Andes of Ecuador, 0°28´S. *Journal of Geophysical Research*. 109. p.pp. 1–17.

Freymueller, J.T., Kellogg, J.N. & Vega, V. (1993). Plate Motions in the North Andean Region. *Journal of Geophysical Research*. 98 (B12). p.pp. 853–863.

Gaffen, D.J., Santer, B.D., Boyle, J.S., Christy, J.R., Graham, N.E. & Ross, R.J. (2000). Multidecadal Changes in the Vertical Temperature Structure of the Tropical Troposphere. *Science*. 287. p.pp. 1242–1246.

Garibotti, I.A. & Villalba, R. (2009). Lichenometric dating using Rhizocarpon subgenus Rhizocarpon in the Patagonian Andes, Argentina. *Quaternary Research*. [Online]. 71 (3). p.pp. 271–283. Available from: http://www.sciencedirect.com/science/article/pii/S0033589409000106.

Giese, B.S., Urizar, S.C. & Fuckar, N.S. (2002). Southern Hemisphere Origins of the 1976 Climate Shift. *Geophysical Research Letters*. 29 (2).

Gilbert, J.S., Stasiuk, M.V., Land, S.J., Adam, C.R., Murphy, M.D., Sparks, R.S.J. & Naranjo, J.A. (1996). Non-explosive , constructional evolution of the ice-filled caldera at Volcán Sollipulli. *Bull Volcanol*. 58. p.pp. 67–83.

Glasser, N.F., Harrison, S., Winchester, V. & Aniya, M. (2004). Late Pleistocene and Holocene palaeoclimate and glacier fluctuations in Patagonia. *Global and Planetary Change*. 43. p.pp. 79–101.

Gómez-Tuena, A., Orozco-Esquivel, M.T. & Ferrari, L. (2007). Igneous petrogenesis of the Trans-Mexican Volcanic Belt. In: S. A. Alaniz-Alvarez & A. F. Nieto-Samaniego (eds.). *Geology of México::Celebrating the Centenary of the Geological Society of México: Geological Society of America Special Paper 422*. Querétaro, Mexico: The Geological Society of America, pp. 129–181.

Govett, M. (2017). *ESRL Radiosonde Database*. [Online]. 2017. Available from: https://esrl.noaa.gov/raobs/General_Information.html. [Accessed: 6 March 2017].

Hoyos-Patiño, F. (1998). Glaciers of Colombia. In: R. Williams & J. Ferrigno (eds.). *Satellite Image Atlas of Glaciers of the World*. Washington: U.S. Geological Survey, pp. 11–30.

Huggel, C. (2009). Recent extreme slope failures in glacial environments: effects of thermal perturbation. *Quaternary Science Reviews*. [Online]. 28 (11–12). p.pp. 1119–1130. Available from: http://dx.doi.org/10.1016/j.quascirev.2008.06.007.

Huggel, C., Caplan-Auerbach, J., Waythomas, C.F. & Wessels, R.L. (2007a). Monitoring and modeling ice-rock avalanches from ice-capped volcanoes : A case study of frequent large avalanches on Iliamna Volcano , Alaska. *Journal of Volcanology and Geothermal Research*. 168. p.pp. 114–136.

Huggel, C., Ceballos, J.L., Pulgari, B., Ramírez, J. & Thouret, J. (2007b). Review and reassessment of hazards owing to volcano – glacier interactions in Colombia. *Annals of Glaciology*. 45. p.pp. 128–136.

Husker, A. & Davis, P.M. (2009). Tomography and thermal state of the Cocos plate subduction beneath Mexico City. *Journal of Geophysical Research*. 114 (December 2008). p.pp. 1–15.

Huybers, P. & Langmuir, C. (2009). Feedback between deglaciation, volcanism, and atmospheric CO2. *Earth and Planetary Science Letters*. [Online]. 286 (3–4). p.pp. 479–491. Available from: http://dx.doi.org/10.1016/j.epsl.2009.07.014.

Jellinek, A.M., Manga, M. & Saar, M.O. (2004). Did melting glaciers cause volcanic eruptions in eastern California? Probing the mechanics of dike formation. *Journal of Geophysical Research*. 109. p.pp. 1–10.

Jordan, E. & Hastenrath, S.L. (1998). Glaciers of Ecuador. In: R. Williams & J. Ferrigno (eds.). *Satellite Image Atlas of Glaciers of the World*. Washington: U.S. Geological Survey, pp. 31–50.

Jull, M. & Mckenzie, D. (1996). The effect of deglaciation on mantle melting beneath Iceland. *Journal of Geophysical Research*. 101 (B10). p.pp. 21815–21828.

Kilian, R. & Lamy, F. (2012). Invited review A review of Glacial and Holocene paleoclimate records from southernmost Patagonia (49-55° S). *Quaternary Science Reviews*. [Online]. 53. p.pp. 1–23. Available from: http://dx.doi.org/10.1016/j.quascirev.2012.07.017.

Kim, J., Schneider, R.R., Hebbeln, D. & Peter, J.M. (2002). Last deglacial sea-surface temperature evolution in the Southeast Pacific compared to climate changes on the South American continent. *Quaternary Science Reviews*. 21. p.pp. 2085–2097.

Kim, Y., Clayton, R.W. & Jackson, J.M. (2010). Geometry and seismic properties of the subducting Cocos plate in central Mexico. *Journal of Geophysical Research*. 115. p.pp. 1–22.

Lescinsky, T. & Fink, H. (2000). Lava and ice interaction at stratovolcanoes: Use of characteristic features to determine past glacial extents and future volcanic hazards. *Journal of Geophysical Research*. 105.

Liu, T., Kinouchi, T. & Ledezma, F. (2013). Remote Sensing of Environment Characterization of recent

glacier decline in the Cordillera Real by LANDSAT, ALOS, and ASTER data. *Remote Sensing of Environment*. [Online]. 137. p.pp. 158–172. Available from: http://dx.doi.org/10.1016/j.rse.2013.06.010.

Lliboutry, L. (1998). Glaciers of Chile and Argentina. In: R. Williams & J. Ferrigno (eds.). *Satellite Image Atlas of Glaciers of the World*. Washington: U.S. Geological Survey, pp. 109–206.

Lliboutry, L. (1956). *Nieves y glaciares de Chile*. Santiago de Chile: Edicioned de la Universidad de Chile.

Maclennan, J., Jull, M., Mckenzie, D., Slater, L. & Gro, K. (2002). The link between volcanism and deglaciation in Iceland. *Geochem. Geophys. Geosyst.* 3 (11). p.pp. 1–25.

Masiokas, M.H., Rivera, A., Espizua, L.E., Villalba, R., Delgado, S. & Carlos, J. (2009). Glacier fluctuations in extratropical South America during the past 1000 years. *Palaeogeography, Palaeoclimatology, Palaeoecology*. [Online]. 281 (3–4). p.pp. 242–268. Available from: http://dx.doi.org/10.1016/j.palaeo.2009.08.006.

McGuire, B. (2013). Hazardous responses of the solid Earth to a changing climate. In: B. Mcguire & M. Maslin (eds.). *Climate Forcing of Geological Hazards*. John Wiley & Sons Ltd., pp. 1–33.

McGuire, B. (2015). Implications for hazard and risk of seismic and volcanic responses to climate change in the high-mountain cryosphere. In: C. Huggel, M. Carey, J. J. Clague, & A. Kääb (eds.). *The High-Mountain Cryosphere*. Cambridge: Cambridge University Press, pp. 109–126.

McGuire, W.J., Jones, A.P. & Neuberg, J. (1996). Volcano instability: a review of contemporary themes. *Geological Society Special Publications*. (110). p.pp. 1–23.

Morales-Arnao, B. (1998). Glaciers of Peru. In: R. Williams & J. Ferrigno (eds.). *Satellite Image Atlas of Glaciers of the World*. Washington, pp. 51–79.

NASA (2017). *Landsat 7*. [Online]. 2017. Available from: https://landsat.gsfc.nasa.gov/landsat-7/. [Accessed: 27 February 2017].

Ortiz-Guerrero, N., Brown, S.K., Delgado Granados, H. & Lombana-Criollo, C. (2015). Global monitoring capacity: development of the Global Volcano Research and Monitoring Institutions Database and analysis of monitoring in Latin America. In: S. C. Loughlin, R. S. J. Sparks, S. K. Brown, S. F. Jenkins, & C. Vye-Brown (eds.). *Global Volcanic Hazards and Risk*. Cambridge: Cambridge University Press, pp. 323–333.

Pagli, C. & Sigmundsson, F. (2008). Will present day glacier retreat increase volcanic activity? Stress induced by recent glacier retreat and its effect on magmatism at the Vatnajökull ice cap, Iceland. *Geophysical Research Letters*. 35. p.pp. 3–7.

Pardo, M. & Sufirez, G. (1995). Shape of the subducted Rivera and Cocos plates in southern Mexico Seismic and tectonic implications. *Journal of Geophysical Research*. 100 (B7). p.pp. 357–373.

Paul, F. (2002). Changes in glacier area in Tyrol, Austria, between 1969 and 1992 derived from Landsat 5 Thematic Mapper and Austrian Glacier Inventory data. *International Journal of Remote Sensing*. [Online]. 23 (4). p.pp. 787–799. Available from: http://dx.doi.org/10.1080/01431160110070708.

Paul, F., Barrand, N., Baumann, S., Berthier, E., Bolch, T., Casey, K., Frey, H., Joshi, S.P., Konovalov, V., Le Bris, R., Mölg, N., Nosenko, G., Nuth, C., Pope, A., Racoviteanu, A., Rastner, P., Raup, B., Scharrer, K., Steffen, S. & Winsvold, S. (2013a). On the accuracy of glacier outlines derived from remote sensing data. *Annals of Glaciology*. 54 (63). p.p. 171–182(12).

Paul, F., Bolch, T., Kääb, A., Nagler, T., Nuth, C., Scharrer, K., Shepherd, A., Strozzi, T., Ticconi, F., Bhambri, R., Berthier, E., Bevan, S., Gourmelen, N., Heid, T., Jeong, S., Kunz, M., Rune, T., Luckman, A., Peter, J., Boncori, M., Moholdt, G., Muir, A., Neelmeijer, J., Rankl, M., Vanlooy, J. & Niel, T. Van (2013b). Remote Sensing of Environment The glaciers climate change initiative : Methods for creating glacier area , elevation change and velocity products. *Remote Sensing of Environment*. [Online]. Available from: http://dx.doi.org/10.1016/j.rse.2013.07.043.

Paul, F., Bolch, T., Kääb, A., Nagler, T., Nuth, C., Scharrer, K., Shepherd, A., Strozzi, T., Ticconi, F., Bhambri, R., Berthier, E., Bevan, S., Gourmelen, N., Heid, T., Jeong, S., Kunz, M., Rune, T., Luckman, A., Peter, J., Boncori, M., Moholdt, G., Muir, A., Neelmeijer, J., Rankl, M., Vanlooy, J. & Niel, T. Van (2013c). The glaciers climate change initiative: Methods for creating glacier area, elevation change and velocity products. *Remote Sensing of Environment*. [Online]. Available from: http://dx.doi.org/10.1016/j.rse.2013.07.043.

Paul, F., Huggel, C., Kellenberger, T. & Maisch, M. (2003). Comparison of TM-derived glacier areas with higher resolution data sets. *EARSeL eProc*. 2 (1). p.pp. 15–21.

Paul, F. & Mölg, N. (2014). Hasty retreat of glaciers in northern Patagonia from 1985 to 2011. *Journal of Glaciology*. 60 (224). p.pp. 1033–1043.

Paul, F., Winsvold, S.H., Kääb, A., Nagler, T. & Schwaizer, G. (2016). Glacier Remote Sensing Using Sentinel-2. Part II: Mapping Glacier Extents and Surface Facies, and Comparison to Landsat 8. *Remote Sensing*. 8 (575). p.pp. 1–15.

Peduzzi, P., Herold, C. & Silverio, W. (2010). Assessing high altitude glacier thickness, volume and area changes using field, GIS and remote sensing techniques: the case of Nevado Coropuna (Peru). *The Cryosphere*. 4 (3). p.pp. 313–323.

Pfeffer, W.T., Arendt, A.A., Bliss, A., Bolch, T., Cogley, J.G., Gardner, A.S., Hagen, J., Hock, R., Kaser, G., Kienholz, C., Miles, E.S., Moholdt, G., Rastner, P., Raup, B.H., Paul, F., Radic, V., Mo, N., Rich, J., Sharp, M.J. & Consortium, T.H.E.R. (2014). The Randolph Glacier Inventory: a globally complete inventory of glaciers. *Journal of Glaciology*. 60 (221). p.pp. 537–552.

Pinel, V. & Jaupart, C. (2005). Some consequences of volcanic edifice destruction for eruption conditions. *Journal of Volcanology and Geothermal Research*. 145. p.pp. 68–80.

Rabatel, A., Francou, B., Soruco, A., Gomez, J., Ceballos, J.L., Vuille, M., Sicart, J., Huggel, C., Rabatel, A., Francou, B., Soruco, A. & Gomez, J. (2013). Current state of glaciers in the tropical Andes: a multi-century perspective on glacier evolution and climate change. *The Cryosphere*. 7. p.pp. 81–102.

Raup, B., Kääb, A., Kargel, J.S., Bishop, M.P., Hamilton, G., Lee, E., Paul, F., Rau, F., Soltesz, D., Singh Khalsa, J.S., Beedle, M. & Helm, C. (2007). Remote sensing and GIS technology in the Global Land Ice Measurements from Space (GLIMS) Project. *Computers & Geoscience*. 33. p.pp. 104–125.

Rignot, E., Rivera, A. & Casassa, G. (2003). Contribution of the Patagonia Icefields of South America to Sea Level Rise. *Science*. 302 (OCTOBER). p.pp. 434–438.

Rivera, A. & Bown, F. (2013). Recent glacier variations on active ice capped volcanoes in the Southern Volcanic Zone (37° - 46°), Chilean Andes. *Journal of South American Earth Sciences*. [Online]. 45. p.pp. 345–356. Available from: http://dx.doi.org/10.1016/j.jsames.2013.02.004.

Rivera, A., Bown, F., Cawkell, F., Bravo, C., Rada, C. & Zenteno, P. (2009). Glacier advance at Volcán Michinmahuida; a consequence of the ongoing eruption of Volcán Chaitén ? *XII Congreso Geológico Chileno*. p.pp. 4–7.

Rivera, A., Bown, F., Mella, R., Wendt, J., Casassa, G., Rignot, E., Clavero, J. & Brock, B. (2006). Ice volumetric changes on active volcanoes in southern Chile. *Annals of Glaciology*. 43. p.pp. 111–122.

Rivera, A., Bravo, C. & Buob, G. (2017). Climate change and land ice. *The International Encyclopedia of Geography*.

Rivera, A., Brown, F., Carrión, D. & Zenteno, P. (2012). Glacier responses to recent volcanic activity in Southern Chile. *Environmental Research Letters*. 7.

Rivera, A., Corripio, J.G., Brock, B., Clavero, J. & Wendt, J. (2008). Monitoring ice-capped active Volcán Villarrica, southern Chile, using terrestrial photography combined with automatic weather stations and global positioning systems. *Journal of Glaciology*. 54 (188). p.pp. 920–930.

Rosenblüth, B., Fuenzalida, H.A. & Aceituno, P. (1997). Recent Temperature Variations in Southern South America. *International Journal of Climatology*. 17. p.pp. 67–85.

Schauwecker, S., Rohere, M., Huggel, C., Endries, J., Montoya, N., Neukom, R., Perry, B., Salzmann, N., Schwarb, M. & Suarez, W. (2017). The freezing level in the tropical Andes, Peru: An indicator for present and future glacier extents. *Journal of Geophysical Research: Athmosphere*. p.pp. 5172–5189.

Schneider, D., Delgado Granados, H. & Huggel, C. (2008). Assessing lahars from ice-capped volcanoes using ASTER satellite data , the SRTM DTM and two different flow models: case study on Iztaccíhuatl (Central Mexico). *Natural Hazards and Earth System Science*. 8 (3). p.pp. 559–571.

Seidel, D. & Free, M. (2003). Comparison of lower- tropospheric temperature climatologies and trends at low and high elevation radiosonde sites. *Climatic Change*. 59. p.pp. 53–74.

Siebert, L., Simkin, T. & Kimberly, P. (2010). *Volcanoes of the World*. 3rd Editio. Los Angeles: University of California Press.

Sigmundsson, F., Pinel, V., Lund, B., Albino, F., Pagli, C., Geirsson, H. & Sturkell, E. (2010). Climate effects on volcanism: influence on magmatic systems of loading and unloading from ice mass variations, with examples from Iceland. *Philosophical Transactions of the Royal Society*. 368. p.pp. 2519–2534.

Sold, L., Huss, M., Machguth, H., Joerg, P.C., Vieli, G.L., Linsbauer, A., Salzmann, N., Zemp, M. & Hoelzle, M. (2016). *Mass Balance Re-analysis of Findelengletscher , Switzerland ; Benefits of Extensive Snow Accumulation Measurements*. 4 (February).

Stern, C.R. (2004). Active Andean volcanism: its geologic and tectonic setting. *Revista Geológica de Chile*. 31 (2). p.pp. 161–206.

Troncoso, L., Bustillos, J., Romero, J.E., Carrillo, J., Montalvo, E. & Izquierdo, T. (2017). Hydrovolcanic ash emission between August 14 and 24, 2015 at Cotopaxi Volcano (Ecuador): Characterization and eruption mechanisms. *Journal of Volcanology and Geothermal Research*. [Online]. Available from: http://dx.doi.org/10.1016/j.jvolgeores.2017.05.032.

Tuffen, H. (2010). How will melting of ice affect volcanic hazards in the twenty-first century? *Philosophical Transactions of the Royal Society*. 368. p.pp. 2535–2558.

Tuffen, H. & Betts, R. (2010). Volcanism and climate: chicken and egg (or vice versa)? *Philosophical Transactions of the Royal Society*. 368. p.pp. 2585–2588.

U.S. Geological Survey (2016a). *Landsat 8*. [Online]. 2016. Available from:

https://landsat.usgs.gov/landsat-8. [Accessed: 15 March 2017].

U.S. Geological Survey (2016b). *What are the band designations for the Landsat satellites?* [Online]. 2016. Available from: https://landsat.usgs.gov/what-are-band-designations-landsat-satellites. [Accessed: 27 February 2017].

Vaughan, D.G., Comiso, J.C., Allison, I., Carrasco, J., Kaser, G., Kwok, R., Mote, P., Murray, T., Paul, F., Ren, J., Rignot, E., Solomina, O., Steffen, K. & Zhang, T. (2013). Observations: Cryosphere. In: T. F. Stocker, D. Qin, G.-K. Plattner, M. Tingnor, S. k. Allen, J. Boschung, A. Nauels, Y. Xia, V. Bex, & P. M. Midgley (eds.). *Climate Change 2013: The Physical Science Basis. Contribution of Working Group I to the Fifth Assessment Report of the Intergovernmental Panel on Climate Change*. United Kingdom and New York USA: Cambridge University Press, Cambridge.

Vázquez-selem, L. & Heine, K. (2004). Late Quaternary glaciation of México. In: J. Ehlers & P. L. Gibbard (eds.). *Quaternary Glaciations—Extent and Chronology*. Holland: Elsevier B.V., pp. 233–242.

Vuille, M., Francou, B., Wagnon, P., Juen, I., Kaser, G., Mark, B.G. & Bradley, R.S. (2008). Climate change and tropical Andean glaciers: Past , present and future. *Earth-Science Reviews*. 89. p.pp. 79–96.

White, S.E. (2002). Glaciers of Mexico. In: S. Richard, J. Williams, & J. G. Ferrigno (eds.). *Satellite Image Atlas of Glaciers of the World*. Washington: U.S. Geological Survey, pp. 383–405.

Wilson, M. (1989). *Igneous Petrogenesis*. Dordrecht: Springer.

Winchester, V. & Harrison, S. (1996). Recent Oscillations of the San Quintin and San Rafael Glaciers , Patagonian Chile. *Geografiska Annaler*. 78 (1). p.pp. 35–49.

Appendix

Maps showing glacier outline for all three time steps:

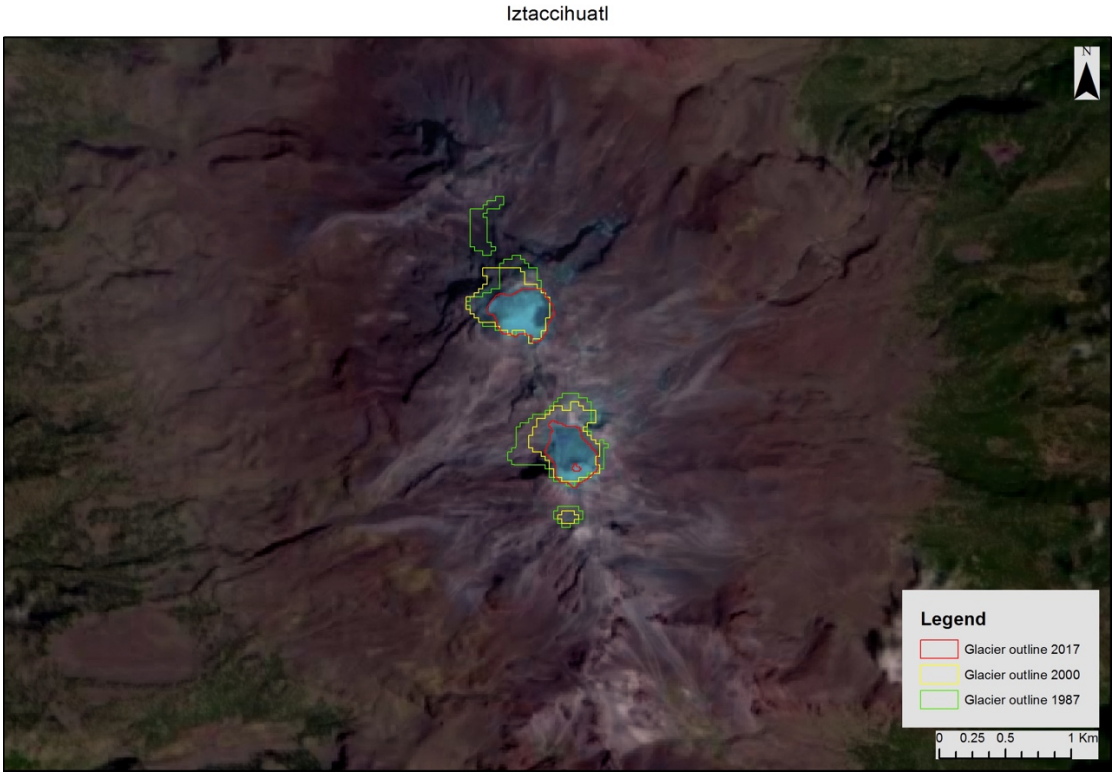

Figure A 1:Glacier outlines of Iztaccíhuatl (Mexico).

Figure A 2: Glacier outlines of Popocatepetl (Mexico).

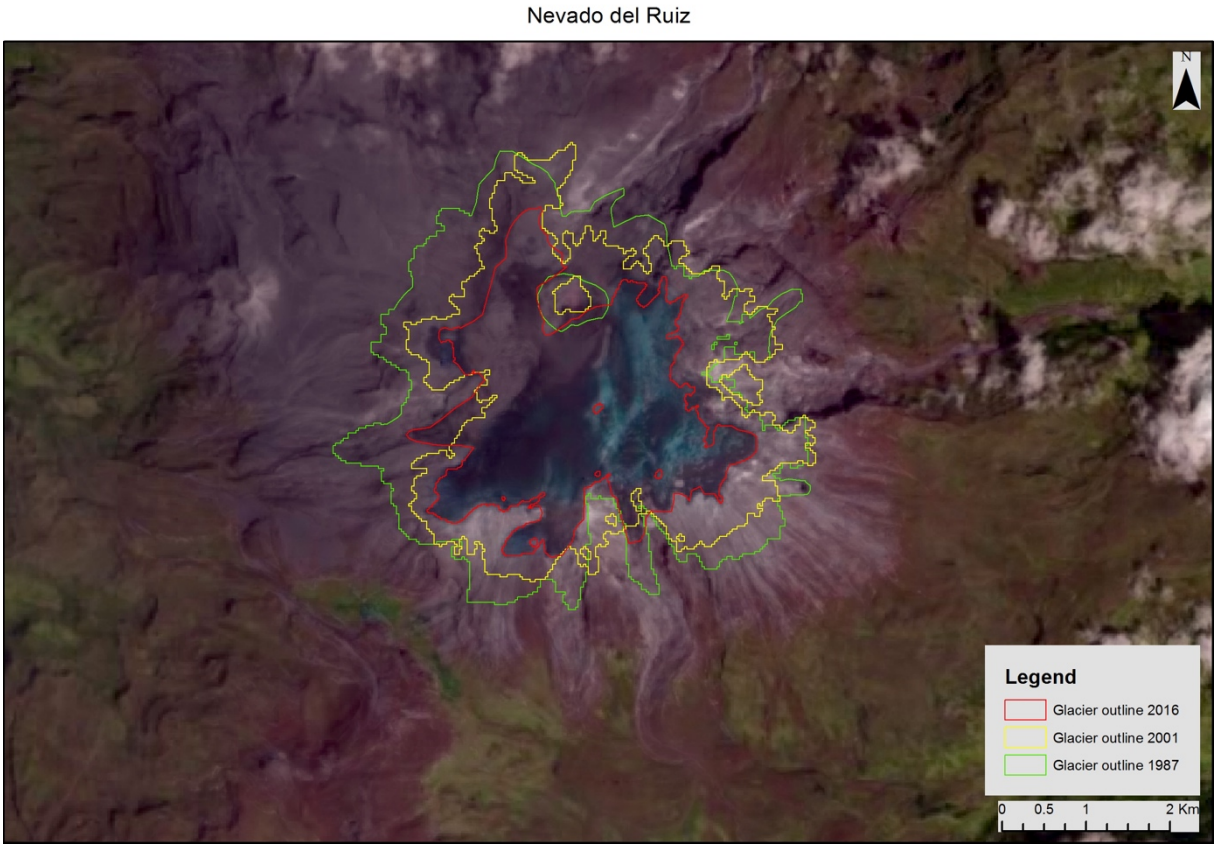

Figure A 3: Glacier outlines of Nevado del Ruiz (Colombia).

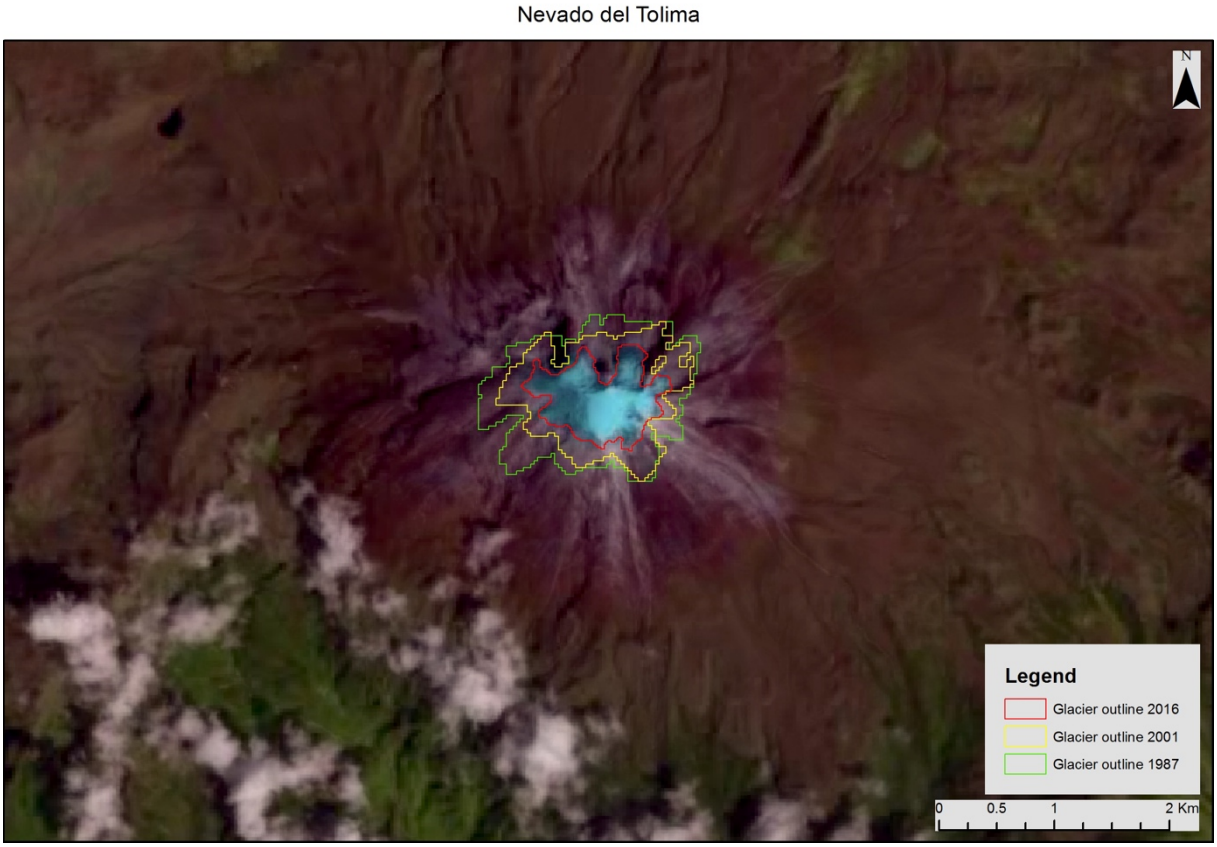

Figure A 4: Glacier outlines of Nevado del Tolima (Colombia).

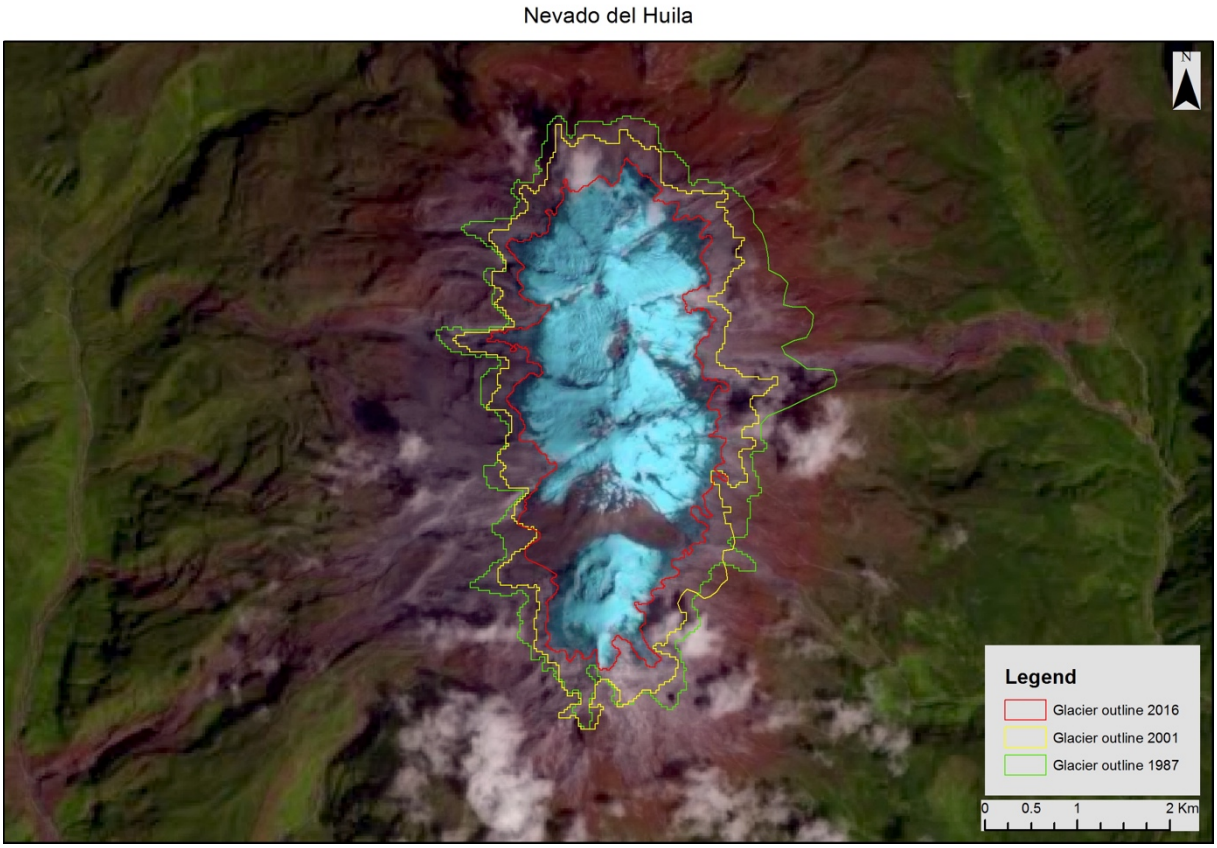

Figure A 5: Glacier outlines of Nevado del Huila (Colombia).

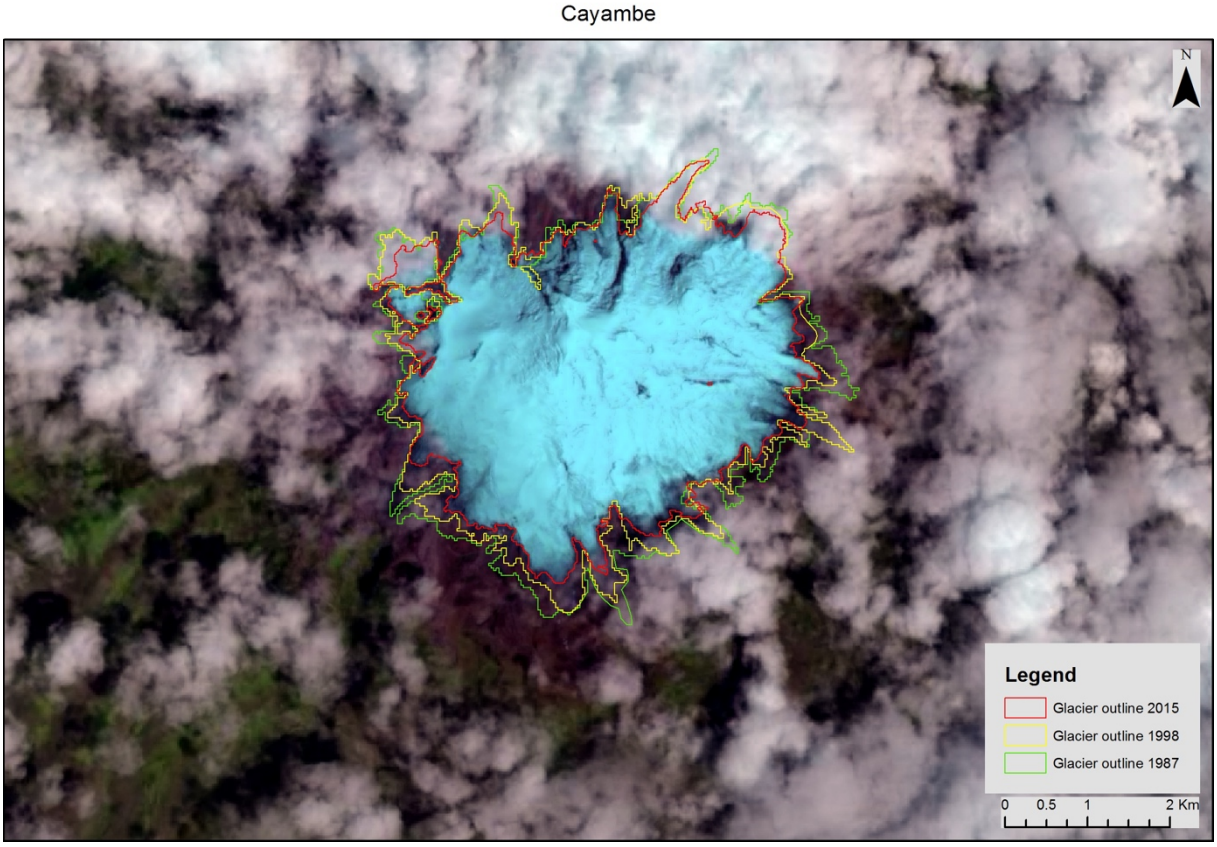

Figure A 6: Glacier outlines of Cayambe (Ecuador).

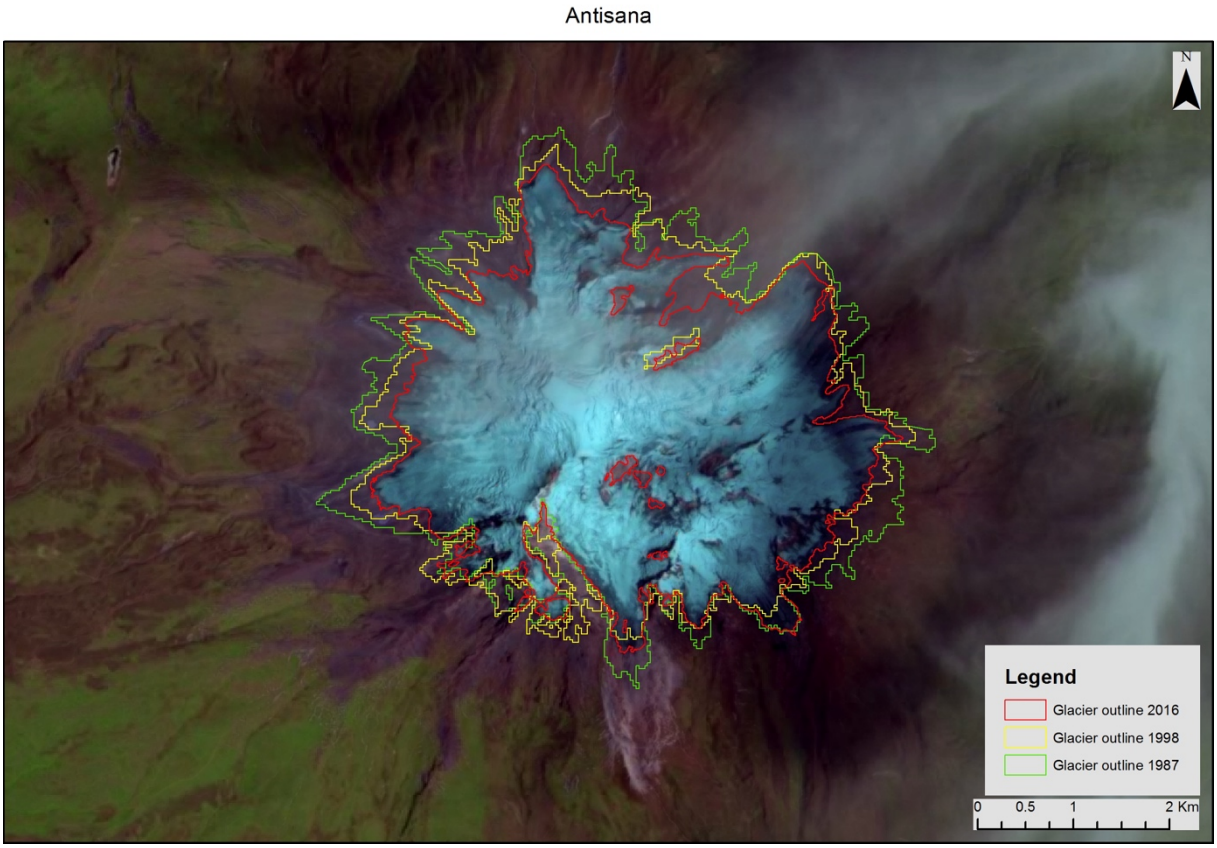

Figure A 7: Glacier outlines of Antisana (Ecuador).

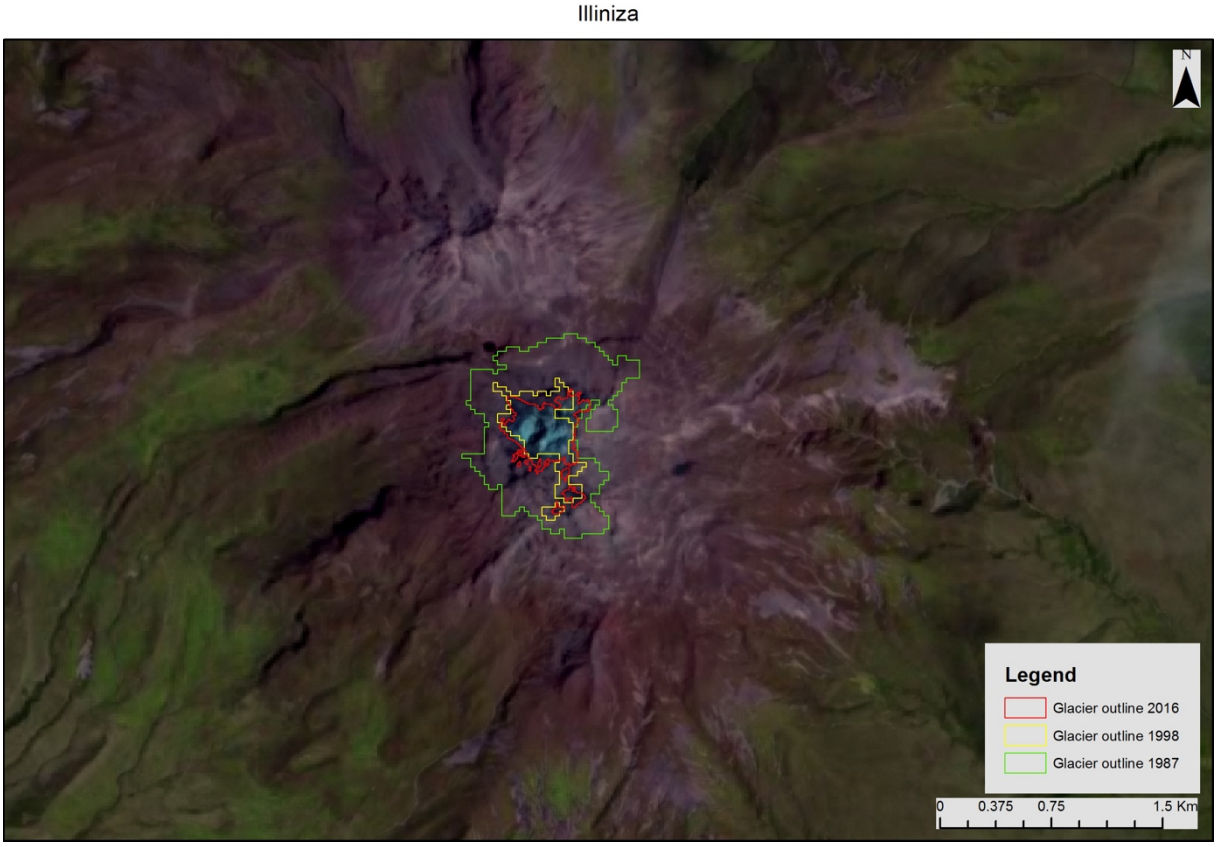

Figure A 8: Glacier outlines of Illiniza (Ecuador).

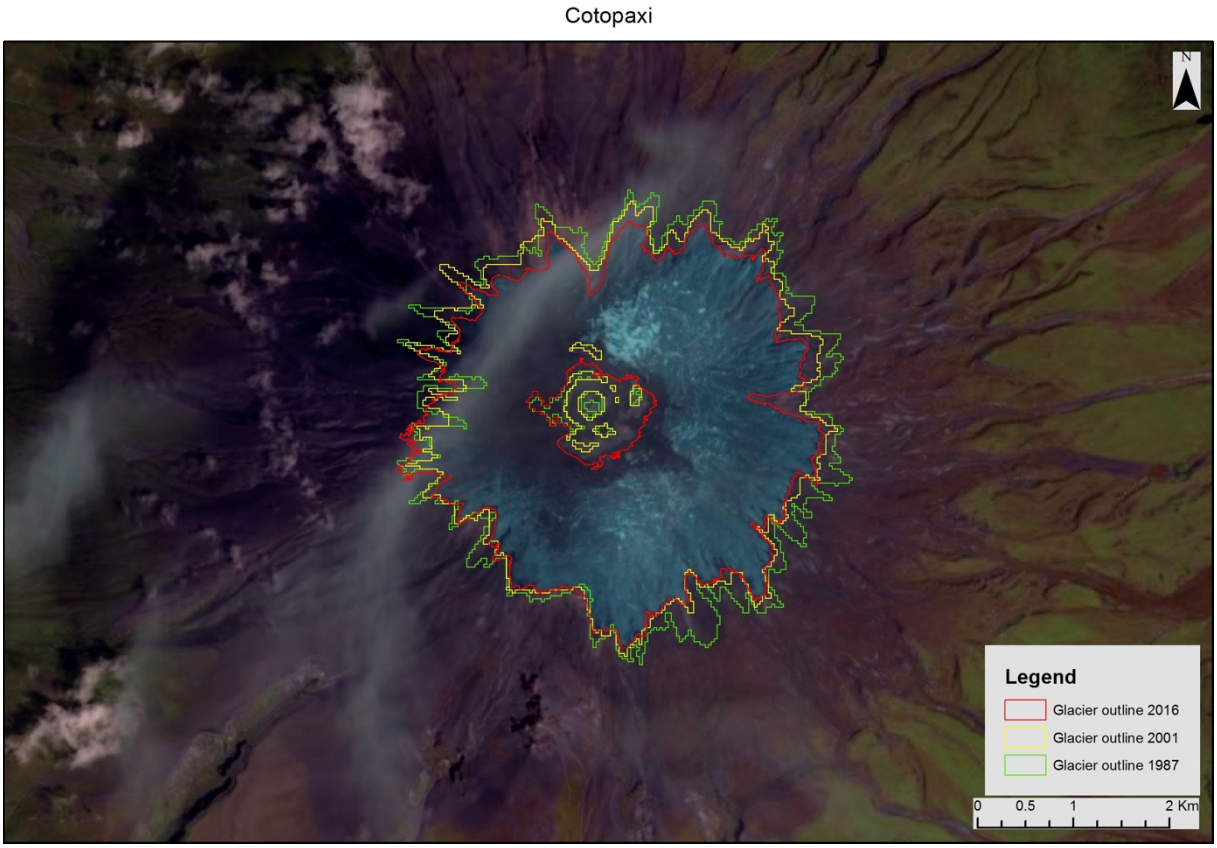

Figure A 9: Glacier outlines of Cotopaxi (Ecuador).

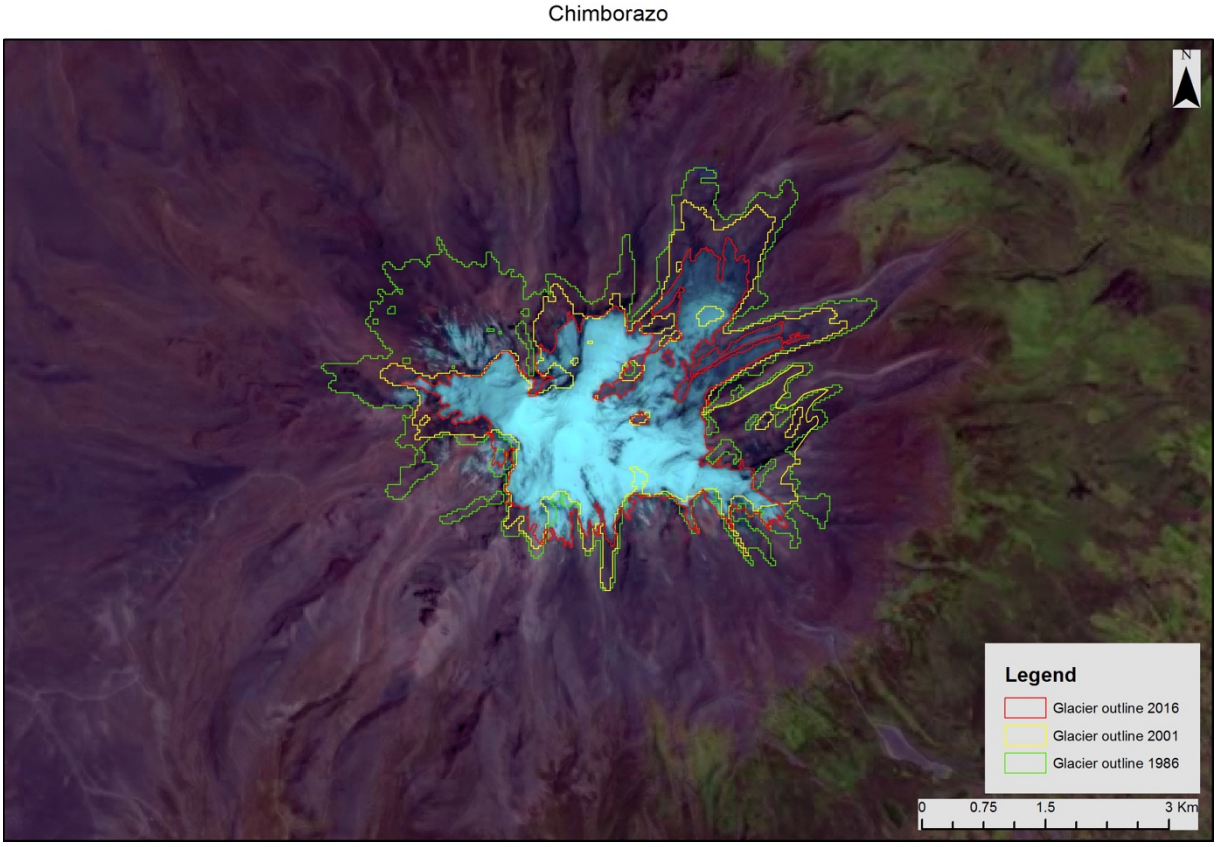

Figure A 10: Glacier outlines of Chimborazo (Ecuador).

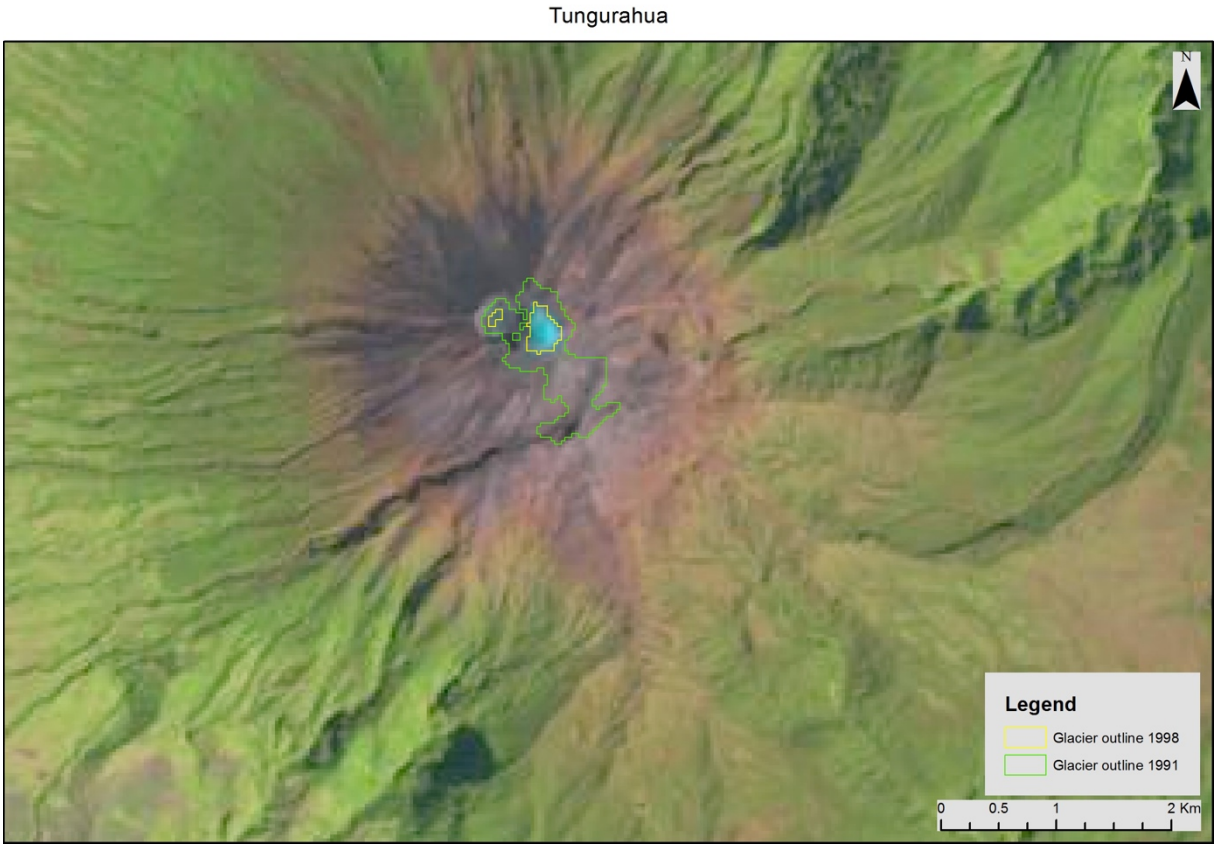

Figure A 11: Glacier outlines of Tungurahua (Ecuador).

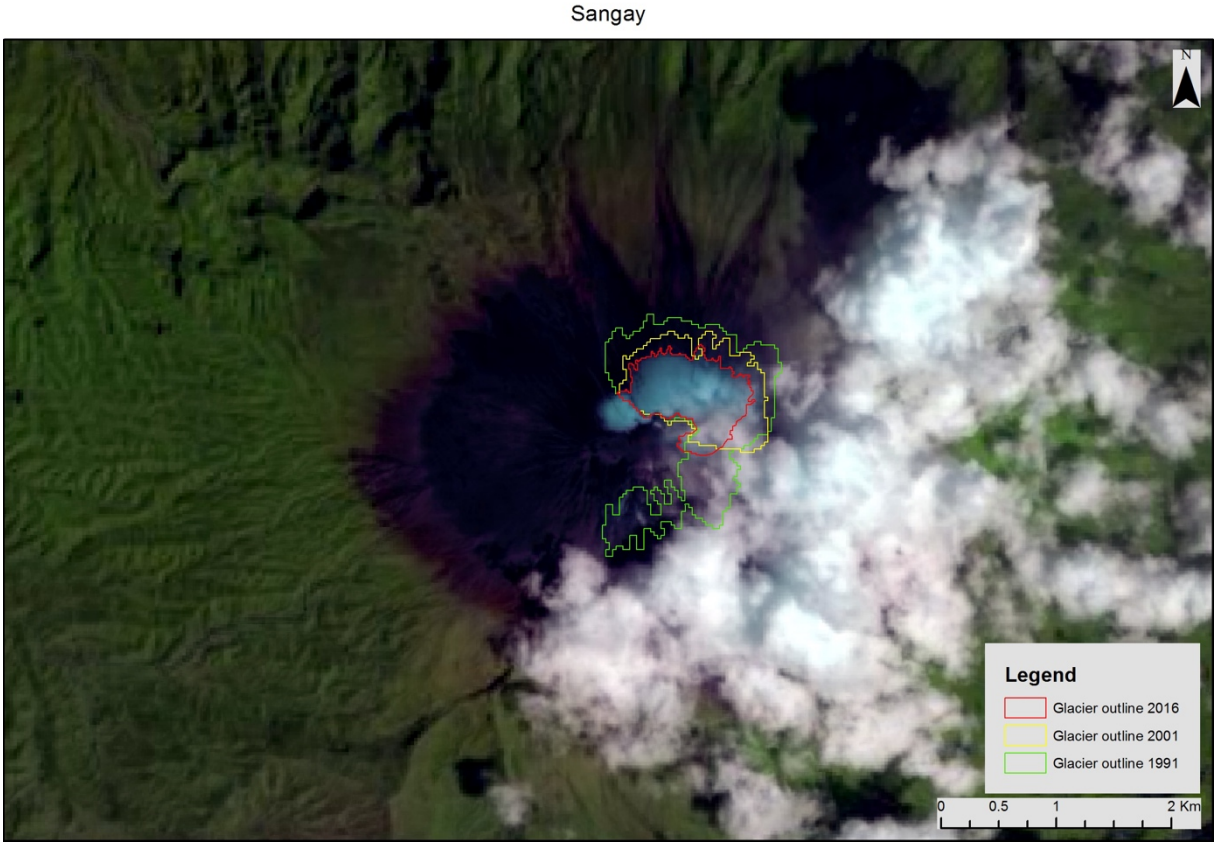

Figure A 12: Glacier outlines of Sangay (Ecuador).

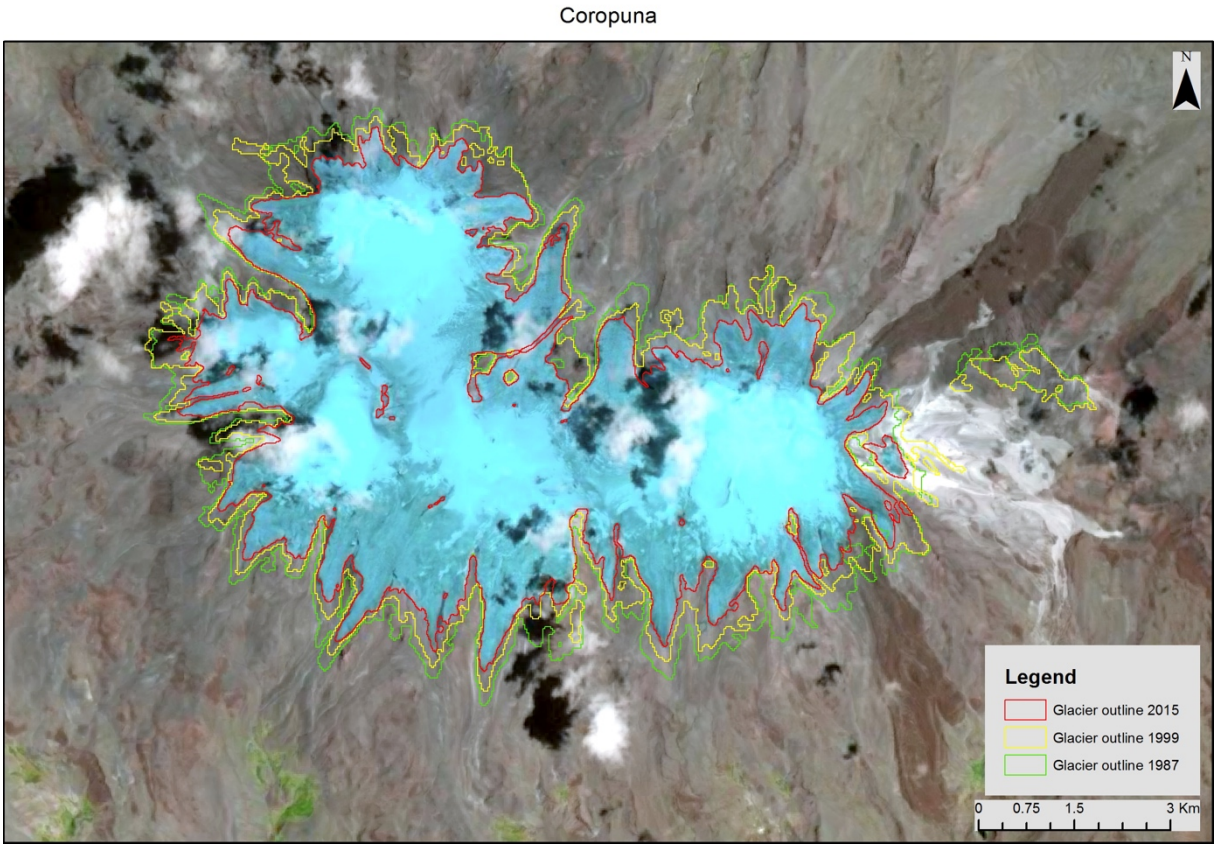

Figure A 13: Glacier outlines of Coropuna (Peru).

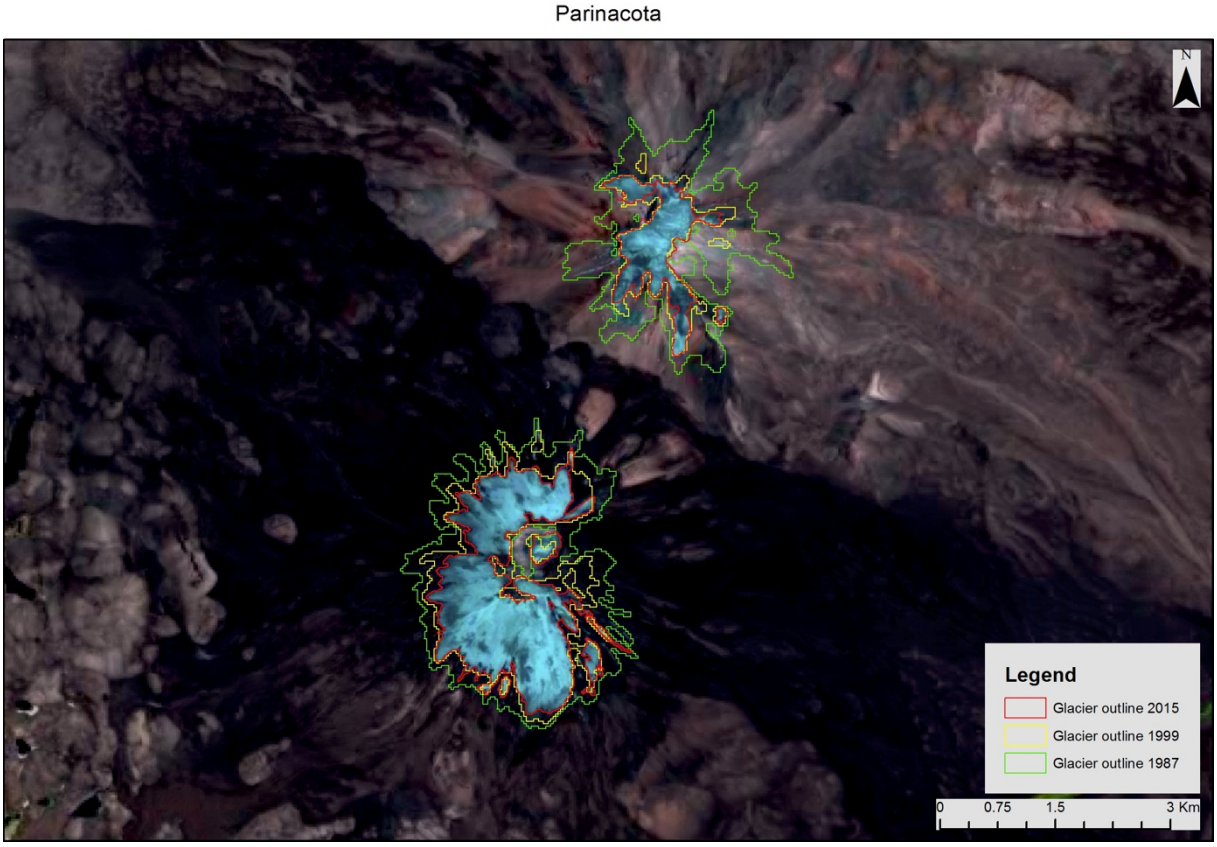

Figure A 14: Glacier outlines of Parinacota (south) and Pomerape (north) (Bolivia/Chile).

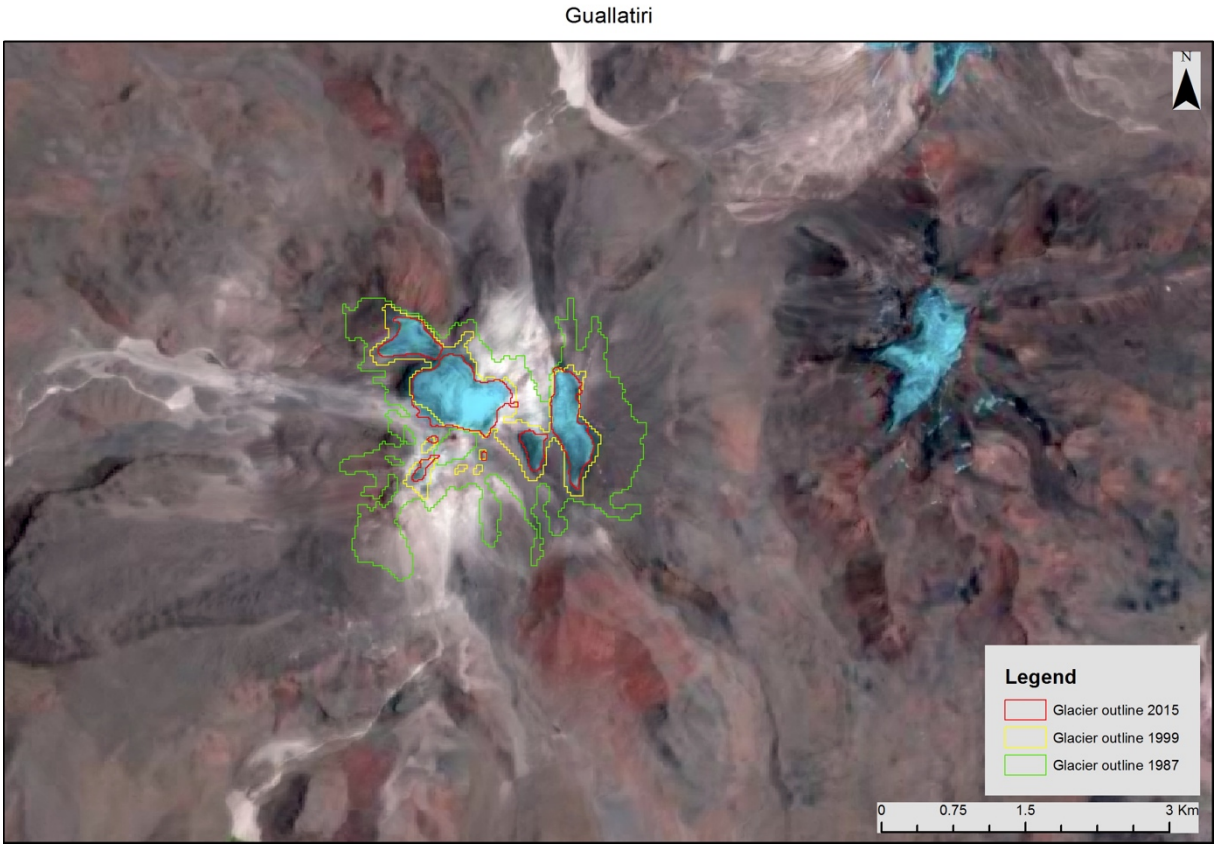

Figure A 15: Glacier outlines of Guallatiri (Bolivia/Chile).

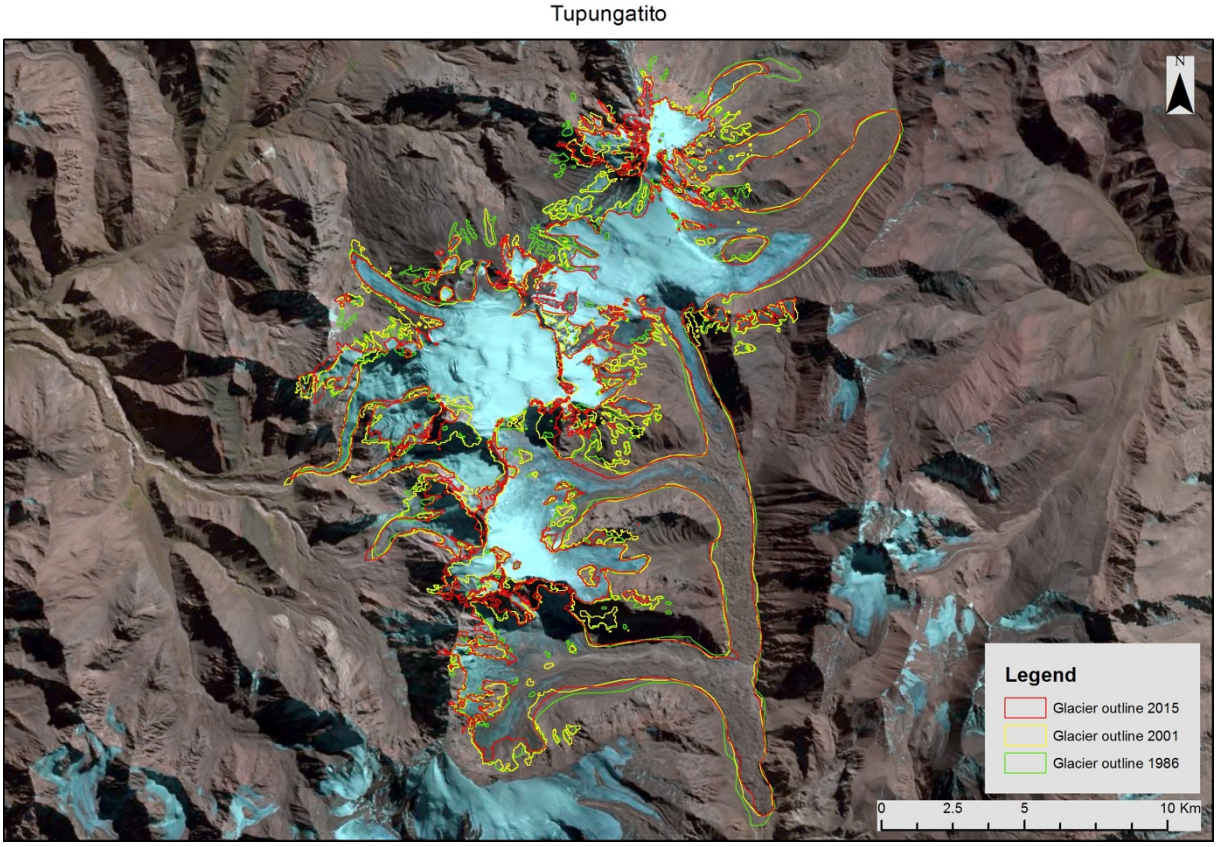

Figure A 16: Glacier outlines of Tupungatito (Chile).

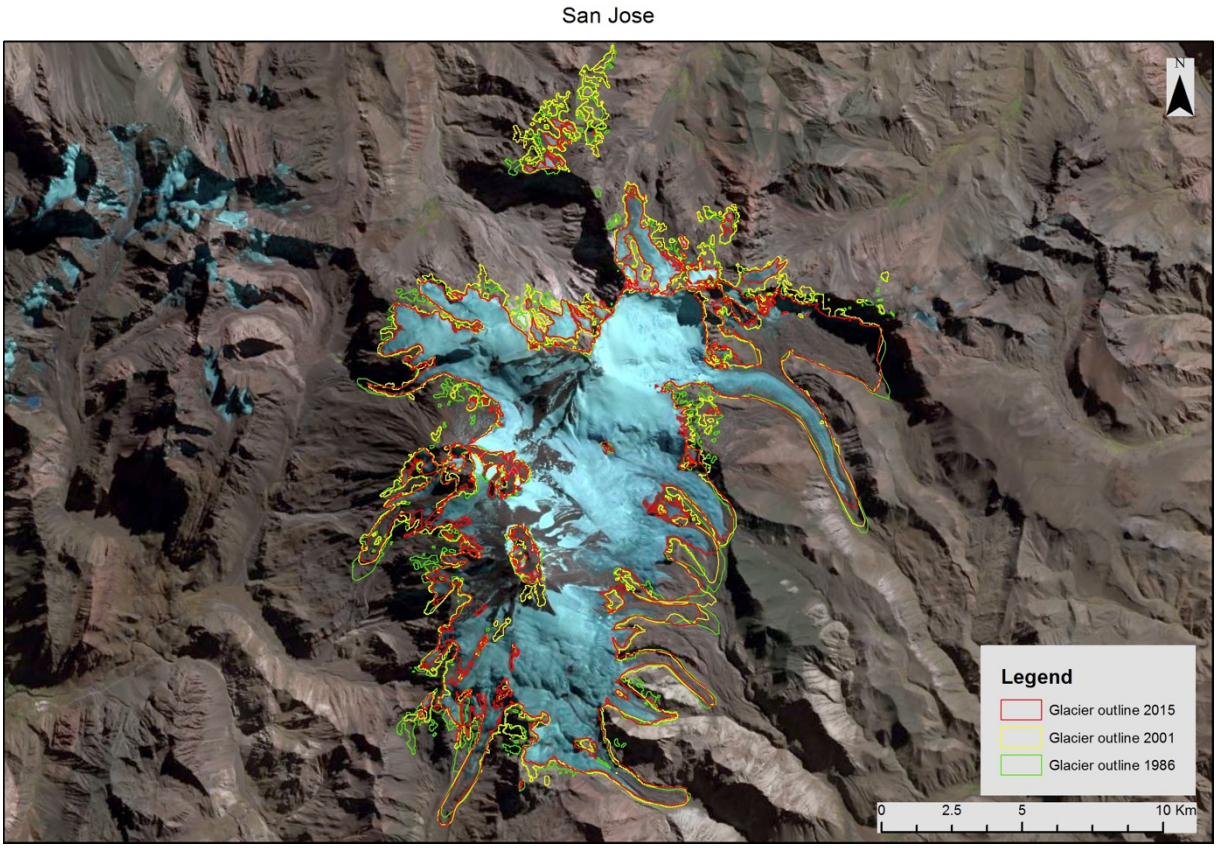

Figure A 17: Glacier outlines of San Jose (Chile/Argentina).

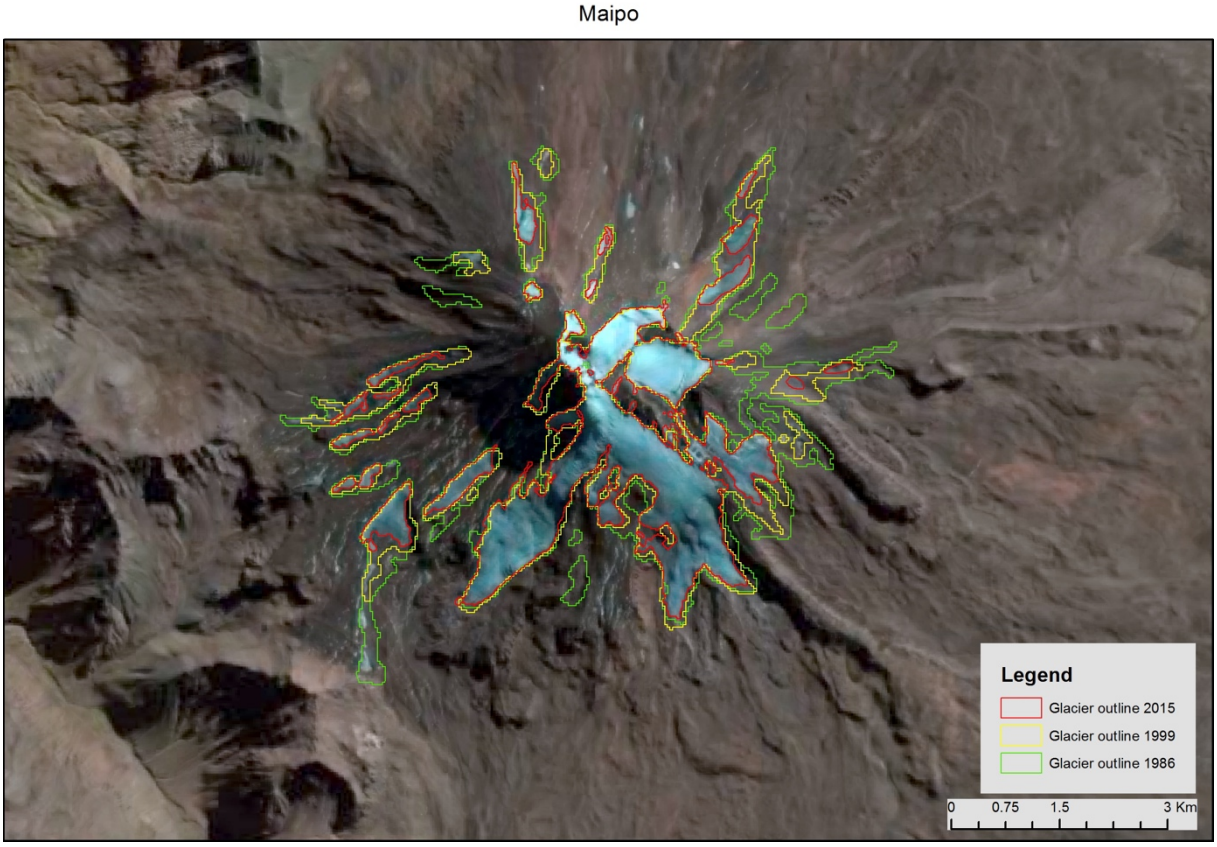

Figure A 18: Glacier outlines of Maipo (Chile/Argentina).

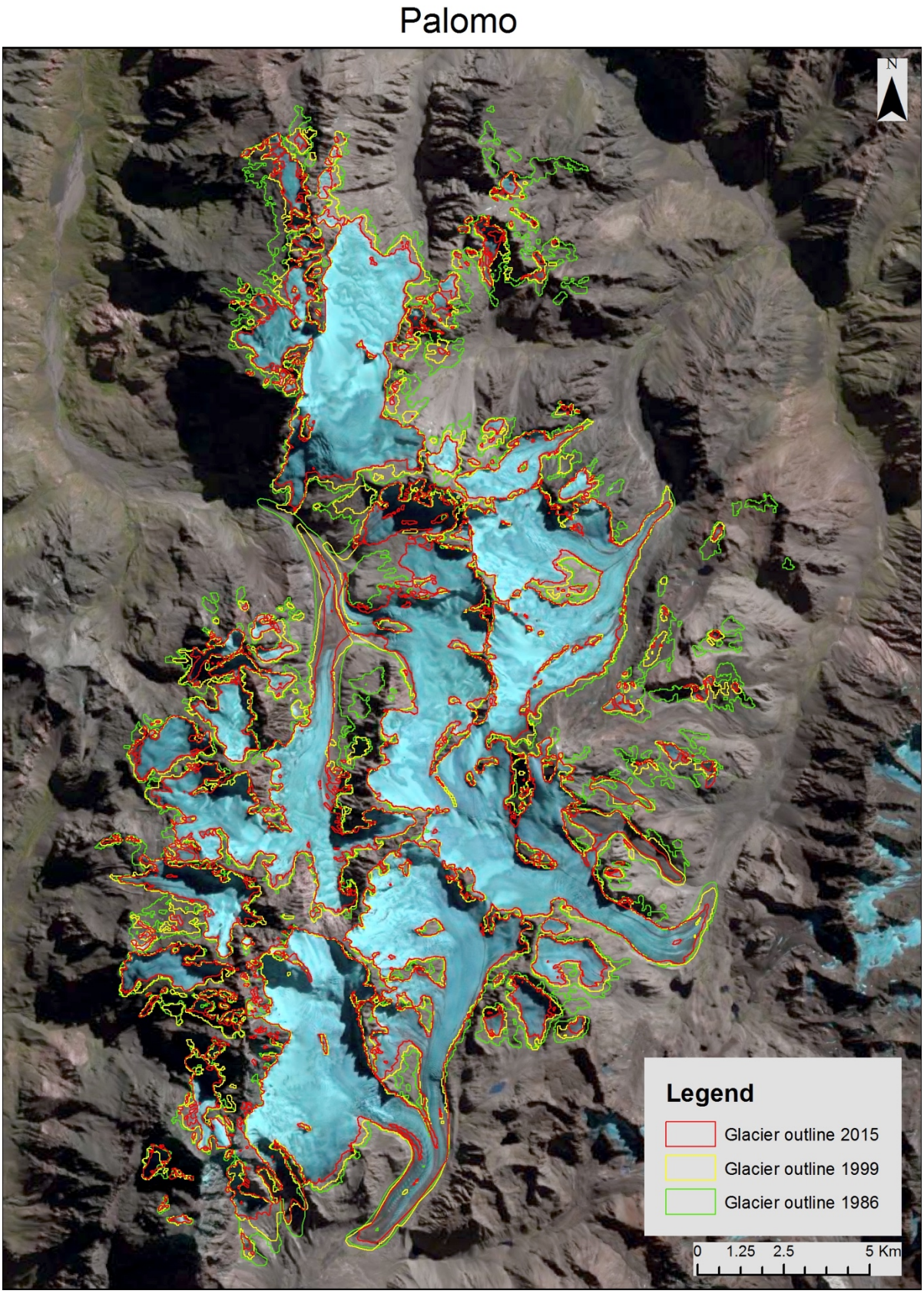

Figure A 19: Glacier outlines of Palomo (Chile).

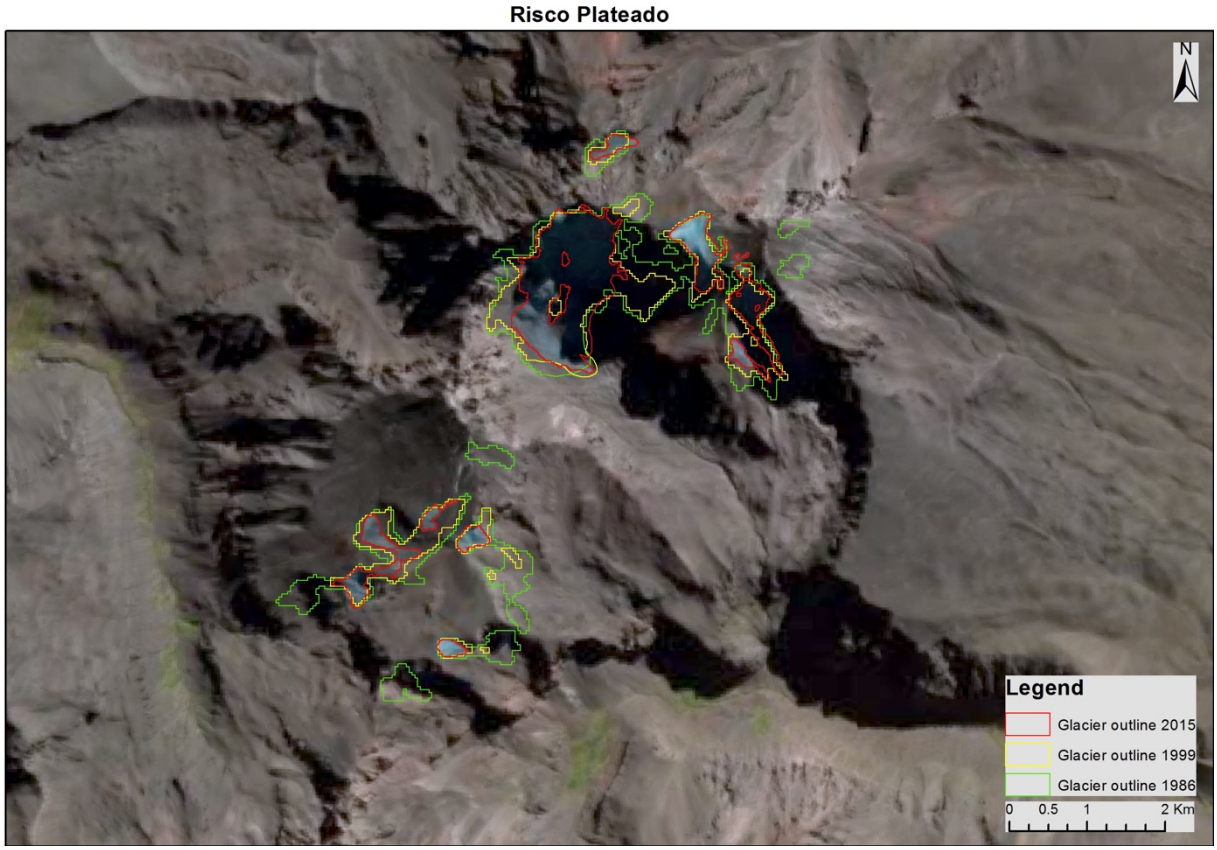

Figure A 20: Glacier outlines of Risco Plateado (Argentina).

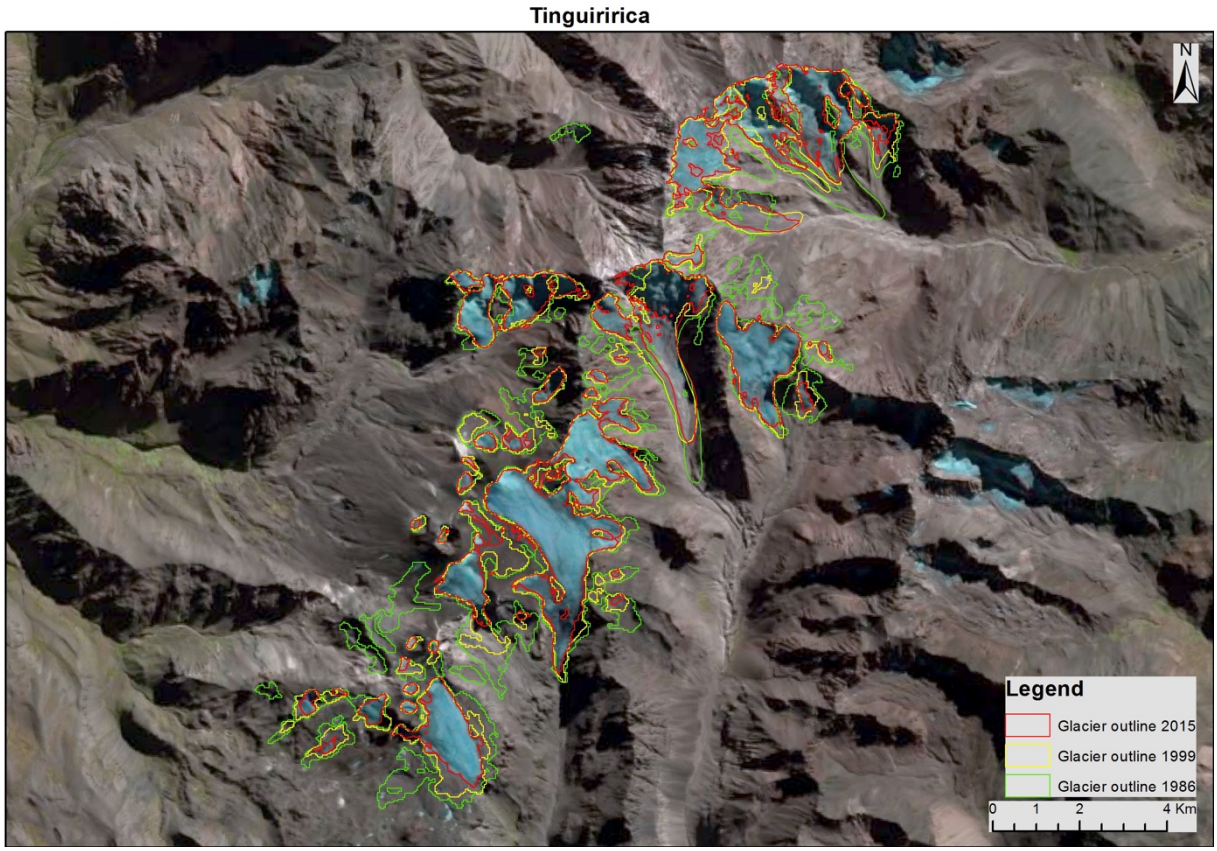

Figure A 21: Glacier outlines of Tingiririca (Chile).

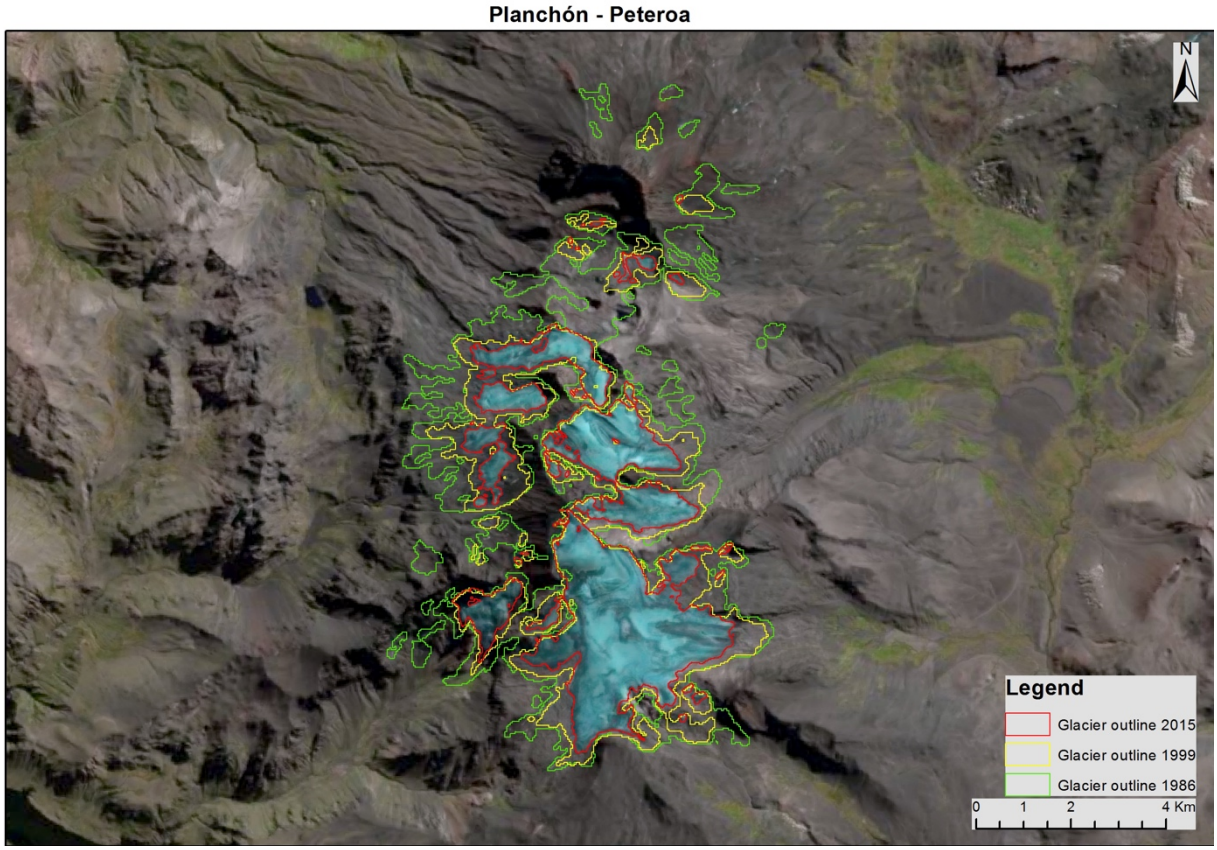

Figure A 22: Glacier outlines of Planchón-Peteado (Chile/Argentina).

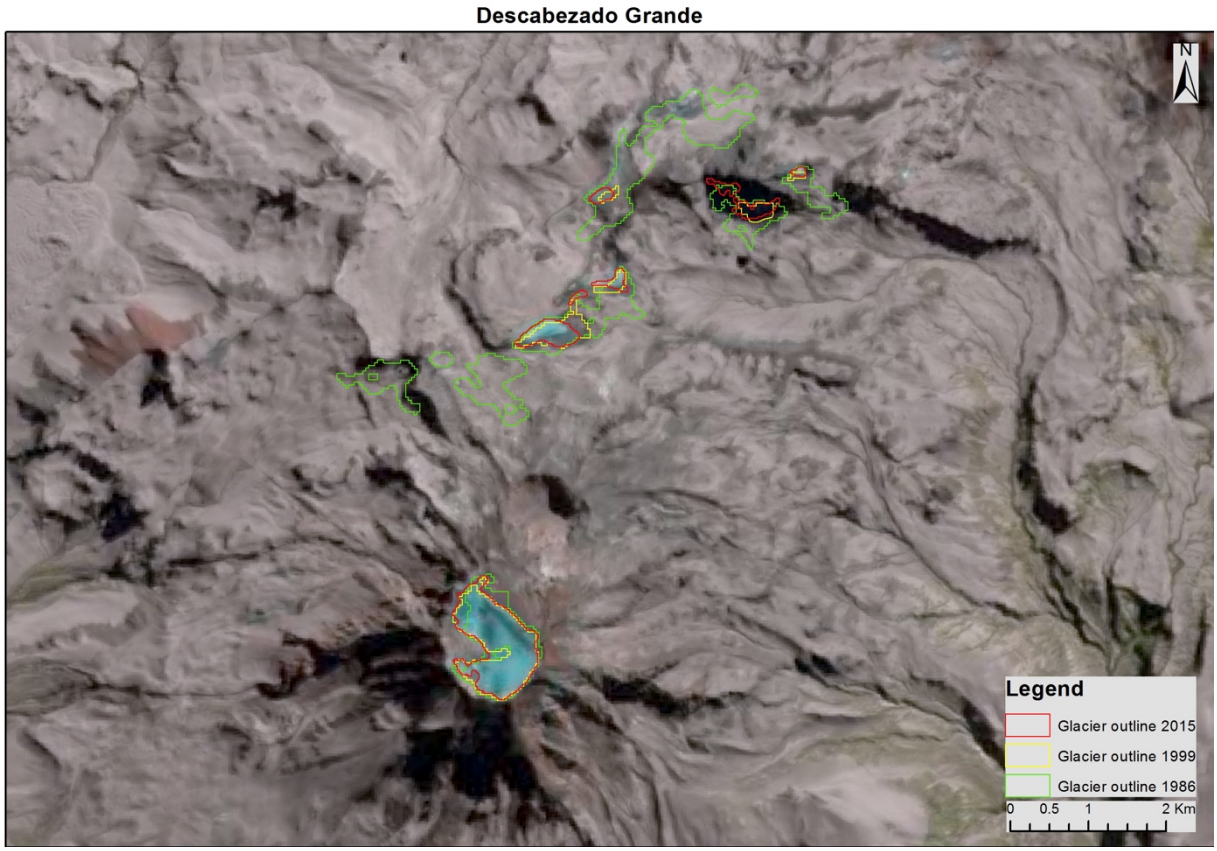

Figure A 23: Glacier outlines of Descabezado Grande (Chile).

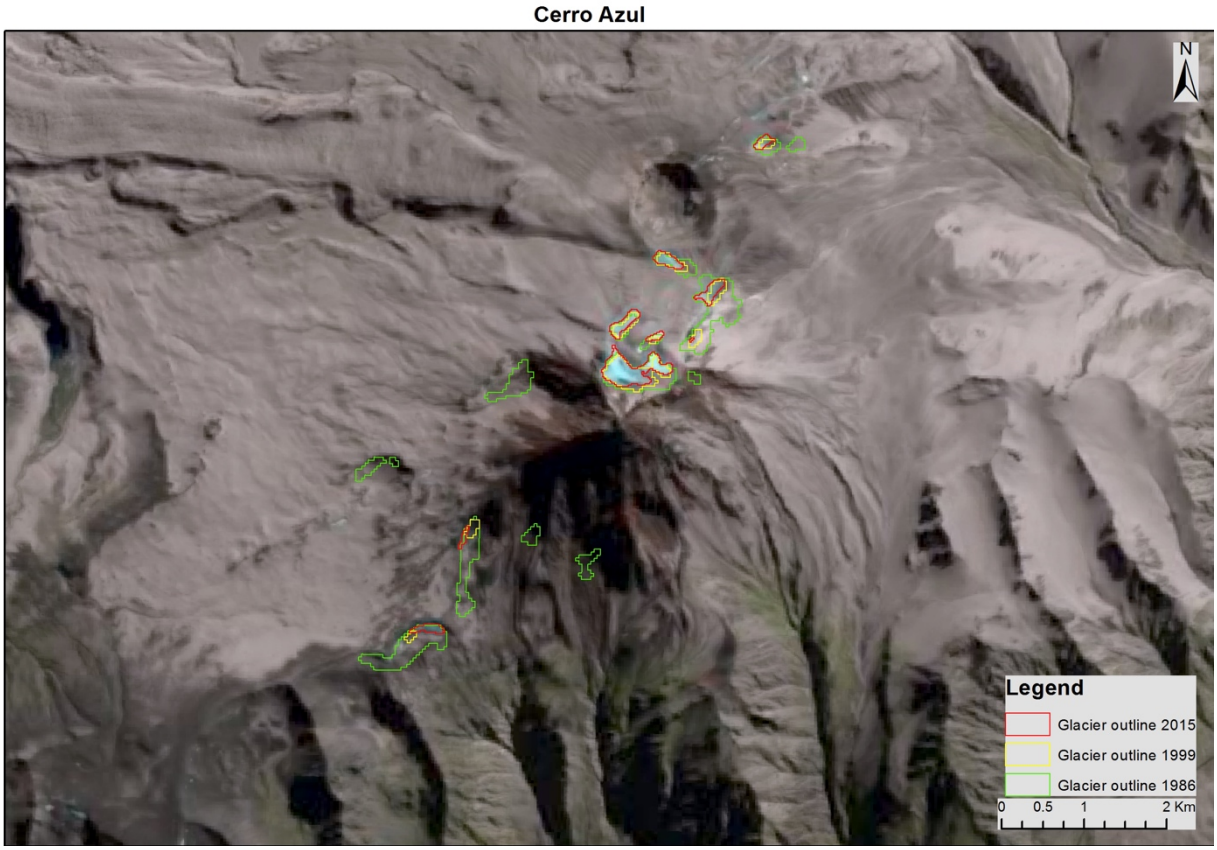

Figure A 24: Glacier outlines of Cerro Azul (Chile).

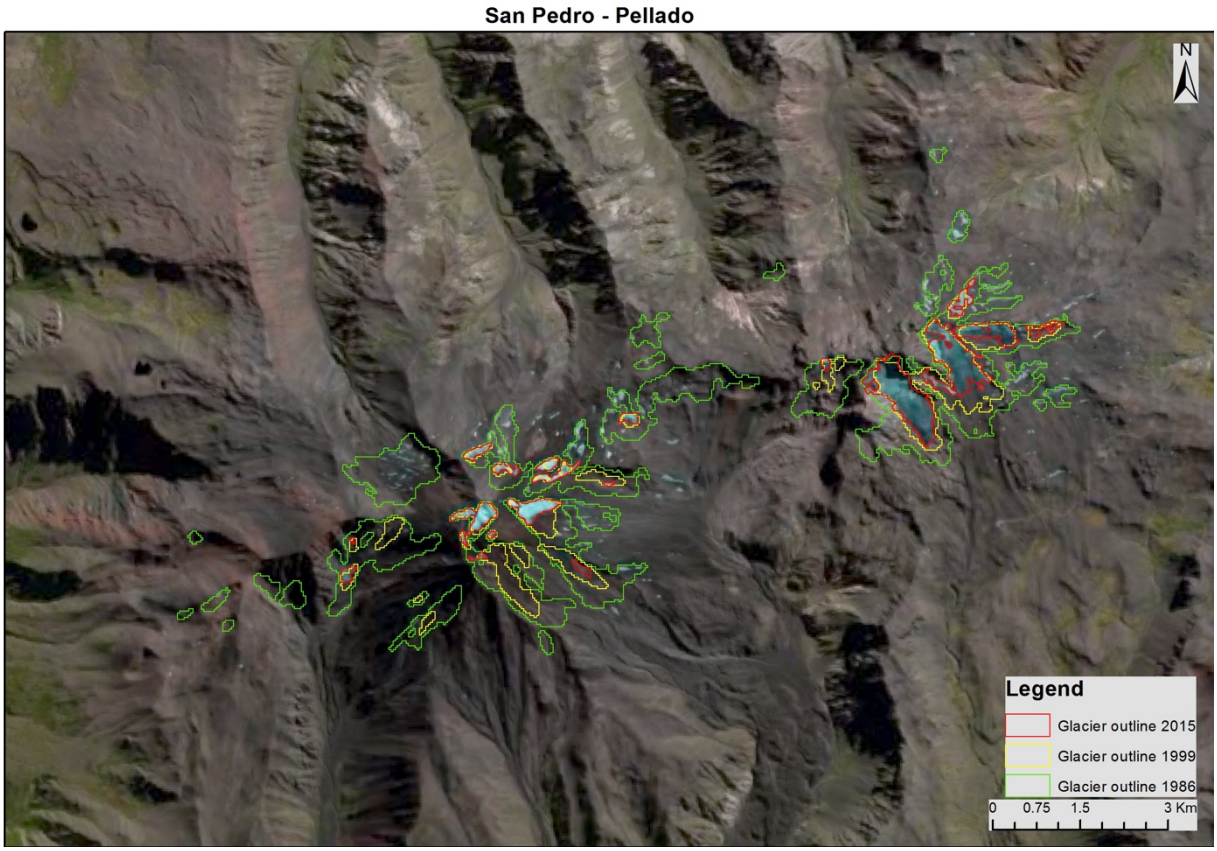

Figure A 25: Glacier outlines of San Pedro - Pellado (Chile).

Figure A 26: Glacier outlines of Nevado de Longavi (Chile).

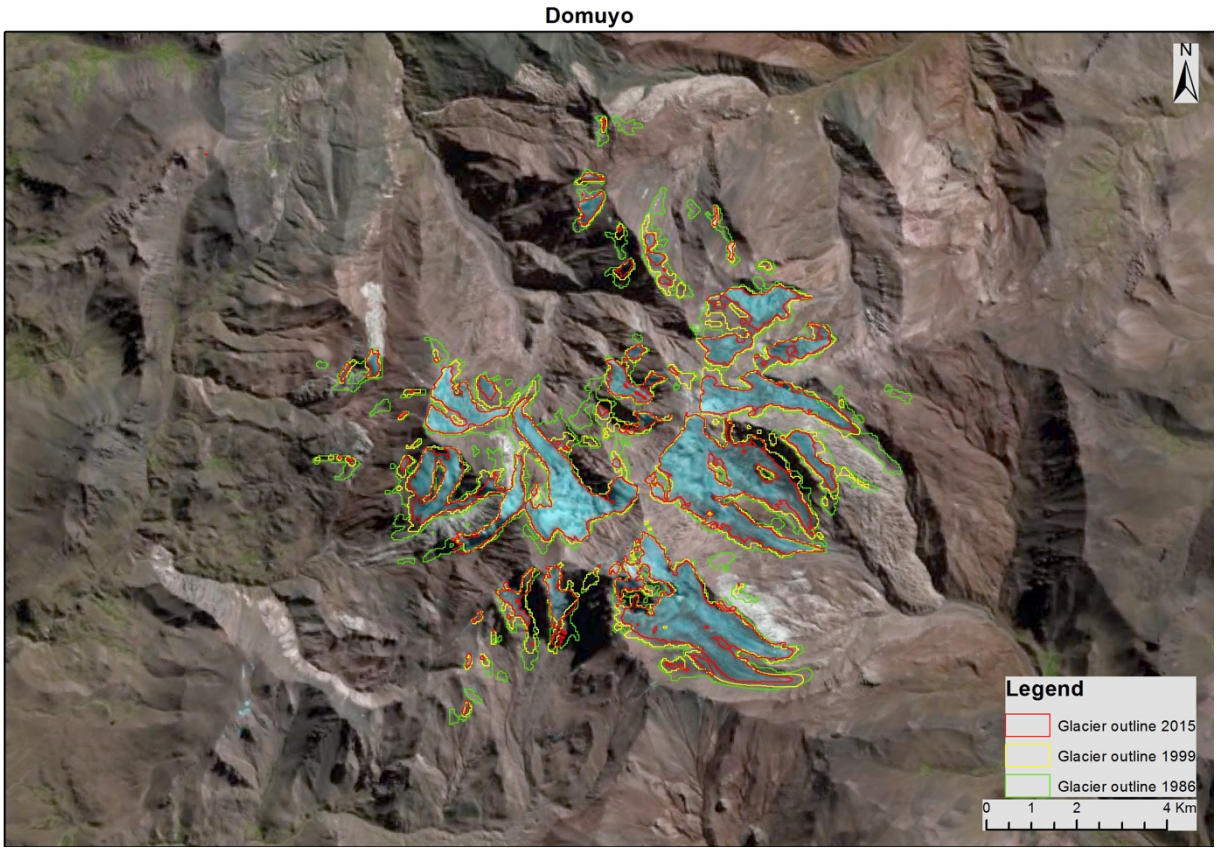

Figure A 27: Glacier outlines of Domuyo (Argentina).

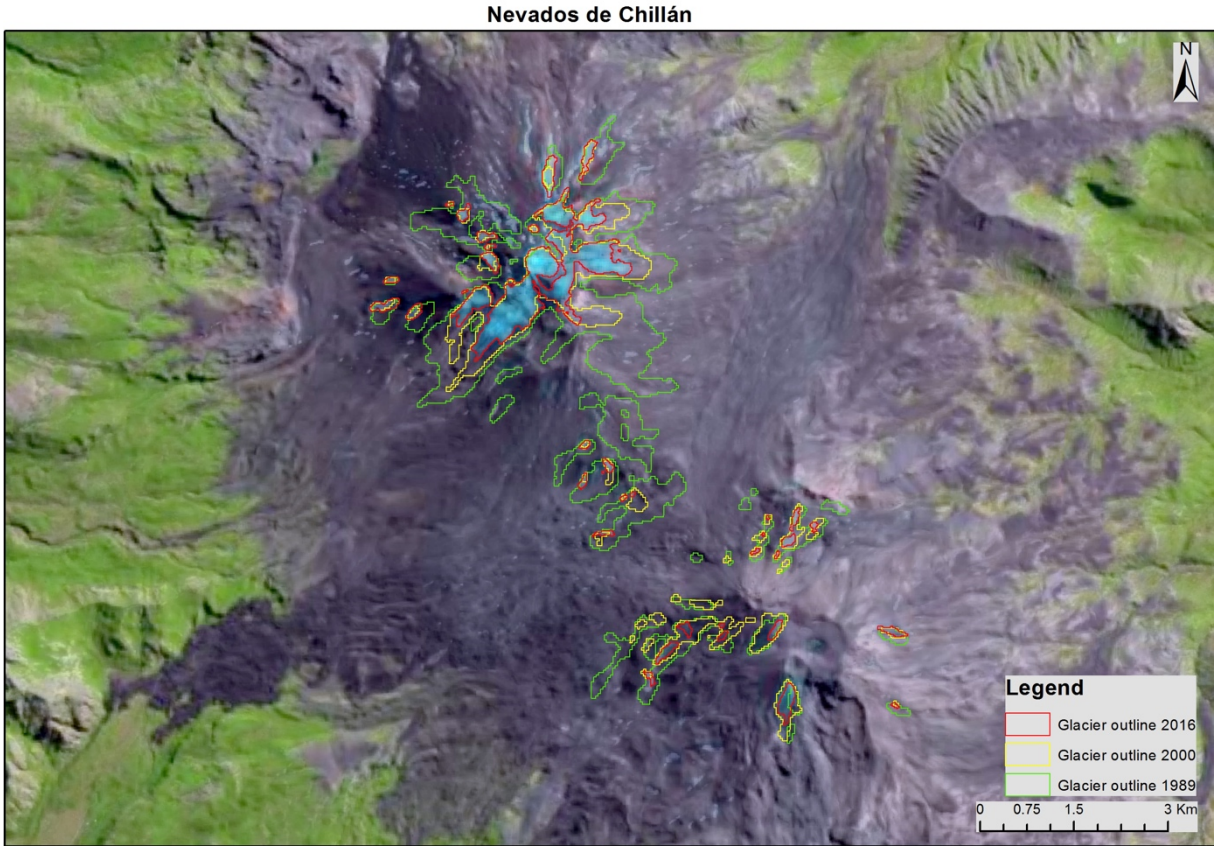

Figure A 28: Glacier outlines of Nevados de Chillán (Chile).

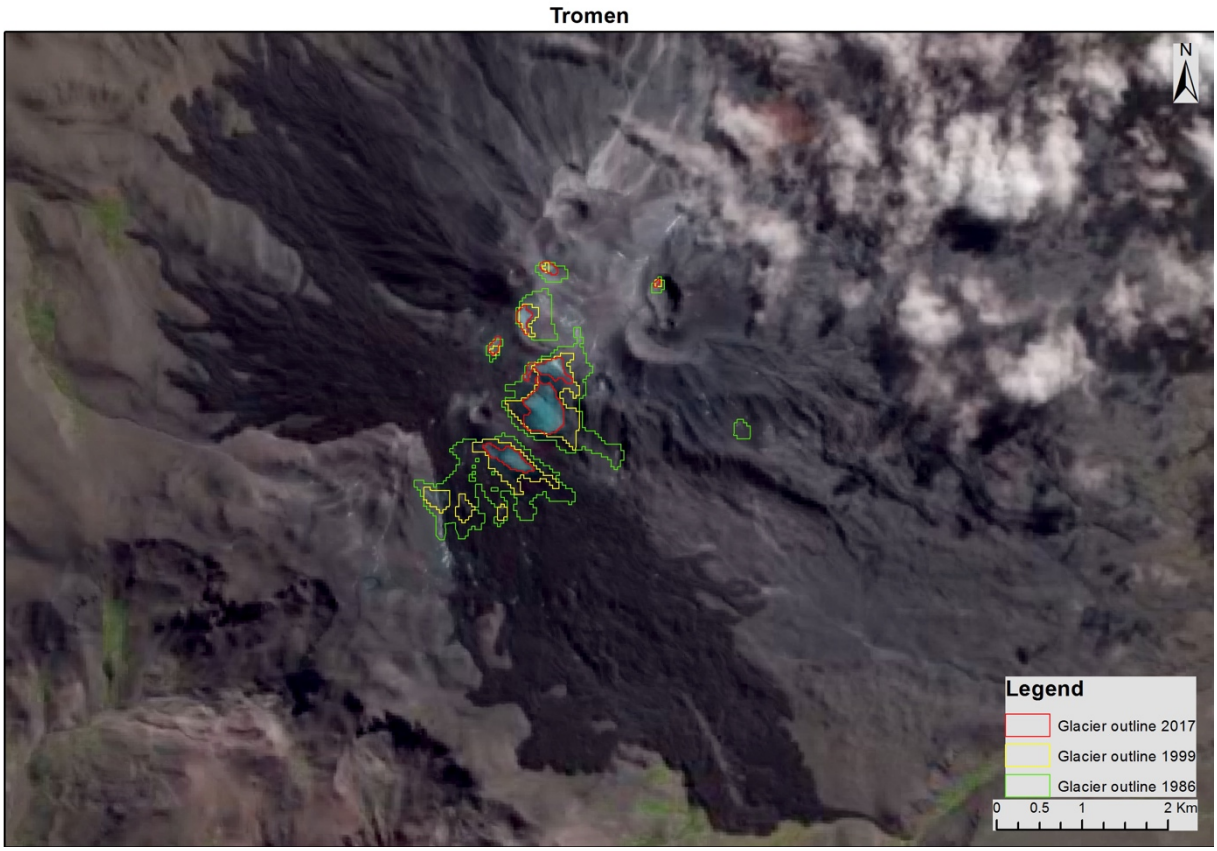

Figure A 29: Glacier outlines of Tromen (Argentina).

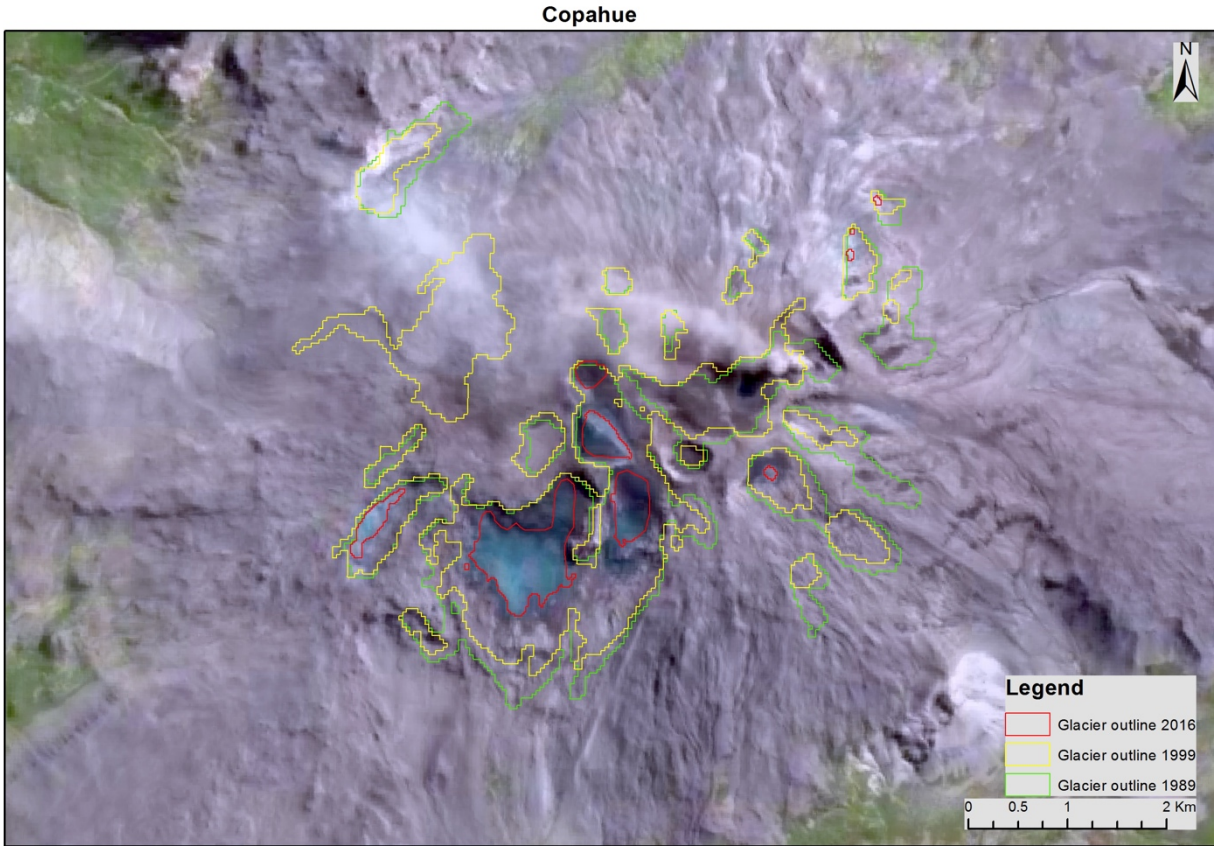

Figure A 30: Glacier outlines of Copahue (Chile/Argentina).

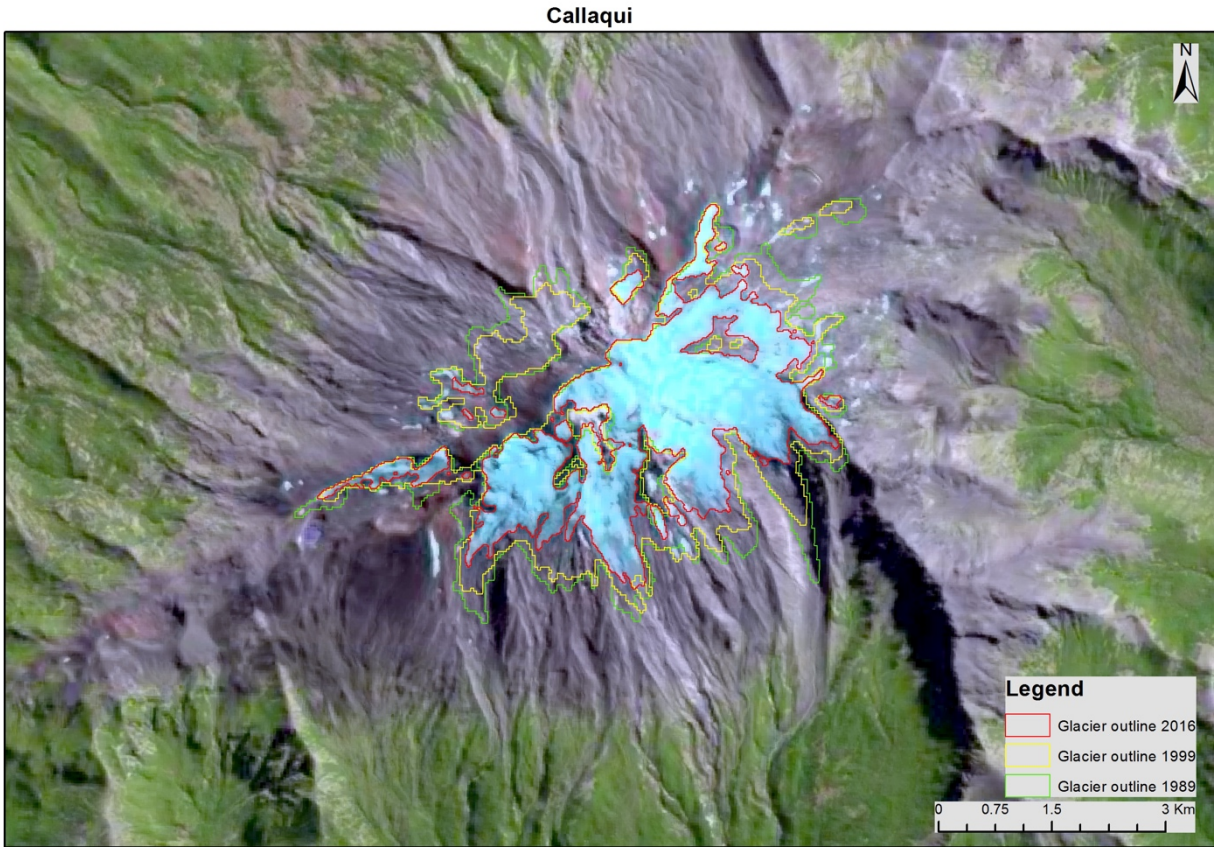

Figure A 31: Glacier outlines of Callaqui (Chile).

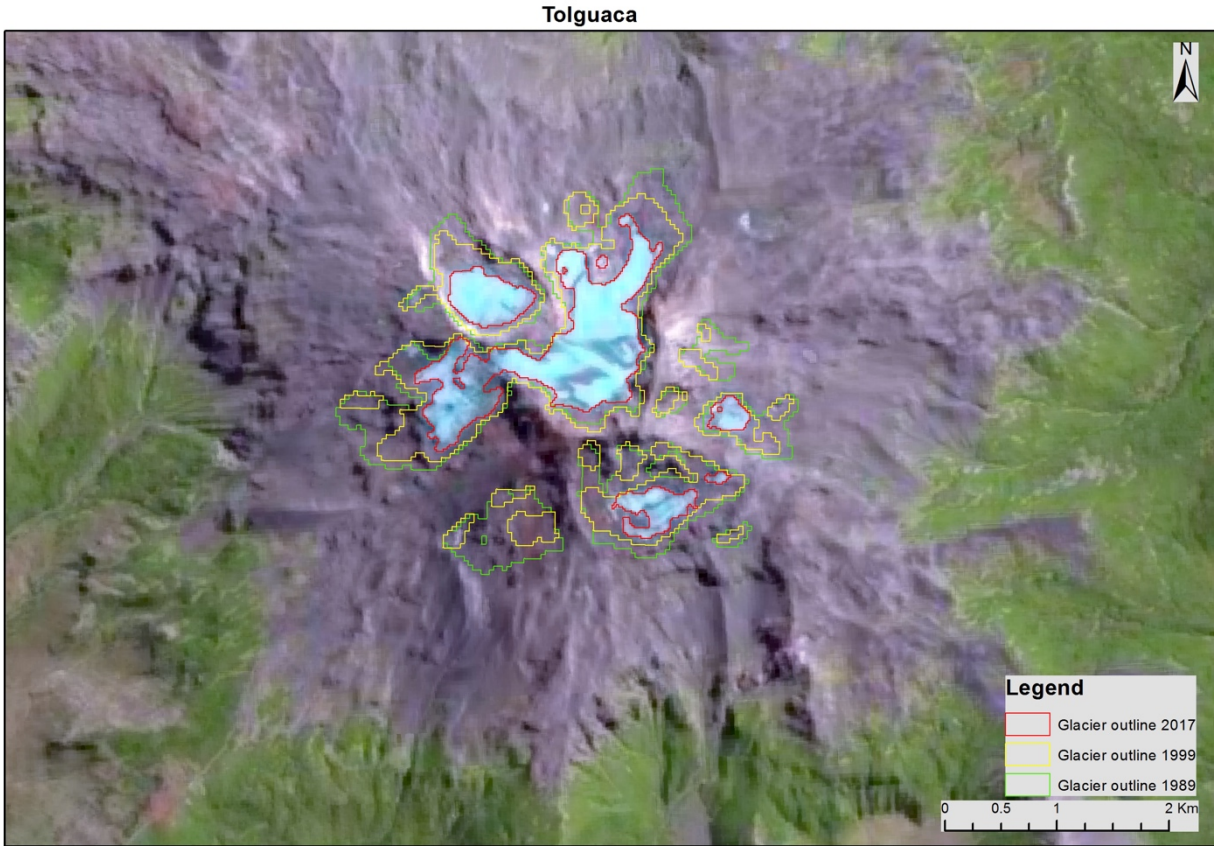

Figure A 32: Glacier outlines of Tolguaca (Chile).

Figure A 33: Glacier outlines of Lonquimay (Chile).

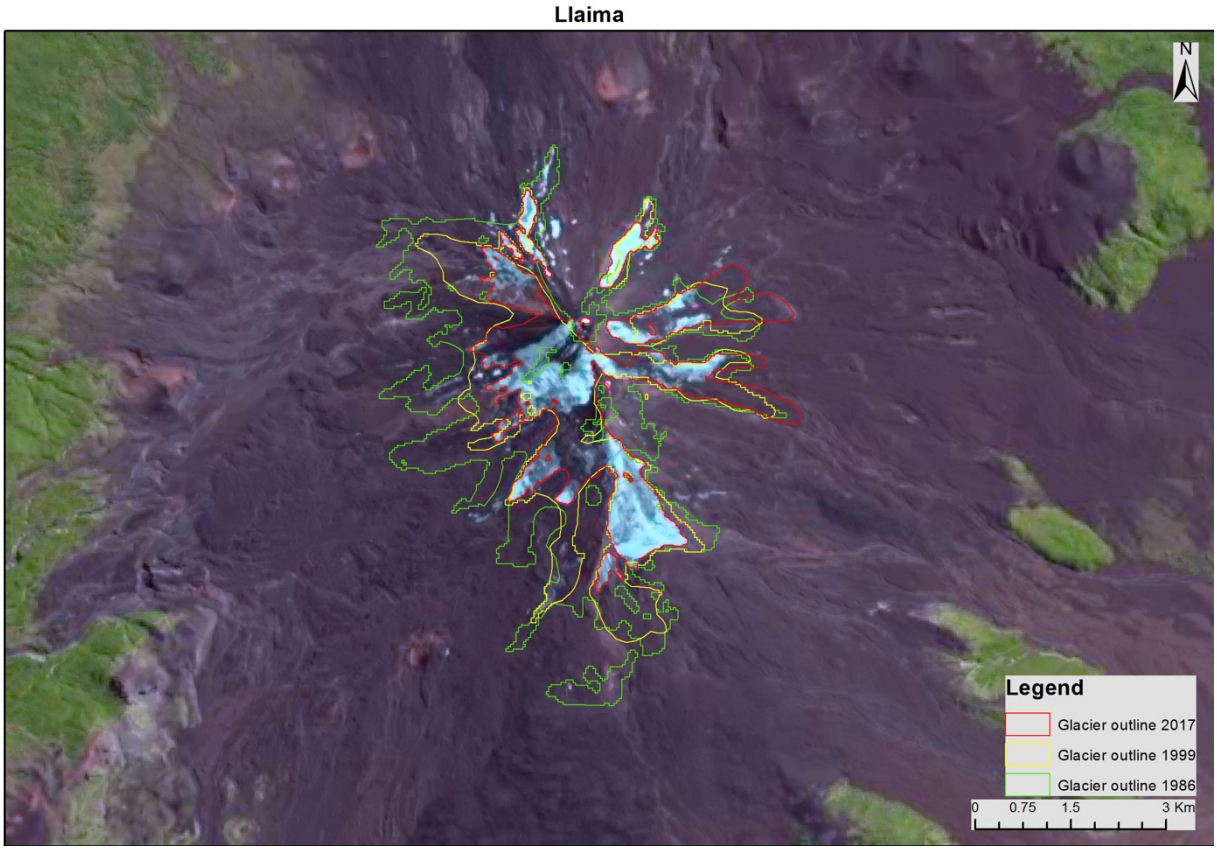

Figure A 34: Glacier outlines of Llaima (Chile).

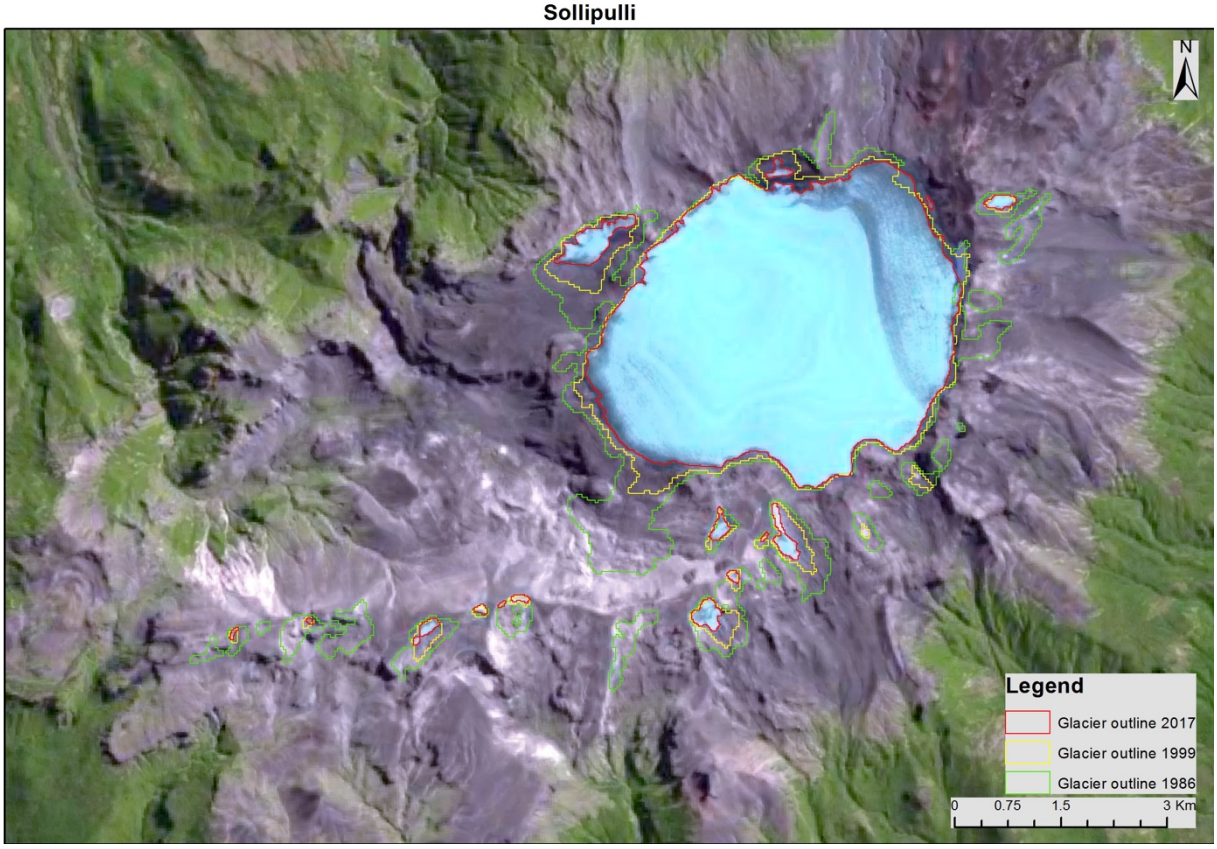

Figure A 35: Glacier outlines of Sollipulli (Chile).

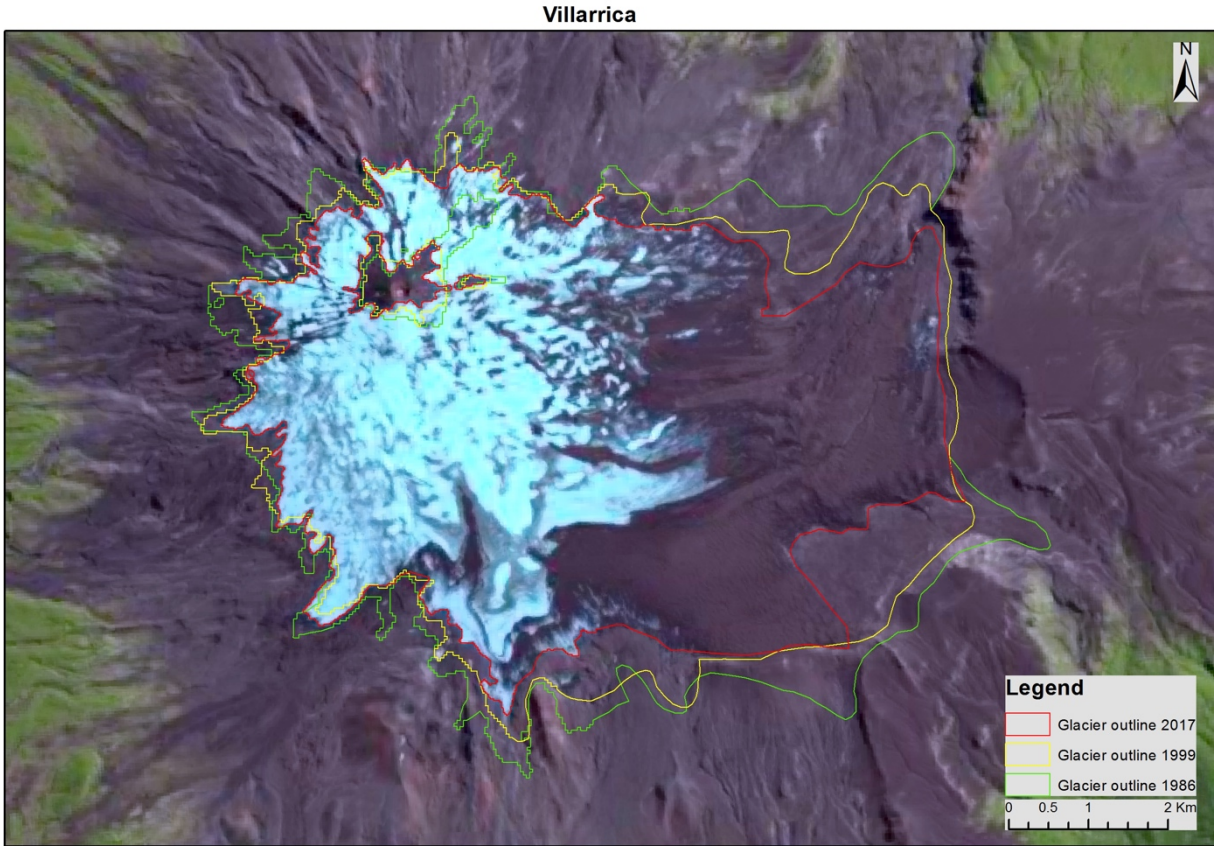

Figure A 36: Glacier outlines of Villarrica (Chile).

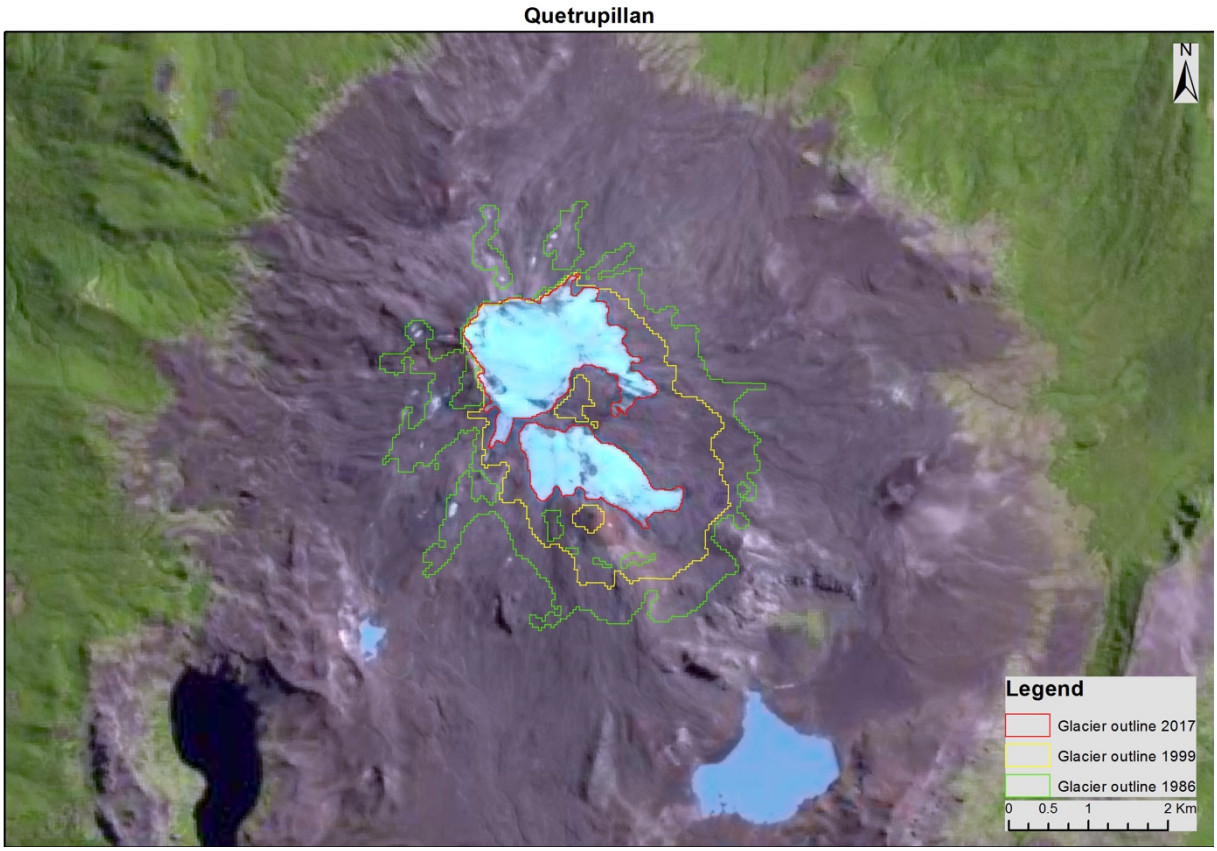

Figure A 37: Glacier outlines of Quetrupillan (Chile).

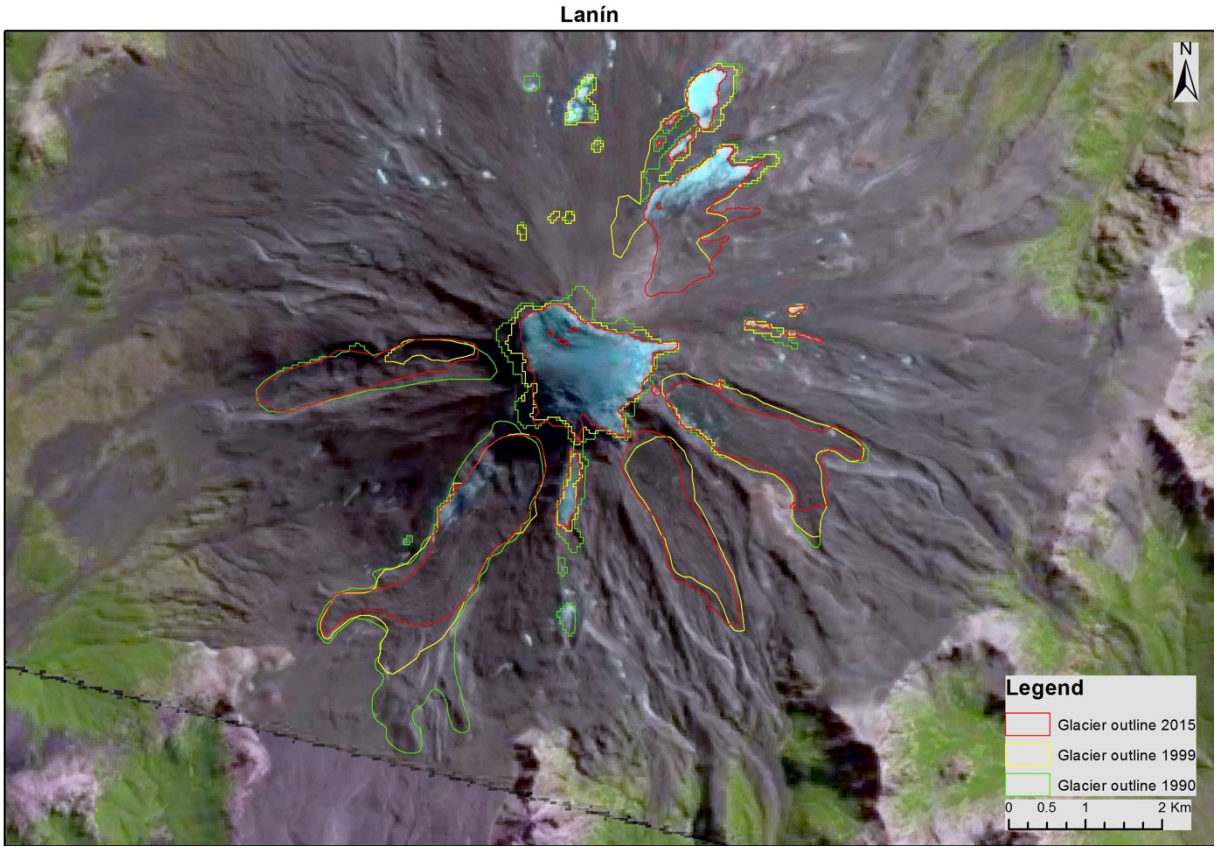

Figure A 38: Glacier outlines of Lanín (Chile/Argentina).

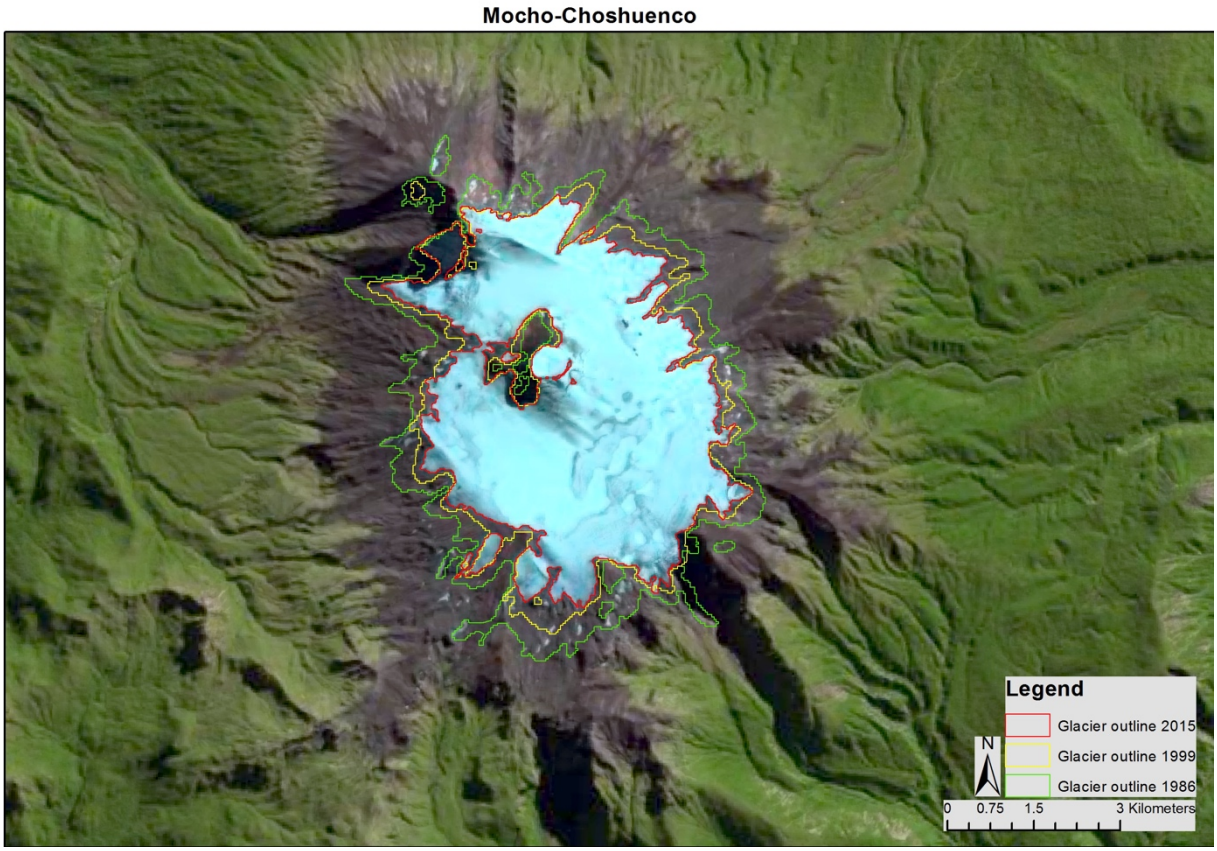

Figure A 39: Glacier outlines of Mocho - Choshuenco (Chile).

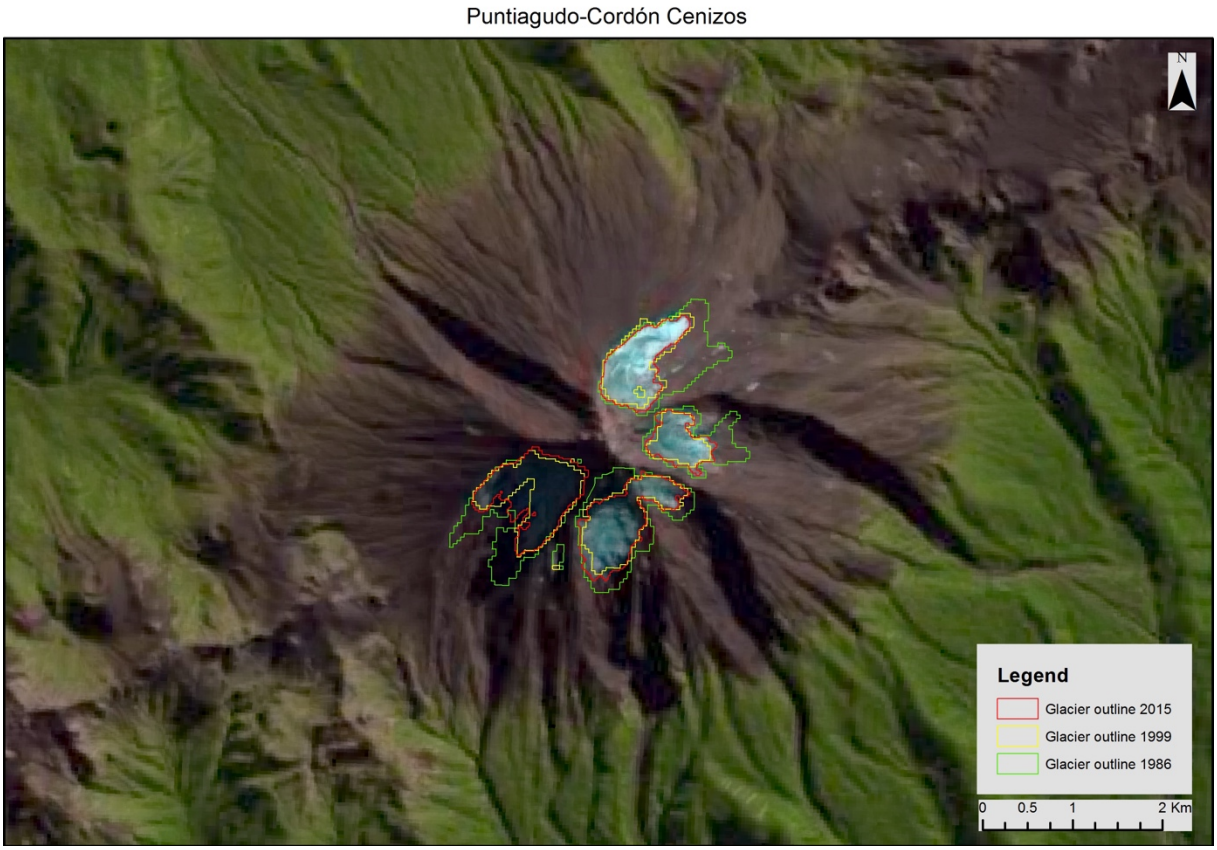

Figure A 40: Glacier outlines of Puntiagudo-Cordón Cenizos *(Chile).*

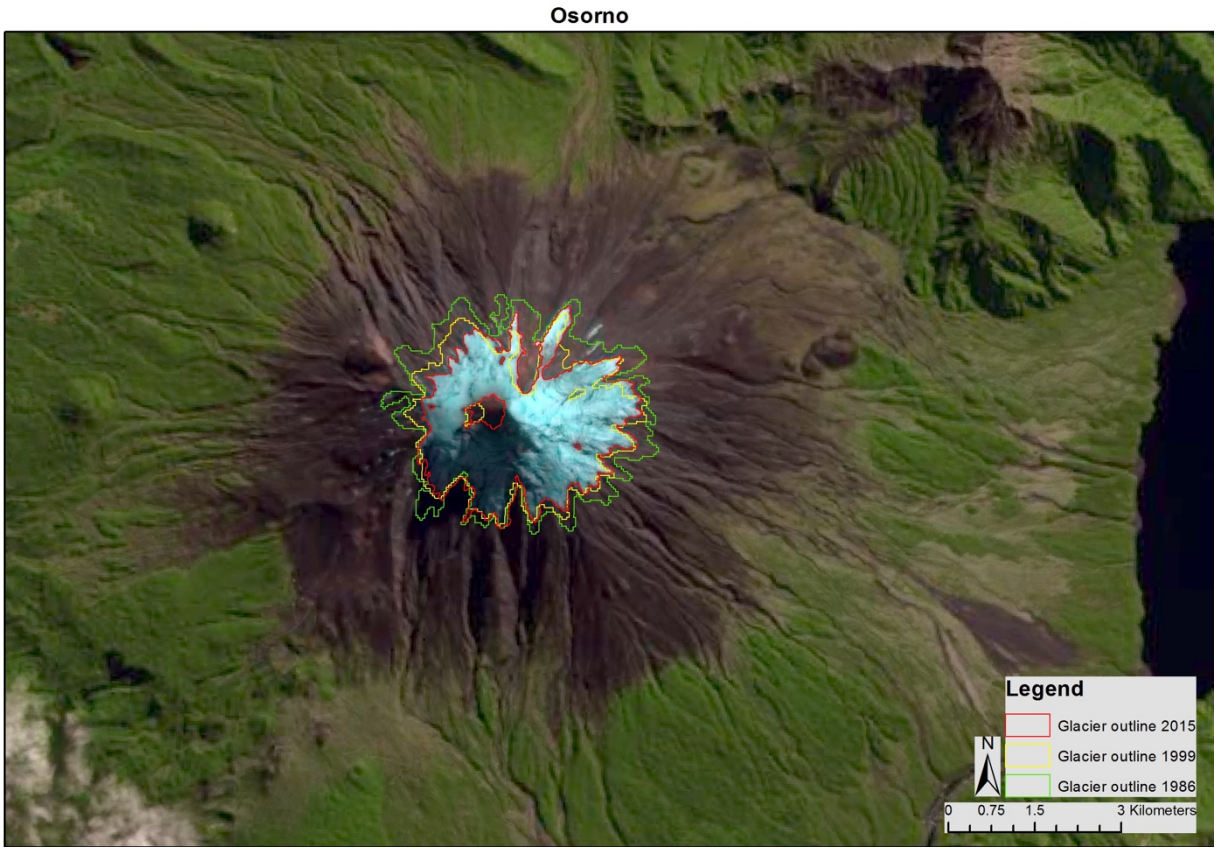

Figure A 41: Glacier outlines of Osorno (Chile).

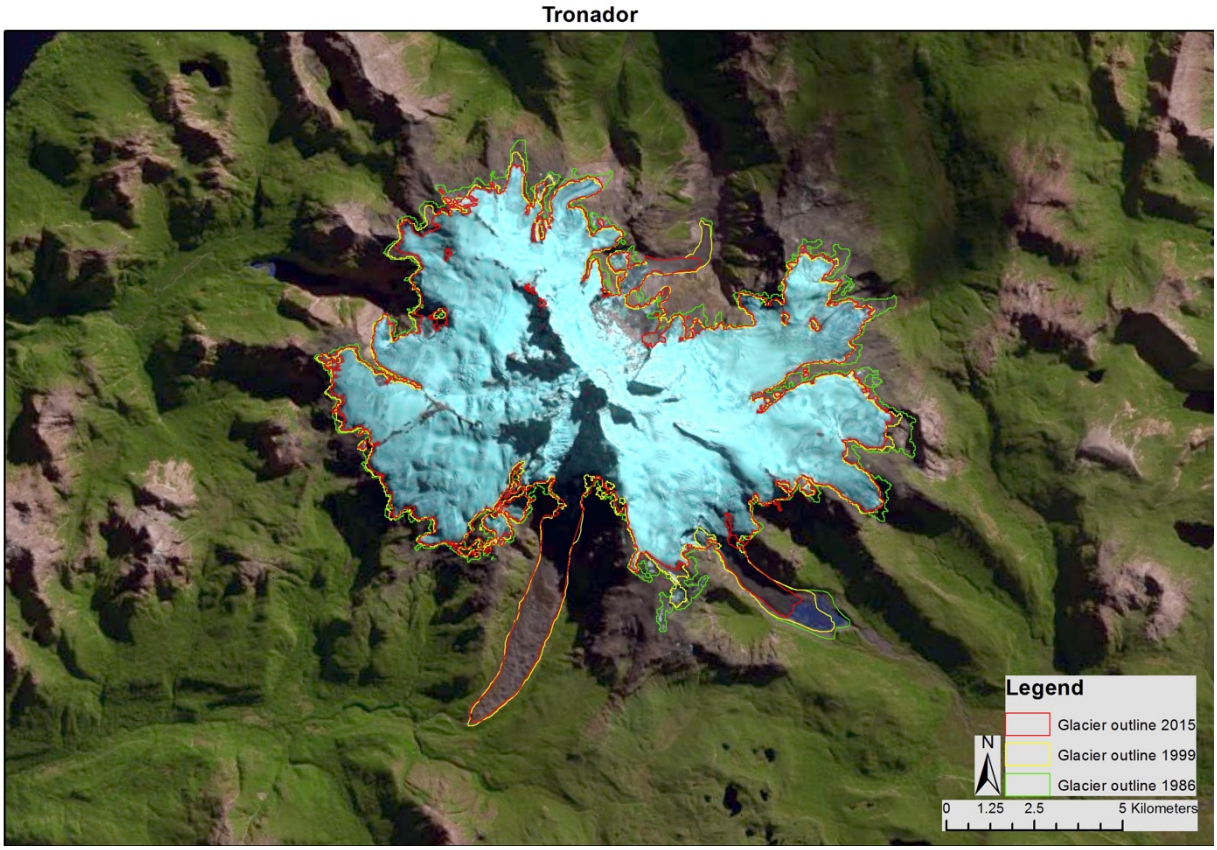

Figure A 42: Glacier outlines of Tronador (Chile/Argentina).

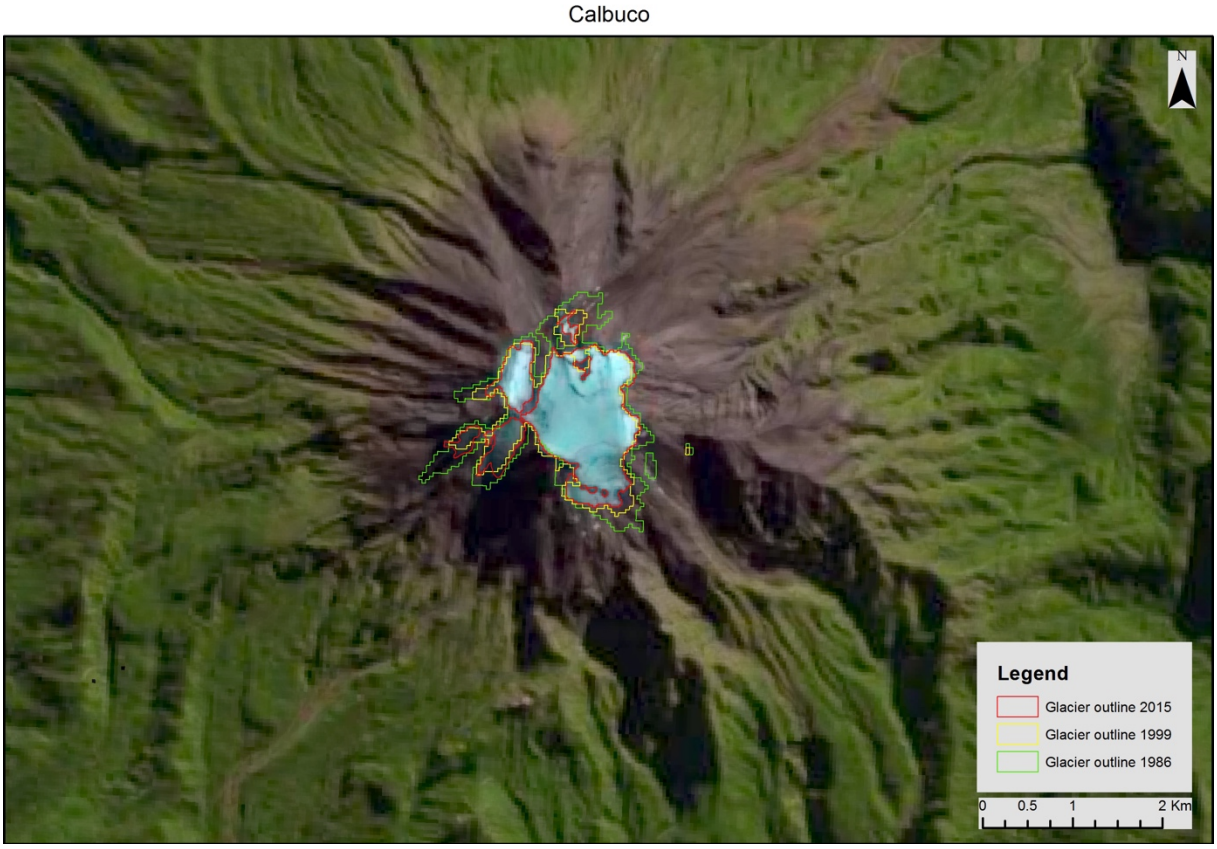

Figure A 43: Glacier outlines of Calbuco (Chile).

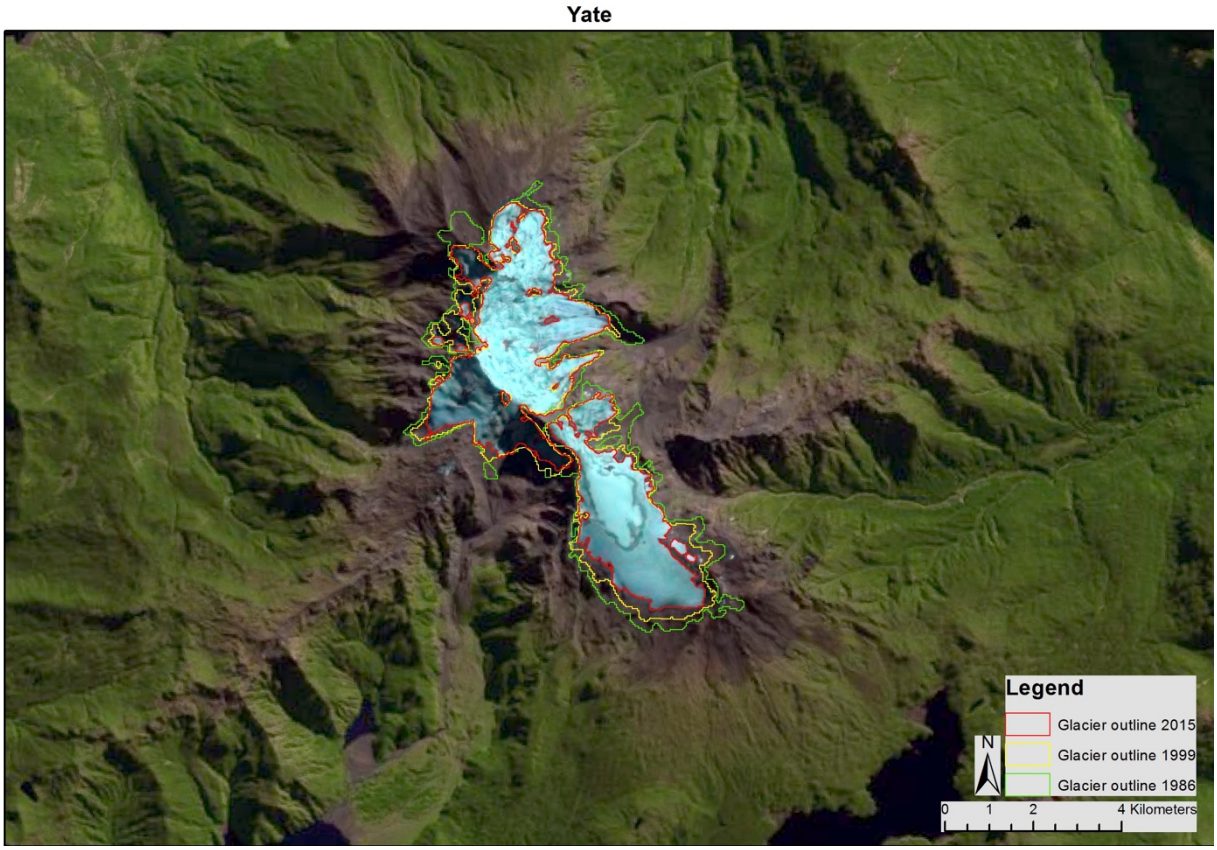

Figure A 44: Glacier outlines of Yate (Chile).

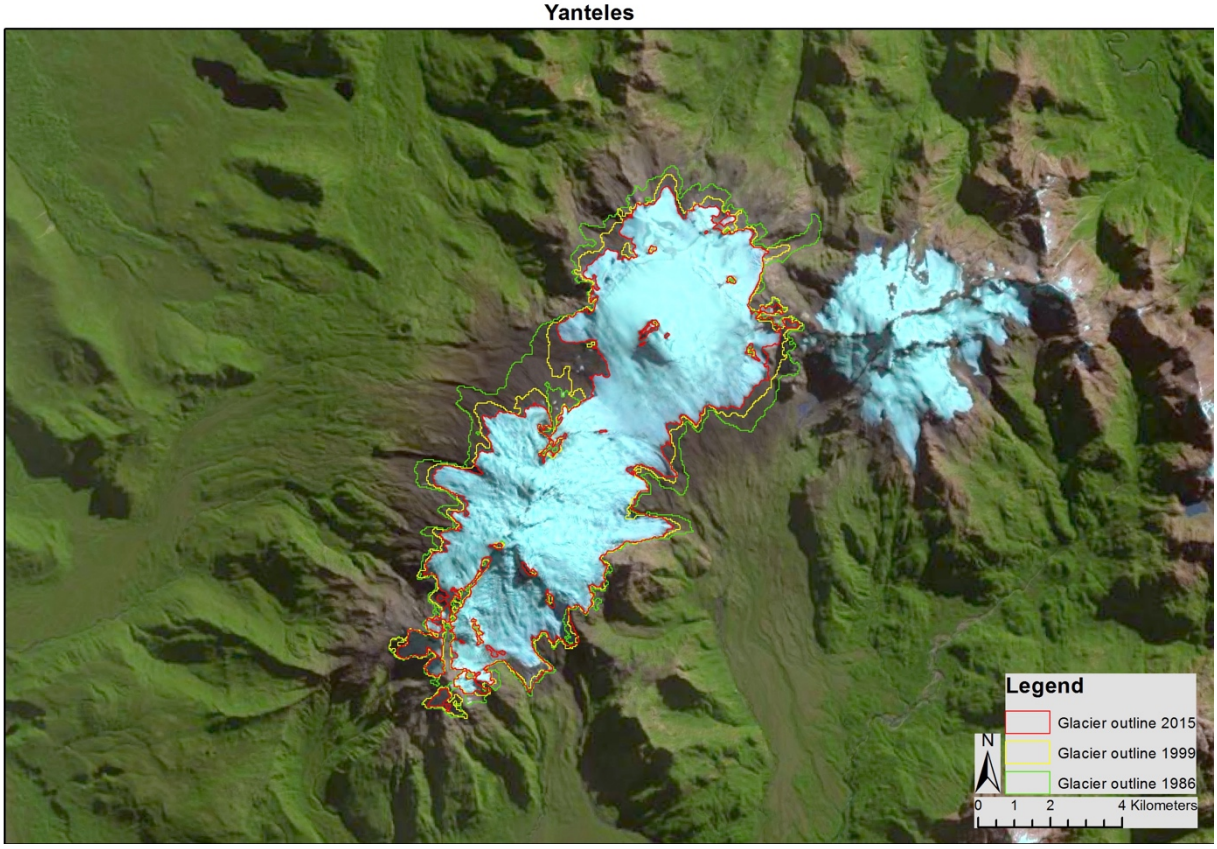

Figure A 45: Glacier outlines of Yanteles (Chile).

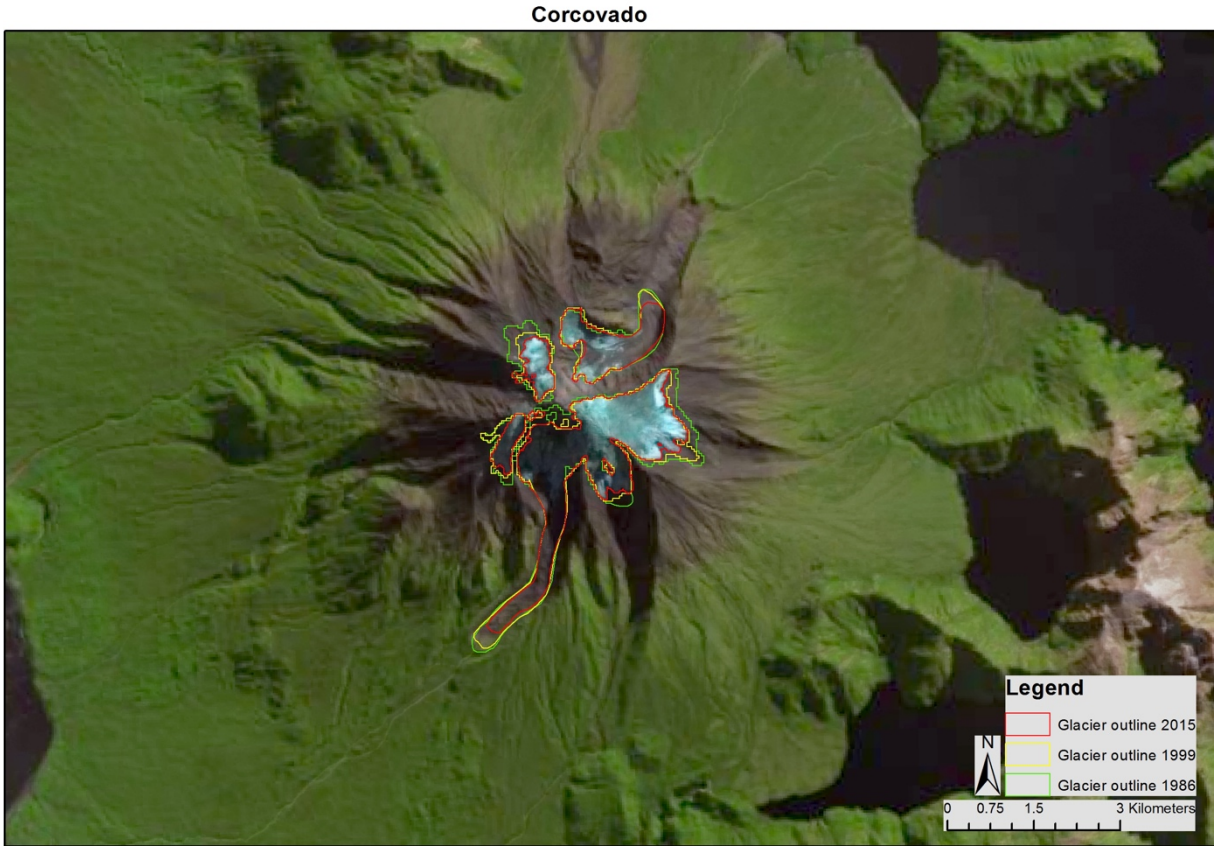

Figure A 46: Glacier outlines of Corcovado (Chile).

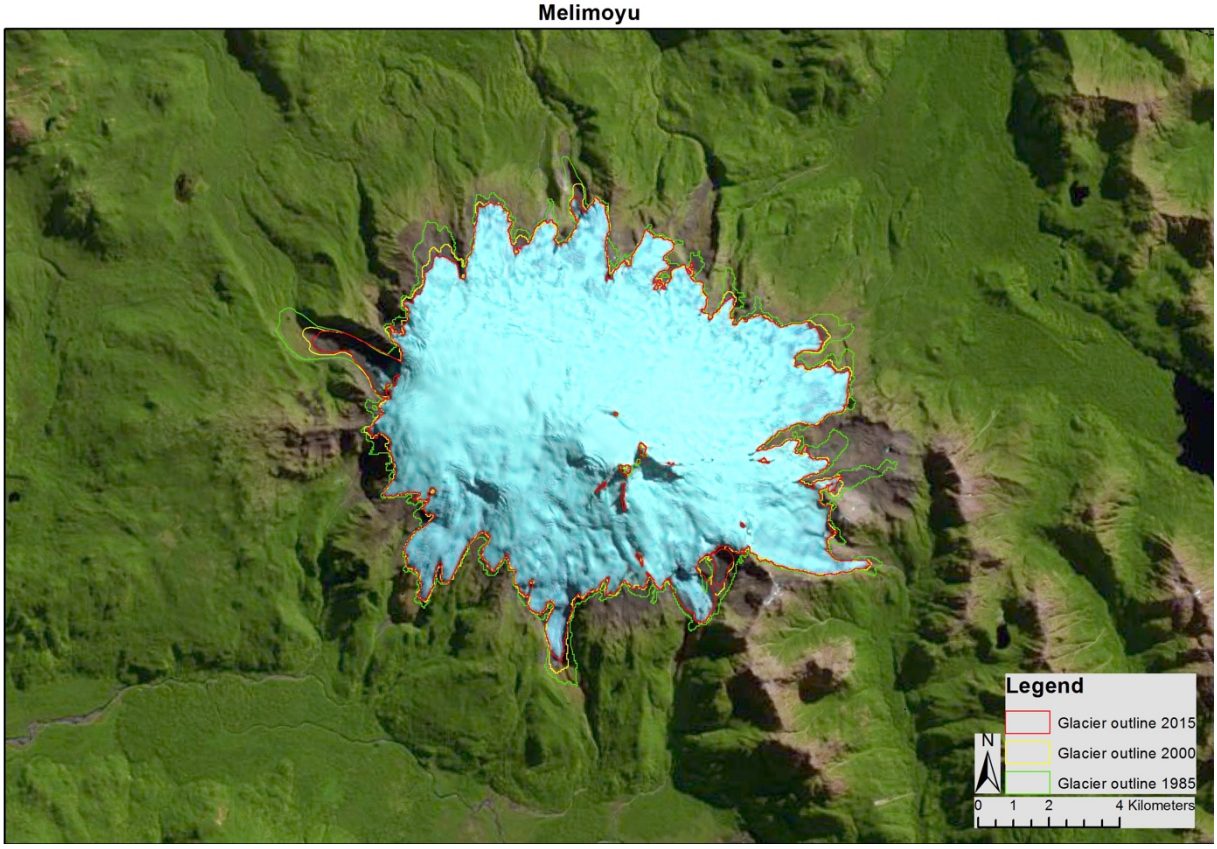

Figure A 47: Glacier outlines of Melimoyu (Chile).

Figure A 48: Glacier outlines of Menolat (Chile).

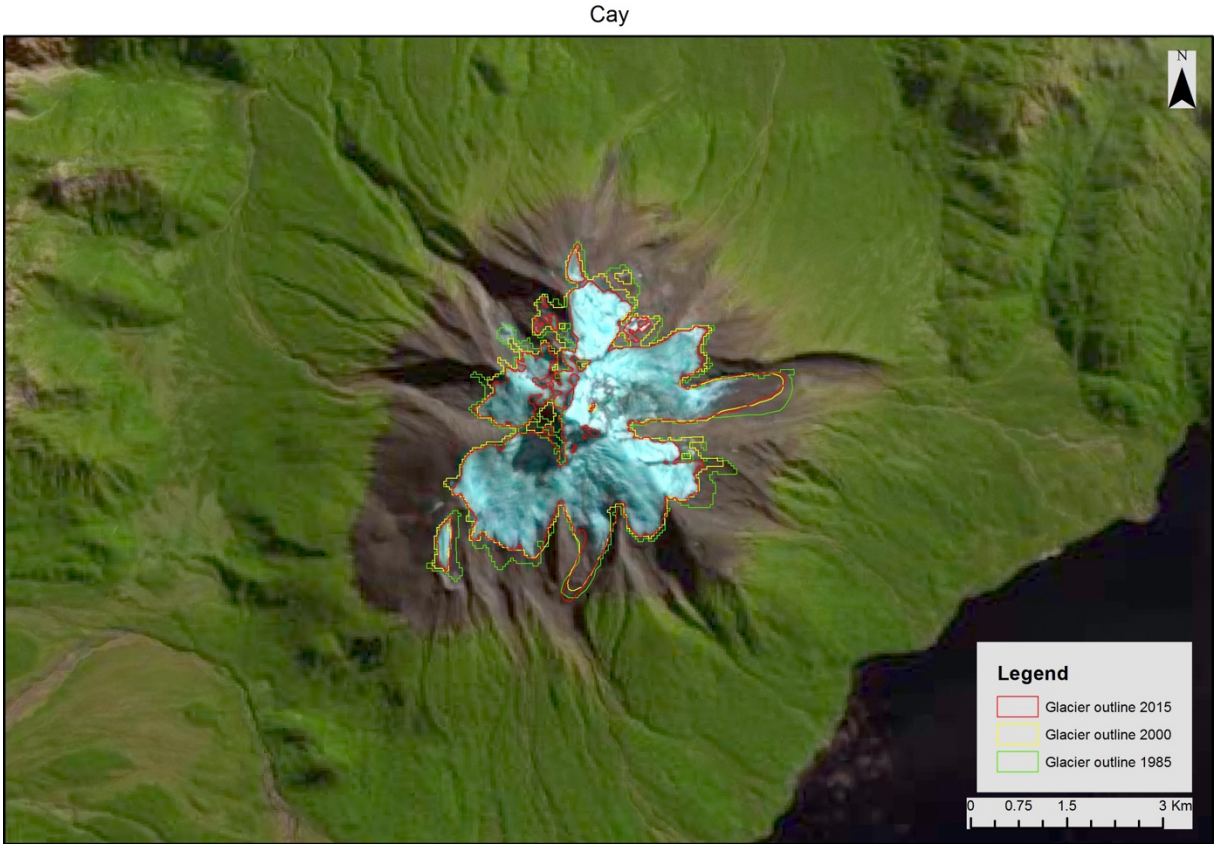

Figure A 49: Glacier outlines of Cay (Chile).

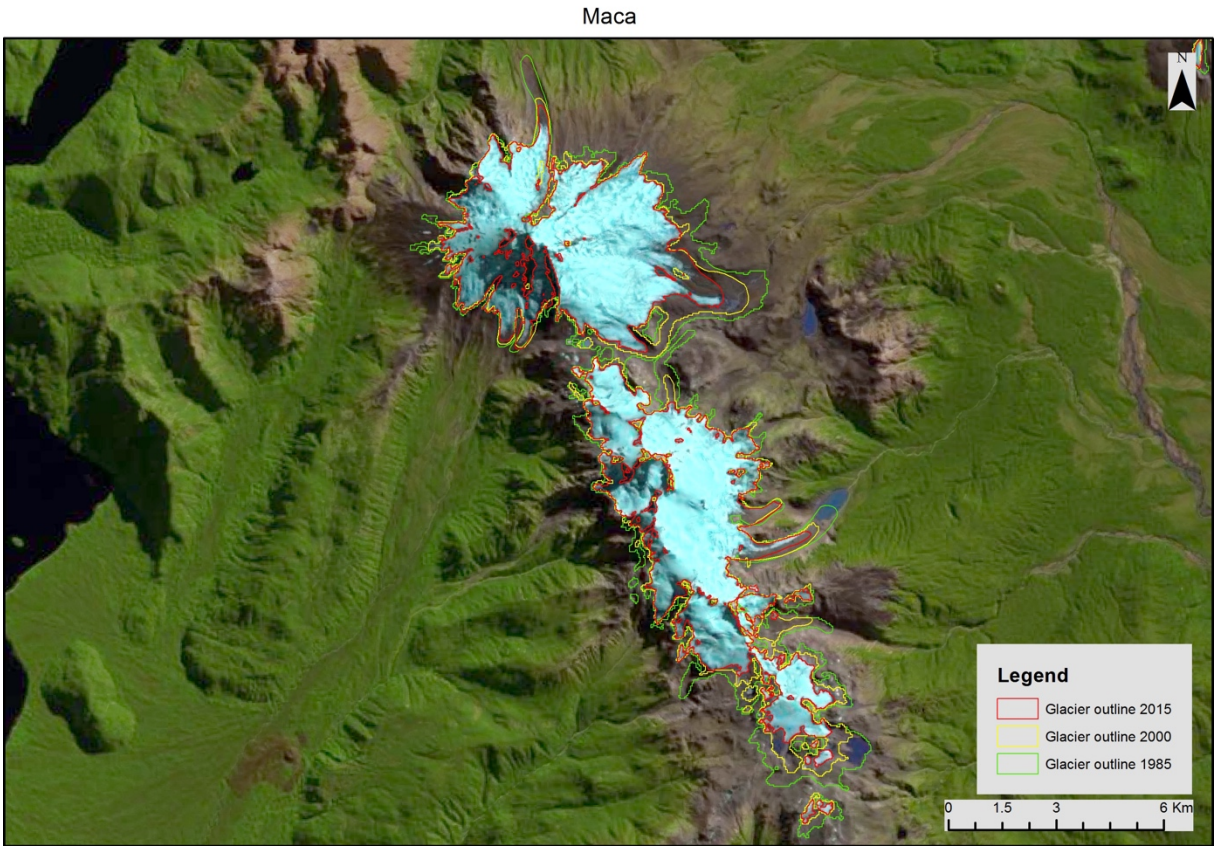

Figure A 50: Glacier outlines of Maca (Chile).

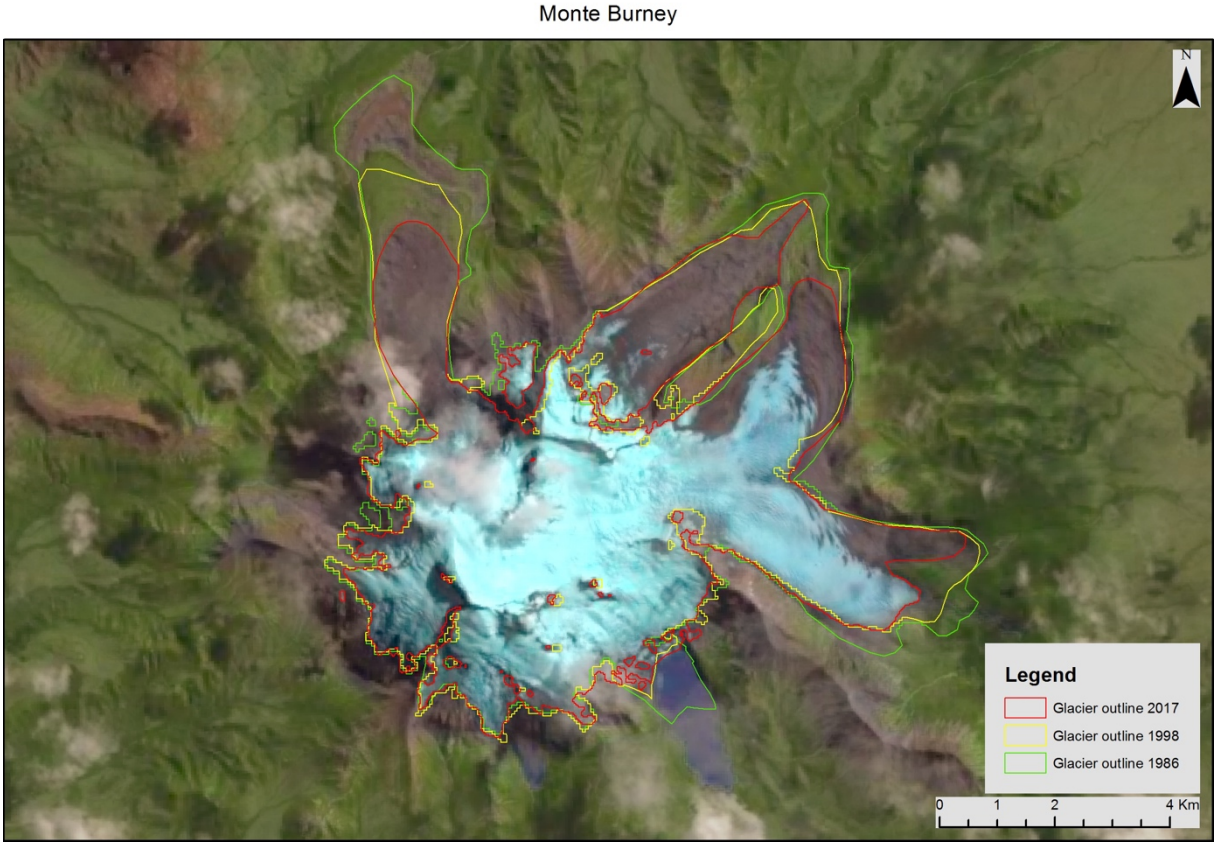

Figure A 51: Glacier outlines of Monte Bruney (Chile).

Table A 1: List of analysed volcanoes including Long./Lat., analyse date and used satellite.

Volcano name	Latitude	Longitude	Path/Row	Anal date 1985	Satellite 1985	Anal date 2000	Satellite 2000	Anal date 2015	Sentinel-2 2015
Antisana	-0.49	-78.14	P10R60	21/01/87	Landsat TM	21/12/98	Landsat TM	02/02/16	Sentinel-2
Antuco	-37.42	-71.35	P233R86	01/03/89	Landsat TM	31/03/00	Landsat ETM+	19/03/16	Landsat OLI
Azul, Cerro	-35.66	-70.77	P232R85	22/02/86	Landsat TM	26/02/99	Landsat TM	11/04/15	Landsat OLI
Calabozos	-35.57	-70.5	P232R85	22/02/86	Landsat TM	26/02/99	Landsat TM	11/04/15	Landsat OLI
Calbuco	-41.33	-72.61	P232R89	26/03/86	Landsat TM	10/02/99	Landsat TM	11/04/15	Landsat OLI
Callaqui	-37.93	-71.44	P233R86	01/03/89	Landsat TM	16/01/99	Landsat TM	19/03/16	Landsat OLI
Cay	-45.06	-72.98	P232R91	07/03/85	Landsat TM	08/03/00	Landsat ETM+	26/03/15	Landsat OLI
Cayambe	0.02	-77.99	P10R60	05/01/87	Landsat TM	21/12/98	Landsat TM	18/11/15	Landsat OLI
Chimborazo	-1.46	-78.81	P10R61	02/03/86	Landsat TM	11/03/01	Landsat ETM+	20/11/16	Landsat OLI
Copahue	-37.86	-71.18	P233R86	01/03/89	Landsat TM	16/01/99	Landsat TM	19/03/16	Landsat OLI
Corcovado	-43.2	-72.79	P232R90	26/03/86	Landsat TM	10/02/99	Landsat TM	11/04/15	Landsat OLI
Coropuna	-15.55	-72.64	P04R71	24/11/86	Landsat TM	14/11/00	Landsat TM	26/11/16	Landsat OLI
Cotopaxi	-0.69	-78.43	P10R60	26/03/87	Landsat TM	11/03/01	Landsat ETM+	02/02/16	Sentinel-2
Descabezado Grande	-35.56	-70.74	P232R85	22/02/86	Landsat TM	26/02/99	Landsat TM	11/04/15	Landsat OLI
Domuyo	-36.62	-70.43	P232R85	22/02/86	Landsat TM	26/02/99	Landsat TM	11/04/15	Landsat OLI
Guallatiri	-18.42	-69.09	P01R73	08/12/87	Landsat TM	17/12/99	Landsat ETM+	05/12/15	Landsat OLI
Huila, Nevado del	2.93	-76.03	P09R58	14/01/87	Landsat TM	12/01/01	Landsat ETM+	14/01/16	Landsat OLI
Illiniza	-0.66	-78.72	P10R60	26/03/87	Landsat TM	21/12/98	Landsat TM	02/02/16	Sentinel-2
Iztaccihuatl	19.17	-98.64	P26R47	26/03/87	Landsat TM	22/04/00	Landsat ETM+	19/02/17	Sentinel-2
Lanín	-39.65	-71.51	P232R88	25/02/90	Landsat TM	10/02/99	Landsat TM	26/03/15	Landsat OLI
Llaima	-38.71	-71.73	P232R87	26/03/86	Landsat TM	26/02/99	Landsat TM	06/03/17	Landsat OLI
Longavi, Nevado de	-36.2	-71.16	P233R85	17/03/89	Landsat TM	31/03/00	Landsat ETM+	22/03/17	Landsat OLI
Lonquimay	-38.38	-71.59	P232R87	26/03/86	Landsat TM	26/02/99	Landsat TM	06/03/17	Landsat OLI
Macá	-45.14	-73.14	P232R91	07/03/85	Landsat TM	08/03/00	Landsat ETM+	26/03/15	Landsat OLI
Maipo	-34.17	-69.83	P232R84	22/02/86	Landsat TM	26/02/99	Landsat TM	27/04/15	Landsat OLI
Melimoyu	-44.07	-72.87	P232R91	07/03/85	Landsat TM	08/03/00	Landsat ETM+	26/03/15	Landsat OLI
Mentolat	-44.7	-73.07	P232R91	07/03/85	Landsat TM	08/03/00	Landsat ETM+	26/03/15	Landsat OLI
Michinmahuida	-42.81	-72.45	P232R90	26/03/86	Landsat TM	10/02/99	Landsat TM	11/04/15	Landsat OLI
Mocho-Choshuenco	-39.94	-72.03	P232R88	26/03/86	Landsat TM	10/02/99	Landsat TM	11/04/15	Landsat OLI
Monte Burney	-52.32	-73.36	P231R96	14/01/86	Landsat TM	16/02/98	Landsat TM	04/02/17	Landsat OLI
Mount Hudson	-45.91	-72.96	P232R92	07/03/85	Landsat TM	08/03/00	Landsat ETM+	12/03/16	Landsat OLI
Nevados de Chillán	-36.84	-71.4	P233R86	01/03/89	Landsat TM	31/03/00	Landsat ETM+	19/03/16	Landsat OLI

Osorno	-41.11	-72.5	P232R89	26/03/86	Landsat TM	10/02/99	Landsat TM	11/04/15	Landsat OLI
Palomo	-34.6	-70.34	P232R84	22/02/86	Landsat TM	26/02/99	Landsat TM	27/04/15	Landsat OLI
Parinacota	-18.15	-69.14	P01R73	08/12/87	Landsat TM	17/12/99	Landsat ETM+	05/12/15	Landsat OLI
Pico de Orizaba	19.04	-97.27	P25R47	16/03/86	Landsat TM	04/02/98	Landsat TM	25/02/17	Sentinel-2
Planchón-Peteroa	-35.27	-70.58	P232R85	22/02/86	Landsat TM	26/02/99	Landsat TM	11/04/15	Landsat OLI
Popocatepetl	19.03	-98.63	P26R47	26/03/87	Landsat TM	22/04/00	Landsat ETM+		
Puntiagudo-Cordón Cenizos	-40.98	-72.27	P232R88	26/03/99	Landsat TM	10/02/99	Landsat TM	11/04/15	Landsat OLI
Puyehue-Cordón Caulle	-40.58	-72.11	P232R88	26/03/86	Landsat TM	10/02/99	Landsat TM	11/04/15	Landsat OLI
Quetrupillan	-39.51	-71.71	P232R87	26/03/86	Landsat TM	10/02/99	Landsat TM	06/03/17	Landsat OLI
Risco Plateado	-34.93	-70.01	P232R84	22/02/86	Landsat TM	26/02/99	Landsat TM	27/04/15	Landsat OLI
Ruiz, Nevado del	4.88	-75.32	P09R57	14/01/87	Landsat TM	01/12/01	Landsat ETM+	14/01/16	Landsat OLI
Sabancaya	-15.77	-71.87	P04R71	21/11/86	Landsat TM	14/11/00	Landsat TM	25/10/16	Landsat OLI
San Jose	-33.77	-69.88	P232R83	06/02/86	Landsat TM	11/03/01	Landsat ETM+	27/04/15	Landsat OLI
San Pedro-Pellado	-35.98	-70.82	P232R85	22/02/86	Landsat TM	26/02/99	Landsat TM	11/04/15	Landsat OLI
Sangay	-2.01	-78.34	P10R61	18/12/91	Landsat TM	11/03/01	Landsat ETM+	20/11/16	Landsat OLI
Santa Isabel, Nevado del	4.8	-75.37	P09R57	14/01/87	Landsat TM	01/12/01	Landsat ETM+	14/01/16	Landsat OLI
Sollipulli	-38.98	-71.53	P232R87	26/03/86	Landsat TM	26/02/99	Landsat TM	06/03/17	Landsat OLI
Tinguiririca	-34.79	-70.32	P232R84	22/02/86	Landsat TM	26/02/99	Landsat TM	27/04/15	Landsat OLI
Tolguaca	-38.31	-71.65	P233R86	01/03/89	Landsat TM	16/01/99	Landsat TM	03/03/17	Landsat OLI
Tolima, Nevado del	4.66	-75.33	P09R57	14/01/87	Landsat TM	12/01/01	Landsat ETM+	14/01/16	Landsat OLI
Tromen	-37.15	-70.05	P232R86	26/03/86	Landsat TM	26/02/99	Landsat TM	31/03/17	Landsat OLI
Tronador	-41.16	-71.89	P232R89	26/03/86	Landsat TM	10/02/99	Landsat TM	11/04/15	Landsat OLI
Tungurahua	-1.47	-78.44	P10R61	18/12/91	Landsat TM	21/12/98	Landsat TM		
Tupungatito	-33.43	-69.79	P232R83	06/02/86	Landsat TM	11/03/01	Landsat ETM+	27/04/15	Landsat OLI
Villarrica	-39.43	-71.92	P232R87	26/03/86	Landsat TM	10/02/99	Landsat TM	06/03/17	Landsat OLI
Yanteles	-43.49	-72.8	P232R90	26/03/86	Landsat TM	10/02/99	Landsat TM	11/04/15	Landsat OLI
Yate	-41.78	-72.39	P232R89	26/03/86	Landsat TM	10/02/99	Landsat TM	11/04/15	Landsat OLI

Personal declaration

Name: Johannes Reinthaler

Matriculationnumber: 15-727-720

Definitive title of the master thesis: Analysis of decadal glacier changes on active volcanoes in Latin America

I hereby declare that the submitted thesis is the result of my own, independent work. All external sources are explicitly acknowledged in the thesis. Additionally, I affirm that I did not use the contents of this work for obtaining credits otherwise.

Signature:

Date, signature of the candidate: .....